

COMMON ALLELES OF THE SLAM/CD2 FAMILY ARE ASSOCIATED WITH
MURINE LUPUS

APPROVED BY SUPERVISORY COMMITTEE

Edward K. Wakeland, Ph.D.

James M. Forman, D.M.D, Ph.D.

Michael Bennett, M.D.

Chandra Mohan, M.D., Ph.D.

Porunelloor A. Mathew, Ph.D.

Acknowledgements

There are numerous people to thank for all of their support during my time at the Center for Immunology at UT Southwestern. I'm extremely grateful to my mentor, Dr. Edward K. Wakeland, for welcoming as one of his first graduate students. He has provided me with a wonderful opportunity to learn and develop as an independent scientist, and has always been extremely encouraging of my efforts.

I would also like to thank my many colleagues, many of whom have become very good friends, for all of their help and support over the years. And finally, I'd like to acknowledge my family and all of my friends, who have been a source of great motivation and encouragement, and have always been there through the good times and the bad. I will always treasure all of the wonderful times we've shared.

COMMON ALLELES OF THE SLAM/CD2 FAMILY ARE ASSOCIATED WITH
MURINE LUPUS

By
Nisha Limaye

DISSERTATION

Presented to the Faculty of the Graduate School of Biomedical Sciences

The University of Texas Southwestern Medical Center at Dallas

In Partial Fulfillment of the Requirements

For the Degree of

DOCTOR OF PHILOSOPHY

The University of Texas Southwestern Medical Center at Dallas

Dallas, Texas

April, 2005

Common Alleles of the SLAM/CD2 Family are Associated with Murine Lupus

Publication No. _____

Nisha Limaye

The University of Texas Southwestern Medical Center at Dallas

Supervising Professor: Dr. Edward K. Wakeland

The *Sle1b* locus on telomeric mouse chromosome 1 mediates a break in tolerance to chromatin in the NZM2410 model of the autoimmune disease Systemic Lupus Erythematosus (SLE). B6.*Sle1b* congenic mice produce anti-nuclear autoantibodies (ANAs), and have elevated activated B and CD4⁺ T cells, and mild splenomegaly. Fine mapping of *Sle1b* positioned it within a ~900 kb region between 171.3 and 172.2 Mb. A contig of 100 B6-derived Bacterial Artificial Chromosomes (BACs) was constructed across *Sle1b*, and sequencing of six BACs that form an overlapping tiling path across it revealed that the interval contains 24 genes, 19 of which are expressed in the spleen, and 14 of which are in B and CD4⁺ T cells. We carried out extensive candidate gene analyses on the spleen-expressed genes, including sequencing of all the exons and flanking introns in the lupus-resistant B6 and susceptible B6.*Sle1b* parental strains, as well as Quantitative Real-time PCR on B and CD4⁺ T cell cDNA to detect any potentially functional polymorphisms between them. These

analyses showed that the SLAM/CD2 family of seven immunoregulatory receptors, clustered within the locus, are by far the best candidates to be the *Sle1b* gene(s). The members of this family play important roles in intercellular interactions, activation, and function, by engaging in homophilic interactions with themselves or with each other, on a wide variety of immune cell types. Sequence analyses of their extracellular ligand-binding immunoglobulin (Ig) domains revealed that the cluster forms two stable, linked haplotypes of alleles in 33 common inbred laboratory strains of mice. The B6-like haplotype is found only in a small set of C57-strains, while the B6.*Sle1b*-like haplotype is found in all of the remaining, including the autoimmune-prone MRL, NOD, and NZB, as well as non-autoimmune strains like 129, Balb/c, and C3H. Introgression of this common haplotype from 129 onto B6 also potentiates autoimmunity, causing phenotypes similar to those of B6.*Sle1b* mice, which derive this interval from the NZW parent of NZM2410. Autoimmunity is mediated, not by a rare mutation peculiar to the region from NZW, but instead by common polymorphic variants of this family, in combination with the downstream signaling and effector molecules and pathways present in the B6 genetic background, underlining the importance of epistasis in such complex, multigenic autoimmune phenotypes. An examination of the SLAM/CD2 Ig domains in a large group of wild-outbred and wild-derived inbred strains belonging to different species of *Mus*, and sub-species of *Mus musculus*, has shown that the “disease” alleles of this family are also very common in these populations, demonstrating that their prevalence in the lab strains is not simply an artifact of their inbreeding. The genes also show the presence of ancestral or trans-species polymorphisms, indicative of maintenance of these alleles by balancing selection, although we do not yet know what precisely drives it. The small size of the *Sle1b* susceptibility interval, and the presence of this linked cluster of attractive candidate genes within it, makes it hard to identify which gene or combination of genes within this family is actually responsible for the autoimmunity by any further

recombinational analysis. We have instead turned to a BAC-transgenic rescue strategy by which to localize the gene to a single B6-derived BAC, by its ability to complement the ANA-production phenotype and rescue autoimmunity in B6.*Sle1b* mice. We believe the strategy is feasible because *Sle1b* has a strong allele dose effect, so that the presence of a B6 allele of the *Sle1b* gene causes a large drop in penetrance of ANA-production, from about 90% in nine month old B6.*Sle1b* females, to about 33% in (B6 X B6.*Sle1b*) F1s. Our data show that none of the non-SLAM/CD2 candidates within the region is able to rescue B6.*Sle1b* mice, despite being demonstrably expressed from their BAC-transgenes. BACs carrying certain SLAM/CD2 family members have given us some promising preliminary data, but completion of this analysis will require the characterization of a BAC carrying our single most promising candidate gene, Ly108. This functional, *in vivo* method, we believe, will allow us to definitively identify the *Sle1b* gene.

TABLE OF CONTENTS

Abstract.....	iv
Table of Contents	vii
Publications	xi
List of Figures.....	xii
List of Tables	xiv
CHAPTER 1: Introduction.....	1
<i>SLE as a Single-Gene Effect: Complement and SLE</i>	<i>1</i>
<i>SLE is a Complex, Multigenic Disease: Multiple loci are linked to susceptibility in humans</i>	<i>4</i>
<i>Polymorphic genes associated with SLE in human studies, with supporting evidence from</i> <i>synthetic mouse models of lupus</i>	<i>7</i>
The MHC and lupus.....	7
TNF- α and TNFR2	8
PTPN22.....	9
PD-1	10
CTLA4.....	11
IL-10	12
Activating and Inhibitory Fc γ Rs	13
CRP and SAP.....	15
<i>Synthetic Mouse Models of Lupus</i>	<i>17</i>
<i>Spontaneous Mouse Models of SLE.....</i>	<i>19</i>
<i>Linkage analysis and congenic dissection in the NZM2410 model of autoimmunity.....</i>	<i>21</i>
<i>The importance of epistasis in autoimmunity</i>	<i>23</i>

<i>Susceptibility genes identified in spontaneous mouse models of SLE: Ifi202, Cr2, and the SLAM/CD2 family</i>	25
<i>The SLAM/CD2 Family of Immunoregulatory Receptors</i>	28
The receptor-ligand pair Cd48 and Cd244.....	29
Cd150.....	32
Cs1	36
Cd84.....	37
CD229.....	37
Ly108.....	38
<i>SAP and EAT2: Downstream adaptors of the SLAM/CD2 family</i>	40
<i>The importance of SAP in immune regulation</i>	41
Chapter II. Methods	45
<i>Mice and Mouse Strain DNA</i>	45
<i>BAC Contig Construction</i>	46
<i>BAC DNA Extraction and Insert Sequencing</i>	46
<i>BAC-transgene Construct Preparation</i>	47
<i>PCR Genotyping</i>	48
<i>Preparation of genomic DNA from tail lysates</i>	49
<i>Cell Preparation</i>	49
<i>Preparation of cDNA</i>	49
<i>Quantitative RT-PCR</i>	49
<i>PCR Amplification and Sequencing of Products</i>	50
<i>Phylogenetic analysis of sequence data</i>	51
<i>Likelihood analysis of codon selection</i>	51
<i>Serology</i>	51

<i>Sequencing-based Single-nucleotide polymorphism (SNP) Assays</i>	52
Primers used to on genomic DNA determine copy number/ heterozygosity vs homozygosity	55
Primers used to detect expression of candidate B6-transgenes in splenic cDNA.....	56
<i>Flow Cytometric Analysis and Antibodies</i>	59
Statistical Analysis.....	59
CHAPTER III. Association of Extensive Polymorphisms in the SLAM Family Gene	
Cluster with Murine Lupus	64
Introduction.....	64
Results.....	66
<i>Sequencing and construction of a molecular map of the Sle1b congenic interval.</i>	66
<i>Extensive polymorphisms distinguish the SLAM/CD2 family genes in B6 and B6.Sle1b</i> 66	
<i>Polymorphic SLAM/CD2 family haplotypes and the development of autoimmunity</i>	70
Discussion.....	73
CHAPTER IV. Retention of Autoimmune Susceptibility Alleles in Natural Populations	
.....	91
Introduction.....	91
Results.....	94
<i>SLAM/CD2 Haplotypes in common laboratory strains are present in multiple Mus sub-</i> <i>species.</i>	94
<i>The SLAM/CD2 family Ig regions show the presence of ancestral polymorphism</i>	96
<i>Codon-substitution analyses on the SLAM/CD2 Ig show that Cd229, Cd48 and Cd84 are</i> <i>the best candidates for having codons under selection</i>	98
<i>CTLA4 polymorphism linked to autoimmunity is common in multiple Mus species and</i> <i>sub-species</i>	101

Discussion.....	103
CHAPTER V. Identification of the <i>Sle1b</i> Gene by BAC-Transgenic Rescue: SLAM/CD2 Members Remain the Strongest Candidates to Mediate Autoimmunity.....	120
Introduction.....	120
Results.....	124
<i>Characterization of BAC 41-Tg lines: B6-alleles of <i>Usp23</i> and <i>Nit1</i> on BAC 41 do not cause a drop in penetrance of ANA-production.</i>	<i>125</i>
<i>Characterization of BAC 47- Tg lines: B6-Ref2bp does not cause a drop in ANA production.</i>	<i>127</i>
<i>Characterization of BAC 25-Tg lines: A modest but consistent drop in ANA penetrance caused by BAC 25, carrying the B6 alleles of SLAM/CD2 family members <i>Cd229</i> (<i>Ly9</i>), <i>Cs1</i>, and <i>Cd244</i> (<i>2B4</i>).</i>	<i>128</i>
<i>Characterization of BAC 40-Tg lines: A significant, but inconsistent, drop in ANA production in the presence of the B6-BAC carrying SLAM/CD2 family members <i>Cd48</i> and <i>Cd150</i> (<i>Slam</i>).</i>	<i>130</i>
<i>Characterization of BAC 95-Tg lines: A mild and inconsistent drop in ANA-penetrance in BAC-Tgs with the B6 alleles of <i>Nicastrin</i>, <i>Copa</i>, and <i>Pxf</i>.</i>	<i>133</i>
<i>Flow cytometric analysis of splenic cell populations in BAC-Tg lines: No obvious differences from the parental B6.<i>Sle1b</i> strain in any group except BAC 95(1254)-Hom</i>	<i>135</i>
Discussion.....	137
CHAPTER VI. Discussion	162
References.....	169
VITAE.....	216

Publications

Limaye N, Belobrajdic K, Chan, A, Wandstrat A, Bonhomme F, Edwards SE, Wakeland EK. Retention of Autoimmune Susceptibility Alleles in Natural Populations. *Manuscript in preparation*.

Nguyen C, Mooney J, Subramanian S, **Limaye N**, Schatzle J, Wakeland EK. Phenotypic characterization of the SLAM family and its impact on lymphocyte activation in *Sle1b* mice. *Manuscript in preparation*.

Limaye N¹, Wandstrat AE¹, Nguyen C¹, Chan AY, Subramanian S, Tian X-H, Yim Y-S, Pertsemlidis A, Gardner, Jr. HR, Morel L, Wakeland EK. (2004) Association of extensive polymorphisms in the SLAM/CD2 gene cluster with murine lupus. *Immunity* 21(6):769-80.
(¹These authors contributed equally to this study)

Limaye N, Mohan C. Pathogenicity of anti-DNA/glomerular autoantibodies - weighing the evidence. *Drug Discovery Today: Disease Models*. *Manuscript in press*.

Nguyen C, **Limaye N**, Wakeland EK (2002) Susceptibility genes in the pathogenesis of murine lupus. *Arthritis Res* 4 (Suppl 3): S255-63.

List of Figures

<i>Multi-step pathway model of autoimmunity</i>	25
<i>Sample output from the sequencing-based SNP assay</i>	54
Figure 1A. <i>Complete BAC contig of the Sle1b interval</i>	77
Figure 1B. <i>Molecular map and tiling path of BACs across Sle1b</i>	79
Figure 2A-B. <i>Sequence alignment of ligand-binding domains of rat/human CD2</i> <i>with B6 and NZW Cd84 and Cd229</i>	82
Figure 2C. <i>Amino acid sequence alignment of Cd244 from B6, and the 4-gene</i> <i>expanded locus in B6.Sle1b</i>	83
Figure 3A-B. <i>Expression of candidate genes in CD4+ T and B cells from B6.Sle1b</i> <i>as compared to B6</i>	84
Figure 4A-B. <i>Haplotype analysis of the Sle1b interval</i>	85
Figure 5. <i>SLAM/CD2 haplotypes found in laboratory and wild-derived inbred strains</i>	88
Figure 6. <i>Analysis of mice congenic for the Sle1b region from NZM2410, 129, and</i> <i>Cast/Ei, on the B6 genetic background</i>	89
Figure 7. <i>Estimated evolutionary distribution and distances between Mus species</i>	108
Figure 8. <i>SLAM/CD2 alleles found in inbred strains from distinct Mus taxa</i>	109
Figure 9. <i>Phylogenetic tree of the Mitochondrial D-loop region</i>	110
Figure 10. <i>Phylogenetic tree of Cd229 Ig domains</i>	111
Figure 11. <i>Phylogenetic tree of Cd48 Ig domains</i>	112
Figure 12. <i>Phylogenetic tree of Cd84 Ig domains</i>	113
Figure 13. <i>Phylogenetic tree of Ly108 Ig domains</i>	114
Figure 14. <i>Phylogenetic tree of Cs1 Ig domains</i>	115
Figure 15. <i>Phylogenetic tree of Cd1501 Ig domains</i>	116

Figure 16A-B. <i>Sequence alignment of ligand-binding domains of rat/human CD2</i> <i>with mouse Cd84 and Cd229 residues under selection</i>	118
Figure 17. <i>Sle1b has an allele-dose effect on ANA production</i>	140
Figure 18. <i>Schematic representation of the BAC-transgenic rescue strategy</i>	141
Figure 19. <i>Breeding scheme used to generate BAC-transgenic rescue test-progeny</i>	143
Figure 20A-C. <i>BAC-41 transgenic lines: Copy number and transgene expression</i>	144
Figure 20D-E. <i>BAC-41 transgenic lines: ANA-penetrance and splenomegaly</i>	145
Figure 21A-B. <i>BAC-47 transgenic lines: Copy number and transgene expression</i>	146
Figure 21C-D. <i>BAC-41 transgenic lines: ANA-penetrance and splenomegaly</i>	147
Figure 22A-C. <i>BAC-25 transgenic lines: Copy number and transgene expression</i>	148
Figure 22D-E. <i>BAC-25 transgenic lines: B6-2B4 expression on NK cells</i>	149
Figure 22F-G. <i>BAC-25 transgenic lines: B6-2B4 expression on CD8+ T cells</i>	150
Figure 22H-I. <i>BAC-25 transgenic lines: B6-2B4 expression on B220+ cells</i>	151
Figure 22J-K. <i>BAC-25 transgenic lines: ANA-penetrance and splenomegaly</i>	152
Figure 23A-C. <i>BAC-40 transgenic lines: Copy number and transgene expression</i>	153
Figure 23D-F. <i>BAC-40 transgenic lines: Cd48 cell surface expression</i>	154
Figure 23G-H. <i>BAC-40 transgenic lines: ANA-penetrance and splenomegaly</i>	155
Figure 24A-D. <i>BAC-95 transgenic lines: Copy number and transgene expression</i>	156
Figure 24E-F. <i>BAC-95 transgenic lines: ANA-penetrance and splenomegaly</i>	157
Figure 25. <i>A comparison of ANA titers in a subset of BAC-transgenic lines</i>	158
Figure 26. <i>A model depicting how SLAM/CD2 members mediate autoimmunity on the</i> <i>B6 genetic background</i>	168

List of Tables

<i>Susceptibility loci identified in human linkage analysis with SLE stratified by symptoms.....</i>	<i>6</i>
<i>Primers used in sequencing-based SNP assays.....</i>	<i>55</i>
Table 1. <i>Primers used for Real-time quantitative PCR.....</i>	<i>61</i>
Table 2. <i>Primers used for PCR-sequencing.....</i>	<i>62</i>
Table 3. <i>Synonymous and non-synonymous SNPs in candidate genes between B6 and B6.Sle1b.....</i>	<i>80</i>
Table 4. <i>Amino acid residue changes between B6 and B6.Sle1b.....</i>	<i>81</i>
Table 5. <i>SNPs analyzed in the haplotype analysis of B6, B6.Sle1b, and the panel of inbred strains listed.....</i>	<i>86</i>
Table 6. <i>Amino acid changes between B6 and multiple autoimmune congenic strains.....</i>	<i>90</i>
Table 7A. <i>List of wild-derived inbred strains.....</i>	<i>106</i>
Table 7B. <i>List of wild, outbred mouse dnas.....</i>	<i>107</i>
Table 8. <i>Codon-substitution (d_N/d_S) analysis of SLAM/CD2 genes and CTLA4.....</i>	<i>117</i>
Table 9. <i>An exon 2 SNP in CTLA4 associated with autoimmunity is prevalent in multiple Mus species.....</i>	<i>119</i>
Table 10. <i>List of BAC-transgenic lines generated and analyzed for rescue of Sle1b.....</i>	<i>142</i>
Table 11A. <i>Flow cytometric analysis of basic cell lineages in BAC-transgenic lines.....</i>	<i>159</i>
Table 11B. <i>Flow cytometric analysis of CD4+ T cell activation in BAC-transgenic lines...160</i>	
Table 11C. <i>Flow cytometric analysis of T and B cell activation in BAC-transgenic lines....161</i>	

Chapter I. Introduction

The autoimmune disorder Systemic Lupus Erythematosus (SLE) is a complex disease characterized by a loss in tolerance to ubiquitous self-antigens, with the production of anti-nuclear autoantibodies (ANAs) to nucleosomal chromatin, ds and ss DNA, as well as a variety of other antigens like ribonucleoproteins and complement components, resulting in autoantibody-mediated tissue injury. Disease pathology can be manifested in a wide variety of symptoms, including rashes, glomerulonephritis (GN), vasculitis, and central nervous system damage. Diagnosis of the disorder is complicated by this heterogeneity in clinical symptoms, and current guidelines require 4 out of 11 disease criteria to be fulfilled in order to classify a patient as having lupus (reviewed in 1). The disease is strongly race and gender-biased, with a female to male ratio of incidence of 9:1, and disease onset usually occurring during the child-bearing years. Incidence is also greater amongst African-American and Hispanic populations than amongst Caucasians (1, 2).

The genetic basis of SLE is borne out by a ten-fold higher concordance rate in monozygotic twins than in dizygotic twins, and by an increased rate of incidence (λ) amongst siblings of affected patients as compared to the general population (2, 3).

SLE as a Single-Gene Effect: Complement and SLE

SLE rarely occurs as a strongly deleterious single-gene defect in humans. Homozygous deficiencies in C1q, C2, and C4, early components of the complement system, cause lupus with a very high penetrance or rate of incidence in individuals who have these inherited defects. The incidence in people with homozygous deficiency of C1q, which is rare and has been recorded and followed in only 42 cases, is greater than 90% (4). C1q is encoded by three genes in tandem on chromosome 1, and a molecular analysis of 12 families showed

that C1q deficiency was caused by single mutations in one of the three genes in each case. While C1q protein was detectable in some, there was no functional C1q activity in any of the cases. Unlike in humans, where complete deficiency in C1q can mediate lupus in a monogenic, almost completely penetrant fashion, the effects of a targeted deletion of C1q in the mouse depend very much on genetic background (5, 6). C1q-deficiency has no autoimmune phenotypes on either the C57Bl/6 (B6) or 129 genetic backgrounds; however, on a mixed 129 /B6 background, which is predisposed to autoimmunity (7), it accelerates anti-nuclear autoantibody (ANA) production and glomerulonephritis (GN), with an increased number of apoptotic bodies observed in the glomeruli of C1q^{-/-} mice, and impaired phagocytosis of apoptotic cells by peritoneal macrophages (8). C1q-deficiency slightly exacerbates disease in the already strongly autoimmune Fas-defective MRL/*lpr* strain, and it has an even greater effect on the mild autoimmunity usually observed in MRL/Mp mice, elevating ANA-production, and causing mortality due to GN (5). Both B6 and MRL mice lacking C1q show splenic monocytosis; in the autoimmune-prone MRL strain, this is also accompanied by splenic hypercellularity, chronic B and CD4 T cell activation, increased splenic plasma cells, decreased marginal zone B cells, and increased total plasma IgM, but not IgG (6).

C4 is encoded by two tandemly duplicated genes in the Class III region of human MHC. This means that there are from two to eight copies in the diploid genome, coding for the C4A and C4B isoforms. A null allele for both occurring together is therefore rare, but of the 28 recorded cases, >75% had SLE (4, 9). Heterozygous mutations in either C4A or C4B are more common (10), and some studies in fact estimate a fairly high incidence of such deficiencies amongst SLE patients of multiple ethnicities (11). Since these C4 deficiencies are linked to certain MHC haplotypes, however, it is difficult to ascertain which of these actually represent susceptibility factors (10). As in the case of C1q, targeted deletions of C4

in the mouse have genetic background-dependent effects (12, 13). On the B6/129 mixed background, C4-deficiency has been associated with ANA production, glomerular immune complex (IC) deposition, GN and splenomegaly as the mice age, as well as elevated activation of T and B cells, and impaired IC clearance from plasma (12). A later study found anti-dsDNA IgM and IgG in C4-deficient B6, (B6X129), and BalbX(B6X129) mixed background mice, but no renal disease accompanying IC deposition on the B6 background (13).

Finally, homozygous C2 deficiency, which occurs more commonly, in about 1 in 20,000 Caucasians, has the lowest incidence of SLE associated with it (about 10%, 4). A common cause of the deficiency, a 28 base-pair deletion, was found to occur more frequently in a group of North American Caucasian SLE patients than in controls, but the deletion was not found in African-American patient or control groups (14), reflecting the heterogeneity in predisposing genetic factors in different ethnic groups often observed in SLE.

The exacerbating effects of complement deficiencies on autoimmunity seem counter-intuitive, as antibody-mediated damage is often thought to be caused by immune complex deposition followed complement-fixation (10). Complement components may be protective against autoimmunity due to their role in clearing immune complexes and apoptotic cells and debris effectively so that they are not presented as antigens in the context of injury or inflammation where they may trigger autoimmunity (10), and their ability to regulate potentially autoreactive B cells by enhancing self-antigen presentation to immature B cells, which get negatively selected as a result (15).

SLE is a Complex, Multigenic Disease: Multiple loci are linked to susceptibility in humans

As is evident from these reports on complement-deficiency mediated SLE, strongly deleterious, single-gene deficiencies account for a very small proportion of the affected population in humans. The genetic factors that more commonly mediate susceptibility to lupus have been hard to elucidate, due to the fact that it primarily occurs as a complex, multigenic disease. Combinations of multiple, polymorphic genes act in concert to cause the phenotypes associated with SLE. In addition, amongst the heterogeneous human population, the same host of symptoms can be caused by different sets of genes. For both these reasons, contributing genes may not have very strong individual effects on the overall outcome of disease pathology, making them hard to detect in the context of whole-genome scans of patient populations. Added to this, environmental and stochastic processes seem to play an important role in lupus: even in genetically identical inbred strains of mice harboring lupus-susceptibility loci, the autoimmune phenotypes mediated by these genes are invariably incompletely penetrant. Thus, even individuals harboring the necessary genetic susceptibility factors may show attenuated, or even no disease phenotypes, weakening our ability to detect them. Despite these difficulties, a large number of loci have been linked to susceptibility to SLE in whole-genome linkage studies, in which microsatellite markers (repeat-length polymorphisms) across the entire genome are tested for the association of certain alleles with disease, i.e., the enrichment of specific alleles in affected patients as compared to unaffected relatives. These genome scans, usually done on families with at least two affected siblings, and sometimes including an extended pedigree of affected and unaffected family members, are followed by more detailed candidate gene analyses including transmission- disequilibrium testing (Tdt) and case control studies on certain genes within the implicated intervals.

Nine large-scale genome-wide screens have been carried out, which point to more than 50 different loci, about 15 of which are significantly linked to SLE susceptibility; these are discussed below. Lupus-linked loci on chromosome 1 include **1q22-24** (16, 17, 18), which contains the Fcγ receptors for IgG-immune complexes, the acute phase C-reactive protein (CRP) and Serum Amyloid P component (SAP) , and the SLAM/CD2 family of immunoregulatory receptors; and **1q41-42** (16,17, 19; supported by data from 20 and 21, and confirmed by 22, 23). Tsao et al (24) found transmission disequilibrium of an 85 base pair (bp) allele of a polymorphic repeat-length marker in the 5' region of the poly ADP ribose polymerase gene (PARP), which plays a role in DNA repair and apoptosis, making it a good candidate in the region. The association was not, however, reproducible by multiple groups, suggesting the gene may actually lie centromeric to PARP (25). These chromosome 1 loci correspond to the *Sle1a*, *b*, and *d* regions, which are associated with autoimmune-susceptibility in the NZM2410 spontaneous murine model of lupus (26).

On chromosome 2, the **2q37** region has been associated with lupus-susceptibility in Icelandic and Swedish families (27), and a region at **2q33** has recently been identified amongst Caucasian American families (18). Other chromosomal loci implicated include **4p15-16** (28, 27, 16); the HLA, C4 and TNF-α containing **6p11-22** (20, 21), and **16q12-13** (20, 21, 18), which harbors the NOD2 LPS-response gene, associated with susceptibility to Crohns disease (29). In a recent study, **17p12-q11** was associated with lupus in Argentine families (30), and on the same chromosome, **17q21-23** has also been linked to the disease, primarily in non-Caucasian American families (18). Other new loci emerging from recent studies include **3p24**, **10q23-24**, **13q32**, **18q22-23** (18), and **12q24** (31). Several more loci than are listed here, it must be emphasized, have been detected in these studies, albeit more weakly; the duplication of some of these in multiple studies indicates that they may indeed harbor genes that contribute to autoimmunity.

Disease heterogeneity can be a major complicating factor in detecting regions contributing to SLE in whole genome-scans: the disease represents a wide variety of symptoms which may in fact have different etiologies, which may be hard to detect when they are grouped together under one banner. Numerous loci associated with autoimmunity have recently been uncovered by analyzing the genetic basis of lupus stratified by its specific symptoms. The pedigrees used in these studies included African American, European American and Hispanic families. A list of the loci linked to disease in patients stratified by symptoms, is given in tabular form below. Included are the categories used to stratify disease, the implicated loci, and ethnicity of the pedigrees for which the associations were found, if they did not apply to all racial groups(AA : African American, EA : European American).

Renal disease	2q34-35 (AA), 11p15.6 (AA), 10q22.3 (EA)	32
Thrombocytopenia	1q22-23 , 11p13 (AA)	33
Discoid lupus erythematosus	11p13 (AA)	34
Hemolytic anemia	11q14 (AA)	35
Vitiligo	17p13 (EA)	36
Rheumatoid arthritis	5p15.3 (EA)	37, confirmed by 38
dsDNA	18q21.1 (AA), 19p13.2 (EA)	39
Anti-nucleolar Abs	11q14 (AA)	40
Neuropsychiatric symptoms	4p16 (EA)	41

A striking observation made by reviewers of the field, is that the susceptibility loci linked to multiple complex autoimmune diseases including type 1 diabetes (T1D), rheumatoid arthritis (RA) and SLE, often cluster together at certain chromosomal regions

(reviewed in 3, 42). This may be due to common genes conferring susceptibility to pathogenic processes common to multiple autoimmune diseases, as in the case of PTPN22, which is associated with risk to T1D, RA, and lupus (43, 44, 45,46), or CTLA4, which is associated with T1D, autoimmune thyroiditis, and Graves disease (reviewed in 47, 48). Alternatively, it could reflect the presence of functionally related groups of genes that are grouped within these intervals and play roles in dysregulating related pathways in the different disorders, as in the case of the Major Histocompatibility Locus (MHC). The region harbors numerous immunologically relevant genes involved in antigen processing and presentation, along with genes like TNF α and HSP70 in close linkage, such that it difficult to distinguish between their various effects on diseases including lupus, RA and T1D (49).

Polymorphic genes associated with SLE in human studies, with supporting evidence from synthetic mouse models of lupus

Whole genome scans followed by candidate gene analyses have yielded a variety of genes that have been associated with lupus. The associations are often inconsistent in different populations, and sometimes even within the same population, reflecting the heterogeneity of the disease in humans. Support for their role in autoimmunity comes in the form of functional or mechanistic studies that explain how they may mediate disease, and from synthetic mouse models, in which autoimmunity is caused by targeted deletion or transgenic overexpression of these same genes.

The MHC and lupus

The major histocompatibility (MHC) genes lie in the human leukocyte antigen (HLA) region, spanning about 3.6 Mb at 6p21.3 (50), a region that has shown linkage to SLE (20, 21). There is some evidence that certain alleles of the highly polymorphic class II MHC DR

and DQ genes may be associated with lupus susceptibility. The most consistent, but modest, associations are with the DRB1 alleles DR2 (DRB1*1501) and DR3 (DRB1*0301) in white populations, although the association has not been consistent in other ethnic groups. Strong linkage disequilibrium makes it hard to distinguish between the effects of MHC and other tightly linked genes within this region, like TNF- α and C4, null alleles of which have also been associated with SLE (1, 51, 52). Graham et al (51) used dense microsatellite mapping across the HLA region in an effort to do just this, and identified three risk-associated haplotypes that showed transmission disequilibrium in SLE families and were present significantly more frequently in patients than in case controls. Again, this was in Caucasian populations. The DR2 /DQ6 and DR8/DQ4 haplotypes could be narrowed down to include primarily just the class II region, but the DR3/DQ2 haplotype, associated with the highest risk, formed part of the extended HLA A1-B8-DR3 haplotype, which could not be narrowed further due to strong linkage disequilibrium. This haplotype contains the TNF-308A and C4-null alleles that are linked to SLE in other studies, making it hard to distinguish as yet between the effects of these genes and class II MHC in mediating susceptibility (1, 53, 54).

TNF- α and TNFR2

Polymorphisms in TNF- α , within the class II MHC region, as well as TNFR2, its high-affinity receptor in the 1p36 locus, have been associated with SLE, somewhat inconsistently. The important role of TNF- α in inflammatory and apoptotic immune processes (55), and correlations between levels of TNF α and its soluble receptors and SLE disease activity (56, 57), make both potential candidate genes within their respective intervals. A single nucleotide polymorphism (SNP) in the TNF α promoter region (TNF 308G/A) has been associated with SLE, most often in Caucasians (58, 59, 60), but also in African Americans in one study (61). Other studies, however, have failed to detect the

association in Caucasians (62, 63, 64), as well as other ethnic populations (62, 64, 65). This SNP is thought to affect transcriptional regulation of the gene by modifying a transcription factor binding site, with the susceptible allele increasing transcriptional activity (as reviewed in 66); although other groups have found no effect of the SNP on transcriptional binding and activity (67). Thus, it remains unclear whether it represents a risk factor, or has been associated with lupus due to its previously-discussed linkage with other genes. The association between the 196R allele of TFR2 (TNFR2 196M/R) was found in Japanese SLE patients in two different studies (68, 69), but not in a third (70). The association has not been observed in Caucasians (63, 71) or in Vietnamese patients (72), although this could simply reflect differences in genetic susceptibility between various populations.

PTPN22

Two studies on three independent cohorts have found an association of PTPN22 (protein tyrosine phosphatase non-receptor 22) with SLE in Caucasians (45, 46). The gene is located in the 1p13 region, which has been linked weakly with susceptibility (20). The phosphatase has been found to be important in downregulating T cell receptor signaling in effector/memory T cells, and mice deficient in its ortholog PEP (PEST Domain-Enriched Tyrosine Phosphatase) exhibit an enhanced number and function of effector/memory T cells, spontaneous development of germinal centers with splenomegaly, and elevated levels of serum IgG1, IgG2a, and IgE, although there is no increase in ANA or anti-ds or anti-ss DNA antibodies (73). The particular SNP associated with disease results in an amino acid change from arginine to tryptophan (PTPN22 620 R/W; 45, 46) in the SH3-binding domain, and has been found to be important in binding to Csk (C-terminal Src tyrosine kinase; 43), association with which is important in PEP's inhibitory function (74).

PD-1

Another molecule that plays a role in the inhibition or downregulation of T cell responses, programmed cell death-1 (PD-1 or PDCD-1), has also been associated with lupus susceptibility in humans. Fine mapping of the 2q37 locus linked to SLE in Nordic families (27) was carried out to narrow down the interval (75), revealing the presence of PD-1 as a strong candidate gene. PD-1 is a transmembrane protein with an immunoreceptor tyrosine-based inhibitory motif (ITIM: V/I X Y XX L) in its cytoplasmic region. Upon engagement with its ligands PD-L1 and PD-L2, which are expressed on non-lymphoid tissues and APCs, it results in the attenuation of B and T cell receptor-induced signaling by recruitment of the protein tyrosine phosphatase SHP-2 (reviewed in 76). An intronic SNP in the gene (PD1.3 G/A) has been associated with SLE susceptibility in Swedish, European American and Mexican groups (77). An oligonucleotide containing the susceptibility allele (A) of the SNP was shown to bind the runt-related transcription factor (RUNX or AML-1) less efficiently in electromobility shift assays (EMSA), and it has been hypothesized that this modification of an enhancer binding element may be the mechanism by which it mediates susceptibility to SLE (77). Support for this hypothesis comes from studies relating regulatory SNPs in RUNX-binding regions to susceptibility to two other autoimmune diseases, RA (78) and psoriasis (79). Following this, two other groups also found an association between PD-1 and SLE, but neither was able to replicate the association with this particular SNP. Instead, one group (80) identified another intronic SNP (6867 C/G), located in a potential binding-site for a transcriptional repressor as being significantly associated with disease in Danish Caucasians. Another study on a large Spanish cohort actually found the G, rather than the A, allele of the PD1.3 SNP associated with lupus-susceptibility (81). While different alleles or SNP-haplotypes of the PD-1 gene could well be mediating susceptibility in different ethnic populations, it is unlikely that the two possible alleles of the same SNP are each causative of

disease in different populations. The data do support a role for the gene in lupus, although the specific “autoimmune” alleles, and the functional or mechanistic basis for their association, will require further investigation. A targeted deficiency in the gene causes late-onset autoimmunity in B6 mice, including GN with C3, IgG3 and IC deposition, proliferative arthritis, mild splenomegaly and increased responsiveness of B cells to stimulation. The mice also show impaired T cell self-tolerance (82, 83). The addition of the *lpr* mutation of the Fas gene accelerates and exaggerates these phenotypes (82). In BALB/c mice, on the other hand, the autoimmunity observed is cardiac-specific, with the mice developing dilated cardiomyopathy with high titers of circulating antibodies against a cardiomyocyte-specific protein (84).

CTLA4

The association of CTLA4 with lupus has been inconsistent, although it lies within an interval linked to autoimmunity (2q33, 18), and is certainly a good candidate gene to mediate lupus susceptibility, having been associated with susceptibility to other autoimmune disorders including T1D, autoimmune hypothyroidism and Graves disease (47, 48). More than ten studies have investigated the association of four SNPs (-1722T/C, -1661A/G, -318C/T and +49G/A) in the 5' promoter region and exon 1 of CTLA4 to SLE in a wide variety of ethnic populations; their findings are detailed in a recent study by Parks et al (85). Only two have shown an association with the most widely studied of these polymorphisms, +49G /A, usually studied in conjunction with the -318C/T SNP, and two with the -1722 T/C promoter region SNP, findings which have not been replicated in any of the other studies, including the recent one by Parks et al (85). An association between a dinucleotide AT repeat polymorphism in the 3'UTR of the gene has also been found (86, 87), while a recent study found an association between a different SNP in the 3' region (CT60 A/G), but failed to find an association with

the repeat marker (88). The 3`repeat has been found to form a haplotype with the exon 1 polymorphism, and may also be linked to the CT60 SNP, as alleles at these three loci seem to go together (88, 86) . It is therefore possible that inconsistencies in the association studies arise from differences in the occurrence or prevalence of certain *haplotypes* of these CTLA4 polymorphisms amongst various groups, and studies investigating their association (rather than that of individual SNPs) with disease, may yield more promising results.

IL-10

Polymorphic haplotypes of the IL-10 promoter region that are associated with increased IL-10 production have been associated with SLE in African-American, Chinese, and Vietnamese patients (89, 90, 72). Supporting its role in disease pathogenesis, serum levels of the cytokine have been correlated with disease activity (91, 92), and levels of IL-10 production by monocytes and B cells are elevated in first and second-degree relatives of SLE patients (93). Increased IL-10 production may in turn play a role in B cell hyperactivity and autoantibody production, as evidenced by the finding that recombinant IL-10 greatly increases spontaneous IgM and IgG production by SLE peripheral blood mononuclear cells (PBMCs), while anti-IL10 mAbs can inhibit the *in vivo* production of anti-dsDNA autoantibodies by SLE PBMCs injected into SCID mice (94). SLE PBMCs have been found to proliferate less in response to stimulation by irradiated allogeneic dendritic cells (95). Within the patient group, serum levels of IL-10 were found to be higher amongst the poor responders, and the addition of blocking anti-IL10 antibodies increased their proliferative response. In addition, the presence of IL-10 in SLE PBMC supernatants correlated with the ability to inhibit the allogeneic proliferative responses of normal PBMCs (95). This effect of IL-10 seems to occur due to the resulting downregulation of IL-12 production (95). Finally, administration of anti-IL-10 monoclonal antibody (mAb) to SLE patients was found to

improve disease symptoms and reduce steroid dependence in five cases (96), making it a good example of how the implication of molecules or immunologic pathways in disease pathogenesis can be of value in providing us with therapeutic targets.

Activating and Inhibitory FcγRs

The FcγRs consist of a set of stimulatory and inhibitory receptors for IgG, with varying affinities for the different isotypes, and different signaling properties upon ligand binding (reviewed in 97). The activating high-affinity IgG FcγRI and intermediate-affinity FcγRIIIa and b (and the low-affinity FcγRIIa and c, absent in the mouse) modulate a variety of immune functions including immune-complex clearance, antibody-dependent cellular cytotoxicity (ADCC), phagocytosis, and the release of cytokines, reactive oxidants and proteases by phagocytes. The inhibitory low-affinity FcγRIIb receptor can downregulate cell signaling, and negatively regulate antibody production and immune-complex mediated activation (97). This is one example of receptors with similar ligand-specificities but different, even opposing, cytoplasmic signaling components and effects, a dysregulation in the balance between which can, in certain genomic contexts, contribute to susceptibility to immunological diseases. The receptors lie in the 1q23 region, which has consistently been linked to lupus in humans, and which harbors numerous other promising candidate genes emerging from studies on murine models of lupus, including the SLAM/CD2 family and the complement receptor Cr2.

The 131H/R polymorphism of FcγRIIa and the 158V/F polymorphism of FcγRIIIa are the most widely studied of the FcγR polymorphisms associated with autoimmunity. The susceptibility alleles of these receptors (R and F, respectively) lower their binding affinity for IgG2, and IgG1 and 3 respectively (98, 99), which can affect the ability to clear immune complexes (100). Another commonly studied polymorphism is the FcγRIIb NA1/NA2,

encoding the HNA1a and 1b products respectively. While these don't show a difference in binding affinity, neutrophils carrying the NA2 susceptibility-allele have a lower FcγR-phagocytic response, which may be due to a weaker oxidative burst and degranulation response (101, 102). The association between these FcγR polymorphisms and lupus is somewhat inconsistent across the numerous studies done in various populations (reviewed in 97). Many have found associations with specific clinical features, rather than an overall association with the disease. This would seem to suggest that, in some groups, rather than constituting strong, independent risk factors, the FcγRs influence disease course and outcome (103, 104, 105, 106). In Swedish and Mexican patients, a haplotype consisting of both the FcγRIIa and IIIa alleles was found to be the risk factor (107, 108), and recently, a SNP in the inhibitory FcγRIIb (232 I/T) has been found to confer susceptibility in three different East Asian populations (109, 110, 111), although its mode of effect is not yet clear.

Support for the role of FcγRs in immune regulation and autoimmunity comes from mice deficient in the activating or inhibitory receptors. Targeted deletion of the common γ chain abolishes the expression of the activating FcγRI and FcγRIII, and has an ameliorative effect on autoantibody-triggered experimental hemolytic anemia and thrombocytopenia (112). The deletion on the spontaneously autoimmune (NZB X NZW) F1 background reduces GN disease severity despite the presence of ANAs and IC deposition (113), and mice without these activating receptors are protected from anti-glomerular basement membrane (GBM)-induced GN and experimental antigen-induced arthritis (114, 115). These data support a role for these receptors in the effector phase of disease, and end-organ damage, rather than disease initiation.

Certain autoimmune-prone strains of mice (NOD, NZB, BXSB and MRL) have been shown to have reduced levels of the inhibitory FcγRIIb on their activated and germinal-center B cells, associated with a deletion polymorphism in the promoter region of the gene (116,

117). In addition, deletion of the Fc γ RIIb gene can result in spontaneous lupus-like disease in mice, but this effect is background-specific (118). Knockout mice on the B6 genetic background produce ANAs with H2A/H2B/DNA subnucleosomal specificity. They have splenomegaly with high numbers of plasma cells and germinal centers, indicative of chronic immune activation, and multi-organ inflammation, including immune-complex mediated GN and vasculitis. Kidney damage causes proteinuria by about 4-5 months of age, and by 8-10 months, they have increased B and T cell activation markers, and increased mortality. These autoimmune phenotypes, however, are not at all evident on the Balb/c background (118). Retroviral-transduction mediated increases in the level of expression of the receptor on a proportion of B cells can ameliorate autoimmunity in B6.Fc γ RIIb-deficient mice, as well as in the low Fc γ RIIb-expressing NZM2410 and BXSB strains (119), perhaps due to its role in holding the accumulation of autoreactive plasma-B cells in check (120).

CRP and SAP

The acute phase C-reactive protein lies within the same susceptibility locus as the Fc γ Rs. A SNP within the gene's 3' region (CRP4 G/A) was recently shown to be in transmission disequilibrium in SLE, in a study that predominantly included European Caucasian families, but also small numbers of families of other ethnicities (121). The SNP was also associated with the presence of ANAs in patients and their siblings, and was one of two SNPs shown to independently contribute to lower basal serum levels of CRP (121). CRP binds to nuclear antigens including chromatin and snRNP that play an important role in SLE pathogenesis, and can also interact with apoptotic cells, a possible source of nuclear antigenic material. It can activate the complement cascade, and binds Fc γ Rs, which would make it possible for phagocytic cells to engulf CRP-associated material, contributing to the clearance of immune complexes. CRP has, in addition, been shown to reduce immune responses to the

molecules it binds (reviewed in 122, 123). Thus, polymorphic variants of the gene that cause lower expression levels could certainly contribute to autoimmune susceptibility. In mice, CRP is only present in trace amounts in the serum, and is minimally elevated in the acute-phase response. A study by Szalai et al (124) showed that in the (NZB X NZW) F1 spontaneous murine model of autoimmunity, the expression of a human transgene for CRP delayed the onset and reduced the severity of renal disease, supporting a protective role for CRP in autoimmunity. While serum levels of anti-dsDNA IgM were only transiently reduced, and IgG levels actually increased, kidney deposition of IgM and IgG were much reduced. The CRP transgene, which consisted of genomic DNA for the CRP gene as well as 17 kb of the 5' and 11 kb of the 3' flanking sequence, was found to be expressed in the kidney in these mice, suggesting that its protective effect may be exerted locally (124).

Serum Amyloid P component (SAP) lies adjacent to CRP in both mouse and humans, and it is the major acute phase protein in the case of the mouse. It shares many similarities with CRP, including a large degree of nucleotide identity, the ability to bind nuclear material and late apoptotic cells, interaction with complement and the Fc receptors (reviewed in 125, 123). Support for a role for CRP/SAP in autoimmunity comes from mice deficient for SAP, which show an increase in the ANA production already observed in the mixed B6/129 background strain, as well as GN in females (126). ANA production is also observed on the B6 genetic background, but the deficiency fails to cause any autoimmunity in 129 mice (127). SAP has been shown to reduce the degradation of chromatin both *in vivo* and *in vitro*, suggesting that it functions to decrease the immunogenicity of the autoantigen in this manner (126). The expression of transgenic human SAP on the SAP-deficient B6 background, however, fails to rescue the autoimmune phenotype (127). Finally, the study that found an association of CRP with lupus in humans, also examined three SNPs identified in the SAP gene, but failed to find any association with autoimmune susceptibility (127).

Most of the polymorphisms associated with susceptibility to lupus in humans probably hold true only in certain populations, given the heterogeneity inherent in human genes and in the disease; added to these are variations in the experimental and statistical parameters employed in different studies. Therefore, it is not surprising that data on many candidate genes being studied for their association with lupus are not completely consistent. Precise mechanistic or functional links between these susceptibility alleles and the autoimmunity they mediate would strengthen their case greatly, but these are lacking in many cases. Even in their absence, however, such studies certainly provide us with insights into the pathways which regulate normal immunity which, when dysregulated, have pathogenic outcomes. These provide us with many potentially useful therapeutic targets, which can be modulated to counter the deleterious effects of the primary disease genes.

Synthetic Mouse Models of Lupus

Synthetic mouse models of lupus provide us with another very useful source of information on the pathways and checkpoints which, when perturbed, potentiate autoimmunity. In these models, aberrant expression of genes (in knockouts or transgenics) can cause or exacerbate autoimmune phenotypes. Such synthetic models are numerous, and while the specific genes they implicate are not necessarily involved in spontaneously occurring SLE, they do tell us much that is useful about the pathogenic mechanisms involved in disease, and provide us with additional therapeutic targets.

One class of genes that has been implicated by synthetic mouse models are those involved in the appropriate handling and clearance of apoptotic material. These include the C1q, C4, SAP, and common Fc γ chain knockouts described earlier, as well as mice with

deficiencies in the nuclease Dnase1 (128) and the membrane tyrosine kinase c-mer, which indirectly binds phosphatidylserine (PS) on apoptotic bodies (129). Mice lacking the protein Ro, found bound to small RNAs in cells, also develop lupus-like autoimmunity along with sensitivity to UV irradiation when on the B6 background, presumably because of defective sequestering of the ribonucleoprotein antigens from the immune system (130).

A second class of genes is involved in B and T cell apoptosis, and perturbations in their expression cause potentially autoreactive lymphocytes to escape cell death and accumulate, allowing them to do damage. Deficiencies in the expression or function of the FAS and FAS-L genes in the form of the *lpr* and *gld* mutations respectively, or in FAS-null mice, cause lymphoproliferation with an accumulation of CD4-CD8- double negative T cells, splenomegaly, lymphadenopathy, autoantibody production, and lymphocyte infiltration and end organ damage (131, 132, 133, 134). Transgenic mice overexpressing the anti-apoptotic molecule bcl-2 in B cells on the mixed B6/SJL genetic background also develop lupus-like autoimmunity, due to prolonged B cell survival (135), and conversely, targeted deletion of the pro-apoptotic Bim molecule also leads to increased cell survival, with an accumulation of CD4-CD8- thymocytes, ANA production, and GN (136). Mice transgenic for IEX-1 (Immediate Early response gene X-1; 137), and those deficient for TSAd (T cell-specific adaptor protein; 138) develop lupus-like phenotypes due to impaired T cell apoptosis. The PI3K/Akt pathway is implicated in the development of the lupus by the autoimmune phenotypes observed in mice that are heterozygous for a deletion of the phosphatase Pten, an inhibitor of the pathway which causes an impairment in Fas-mediated apoptosis (139), and in mice transgenic for an active form of PI3K expressed in their T cells, which results in a reduction in spontaneous apoptosis (140).

Aberrant expression of genes like PTPN22, PD-1, and FcγRIIb, described earlier, which modulate immune cell activation and affect their proliferation or function, can also contribute to autoimmunity. This third group includes surface receptors and ligands, as well as their downstream signaling partners. Thus, mice transgenic for Blys (B lymphocyte stimulator, or TALL-1/BAFF), are rendered autoimmune due to the survival and inappropriate proliferation of B cells (141), and lupus-like phenotypes are also observed in mice deficient in TACI (transmembrane activator and calcium modulator and cyclophilin ligand), an inhibitory receptor for this molecule (142). Decay accelerating factor (Daf) deficiency exaggerates autoimmunity on the MRL/lpr genetic background, with the mice exhibiting dermatitis along with the other lupus-like phenotypes (143), and the overexpression of CD40L on B cells causes ANA production and GN in a fraction of the transgenics (144). Intracellular signaling molecules, the absence of which cause autoimmunity, include the Src tyrosine kinase Lyn (145), PKCδ, a member of protein kinase C family (146), and Gadd45a, a component of the p53 pathway (147).

Several additional genes are also included in each of these groups, indicating that the fine balance between appropriate immune surveillance and inappropriate responses to self is maintained by numerous checkpoints, the disruption of any of which can potentiate autoimmunity.

Spontaneous Mouse Models of SLE

In addition to the numerous synthetic models of lupus, certain strains of mice spontaneously develop disease-phenotypes that resemble human lupus. While there are variations in the specific phenotypes observed in the different lupus-prone strains, typically these models exhibit high levels of ANAs, splenomegaly and lymphadenopathy, and

immune-complex mediated GN (1, 2). The commonly used spontaneous mouse models of SLE include the MRL/*lpr* strain, in which the autosomal recessive mutation in the FAS gene disrupts apoptosis of B and T cells, causing autoimmunity on the MRL genetic background, and the BXSB/*Yaa* strain, in which the unidentified Y-linked autoimmune accelerator gene (*Yaa*) causes severe autoimmunity only in males, uncommon in human lupus. Other models include the (NZBXSWR) F1 (SWF1), the (NZB X NZW) F1 (BWF1), and the NZM/Aeg2410 recombinant inbred strain derived from this cross (1, 2).

In all of these models, pathogenicity is mediated in a complex, multigenic fashion, as in humans, making it challenging to dissect the genetic basis of their autoimmunity. Unlike in the human system, however, these mice are inbred and therefore genetically identical, and, in addition, amenable to genetic manipulation in the form of prescribed mating schemes with lupus-resistant strains. This makes linkage analysis easier to carry out in this system, where it is a powerful and sensitive tool. Studies that follow the inheritance of repeat-length polymorphisms in autoimmune versus non-autoimmune offspring in crosses between these lupus-susceptible and resistant strains like C57Bl/6 (B6) have yielded numerous loci, many of which, strikingly, cluster around telomeric chromosome 1, the middle of chromosome 4, and on chromosomes 7 and 17 (reviewed in 42, 148).

The loci identified in linkage analyses typically have a 95% confidence interval of about 20-25cM or more, and contain hundreds of genes. The functional identification of disease-genes and the pathways they are involved in requires a narrowing of the list of candidates to a more manageable number, as well as some understanding of the manner in which the locus contributes to autoimmunity, i.e., the component phenotype that it mediates. Congenic dissection is a powerful approach used for just this purpose. It involves the introgression of individual susceptibility loci from an autoimmune strain, onto a non-

autoimmune genetic background, allowing for the identification of the specific phenotypes associated with each locus in isolation from the others. The use of marker-assisted selection, in which the purity of the genome is followed using repeat-length polymorphisms between the parental strains, reduces the number of generations required to obtain the desired congenic: mice that retain the locus of choice from the autoimmune parent, with the least amount of contamination from it in the rest of the genome, are the ones selected for further mating back to the resistant strain. In this manner, a congenic is obtained that carries one autoimmune-associated interval, but is otherwise identical to the resistant strain, and the complex disease is broken down into its individual component phenotypes. Further recombinant analysis and fine mapping are used to narrow the susceptibility interval down to a reasonable size, and finally, the genes within are assessed for their candidacy.

Linkage analysis and congenic dissection in the NZM2410 model of autoimmunity

The congenic dissection approach has been used very effectively on the NZM2410 model of lupus, a recombinant inbred strain which derives about 75% of its genome from the New Zealand White (NZW) strain, and 25% from New Zealand Black (NZB). It develops splenomegaly, expansion of CD4 T and B cells, high titers of ANAs, and GN with about an 85% penetrance by 12 months of age, in both males and females (149, 150). Linkage analysis performed on backcross (BC1) progeny between (NZM X B6) F1 X NZM mice, revealed the presence of multiple loci that potentiate autoimmunity when homozygous for the NZM allele. These include *Sle1* on chromosome 1, *Sle2* on chromosome 4, and *Sle3* on chromosome 7, with an additional locus in the H2 region on chromosome 17, for which GN susceptibility was associated with heterozygosity rather than homozygosity for the NZM allele (151). *Sle1* and *Sle3* are both derived from the NZW parental strain of NZM2410, while *Sle2* is a recombinant, 60% of which is derived from NZW, and 40% from NZB (152). Additional loci

were revealed in further linkage analyses examining the inheritance of GN and a variety of serological phenotypes in (NZM X B6) F2 progeny, and the chromosome 7 *Sle3* locus was found to correspond to two independent loci, the more distal *Sle3* and proximal *Sle5* (153).

The production of congenic strains carrying each of the NZM-loci on the B6 background, B6.NZMc1 (B6.*Sle1*, with NZM-derived *Sle1* on the B6 background), B6.NZMc4 (B6.*Sle2*) and B6.NZMc7 (B6.*Sle3*, 5), allowed for a functional analysis of this lupus model (154).

Sle1 causes a break in tolerance to chromatin, and B6.*Sle1* congenic mice have splenomegaly (155) and produce anti-nuclear antibodies with specificity for H2A/H2B/dsDNA subnucleosomes, with about a 75% penetrance in both sexes by 7-9 months of age, although the onset of the phenotype is earlier in females (156). They have an elevated percentage of CD4⁺ T cells expressing the activation marker CD69 and B cells expressing B7.2. Their T cells exhibit reactivity to core histones, and their B cells spontaneously produce anti-H2A/H2B/dna IgG. They don't, however, exhibit any obvious lymphocyte hyperactivity or differences in apoptosis, making this phenotype quite specific (156). The abnormalities caused by the locus are intrinsic to both the B and the T cells (157, 158). Despite the presence of ANAs, this locus by itself is not sufficient to cause full-blown pathogenicity. Its importance in initiation of the disease that culminates in mortality due to GN, however, is exhibited by the fact that bicongenic mice carrying *Sle1* with either *Sle2*, *Sle3* or the BXSB-derived male-specific *Yaa* gene on the B6 background, have fatal GN with varying penetrance, whereas combinations of any of the other loci does not have such an effect (159).

Sle2 causes spontaneous B cell hyperactivity, thereby serving to amplify the autoimmune response initiated by *Sle1*. Splenic B cells in B6.*Sle2* mice are increased, and

have an activated phenotype. They also have an increased percentage of CD23^{low}, probably immature, B cells in the spleen, a reduced percentage of mature B cells in the bone marrow, and expanded splenic and peritoneal B1a populations as they age. B6.*Sle2* B cells are hyper-responsive to stimuli *in vivo* and *in vitro*, and their spontaneous hyperactivity is reflected in the higher serum levels of polyclonal, polyreactive IgM (160).

The *Sle3* locus affects the T cell compartment, and B6.*Sle3* mice have an elevated ratio of CD4⁺: CD8⁺ T cells in both spleen and lymph node early on, and an increase in activated CD4⁺ T cells and diffuse spleen architecture as they age. They exhibit increased T-dependent immune responses, and their T cells have stronger *in vitro* proliferative and reduced apoptotic responses to stimulation. As they age, their B cells also become activated, and this activation is reflected in elevated levels of polyclonal IgG and IgM, and low grade ANAs in their serum. The incidence of severe GN in this strain in isolation is about 18%, although in combination with *Sle1*, *Sle3* causes severe GN with a high penetrance, especially in females, where over 90% have severe GN by 12 months of age, with a mortality of about 40% in males and 60% in females by this time (154, 155, 161).

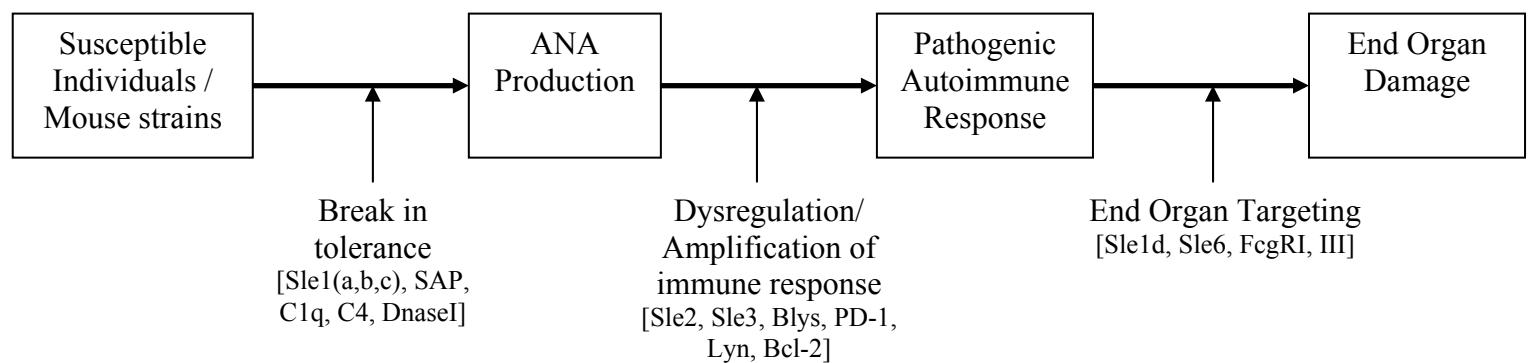
In this manner, each of the loci identified by linkage in the NZM2410 models contributes a different, but important aspect of the overall phenotype, together mediating highly penetrant, severe lupus. Their reconstitution of the autoimmune phenotype has actually been shown by putting all three loci together in a tri-congenic strain on the B6 background, which exhibits severe autoimmunity, and fatal GN (159).

The importance of epistasis in autoimmunity

Although the NZW parental genome contains both *Sle1* and *Sle3*, and part of *Sle2*, it shows only very mild autoimmunity, with some anti-ss DNA autoantibody production, and Ig deposition in glomeruli at an advanced age, but no nephritis (162). This indicated the

presence of autoimmune-suppressive genes in the genome of this strain, and linkage analysis performed on (B6.*Sle1* X NZW) F1 X NZW backcross progeny identified four suppressive loci, *Sles* (SLE suppressors) 1-4, on chromosomes 17, 4, 3, and 9 respectively, and two enhancers, *Sle3*, and the novel locus *Sle6* on chromosome 5, associated with nephritis (163). Bicongenic analysis further has shown that *Sles1* specifically suppresses *Sle1* but not *Sle2* or *Sle3*, and is sufficient to shut down the autoimmunity in (B6.*Sle1* X NZW) F1 mice. The locus lies on chromosome 17, in the complement region of the MHC, and accounts for the original linkage to NZM-heterozygosity for the H2 region (163). Genetic dissection of this model demonstrates that autoimmunity is the result of complex epistatic interactions between numerous loci with enhancing and suppressive effects, acting together. Thus, NZW, despite carrying all the susceptibility intervals required, does not exhibit any pathology, due to the additional presence of suppressor loci like *Sles1* (163). Interactions of these susceptibility loci, each of which is fairly innocuous in isolation, however, leads to severe, penetrant GN in tri-congenic B6.*Sle1/2/3* mice, which lack the suppressive modifiers present on the NZW background (159). Epistasis accounts for the fact that the highly autoimmune BWF1 and NZM2410 models result from interactions between genomic regions from the very mildly autoimmune parental NZW and NZB strains. The numerous synthetic mouse models described that show strong genetic background effects also, in fact, point to the importance of epistasis in autoimmunity, and additional examples of the phenomenon include the interaction of *Sle1* with *Yaa* (159), and with the *lpr* mutation in FAS (164).

The work described here allows us to propose a multi-step model of autoimmunity, as shown in the following figure, adapted from (1):



In this model, Pathway 1 leads to the initial loss in tolerance to nuclear antigens, and is mediated by genes like *Sle1*, *FcγRIIb*, *SAP*, *C1q* and *Dnase1*, which are involved in antigen clearance or the modulation of lymphocyte interactions and the nature of their responses to antigen. Pathway 2 serves to amplify the autoimmune response by dysregulating various components of the immune system. It involves genes like *Sle2* and *3*, *Blys*, *Fas* and *FasL*, and *Bcl-2*, which impact activation and function, proliferation or apoptosis. Finally, Pathway 3 targets end organs like the kidney for damage, and includes genes that may exert a local inflammatory effect like the activating *Fcγ* receptors, and genes like *Sle6* and *Sle1d* (a locus within *Sle1* that potentiates GN), whose nature is not yet clear.

Susceptibility genes identified in spontaneous mouse models of SLE: *Ifi202*, *Cr2*, and the SLAM/CD2 family

Much of the progress made towards identifying the genes within susceptibility loci that mediate disease in the spontaneous models of lupus, has come from studies centered on the telomeric region of chromosome 1, where *Sle1* is located. The region has been identified in multiple linkage analyses on a variety of lupus-prone mouse strains. *Sle1* colocalizes with

the BXSb-derived *Bxs3* locus (165, 166), the SWR-derived *Swrl-1* locus which contributes to autoimmunity in the SNF1 model (167), and *Nba2* and *Lbw7*, which are NZB-derived intervals identified in the context of the BWF1 model (168; 169).

A congenic strain was derived for the *Nba2* locus on the B6 genetic background (B6.*Nba2*; 168), the NZB-derived region of which is quite large, and includes the *Sle1* region. Microarray analysis revealed only two differentially expressed genes out of 11,000 analyzed, in B6.*Nba2* splenocytes as compared to B6; both of these mapped within the *Nba2* locus (170). The interferon inducible genes *Ifi202* and *Ifi203* were found to be highly upregulated and downregulated, respectively, in B6.*Nba2* mice in comparison to B6. This pattern of expression is also observed in parental NZB mice, when compared to NZW. Further investigation of *Ifi202* in a variety of mouse strains indicated that its increased expression correlates with a SNP within its promoter element. It has been hypothesized that the gene may have an anti-apoptotic effect, so that its increased expression results in the accumulation of potentially autoreactive B cells (170), leading to the disease phenotype.

Analysis of recombinants within the *Sle1* congenic region led to the discovery that locus in fact corresponds to a cluster of sub-congenic loci, termed *Sle1a*, *b*, *c* and *d*, and congenic strains for each of these have been derived in order to identify their component phenotypes and causative genes (26, unpublished data from K Tus et al in the lab). The three loci *Sle1 a*, *b* and *c*, all have distinct but related phenotypes, and are involved in the production of anti-nuclear antibodies. *Sle1b* is the most potent of the subcongenic loci, and B6.*Sle1b* mice produce anti-chromatin IgG with the highest penetrance, about 90% in females and 75% in males by 9 months of age, with a fine specificity for H2A/H2B/DNA. They have elevated levels of total serum IgM and IgG, largely due to the presence of these

ANAs, and exhibit splenomegaly, and increased percentages of B and T cells expressing the activation markers CD69 and B7.2, making them most like the B6.*Sle1* congenic (26, 171). *Sle1a* is closely related to *Sle1b* in that it also shows specificity for H2A/H2B/DNA subnucleosomes, although with a much lower penetrance (about 30% and 45% in males and females respectively). In addition, B6.*Sle1a* mice exhibit a higher IgG, but not IgM, response to OVA immunization. They have a decrease in the number of CD4⁺ and CD8⁺ T cells, and an increase in B220⁺ cells. While they have fewer T cells, a higher percentage of their CD4⁺ cells have an activated/memory phenotype (26). *Sle1c* is more distantly related to *Sle1a* and *1b* in its phenotype. It is associated with lower penetrance of ANA production, similar to *Sle1a*, but with no sex difference, and without a marked specificity for any one subnucleosomal component. B6.*Sle1c* mice have lower serum IgM than B6 mice, and elevated percentages of activated/memory CD4⁺ T cells (26). While the B6.*Sle1(a+b)* mouse strain, carrying an interval spanning both loci on the B6 background, seems to recapitulate all of the phenotypes associated with the whole B6.*Sle1* strain, [B6.*Sle1(a+b)* X NZW] F1 mice do not show the GN observed in (B6.*Sle1* X NZW) F1 mice. On the other hand, GN *is* observed in [B6.*Sle1* (113-407) X NZW] F1 mice, which carry *Sle1b* along with an additional telomeric region from NZW on the B6 background. This suggested the presence of an additional locus specifically involved in nephritis, termed *Sle1d*, congenic mice for which have been produced, and are being characterized (K. Tus et al, unpublished data).

Boackle et al (172) have identified the complement receptor gene Cr2, which, by alternative splicing, encodes the CR1 and CR2 receptors for degradation products of the complement components C3 and C4, as the primary candidate for *Sle1c*. The NZW-derived Cr2 gene contains a SNP that introduces a novel N-glycosylation site into the ligand binding domains of these receptors, in the SCR1 region of CR2, and the SCR7 region of CR1.

Furthermore, reduced ligand-binding to recombinant C3dg tetramers is observed in B6.*Sle1c* B cells, along with lower calcium flux in response to stimulation through CR1/CR2 in combination with surface IgM. The expression of complement receptors has been found to be reduced in some SLE patients (173, 174), and early on in autoimmune MRL/*lpr* mice (175). In addition, Cr2-deficiency on the B6/*lpr* background exacerbates the mild, late onset autoimmunity usually observed in these mice (176), supporting a role for complement receptors in autoimmunity.

Finally, we show that members of the SLAM/CD2 family of immune receptors are the strongest candidates for mediating the *Sle1b* phenotype, and may in fact play a fundamental role in autoimmunity in general, in multiple mouse models (Chapter3, 171, Chapter 5). In this context, it is of relevance to examine in detail what is known about the SLAM/CD2 family members, which, along with their downstream signaling partners, are emerging as important regulators of the immune system, and autoimmunity.

The SLAM/CD2 Family of Immunoregulatory Receptors

The SLAM/CD2 family of receptors is expressed on a wide variety of immune cell types and plays important roles in cellular interactions, activation and regulation (reviewed in 177, 178, 179). It is a subset of the CD2 immunoglobulin (Ig) superfamily, and its members include Cd150 (Slam), Cd229 (Ly9), Cd244 (2B4), Cd84, Ly108 (NTB-A, SF2000), Cs1 (CRACC, 19a24, novel Ly9), and Cd48 (Bcm-1, Blast-1). These molecules are characterized by an N-glycosylated extracellular region composed of two immunoglobulin fold (Ig) domains: the non disulfide-bonded N-terminal IgV, involved in ligand-binding, and the membrane-proximal IgC, with its two disulfide bonds; the exception is Cd229 (Ly9), which has two such tandem V-C domains (179). The members of this family (with the exception of

Cd48, a glycosphosphatidylinositol (GPI)-linked protein) have immunoreceptor tyrosine-based switch motifs (ITSMs) in the cytoplasmic region. The motif, T X Y XX V/I, serves to bind SH2 domains on intracellular kinases, phosphatases like SH2-containing 5'-inositol phosphatase (SHIP) and the tyrosine phosphatase SHP-2, and the SH2-domain containing adaptor molecules SLAM-associated protein (SAP or SH2D1A) and EWS/FliI-activated transcript 2 (EAT-2) (178). The SLAM/CD2 family is believed to have arisen by gene duplication from a single molecule (180). They lie clustered on the long arm of chromosome 1 (1q23-24) in humans and its syntenic region at 93.3cM on mouse chromosome 1, and are found to engage in homophilic or heterophilic interactions with one another, forming receptor-ligand pairs within the family. The SLAM/CD2 genes share a common genomic structure: exon 1 encodes the 5' untranslated region (UTR) and the signal sequence, and exons 2 and 3 (as well as 4 and 5 in Cd229) encode the extracellular Ig domains. The transmembrane region is contained in exon 4 (6 in Cd229); finally, the remaining exons encode the cytoplasmic regions involved in downstream signaling by these receptors. Several of the SLAM/CD2 members have multiple isoforms, which typically share the same extracellular domains, but differ in their cytoplasmic regions, due to differences in splicing to downstream exons (179). The most well-studied of this group of genes are Cd150 or Slam, from which the family derives its name, and the receptor-ligand pair Cd48 and Cd244 (2B4). Little is known about the complex interactions and functions of the remaining members.

The receptor-ligand pair Cd48 and Cd244

CD48 was originally cloned as the antigen targeted by a monoclonal antibody (mAb) that inhibited *in vitro* CD3-driven proliferation of mouse CD4⁺ T cells (181). It is a GPI-linked receptor of the SLAM-family, widely expressed on all lymphocytes, macrophages and dendritic cells (181, 182). Cd48 is a high-affinity ligand for Cd244, another member of the

SLAM/CD2 family (183), and it can also bind the CD2 molecule, although with much lower affinity (182, 184). Antibody-mediated cross-linking of Cd48 enhances activation and proliferation of CD4⁺ as well as CD8⁺ T cells, while blocking the receptor has been found to inhibit T cell receptor (TcR)-mediated CD4⁺ T cell activation (181, 182). Cd48-deficient B6 mice have a fairly mild phenotype, exhibiting normal numbers and percentages of the various cellular subsets in their lymphoid organs, except for a slight increase in the percentage of CD4⁺ T cells in the spleen and thymus (185). Activation and proliferation of Cd48-deficient splenocytes and CD4⁺ T cells in response to TcR-stimulation, however, is diminished. In addition, the molecule seems to play an important role in CD4⁺ T cell stimulation not only as a coreceptor on the T cells, but also on irradiated splenocyte stimulators in allo-mixed lymphocyte reactions (185).

Cd244, the high-affinity ligand for Cd48, has been studied in great detail, especially in the context of its role on NK cells in both mouse and human. The picture emerging from these studies is a complicated one, in which Cd244 participates in a variety of intercellular interactions, with different effects depending on the available downstream signaling milieu in the particular cell type and organism being studied.

Cd244 is found predominantly on NK cells, as well as subsets of CD8⁺ T cells and $\gamma\delta$ T cells, monocytes, and basophils (186, 187, 188), and its expression is upregulated upon IL-2 activation of CD8⁺ T cells (189). In the murine system, two isoforms of Cd244, Cd244-L (long) and Cd244-S (short), have been identified (190). Both share identical extracellular ligand-binding domains, but differ in their cytoplasmic signaling regions. Cd244-L contains 4 ITSM motifs along with three additional tyrosine phosphorylation sites. The long isoform binds the phosphatase SHP-2 (but not SHP-1), and has been found to be inhibitory in nature, while Cd244-S, which shares one of these ITSMs and two of the additional tyrosines, but

does not bind either phosphatase, is stimulatory (191). In B6 mouse NK cells, Cd244-L seems to be the predominant isoform expressed (192), which accounts for the fact that the overall effect of engaging Cd244 on B6 NK cells is inhibitory (193, 192). This inhibitory effect of Cd244-engagement seems to occur independent of SAP, and is evident even in SAP-deficient mice (193, 192).

By contrast to its role in their NK cells, Cd244 seems to play an activating role on cytotoxic CD8⁺ T cells from B6 mice, through its interaction with Cd48 on neighboring T cells (194). These differences in function may reflect variations in the signaling molecules that are available and recruited in the two cell types. In fact, the Cd244-Cd48 receptor-ligand pair seem to play stimulatory and inhibitory roles in NK and CD8⁺ T cell function, not only by mediating interactions between these lytic effectors and their target cells, but also through the interactions they mediate between the neighboring activated NK and/or T cell effectors themselves (189, 195).

A recent study by Vaidya et al (196) showed that Cd244-deficient B6 females (but not males) have an increase in the immature CD4-CD8⁻ thymocyte population. A sex difference was also observed in the ability of Cd244-deficient mice to reject Cd48-bearing target melanoma cells. Wild-type B6 mice reject Cd48⁺ cells poorly as compared to Cd48⁻ cells, due to the inhibitory effect of Cd244 engagement upon NK cells. While Cd244-deficient males showed an increased ability to reject these Cd48⁺ cells, as might be expected, females, surprisingly, did not. Thus, there is a gender-specific, Cd48-independent effect of Cd244 deficiency in mice that is yet to be elucidated, but which seems to result from interactions between NK and other cell types (196).

The picture is further complicated by our recent finding that B6 mice are unusual in that they have one Cd244 gene, whereas this locus is expanded to four genes, three of which are transcribed, in most other strains of mice (Chapter 3). Much more information on the

cytoplasmic regions of these additional loci, their distribution and functions, is needed in order to reassess the overall role of Cd244 in mouse strains other than B6.

Cd244 seems to function quite differently in humans than in the B6 mice studied. Only a single transcript, corresponding to Cd244-L, has been identified in humans (197). The product has been found to play an activating role on a variety of human NK cell lines, unlike in the murine system, increasing cytotoxicity and IFN- γ secretion (187, 198). This stimulatory function of Cd244 is dependent on the co-engagement of activating receptors like the natural cytotoxicity receptors Nkp46, Nkp44 and Nkp30 (199), and is reduced by the co-ligation of inhibitory receptors like CD94, part of the CD94/NKG2A complex (198). The presence of SAP is critical to the ability of Cd244 to stimulate NK cell function in humans (200, 201), and the receptor, in fact, acts in an inhibitory manner in cells from XLP patients, which lack any functional SAP (201). This interaction of human Cd244 with SAP is not constitutive, but inducible, and dependent upon tyrosine phosphorylation (202, 203), and less efficient than the association of SAP with Cd150, another of the SLAM/CD2 members. As with Cd150, activation requires the ability of SAP to bind the Src protein tyrosine kinase FynT (202). The role of Cd244 on CD8⁺ cytolytic T cells in humans remains unclear, as it has not yet been possible to show that engagement of Cd244 on these cells has any effect on their cytotoxicity (187, 198).

Cd150

Cd150 or Slam (first characterized as IPO-3; 204), one of two receptors for the measles virus in humans (205), has largely been studied in the context of its modulation of T cell activation and function. It is present on activated/memory populations of a variety of cells: CD4⁺ and CD8⁺ T cells, B cells, macrophages/ monocytes, and dendritic cells. Its expression in cells that are not activated is low. As might be expected from such a pattern of

expression, in vitro stimulation of human T or B cells results in an upregulation of surface levels of the molecule. Cd150 is also present on all thymocytes, with CD4⁺CD8⁺ double positive T cells expressing the highest amounts of the molecule (204, 206, 207, 188). It has rarely been detected in NK cells, even after activation with IL-2 (208), although a study by Sayos et al (203) did find it on a subset of NK cells activated in mice infected with MCMV (murine cytomegalovirus), but not LCMV (lymphocytic choriomeningitis virus).

In humans, SLAM has been found to be a self ligand (209), and the homophilic interaction is of a low affinity. At least four isoforms of the gene are expressed in humans, and these are identical in their extracellular ligand-binding domains, and differ in their 3' regions, due to alternative splicing (206, 210). Two are membrane bound forms, the longer of which contains three ITSM motifs, and the shorter of which shares only the most membrane-proximal of these. A third isoform encodes a cytoplasmic form of the protein, missing the leader sequence, and a fourth encodes a soluble, secreted form of the protein, which lacks the transmembrane domain (206, 210). In mice, two isoforms have been detected: mSLAM1, which contains 3 ITSMs, and mSLAM2, which shares the most 5' of these (207).

SAP-binding of Cd150 is constitutive and critical to the downstream phosphorylation events caused by Cd150 ligand-binding. It competes with SHP-2 phosphatase association, but facilitates the binding of SHIP to CD150 (211, 212, 213, 214). The ability of SAP to recruit and facilitate the activation of FynT is important in its function downstream of the Cd150 receptor (215, 216, 217).

Monoclonal antibody (mAb)-mediated engagement of Cd150 on preactivated human T cells or T cell clones, had a costimulatory effect on proliferation and IFN- γ secretion (208). This activation was found to be IL-2 independent, but dependent on the pre-activated state of the T cells; Cd150 antibody-engagement could not substitute for Cd28 costimulation on naïve

T cells (208). Indeed, numerous studies using antibody-mediated engagement of the molecule on both mouse and human T cells and T cell clones, seemed to point to an important role for Cd150 in supporting Th1 responses by CD4⁺ T cells, and in diminishing or skewing away from Th2 responses (208, 207, 213, 218, 219). These effects of antibody-mediated CD150 costimulation were SAP-independent, occurring in cells deficient for the downstream adaptor molecule (213). In contrast to these findings, however, co-transfection of Cd150 and SAP into a T cell line that does not usually express either, actually inhibited IFN- γ production in response to antigen-stimulation (215).

Clues that antibody engagement of Cd150 might actually have had an antagonistic effect on its overall function, rather than mimicking the effects of ligand-binding by the receptor, first came from studies examining the role of Cd150 on B cells (210). Engagement of Cd150 on human B cells using a FLAG-tagged form the soluble, secreted isoform (sSLAM), caused increased proliferation, by itself, as well as in combination with anti-CD40 and a variety of cytokines including IL-2, 4, 10, 12, and 13, or anti- μ . It had a similar effect on preactivated B cells, and was also found to increase IgM and IgG production. On sorted immature IgD⁺ B cells, it enhanced IgM production, showing that it helps B cell differentiation, but did not result in IgG or IgA production, showing that it may not play a role in class switching (210). Singularly enough, although cross-linking of Cd150 with the use of cells transfected with mSLAM, or beads carrying sSLAM, had the same results, engagement of the receptor with the same monoclonal antibody used in the T cell studies, had none of these costimulatory effects on B cells (210).

The differential effects of Cd150 antibody-binding and ligand-binding may be due to the ability of the antibody to block the homophilic interaction between Cd150 molecules on neighboring cells, or to sequester the receptor away from antigen-stimulation signaling: In

humans, Cd150 has been found to colocalize with the TcR after CD3-stimulation, and be phosphorylated by the Src kinases Lck and Fyn (213).

The generation of a Cd150-deficient mouse has indeed shown that the molecule, in fact, positively regulates the production of IL-4 by CD4⁺ T cells, while negatively regulating the production of IFN- γ by both CD4⁺ and CD8⁺ T cells (220). Stimulation with anti-CD3 and anti-CD28 results in lower IL-4 production, and slightly higher IFN- γ production, in Cd150-deficient T cells, than in wild-type. With polarizing conditions, however, with IL-4 being exogenously supplied, normal levels of IL-4 are secreted. This defect in IL-4 production is also evident with stimulation of antigen-specific TcR-transgenic T cells with APCs and peptide, although normal levels are secreted upon secondary stimulation. The production of both IL-4 and IFN- γ by NKT cells in mice injected with anti-CD3, however, remains normal (220).

The other cellular compartment affected by Cd150- deficiency is macrophages, in which the receptor seems to positively regulate IL-12, TNF α and NO production, while negatively regulating IL-6. Thus, in response to stimulation by LPS or IFN- γ , Cd150-deficient macrophages secrete lower amounts of the inflammatory cytokines, and higher levels of IL-6. They remain functional, however, in terms of phagocytosis, and their ability to stimulate CD4 T cells. These macrophage abnormalities result in an inability of B6 mice to clear *Leishmania major* (220), an intracellular infection that is usually eliminated by these mice through a Th1 response (221). BALB/c mice, which have a Th2 response that fails to clear the infection, and results in footpad swelling (221), make their typical response in the absence of Cd150 (220).

Cs1

Cs1 is found on NK cells, activated CD8⁺ T cells, B cells, and mature dendritic cells (222, 223, 224). Human Cs1 has been found to be homophilic in nature, and ligand-binding by the molecule has the overall effect of increasing the lytic activity of NK cells (225). Cs1 occurs in two splice isoforms in humans: the longer Cs1-L, which contains two of ITSM motifs and seems to be the predominant form in human NK and other cell lines, and Cs1-S, which lacks any ITSMs. The level of expression of both isoforms remains steady upon NK cell stimulation (226). Not much more, however, is known about the relative distributions of the two isoforms in the various Cs1-bearing cell types. While Cs1-L can stimulate NK cell killing of Fc receptor-bearing targets in redirected lysis assays, Cs1-S, it seems, cannot. Differences in baseline killing by RNK-16 rat NK cell transfectants bearing the two different isoforms, indicate that homophilic interactions between Cs1-L molecules on neighboring cells can stimulate NK cytotoxicity even in the absence of a Cs1-specific antibody (226). Crosslinking Cs1-S fails to induce the calcium mobilization observed in the case of Cs1-L, and, while the latter is found to associate with SAP constitutively, but dissociate from it upon pervanadate-stimulation, Cs1-S, lacking ITSMs, does not bind SAP (226). The ability of Cs1-L to activate NK cell killing seems to be independent of SAP, as evidenced by studies with NK cells from SAP-defective XLP patients (224).

Two Cs1 isoforms have been detected in the mouse, the longer of which contains one ITSM motif and one additional Y XX V/I tyrosine phosphorylation motif capable of binding SH2 domains, and the shorter of which shares only the additional SH2-binding motif. The association with SAP observed with human Cs1, is however not evident in the mouse (222).

Cd84

Cd84, present on all thymocytes, B cells, monocytes, platelets, T lymphocytes, and granulocytes (227, 188), has at least five different isoforms (Cd84 a-e) in humans, three of which (a, b, and c) contain two ITSM motifs, and two additional Y XX V/I SH2-binding motifs (227). Its overall expression is upregulated upon activation of T and B cells, and maturation of APCs such as monocytes and dendritic cells. Expression of Cd84 is therefore much higher in memory compared to naive T cells, and slightly higher in memory than in naive B cells (188).

Human Cd84, like human Cs1 and Cd150, seems to engage in homophilic interactions (228). Engagement of the receptor on PBMCs with either mAb or plate-bound Cd84 Ig-fusion protein increased IFN- γ secretion in combination with CD3, indicating a role for Cd84 in T cell stimulation, which may be skewed in the Th0/Th1 direction, as a similar increase in IL-4 secretion was not observed (228).

Mouse Cd84, for which two transcripts or isoforms have been detected (229), has also been reported to be able to interact with itself (although the primary data supporting this observation is unpublished), and ligand-binding seems to be species-specific, with no cross-reactivity between mouse and human forms (228). Cd84 binds SAP, which competes for binding with SHP-1, in a phosphorylation-dependent manner (230, 212). Its costimulation of anti-CD3 mediated proliferation of human T cells, however, appears to occur independent of the association, as SAP-deficient T cells from XLP patients respond similarly (231).

CD229

Cd229 occurs on thymocytes and mature B and T cells, its message being found in all lymphoid tissues except bone marrow (232, 188). In thymocytes, expression is upregulated upon maturation, and it is highest in CD4 and CD8 single-positive thymocytes. Unlike Cd84,

Cd229 expression is not higher on memory than on naïve T cells, but it is slightly higher on memory B cells than in naïve ones (188). Both mouse and human Cd229 are different from the other members of the SLAM/CD2 family in that they have two IgV domains alternating with two IgC domains in the extracellular region (233, 232).

Human Cd229 has been shown to be homophilic in nature (234). The cytoplasmic domain of the molecule contains five SH2-binding tyrosine phosphorylation motifs, two of which are ITSMs (232). As in the case of most of the other family members, these allow it to bind SAP (230), and the ability of SAP to recruit the T cell Src-kinase FynT is important to the phosphorylation of Cd229, and its downstream signaling (217). Little is known about isoform usage in this gene, although the existence of alternatively spliced isoforms is supported by the presence of multiple Cd229 message bands in both mouse and human RNA (232, 171).

Ly108

Ly108 (NTB-A), the single most promising candidate gene in the *Sle1b* interval (Chapter 3, 171), is present on T, B and NK cells in human and mouse (235, 236, 171), and its expression is upregulated upon *in vitro* activation of human B and T cells (237). It has at least two alternatively spliced isoforms in the mouse, Ly108-1 and Ly08-2, which differ in their cytoplasmic domain. Ly108-1 contains two ITSMs, while Ly108-2 has three such motifs (235, 171). In humans, two potential isoforms have been identified, one of which has two ITSMs and an additional SH2-binding motif. The other putative isoform has an extra codon, which would insert an alanine residue in its cytoplasmic region (236).

Human Ly108 has been found to bind itself, and its homophilic interactions tend to be weaker than the higher-affinity Cd244-Cd48 interactions, and similar to the other homophilic Cd150-Cd150 and Cs1-Cs1 interactions (238, 239, 209, 237). The molecule has mainly been

studied in the context of its role in NK cells (236, 238, 239). Engagement of Ly108 by its ligand on target cells stimulates NK cell cytotoxicity, and, as in the case of Cd244, this stimulation is dependent on the presence of activating NK cytotoxicity receptors like NKp30, NKp44, or NKp46 (236, 238). Ly108 stimulates other NK cell functions as well, increasing IFN- γ and TNF- α production (239). The stimulatory effect of Ly108 is dependent on the presence of SAP, and while it seems to have an activating effect overall in normal NK cells, it is inhibitory in SAP-defective NK cells from patients with XLP (236). Ly108 may also be important in the costimulatory interactions of NK cells with one another, as its presence on target cells can actually compete with and inhibit the proliferation that results from the interactions between this protein on neighboring NK cells (238). Thus, it seems to play an emerging role in complex intercellular interactions and regulation, certainly involving NK cells, and potentially many of the other cell types that carry the receptors.

A recent study examining its role in T cells showed that antibody-engagement of Ly108 has a costimulatory effect on human and mouse CD4⁺ T cells, increasing proliferation and IFN- γ secretion in combination with anti-CD3 (237). As in the case of Cd150, it seems play a role in modulating the Th1/Th2 nature of immune responses: antibody-engagement of this receptor enhances *in vitro* Th1 responses by CD4⁺T cells in culture, while soluble human Ly108-Fc fusion protein acts to lower Th1 (IgG2a and IgG3) T-dependent B cell antibody responses while leaving the Th2 (IgG1) responses intact in immunized B6 mice (237). The differential effects of using antibody and fusion protein are reminiscent of similar discrepancies observed in the case of Cd150. Here, the soluble fusion protein may be acting as a self-ligand, or, alternatively, blocking interactions between membrane-bound Ly108 molecules (or other unknown ligands) on different cell types (237). The generation of an Ly108-deficient mouse would be useful in assessing which phenotype (Th1 or Th2) it supports. Finally, the importance of this receptor as a potential therapeutic target in

autoimmune disorders of a Th1 nature is underlined by the fact that the soluble Ly108-Fc construct can ameliorate disease in the experimental autoimmune encephalitis (EAE) model of multiple sclerosis (237).

As is evident from what is currently known about each of its members, the SLAM/CD2 family of proteins has complex, overlapping patterns of expression and function. These receptors are expressed in several isoforms on a wide range of immune cell types, where they interact with themselves or one another, and modulate cell function by engaging a host of downstream signaling molecules. Differences in the levels of expression, isoform usage, and binding-domains of members of the family, such as those observed between B6 and B6.*Sle1b* mice (Chapter 3, 171) as well as other autoimmune strains (240), can therefore have a variety of effects on the quality, strength, and nature of the interactions between different cell types.

SAP and EAT2: Downstream adaptors of the SLAM/CD2 family

The SH2-domain containing adaptor protein SAP acts directly downstream of each of the ITSM-containing members of the SLAM/CD2 family (reviewed in 178, 177). One indication of the importance of these molecules as immunoregulatory receptors, is that mutations or deficiencies in SAP cause X-linked lymphoproliferative disorder or XLP (241, 211, 242). The disease is characterized by immune dysregulation resulting in an inappropriate response to Epstein Barr virus (EBV) infection, including T cell expansion, hypogammaglobulinemia and B cell lymphomas (reviewed in 178,243). While SAP is expressed primarily in T and NK cells (244), EAT-2, a very similar adaptor molecule, is present in APCs including B cells and macrophages (245), indicating that it may be its counterpart and play a similar role with SF members expressed on these cell types. Indeed,

EAT-2 has been found to bind at least four of the ITSM-containing receptors: Cd150, Cd84, Cd229, and Cd244 (245). Both molecules bind the SLAM/CD2 ITSMs in a very similar manner (245, 246), although unlike in the case of SAP's association with Cd150, EAT-2 association is phosphorylation-dependent. As with SAP (215, 216, 217) its ability to recruit Fyn is critical to its function downstream of the SLAM/CD2 receptors (245).

The importance of SAP in immune regulation

The generation and characterization of SAP-deficient mice (247, 248), gives us some idea of the functions of this molecule and its role in mediating the immune dysregulation that results in XLP. Since it acts directly downstream of the SLAM/CD2 family, it also sheds light on some of the overall *in vivo* functions that they participate in.

SAP plays an important role in Th2 T cell responses and T-dependent humoral immunity. When challenged with pathogens like LCMV, *Toxoplasma gondii* or *L. Major*, SAP-deficient mice have an inappropriate immune response, with increased IFN- γ production and T cell activation, impaired IL-4 cytokine production, and hypogammaglobulinemia (247, 248), similar to the features observed in XLP patients, many of which are also present in Cd150-deficient mice (220, 243). The importance of the SAP-mediated signaling pathway in T cell receptor-mediated production of Th2 cytokines like IL-4 and IL-13 (249, 250) is independent of the elevated IFN- γ production observed in these mice (249). While stimulation through the TcR is not able to elicit IL-4 production in the absence of SAP, the T cells remain capable of responding to cytokine stimulation and secreting IL-4 under Th2-polarizing conditions (249).

Not surprisingly, given its importance in the signaling of SLAM/CD2 receptors through SAP, the ability of SAP to bind the Src kinase FynT is critical in its mediation the Th2 pathway in CD4 T cells (249, 250). SAP-deficiency leads to a defect in recruitment of

PKC θ and Bcl-10, and this in turn leads to an impairment in the phosphorylation and ubiquitin-degradation of IKB α , which is important in activation of the p50 component of the NFKB complex. The resultant defective transcription of GATA-3 (249), the master regulator of Th2 differentiation (251), is responsible for the impairment in IL-4 production. SAP-deficient cells have normal levels of T-bet, the Th1 regulator (251).

The profound impairment of Th2 responses, important in providing CD4⁺ T cell help for affinity maturation and class switching in T-dependent B cell immunity, has important effects *in vivo*. The generation of long term T-dependent anti-viral humoral immunity and the formation of germinal centers in response to LCMV infection are defective in the absence of SAP (252). Defects in germinal center formation, and T-dependent, but not T-independent B cell responses to antigen, were also observed by Hron et al (240). Significantly, the lack of T cell help of a Th2 nature makes SAP-deficient 129 mice less susceptible to pristane-induced lupus than wild-type mice, which develop ANAs, anti-ds and anti-ss DNA Abs and rheumatoid factor (RF), as well as renal disease and proteinuria. The mice have an increased susceptibility, however, to the Th1-mediated disease experimentally induced autoimmune encephalomyelitis (EAE) (240). This study demonstrates how Th1 versus Th2-skewed responses can have ameliorative or exacerbating effects on autoimmunity, depending on context. The ability of the SLAM/CD2 family to play a modulatory role on the nature of immune responses, through SAP and the other competing and complementary signaling molecules and pathways, certainly makes the cluster attractive as candidates to potentiate autoantibody-driven autoimmunity in SLE.

Over the next few chapters, I discuss our own findings with regard to the SLAM/CD2 family in the context of the autoimmunity observed in B6.*Sle1b* mice. Analyses of structural and functional polymorphisms in all spleen-expressed candidate genes between the lupus-

resistant B6 and susceptible B6.*Sle1b* strains, demonstrate that the members of this family are the best candidates to mediate a break in tolerance to chromatin. The family forms two tightly-linked haplotypes of alleles in the commonly used laboratory strains of mice. One of these is found in B6 and a few other C57-strains, while the other is in all of the other autoimmune and non-autoimmune strains, causing autoimmunity only in particular genetic contexts: in this instance, the C57Bl/6 background, in B6.*Sle1b* or B6.*I29c1* mice (Chapter 3). The autoimmune-associated alleles of the family members are also very prevalent in wild, outbred populations of mice, indicating that their common occurrence is not just an artifact of inbreeding and the somewhat artificial conditions and environments laboratory inbred strains have been subject to. This is, no doubt, partly because the disease-alleles are only truly pathogenic in certain contexts, i.e., in combination with multiple other susceptibility loci. In addition, however, we find that the different alleles of the SLAM/CD2 family are shared between evolutionarily distant species of *Mus*, and sub-species of *Mus musculus*. Such long coalescence times are indicative of balancing selection, perhaps pathogen-driven, operating to actually retain these alleles over evolutionary time-spans (Chapter 4). Finally, I describe the generation and initial characterization of a series of Bacterial Artificial Chromosome (BAC)-transgenic mice on the B6.*Sle1b* autoimmune-prone genetic background. These transgenics were made from B6-derived BACs spanning the *Sle1b* interval, in order to try and functionally identify the *Sle1b* gene using a BAC-transgenic rescue strategy. Our preliminary data from these studies indicate that the SLAM/CD2 genes remain the best candidates for *Sle1b* (Chapter 4).

Chapter II. Methods

Mice and Mouse Strain DNA. All mice described in this study were females bred and housed in our colony in the UT Southwestern Medical Center Animal Resources Center's specific pathogen free (SPF) facility, under the supervision of Dr. Jose Casco. C57BL/6J (B6) mice were originally obtained from the The Jackson Laboratory (Bar Harbor, ME). The derivation of B6 congenic mice carrying the NZM2410 derived *Sle1b* interval (B6.*Sle1b*) has been described (171, 26). This congenic strain carries the NZM2410-allele of the microsatellite marker D1MIT113, and is flanked by B6 alleles of the markers D1MIT148 on the centromeric side, and D1MIT149 on the telomeric side. The introgression of SLAM/CD2 from 129/SvJ onto C57BL/6 was performed using marker assisted selection protocols (253), and required 5 backcross generations to C57BL/6. The B6.*I29c1* congenic carries a 129-derived congenic interval from *D1MIT148* to *D1MIT115* (roughly 4 Mb) and includes *Sle1b*, but excludes *Sle1a*, *Sle1d*, and *Sle1c*. The B6.*Castc1* congenic strain has a congenic interval similar in size to B6.*Sle1*.

DNAs for the common laboratory inbred strain panel (Table 5 Legend, Chapter 3), and the 15 wild-derived inbred strains (Table 7A, Chapter 4), were obtained from The Jackson Laboratory. DNA from the 33 wild, outbred mice (Table 7B, Chapter 4) was obtained from Dr. F. Bonhomme (Universite MontpellierII, Montpellier, France). Genomic DNA from B6.*Sle1b*, B6.*Castc1*, and B6.*I29c1* congenic mice was prepared from tail lysates of mice, as described under *Preparation of genomic DNA from tail lysates*.

Bacterial Artificial Chromosome (BAC)-transgenic mice were generated by pronuclear injection of each of the purified BAC constructs (described under *BAC-transgene constructs*) into B6 blastocysts at the Transgenic Core at UT Southwestern Medical Center at Dallas, followed by transfer into pseudopregnant B6 females. BAC-transgene positive

founders were detected by PCR-genotyping of tail lysates with common BAC-vector specific primers, flanking the insert on the T7 and Sp6 sides of the circular constructs. The primers used were: Vec(T7)F: TGGTTGCTACGCCTGAATAA with Vec(T7) R: TGCGGAGAAAGAGGTAATGAA (Product size: 200bp; Annealing temp: 56°); and Vec(Sp6)F: CGTTTTTCCAGCTGTCGATT with Vec(Sp6)R: AAACGTACGGCGTCTCTCA (Product size: 300bp; Annealing temp: 56°). BAC transgenes were bred onto the B6.*Sle1b* background by crossing the B6-founders to B6.*Sle1b*, followed by back-crossing of (B6 X BAC Tg-B6.*Sle1b*) F1 progeny to B6.*Sle1b*. [(B6 X Tg-B6.*Sle1b*) X B6.*Sle1b*] mice were typed using the repeat length polymorphic microsatellite marker D1MIT113 to assay for homozygosity of the NZM2410-derived *Sle1b* interval. BAC-transgene positive B6.*Sle1b* homozygous mice were maintained and intercrossed to produce BAC-heterozygous and BAC-homozygous test-progeny, as well as BAC-negative littermates, from each transgenic-line (illustrated in Fig 19 in Chapter 5).

BAC Contig Construction: Construction of the BAC contig was achieved by screening the RPCI-23 library (Children's Hospital Oakland Research Institute, Oakland, CA) and the CalTech BAC library (Invitrogen, Carlsbad, CA) by hybridization with probes derived from *D1Mit148*, *D1Mit146*, *D1Mit113* and *D1Mit149* as well as from genes previously localized to this interval. As BACs were positively mapped to the contig, BAC-end sequencing using the consensus T7 and Sp6 primers was used to generate additional probes (available upon request from Dr. A Wandstrat in the lab). Several markers used were also identified from published YAC and BAC contigs 254-256.

BAC DNA Extraction and Insert Sequencing. BAC DNA was prepared following the Wellcome Trust Centre for Human Genetics and Institute of Molecular Medicine protocol.

(http://www.molbiol.ox.ac.uk/~jmejia/more_protocols.html). For sequencing libraries, BAC DNA was sheared in a nebulizer (Glas-Col, Inc.; Terre Haute, IN) at 150-psi nitrogen for 2.5 minutes. Fragment ends were mended by incubating with 0.2mM dNTPs, 40 units T4 DNA polymerase for 15 min. at RT, and addition of 25 units Klenow for 1-hour at RT. DNA was purified by phenol-chloroform extraction, and ethanol precipitation, and run on a 1% agarose gel. 1-3kb fragments were extracted using the GeneCleanII kit (Qbiogene; Carlsbad, CA) and ligated into the pUC18 vector using the Rapid Ligation Kit (Roche Boehringer Mannheim; Indianapolis, IN). DH5 α TM competent cells (Invitrogen; Carlsbad, CA) were transformed, and plated onto LB plates with 100ug/ml ampicillin, 50ug/ml X-gal, and 1mM IPTG. Plasmid DNA was extracted using an Autogen 740 (AutoGen; Holliston, MA) and sequenced using M13 primers on the Beckman CEQ 2000XL (Beckman Coulter; Fullerton, CA). Sequence was assembled using phred, phrap, and consed (see <http://www.phrap.org>).

BAC-transgene Construct Preparation. BAC constructs are from the RPCI-23 C57Bl/6J-derived BAC library (Children's Hospital Oakland Research Institute, Oakland, CA). Each construct carries ~150-200 kb of genomic B6-derived DNA in the pBACe3.6 vector. The BACs used are: 41 (194d6), 47 (48o11), 25 (171k8), 40 (145f9), 90 (388c4), and 95 (462j8), which form an overlapping tiling path across the minimal *Sle1b* susceptibility locus as shown in Fig 1B, Chapter 3. Briefly, bacterial cultures of clones carrying each BAC were grown in LB Broth (Becton Dickinson, Sparks, MD) containing 50 μ g/mL chloramphenicol (Boehringer Mannheim, Indianapolis, IN), overnight at 37° with shaking at 260-300 rpm. Bacteria from 2 liter cultures were used for each construct to be injected. An alkaline lysis protocol using Qiagen maxiprep solutions P1, P2, and P3 (Qiagen Inc, Valencia, CA) was used, followed by three phenol/chloroform/isoamyl alcohol extractions. BAC-DNA was precipitated using (1/10)th volume 5M NaCl and 1X volume cold isopropanol, and washed

with cold 70% ethanol. It was then resuspended in TE (10 mM Tris, 1mM EDTA), ethidium bromide was added, and it was applied to a CsCl ultracentrifugation gradient. After ultracentrifugation, the lower DNA band, containing uncut BAC-DNA, was pulled using a 1ml syringe and an 18G needle. Ethidium bromide was removed by repeated extraction with 1X volume isoamyl alcohol, until the DNA-TE (lower) layer was clear. DNA was then precipitated out of solution with $(1/10)^{\text{th}}$ volume 3M sodium acetate and 2X volume cold ethanol. DNA was visible at this point, and looped out into an 1.5ml microfuge tube containing TE. DNA was re-precipitated, and finally washed twice with cold 70% ethanol. It was resuspended in a final volume of 400 μL Injection Buffer (10 mM Tris, 0.1 mM EDTA), and stored at 4° until transfer to the Transgenic Core facility. DNA was not prepared more than a week before its scheduled injection date. 3 μL of the DNA obtained was digested using 5 μL Pst1 (10u/ μL) and 1 μL RNaseA at 1mg/mL (both from Invitrogen, Carlsbad, CA), in a 30 μL reaction volume, for 1 hour in a 37° water bath. The reaction was run on an 0.8% agarose gel at 160mV till there was clear separation of the multiple bands, to check for the quality of the product, any background smearing being indicative of sheared genomic/BAC DNA. For injection, BAC-DNA was diluted to 10ng/ μL in Injection Buffer.

PCR Genotyping. Tail clips were obtained at weaning and used to prepare tail lysates.

Briefly, 250 μL of Tail Lysis Buffer (50 mM Tris, pH 8.0/ 50 mM KCl/ 2.5 mM EDTA/ 0.45% NP-40/ 0.45% Tween-20) and 0.4 mg/ml Proteinase K solution (Roche, Indianapolis, IN) were added per tail clip and kept for at least 20 hours in a 55°C water bath. Tail lysates were vortexed and spun down at 14000 rpm for 10 minutes. For a 20 μL PCR reaction, 0.5 μL of tail lysate supernatant was used. PCR products from MIT markers were subsequently run out on 5% agarose gels to resolve the polymorphic bands. All other products were run on 2% agarose gels.

Preparation of genomic DNA from tail lysates. Genomic DNA was obtained from tail lysates by carrying out two phenol/chloroform/isoamyl alcohol extractions, followed by one extraction with chloroform alone. DNA was precipitated out of solution using (1/10)th volume 3M sodium acetate and 2X volume cold ethanol, washed twice with cold 70% ethanol, and resuspended in 100 μ L PCR-grade water.

Cell Preparation. Following the measurement of spleen weight, single cell splenocyte suspensions were prepared, passed through nylon mesh and depleted of red blood cells (RBCs) using ACK Lysis Buffer (0.1mM EDTA/ 0.15M NH₄Cl / 10mM KHCO₃, pH 7.2-7.5). These cells were then used for flow cytometric analyses or to obtain B and CD4⁺ T cells or RNA.

Preparation of cDNA. Spleens were processed as described under *Cell Preparation*, to obtain a single-cell, red blood cell-depleted suspension. Splenic B and CD4⁺ T cells were obtained using Dynabeads mouse pan B (B220) and CD4 magnetic beads respectively (Dyna; Brown Deer, WI). Total RNA was obtained directly from spleen, or from B and T cells, using the Qiagen RNeasy Mini Kit (Valencia, CA) according to manufacturer's instructions, including treatment with DNaseI. cDNA was synthesized using 10 μ L reactions on 1.5 μ g RNA, with the TaqMan Reverse Transcriptase kit using the Oligo dT primer, according to manufacturer's instructions (Applied Biosystems, Foster City, CA).

Quantitative RT-PCR. Quantitative real-time PCR was performed on 10 ng cDNA on the GeneAmp 5700 using SYBR green (Applied Biosystems); primer sequences are included in Table 1. For each primer set, standard curves were generated using serial dilutions of cDNA.

Gapdh was used to normalize for loading. Data is presented as the mean fold difference of B6.*Sle1b* relative to B6 ($n \geq 5$). A Student's t-test was used to determine significance.

PCR Amplification and Sequencing of Products. For all PCR-amplified sequencing products, 100 μ L PCR reactions were performed on 250-500 ng genomic DNA. Primers and cycling conditions used, along with product sizes, are listed in Table 2. Information on additional primer sequences and products, for the exons of all candidate genes within the *Sle1b* interval, are available upon request from Dr. A. Wandstrat in the lab. Amplified products were purified using the High Pure PCR Product Purification Kit (Roche; Indianapolis, IN) or the QIAquick 96 PCR Purification Kit (Qiagen, Valencia, CA).

Where required (in the case of the *Cd244* gene amplification), cleaned products were blunt-end cloned into the pPCR-Script Amp SK(+) vector and XL10-Gold Kan ultracompetent cells were transformed, using the PCR-Script Amp Cloning Kit (Stratagene, La Jolla, CA) according to manufacturer's instructions. The cells were plated onto LB plates with 100 μ g/ml ampicillin, 50 μ g/ml X-gal, and 1mM IPTG. Clones were picked and grown in LB broth containing 100 μ g/mL ampicillin (Boehringer Mannheim), overnight at 37° with shaking at 260-300 rpm. Clones were screened by PCR using M13 primers, and plasmid DNA from positive clones was prepared using the QIAprep Spin Miniprep Kit (Qiagen).

Products were sequenced on the Beckman CEQ2000XL capillary sequencer (Beckman Coulter; Fullerton, CA) or the ABI 3730XL (Applied Biosystems, Foster City, CA), according to manufacturer instructions. The sequencing primers were the same primers used to amplify the products, or, in the case of cloned products, M13 primers. The resulting sequence was edited and assembled using Sequencher software (Gene Codes Corporation; Ann Arbor, MI).

Phylogenetic analysis of sequence data: Phylogenetic analysis of sequence data was carried out by Dr. Scott Edwards (Harvard University, Cambridge, MA). The coding region sequences from the exons of each gene were concatenated together, and phylogenetic trees were made using the neighbor joining method, with a tamura-nei distance method with a gamma rate variation parameter of 0.5.

Likelihood analysis of codon selection: The coding region sequences from the exons of each gene were concatenated together. D_N/d_S analysis was carried out using Yang's codon substitution models (257), a phylogeny-based likelihood ratio test (LRT) that tests for positive selection among different codon positions in a gene, by Dr. Scott Edwards. The log-likelihood value of a Neutral model (Model 1), in which a proportion p_0 of codons is conserved (those with $\omega_0 = d_N/d_S = 0$), and a proportion p_1 is neutral ($\omega_1 = d_N/d_S = 1$), is compared to that of a Discrete Model (Model 3) in which d_N/d_S ratios are estimated for three classes of codons (ω_0 , ω_1 and ω_2) with corresponding proportions p_0 , p_1 and p_2 . The d_N/d_S ratios for the classes in this model are estimated as ω_0 , ω_1 and ω_2 . When $\omega_2 > 1$, this indicates that the codons in this class are under positive selection. If the difference in likelihood between Model 3 and Model 1 is greater than the critical value for a chi-square test with 2 degrees of freedom (5.991), then model 1 can be rejected, thus providing evidence for selection.

Serology. Litters of aging BAC-transgenic females and their negative littermates were bled at 7 and 9 months, and at the 12 month terminal sacrifice. Cohorts of females from all other strains analyzed were similarly serially bled. Sera from these mice are stored at -20°C . Detection of IgG anti-nuclear autoantibodies (ANAs) directed against total histone/dsDNA were performed by ELISA. All coating steps were for 30 minutes at 37°C followed by two

washes in PBS (Sigma-Aldrich). Briefly, Immunlux HB (Dynatech, Chantilly, CA) plates were precoated with 50 μ l/well of methylated BSA (mBSA) and then coated with 50 μ l/well of 50 μ g/ml dsDNA (Sigma-Aldrich; dissolved in PBS and filtered) followed by 50 μ l/well of 10 μ g/ml total histones (Roche). Following the last coating step and wash, plates were incubated overnight at 4°C with 200 μ l/well of ELISA Blocking Buffer (PBS/ 0.1% gelatin/ 3% BSA/ 3 mM EDTA). The following day, test-sera were added at a final dilution of 1:800 in Serum Diluent (PBS/ 0.1% gelatin/ 2% BSA/ 3mM EDTA/ 0.05% Tween-20), and allowed to incubate for 2 hrs at room temperature. Bound IgG was detected using alkaline phosphatase conjugated goat anti-mouse IgG (Roche) and p-nitrophenyl phosphate (Sigma-Aldrich) as the substrate. OD450 was measured on an Elx800 Automated Microplate Reader (Bio-Tek Instruments, Winooski, VT). The raw optical densities for ANA ELISAs were converted to arbitrary U/ml using a standard curve included on each plate, generated by serial dilutions of a monoclonal antibody (3HF1b) derived from an NZM2410 mouse, with the highest (1:250) dilution of the supernatant set at 1000 U/ml.

Sequencing-based Single-nucleotide polymorphism (SNP) Assays. SNP assays were carried out on genomic DNA from tail lysates of every BAC-transgenic mouse, to assess transgene copy number initially, and to distinguish between transgene-heterozygotes and homozygotes in each line. Assays were carried out on splenic cDNA to assay for expression of the B6 (transgenic) allele of each candidate gene contained on that BAC, along with the endogenous B6.*Sle1b* allele.

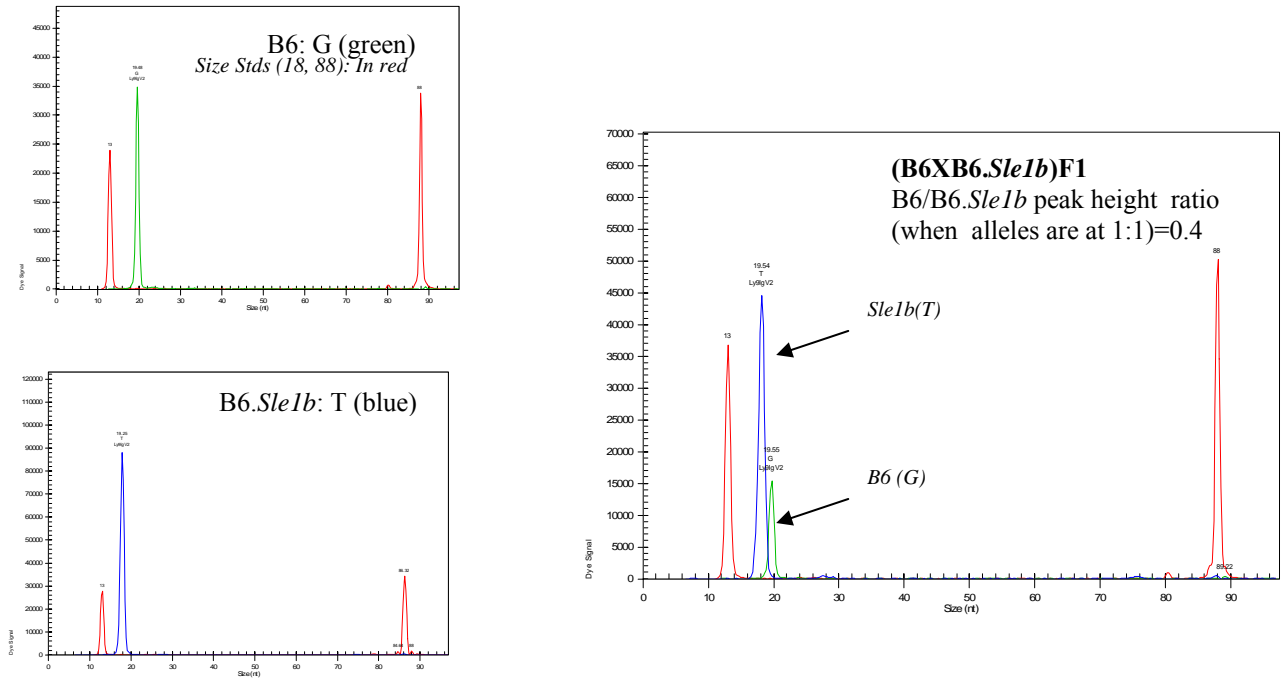
For each gene, primers were designed to amplify a 200-500 bp containing a known SNP between the B6 (transgene) and B6.*Sle1b* (endogenous) alleles. In each case, a 45 μ L PCR reaction was set up using 100ng genomic DNA or spleen cDNA as template, and 15 μ L of the product was run on a 2% agarose gel to verify product size and quality. The remaining

30 μ L was treated with 10U Shrimp Alkaline Phosphatase (SAP; Roche, Indianapolis, IN) and 5U Exo1 (USB, Piscataway, NJ), incubated at 37° for one hour followed by 15 minutes at 75° to inactivate the SAP.

0.5 μ L of each amplified, cleaned PCR product (10-500 fmol dsDNA template) was then used in a 10 μ L “Single base extension” reaction with water, and 5.5 μ L of Ready Mix from the CEQ SNP-Primer Extension Kit (Beckman Coulter, Fullerton, CA), containing dye-labeled ddNTPs, 10X reaction buffer, and polymerase enzyme. Also included was 1pmol of a 20-60 bases-long SNP-interrogation primer (“Single-base Extension” or SbE primer), which stops just short of the SNP. Thus, the single labeled base added to the end of the SbE primer in this reaction depends on whether the amplified template contains the B6 or B6.*Sle1b* alleles, or a mixture of the two. The reaction was cycled in a thermocycler at 96° for 10 seconds, 50° for 5 seconds, and 72° for 30 seconds, for 25 cycles. It was then cleaned with 1U of SAP, incubated at 37° for one hour, followed by incubation for 15 minutes at 75°.

0.5-1 μ L of the SNP reactions were diluted with 0.5 μ L of Size Standard 80 (Beckman Coulter), in Sample Loading Solution (Beckman Coulter), and loaded into a CEQ sample plate with a drop of mineral oil on top. Samples were run on the Beckman CEQ 2000XL capillary sequencer (Beckman Coulter; Fullerton, CA) according to manufacturer’s instructions, using the recommended run program, termed “SNP-1”.

Data were analyzed on the CEQ8000 Genetic Analysis System software (Beckman Coulter). Read-out is in the form of single peaks of different colors corresponding to each of the alleles present in the template (similar to those observed in sequencing reaction), running at the size of the SbE primers. The size standard included also yields two reference peaks, 18 bases and 88 bases in size. A sample obtained from genomic DNA is shown in the figure below:



The peak height from each allele is quantified by the software, and the ratio of B6: Sle1b SNP-alleles is obtained in each case. The higher the B6:Sle1b peak-height ratio, the greater the amount of the B6 allele relative to Sle1b, in the template.

The ratio of the peak heights of the B6 (transgene) and B6.*Sle1b* (endogenous) alleles is normalized to the ratio obtained from (B6 X B6.*Sle1b*) F1 mouse genomic or spleen cDNA, as representing a 1:1 presence of the two alleles. Copy number estimation was done as follows, using a group of BAC-heterozygous DNAs from each line: Let the SNP peak height ratio of B6/B6.*Sle1b* alleles from BAC-transgenic = $R_{(Ex)}$, and SNP peak height ratio of B6/B6.*Sle1b* alleles from (B6 X B6.*Sle1b*)F1 (alleles present 1:1) = $R_{(Ctrl)}$. The “normalized” peak ratio = $R_{(Norm)} = R_{(Ex)} / R_{(Ctrl)}$. If $R_{(Norm)} = N$, then the BAC-Tg contains N-times as many B6 copies as the (two) endogenous B6.*Sle1b* alleles. Therefore, copy number = $(N \times 2)$. This is done to control for the fact that different dye-labeled peaks, even from equal quantities of the four different nucleotides, are not of equal heights. Mice were grouped into heterozygous and homozygous groups based on whether they had lower or higher B6/B6.*Sle1b* ratios.

The primers used to amplify PCR products, the expected product sizes and annealing temperatures, as well as the sizes and sequences of the corresponding SbE primers used for each candidate gene, are listed below. The single dye-labeled base expected to be added to the SbE primer depending on the allele(s) contained in the template, is indicated in bold in each case.

Primers used to determine copy number/ heterozygosity vs homozygosity, on genomic DNA from BAC-transgenics:

BAC41

Tnfsf19 (Dedd) SeqSNP F: AGCAAGAACATGGGCTCTACA

Tnfsf19 (Dedd) SeqSNP R: AACGTAGGGCAGCAAGTCAT

Product size: 250 bp; Annealing temp: 59°

Tnfsf19 SbE primer: CGCTGTGACGAGAGTAACTTTTCG- **C**(B6)/**T**(Sle1b) [24 bp]

BAC47

Ref2bp SeqSNP F: AAGTGGCAGCACGACCTATT

Ref2bp SeqSNP R: AGAGCCACGGCTCCTTGT

Product size: 360bp; Annealing temp: 59°

Ref2bp SbE primer: GCTGTGGATCGATCTGTGACG- **T**(B6)/**C**(Sle1b) [22bp]

BAC25

Ly9 SeqSNP F: GGTAAGGAATCCTGGGAGAGC

Ly9 SeqSNP R: TGAGCACACATAGGCATGGT

Product size: 250 bp; Annealing temp: 66°

Ly9 SbE primer: TGGTCAGAGGTCCTCACCTCC- **G**(B6)/**T**(Sle1b) [23bp]

BAC40

Cd48 SeqSNP F: GCAGCAATGTAACCCTGAAAA

Cd48 SeqSNP R: TCCAGGGTTATCTTCAACTCGT

Product size: 260bp; Annealing temp: 59°

Cd48 SbE primer: TCCGGACATTAGAGATATGAAGTGCACCAT- T(B6)/C(Sle1b)

[31bp]

BAC90

Ly108 gen SeqSNP F: GCATGGTGAGGGATGTTTTT

Ly108 gen SeqSNP R: CTGGCAGGATGTGGTTCTTT

Product size: 400bp; Annealing temp: 59°

Ly108gen SbE primer: TGTCCTTAACTGAGGTCTTTTCTTTTATGTAGAACGA-

C(B6)/T(Sle1b) [39bp]

BAC95

Nic gen SeqSNP F: CCGGAGCTAGACCAGTTGAA

Nic gen SeqSNP R: GCTGCAGAGGGACAGAACTC

Product size: 265bp; Annealing temp: 59°

Nic gen SbE primer: TAAGCATGCTCCATACGTTGTAGTC- G(B6)/A(Sle1b) [26bp]

Primers used to detect expression of candidate B6-transgenes in splenic cDNA:

BAC41

Usp23 cds SeqSNP F: ATGCCCAAGAGTTCCTGAAG

Usp23 cds SeqSNP R: AAATCCTTTCTTGGGGATGG

Product size: 330bp; Annealing temp: 63°

Usp23cds SbE primer: ATGAAGAACCTGAGTTGAGTGATGA- T(B6)/C(Sle1b) [26bp]

Nit1 cds SeqSNP F: ACTGAATGGGGATCTTTTGG

Nit1 cds SeqSNP R: CAGTGGGCTGGACCTGTAAC

Product size: 400bp; Annealing temp: 63°

Nit1cds Sbe primer: GCTTGGTATAGTTGCTTTCTCTCAT- **C(B6)/T(Sle1b)** [26bp]

BAC47

Ref2bp SeqSNP F: AAGTGGCAGCACGACCTATT

Ref2bp SeqSNP R: AGAGCCACGGCTCCTTGT

Product size: 360bp; Annealing temp: 59°

Ref2bp SbE primer: GCTGTGGATCGATCTGTGACG- **T(B6)/C(Sle1b)** [22bp]

BAC25

Ly9 SeqSNP F: GGTAGGAATCCTGGGAGAGC

Ly9 SeqSNP R: TGAGCACACATAGGCATGGT

Product size: 250 bp; Annealing temp: 66°

Ly9 SbE primer: TGGTCAGAGGTCCTCACCTCC- **G(B6)/T(Sle1b)** [23bp]

CS1 SeqSNP F: CTTCACTCAGGGGCATCCTA

CS1 SeqSNP R: CCGTGTAAGGGATTGTGTCA

Product size: 200bp; Annealing temp: 59°

CS1 SbE primer: CTGTCTTGCTGACTATTTTTCATACTA- **T(B6)/C(Sle1b)** [28bp]

BAC40

Cd48 SeqSNP F: GCAGCAATGTAACCCTGAAAA

Cd48 SeqSNP R: TCCAGGGTTATCTTCAACTCGT

Product size: 260bp; Annealing temp: 66°

Cd48 SbE primer: TCCGGACATTAGAGATATGAAGTGCACCAT- **T(B6)/C(Sle1b)**
[31bp]

Slam SeqSNP F: ATTGCCCAGTGATTCTCCAG

Slam SeqSNP R: TTCAGCTGCTTGCAGAATTG

Product size: 260bp; Annealing temp: 66°

Single base extension primer: 320bp; Annealing temp: 59°

Slam SbE primer: AGGATGGCTACCACTTTCAATC- **A(B6)/G(Sle1b)** [23bp]

BAC90

Ly108 cds SeqSNP F: ACACTGCGCAGATAACCACA

Ly108 cds SeqSNP R: GCTCCAGCACACAAAGATGA

Product size: 420bp; Annealing temp: 59°

Ly108cds SbE primer : TTCAAATATATTCTGAGGGTCTTTGAACGA- **C(B6)/T(Sle1b)**
[31bp]

Cd84 cds SeqSNP F: GTCCAGCAGCCATGTACAGA

Cd84 cds SeqSNP R: GCTGCACTGAGGAATAAATGG

Product size: 300bp; Anealing temp: Touchdown to 58° (Annealing 65°, -0.5/cycle, 13X,
followed by 20X at annealing 58°)

Cd84cds SbE primer: TGTTGGCATTCTGTTCGGTTTGTA- **T(B6)/C(Sle1b)** [26bp]

BAC95

Nic cds SeqSNP F: GCAGCTCTTCTCACACATGC

Nic cds SeqSNP R: AGTTTCCCCCTGGAAGAAGA

Product size: 360bp; Annealing temp: 59°

Nic cds SbE primer: TAAGCATGCTCCATACGTTGTAGTC- **G(B6)/A(Sle1b)** [26bp]

Copa SeqSNP F: ACTGGCAACCTGGAGAACTT

Copa SeqSNP R: GGGCCAGTTTGTATCCAATG

Product size: 300bp; Annealing temp: 59°

Copa SbE primer: GGCAGAAATCCCTAGCCTATCTC- **T(B6)/A(Sle1b)** [24bp]

PxfEx2 SeqSNP F: CAAACCCTCCCCAGAACAT

PxfEx2 SeqSNP R: CTTGCTGAGAACTTGCATCG

Product size: 275bp; Annealing temp: 59°

Pxf Ex2 SbE primer: GAGCATCTTTGGCAGTATCTCCTG- **G(B6)/A(Sle1b)** [25bp]

Flow Cytometric Analysis and Antibodies. In each FACs experiment, at least one B6.*Sle1b* BAC-transgene negative littermate was included along with 12 month old female BAC-transgenic mice, and eight experiments also included one 12 month old female B6 control. Cells were blocked with 2.4G2 (American Type Culture Collection, Rockville, MD) on ice. Cells (1.5×10^6 per antibody cocktail) were then stained on ice using optimal amounts of FITC, phycoerythrin (PE), PE-Texas Red, Cychrome, PerCPCy5.5, APC or biotin-conjugated antibodies (Abs) at predetermined dilutions. Four-color combinations of the following antibodies, obtained from BD Biosciences Pharmingen (San Diego, CA) were used for the various analyses: CD45R (RA36B2); CD11b (M1/70); NK1.1 (PK126); CD69 (H1.2F3); CD4 (H129.19); CD8 (53-6.7); CD3 (145-2C11); CD19 (1D3); CD62L (MEL-14); CD44 (1M7), CD48 (HM48-1), and CD244.2(B6; 2B4). After two washes, biotin conjugated Abs were revealed using BD Pharmingen Streptavidin-APC. Appropriate isotype controls for all antibody combinations were included. Stained cells were acquired on a FACsCalibur with CellQuest software (BD Biosciences). Dead cells were excluded on the basis of forward and side scatter properties and 40,000 events within the lymphocyte gate were acquired per sample. Flow cytometric data was analyzed using FlowJo (Tree Star, Ashland, OR).

Statistical Analysis. FACs data were analyzed using non-parametric ANOVAs (Kruskal-Wallis test, followed by Dunn's post-test comparing each group to the background B6.*Sle1b* group) using InStat3 (Graphpad Software, San Diego, CA), and are shown as the Mean percentages \pm SEMs. Comparison of B6 to B6.*Sle1b* was also carried out in separate analyses, using parametric (t-test) or non-parametric (Mann-Whitney) measures as determined by InStat3. Differences in ANA penetrance in BAC-transgenic lines and their

negative littermate control groups were compared using Chi-square tests, and titers were analyzed using the non-parametric ANOVAs described above.

Table 1**(Annealing temp: 55°)**

Gene Name	Direction	Sequence (5' → 3')	Product Size (bp)
<i>B4galt3</i>	For Rev	TTCGACTATTCTCATCCCCACGAT CTTTCTGGACAGTAGGGCAATGCT	112
<i>Ppox</i>	For Rev	CAGATGGTGGCATCTTTGAAGTTG GACAGGCAAGACTTCAGACTCCAA	116
<i>Usp23</i>	For Rev	GAGTGGGAGCCAAGATACCATTTTC CTGGGAGGCAAAGGTCGTAACAT	100
<i>Ucf1</i>	For Rev	TCCGGTATGTGGAGAACAAACAAGA AGGAAATCGTGGATGTACCAGCAT	108
<i>Rpl27</i>	For Rev	GCGATCCAAGATCAAGTCCTTTGT GTCCCTGAACACATCCTTGTGAC	117
<i>Dedd</i>	For Rev	TGTGATATCAGGCTCCGAGTTC GGGTCCTGCTTATTGGAGAAGA	85
<i>Nit1</i>	For Rev	CATCAACACCAAACAAGCAAGAGA GGAGTAATGTCTCGGCAGGGTTT	138
<i>Pfdn2</i>	For Rev	GAGGGCAACAAGGAGCAGATAC ATGAGACGAATGTTGTGCTTTTC	110
<i>Usf1</i>	For Rev	ATGTACAGGGTGATCCAGGTGTCA GGATCACTGCCTGGGTCATAGACT	147
<i>Jam</i>	For Rev	GATCAGTGTCCTCCTCTGTCA ATATCCCGTCCTGAACCAGGAAT	106
<i>Itln</i>	For Rev	AACAGGTGGGGCAATTCTTTCTTT GTGCGCAGGAAATAGAGACCATCT	106
<i>Cd244</i>	For Rev	TCTGAAGAAGTGTTGGTGTCTCA CATCATTATACCAATTCAGGATCTCAA	141
<i>Cd229</i>	For Rev	TCCTGCACCTTCACCCTAATCTG GGGTGTGGCTTCCATCGTATGTAT	108
<i>Cs1</i>	For Rev	AGGAATCCAGTCAGCAACAGTTT AAAAATAGTCAGCAAGACAGCAAA	152
<i>Clpx</i>	For Rev	AACACCAGCATACTTTGCCTCAAAA TCCCAGAGGCTGATTTCTTACTGC	106
<i>Cd48</i>	For Rev	CTTGAAGAAAAACAATGGTGCACCT TTCACGCAGCACTCTCATGTAGT	84
<i>Cd150</i>	For Rev	CAAAACCCAGGAGAACGAGA CGGTGCAGTTGTAGATGCTG	187
<i>Cd84</i>	For Rev	GTCCAGCAGCCATGTACAGACACT GCCAACATCGGAATGAGAATAAGC	104
<i>Ly108</i>	For Rev	TCACAAGTCACTGCCCTCGTTATC CAGGGAGTAGGACTGGGTGATGTT	104
<i>Ltap</i>	For Rev	TGGATCCTGGAGAAGTATTACCAT AATACACCTTGAAGCCAGACACTT	105
<i>Nhlh1</i>	For Rev	TGGAAGCCTTCAACCTAGCCTTC ATGGCCAGGCGTAGGATCTCAAT	99
<i>Nic</i>	For Rev	CTGCTCAACGCCACTCATCAGATT GGTCAACACCCACTTCAGGTCTTC	104
<i>Copa</i>	For Rev	GCCTGTGAGAAAACCCACAGAT CGGTAAGATGCAGCACAAATGTCA	82
<i>Pxf</i>	For Rev	TGCTAATGGCGAACAGTGTCTGAT CCTCAGTTCCCAGTGACTCTGTTG	105
<i>Gapdh</i>	For Rev	TGCACCACCAACTGCTTAG GGATGCAGGGATGATGTTC	172

Table 1: Primers used for Real-time Quantitative PCR. An annealing temperature of 55° was used for all reactions

Table 2**CTLA4 (58°): 700 bp****F: TTCTCCTTGCCATAGCCAAC, R: GGACTCCAAACCAAGGAACA****MitD Loop-1 (55°): 500-600 bp (strain variation)****F: CTTAACACCAGTCTTGTAAC, R: CCTGAAGTAGGAACCAGATG****MitD Loop-2 (62°): 700 bp****F: CCAATGCCCCTTCTCGCT, R: TATAAGGCCAGGACCAAACCT****Cd48 Exon2 IgV (TD56°): 450 bp****F: AAATTTAGGCCACTGGATAGCA, R: CAGTCAACTCCCCTGATTCC****Cd48 Exon3 IgC (55°):****F: GGCTGTGGACAAGAGTCTCC, R: CCTCACACCTTTCTTCCTTCG****Cs1 Exon2 IgV (59°): 300 bp****F: TCACAGCAGCTTCTGGAAGTC, R: GACATGCAGCACATACTCCTG****Cs1 Exon 3 IgC (TD60°): 480 bp****F: AGGACCTGGATGTGGAAGGT, R: CCCACCCTGGTAGTTTCTCA****Cd84 Exon2 IgV (59°): 480 bp****F: TCAAAAGGAGAAGGAACACAAAA, R: TCAGAAATATGGGTGTGGTTTAGA****Cd84 Exon3 IgC (TD55°): 390 bp****F: TCTAAAAAGCTAACAACTGATTGTCAC, R: TTCCCAAAGTGATTTCTGAGG****Cd229 Exon2 IgV1 (60°): 450 bp****F: AATGAACGAAAGGTGGCTTG, R: TCAGTAGGGGATTGGTGGTG****Cd229 Exon3 IgC1 (55°): 450bp****F: GCTTCCCTACCATCACCTTC, R: TCCTCTGTCTCACCGAAACC****Cd229 Exon4 IgV2 (57°): 530bp****F: GTCCTTCAGTGTGGCTTGG, R: CCGCTGGTTCTAATGTTTCC****Cd229 Exon5 IgC2 (57°): 450bp****F: CAAACTCAGGATATCAACCTTGG, R: TATAAACAGCTTAGAACACAAACACTG****Ly108 Exon2 IgV (59°): 470bp****F: GGAACAGAAGGGGGTTATCA, R: GCACTCTCGTAGGCACACAC****Ly108 Exon3 IgC (TD57°): 330bp****F: GCATGGTGAGGGATGTTTTT, R: TCTGGGTCGAAACAGAGACTG**

Table 2 (contd)**Cd150 Exon2 IgV (58°): 450bp****F:** CAAATGTCTCCAGATCTTCCA, **R:** GAACCTTCTAGGCCCTCCTG**Cd150 Exon3 IgC (58°): 400bp****F:** ACAGTTCCGGGACCTTTGTT, **R:** GCATTGGATTTGCCATTGAT**Cd244 Exon2 IgV (TD56°): 500bp****F:** CTGAAGCTTAAGGAAGAGACAGG, **R:** GGTTCCTGGTCAGAGAGTTCTGG**Cd244 Exon3 IgC (60°): 400 bp****F:** CCCACTCTGTCCCTCTGATT, **R:** TGGGTCTCATGTGAATCTGG**Cd244 IgV+C (70°): 900 bp**(to amplify and sequence Cd244 extracellular regions from cDNA):**F:** GGTGTCTCAGGAAAGCCTGT, **R:** GGTGAAGTTCAGGGTGTGGT**Cd244 Allele-specific primers:** for expanded gene locus detection (TD60°): ~300bp**Type1****F:** TCAGGTTAGGGGTCTCAACA, **R:** TGAATTGGTGTAATGGTGGTC**Type 2****F:** TGTCTCAACATGATCTGGAA, **R:** CCTGACTTGGTGTAACAAGAA**Type 3****F:** GTGAGGTGTTTCAACGTGAT, **R:** GATCCTAAATTGGTGTAATTCTGA**Type 4****F:** TCAGGTGAGGTGTCTCAACA, **R:** TCCTGATTTCGTGTAATAATAATGC

Table 2: Primers used to amplify sequencing products. 35 cycles were carried out at the given annealing temperature. TD programs: 14 cycles, annealing temperature drops by 0.5°/cycle; 20 additional cycles at the given annealing temperature.

Chapter III. Association of Extensive Polymorphisms in the

SLAM Family Gene Cluster with Murine Lupus

Introduction

Genetic predisposition is a central element in susceptibility to many common autoimmune diseases, including systemic lupus erythematosus (SLE) (1,3,258). We have used congenic dissection to characterize the susceptibility genes in the lupus-prone NZM2410 mouse (151,156,159). These analyses identified *Sle1*, on murine chromosome 1, as causal for a loss in immune tolerance that leads to anti-nuclear autoantibody (ANA) production, on the B6 background. Interestingly, *Sle1* is syntenic with genomic intervals that are associated with susceptibility to SLE in human linkage studies (16,19).

Fine mapping of *Sle1* revealed a cluster of four loci (designated *Sle1a-Sle1d*) within the B6.*Sle1* congenic interval, each contributing some of the phenotypes originally associated with “*Sle1*” (26). *Sle1b* is the most potent member of this cluster, mediating gender-biased and highly penetrant ANA production in the B6.*Sle1b* congenic strain. *Sle1b* leads to fatal lupus nephritis when combined with the autoimmune-accelerating mutations *lpr* or *yaa*, illustrating the importance of this locus to lupus pathogenesis (259). Analyses of *Sle1* expression in mixed bone-marrow chimeras indicate that genes in the *Sle1* cluster are cell intrinsic, mediating activation phenotypes in both B and T cell lineages developed from B6.*Sle1*-derived bone marrow stem cells (157, 158). These results suggest that all of the susceptibility alleles in the *Sle1* cluster are expressed in lymphocytic lineages, although we have not repeated this experiment with bone marrow that vary at individual *Sle1*-cluster loci.

Under the direction of Dr. A. Wandstrat in the lab, we constructed a BAC contig spanning the *Sle1b* interval using a C57Bl/6J-derived BAC library produced by de Jong and co-workers (260) and the CJ7/129Sv-derived CalTech library (261), shown in Fig 1A. The complete BAC contig of *Sle1b* consists of 100 BACs, ensuring at least 6-fold coverage of the *Sle1b* region. Polymorphic markers derived from this contig positioned the proximal end of *Sle1b* critical interval to a ~10 kb interval between *ApoA2* and *B4galt3*, and the distal end a ~15 kb interval in the *Pxf* region (Fig 1B). This positions *Sle1b* within a genomic segment that is spanned by a tiling path of six C57BL/6J-derived BACs (BAC 41: 194d6, BAC 47: 48o11, BAC 25: 171k8, BAC 40: 145f9, BAC 90: 388c4, and BAC 95: 462j8; Fig 1A and B), which were sequenced to construct a transcriptional map of all the genes in the region (Fig 1B).

Here I describe the genomic characterization and candidate gene analysis of the *Sle1b* interval, which identifies a highly polymorphic seven-member cluster of SLAM/CD2-family genes in the middle of the *Sle1b* critical interval. Analyses of this family reveal extensive sequence and expression-level differences between B6 and B6.*Sle1b* and associate a subset of SLAM/CD2-family members with autoimmunity. Given the well-established role of this family in the modulation of cellular activation and signaling in the immune system, they are ideal candidates for mediating the *Sle1b* phenotype (for reviews see 177, 178, 179, 262, 263).

Results

Sequencing and construction of a molecular map of the *Sle1b* congenic interval.

We assembled more than 8700 high quality sequence reads for the analysis of the BAC inserts in this tiling path, which, when combined with sequence available in public databases (www.genome.ou.edu), provided between 9 to 19-fold coverage for the entire interval and produced a C57BL/6J consensus sequence composed of 10 ordered contigs. This sequence was analyzed using a variety of gene-finding software including PANORAMA (<http://atlas.swmed.edu>), GenescanII (<http://genes.mit.edu/GENSCAN.html>) and HMMgene (<http://www.cbs.dtu.dk/services/HMMgene>), by Dr. A. Wandstrat in the lab.

As shown in Fig. 1B, the *Sle1b* region is located between 171.3Mb and 172.2Mb along chromosome 1. This is a gene-dense 900kb genomic segment that contains 24 expressed genes and two pseudogenes, 19 of which are expressed in the spleen (bolded in Fig. 1B). Most notably, seven members of the SLAM/CD2 gene family (*Cd244*, *Cd229*, *Cs1*, *Cd48*, *Cd150*, *Ly108*, and *Cd84*) are clustered in the center of the *Sle1b* critical interval. These genes encode cell-surface molecules that mediate stimulatory and/or inhibitory signaling during cell-cell interactions between several hematopoietic cell lineages and are the only genes located within the *Sle1b* critical interval with obvious immunological functions (178,263).

Extensive polymorphisms distinguish the SLAM/CD2 family genes in B6 and B6.*Sle1b*

Two features of *Sle1b* were used to evaluate the candidacy of genes within the critical interval: 1) *Sle1b* may be expressed in many tissues, but is expressed in the spleen; and 2) *Sle1b* must be functionally polymorphic between B6 and B6.*Sle1b*. Quantitative real time PCR (RT-PCR) and Northern blot analysis carried out by C. Nguyen in the lab (171), determined that 19 genes within the critical interval are expressed in splenocytes (in bold in

Fig 1B). Functional polymorphisms in these 19 candidate genes were identified via structural and regulatory comparisons of the B6 and B6.*Sle1b* alleles. Structural polymorphisms were found by comparing allelic sequences from B6 and B6.*Sle1b* for each exon, together with relevant surrounding intronic material, and 5' and 3' UTRs. Transcriptional variations in these genes were assessed by real-time quantitative RT-PCR analysis in B and T lymphocytes from age and gender-matched B6 and B6.*Sle1b* mice.

Our analyses revealed extensive polymorphisms between B6 and B6.*Sle1b*, predominantly occurring in genes of the SLAM/CD2-family. The number of synonymous and non-synonymous coding-region polymorphisms found in the SLAM/CD2 family and non-SLAM/CD2 family genes are presented in Table 3. As summarized in Table 4 and Figs. 2 and 3, five members of the SLAM/CD2 family cluster (*Cd244*, *Cd229*, *Cs1*, *Cd48*, and *Cd84*) have transcriptional and structural polymorphisms with potential functional consequences. *Cd229*, *Cd84*, and *Cd48* contain a total of seven non-synonymous mutations in exons encoding their ligand-binding domains. The potential functional consequences of these sequence changes on the structures of the binding domains of these alleles were assessed by aligning their sequences with rat and human CD2, whose molecular structures have been solved (Fig. 2A and B; Cn3D alignment)(264,265). The polymorphism located in *Cd84* was found to be just proximal to the location of the A beta-sheet of the N-terminal V-Ig like domain (Fig. 2A). Of the four polymorphisms in the extracellular region of *Cd229* (Fig 2B), two (a.a. 58 and 70) occur in the C and C' beta sheet of the N-terminal V-Ig like domain respectively. Polymorphisms at amino acid position 109 are in the F beta sheet of the N-terminal C-Ig like domain, while position 118 is just proximal to the G beta sheet. Two recent studies implicate these segments of the binding site in ligand interactions. As shown in Fig. 2B, two of the polymorphisms located in the *Cd229* molecule (a.a. 58 and 118) align

with Interface contact residues in the hCD2-hCD58 structure (265). Furthermore, a recent analysis of Cd229 mutants implicated residues located in the C beta-sheet of the N-terminal V-Ig like domain (such as residue 58) in the homophilic binding of this molecule (234).

The SLAM/CD2 alleles of B6.*Sle1b* also differed from those of B6 in gene copy number. Genomic analysis of *Cd244*, a SLAM/CD2-family gene expressed in NK cells and CD8 T cells (but not B cells), determined that this gene is expanded from a single gene in B6 to a 4-locus cluster in B6.*Sle1b*, all of which encode extracellular ligand-binding domains that are highly divergent from that of the single *Cd244* molecule expressed in B6 (Table 3 and Fig 2C), and one of which seems to be a pseudogene, as evidenced by the presence of a premature stop-codon. Sequence analysis of cloned PCR products from B6.*Sle1b* splenic cDNAs suggests that one of these three *Cd244* genes (“Type 4”, Fig 2C) is expressed preferentially, although transcripts from all three genes are detectable in splenocytes. The nature of the cytoplasmic signaling domains of each of the *Cd244*-genes that form this expansion, and the functional consequences of these extensive variations in *Cd244* structure on NK cell function, remain to be determined.

Six non-SLAM/CD2 family genes in the *Sle1b* interval have one or more non-synonymous mutations (Table 4). *Usp23*, *Nit1*, *Ref2bp*, *Nic*, *Copa*, and *Pxf* are ubiquitously expressed genes having functions in metabolic and cellular processes, rather than immunological roles (266-270). Nicastrin (*Nic*) is a component of the γ -secretase complex, which functions in the intra-membranous proteolysis of, amongst other molecules, Notch, which generates the Notch intracellular domain involved in signaling. The functional implications of its role in the immunological context, however, remain unclear (271). Furthermore, the mutations in these genes are not located in highly conserved positions

(Table 4) or in motifs impacting protein phosphorylation, acetylation and/or glycosylation (based on analysis with PROSITE (www.expasy.ch/prosite)).

In experiments done with C. Nguyen in the lab, we found that four members of the SLAM/CD2-family, *Cd48*, *Ly108*, *Cd84*, and *Cs1*, vary in their expression in splenic B and/or T cells between B6 and B6.*Sle1b* (Fig. 3A and B). *Cd84* and *Ly108* are up-regulated in B cells from B6.*Sle1b* mice, while *Cs1*, *Cd48*, and *Ly108* are down-regulated in B6.*Sle1b* T cells. This differential expression was confirmed in B and T cell subsets at the cell surface level for *Cd48*, the only member for which a commercially available monoclonal antibody that recognizes both the B6 and B6.*Sle1b* alleles exists (data from V. Subramanian, in 171). These variations in expression were detected in young female mice (<12 weeks) well prior to the development of ANA or any other autoimmune phenotypes. In contrast, no variations in expression were found among the non-SLAM/CD2 family positional candidates (Figs 3A and B).

Real time quantitative PCR and Northern blot analysis by C. Nguyen in the lab has shown that there are significant differences in isoform usage for *Ly108* between B6 and B6.*Sle1b*, well prior to the initiation of the disease phenotype (171). *Ly108* produces two splice isoforms (here termed *Ly108-1* and *Ly108-2*) that differ by expressing alternative exons that encode divergent cytoplasmic signaling domains (235). Interestingly, *Ly108-1* contains two TxYxxV/I/A ITSM signaling motifs, while *Ly108-2* contains three, and the variation in isoform expression between B6 and B6.*Sle1b* results in a >5 fold increase in the ratio of *Ly108-1* to *Ly108-2* in B6.*Sle1b* B and T cells (data from C. Nguyen in 171). Such polymorphisms in splice isoform expression are likely to have functional consequences, and have been implicated as candidates for other autoimmune susceptibility loci (48,272,273).

In summary, genomic analyses detected extensive variations between B6 and B6.*Sle1b* within this region, predominantly in the SLAM/CD2-family cluster. Extensive structural and regulatory polymorphisms distinguished six of the seven genes in the SLAM/CD2 cluster. Many of these structural mutations impact molecular domains essential for the functions of these molecules. In addition, four of these genes vary between B6 and B6.*Sle1b* in their lymphocyte expression levels. In contrast, non-SLAM/CD2-family members exhibit much less structural variability and have no detectable changes in expression between B6 and B6.*Sle1b*.

Polymorphic SLAM/CD2 family haplotypes and the development of autoimmunity

The *Sle1b* genomic region was characterized in a panel of inbred laboratory strains to determine whether the highly divergent SLAM/CD2-family gene cluster in B6.*Sle1b* is a unique feature of the genome of the NZM2410 strain. Sequence analysis of the extracellular *Ig* regions of the SLAM/CD2 family revealed that, surprisingly, most of these strains carry alleles throughout the *Sle1b* interval that are indistinguishable from those of the autoimmune B6.*Sle1b*. The analysis was extended to a set of SNPs in genes flanking the SLAM/CD2 family. As shown in Fig. 4A, the SNPs within this genomic segment form two stable haplotypes across all the inbred laboratory strains assayed. The most conserved segment of the haplotype is centered over the SLAM/CD2 family, which deteriorates distal to *Dedd* on the centromeric side and proximal to *Pea15* on the telomeric side. The autoimmune-associated SNP haplotype of B6.*Sle1b*, termed SLAM/CD2 haplotype 2, is the most common version in laboratory strains, being detected in every autoimmune-prone strain analyzed as well as many non-autoimmune strains such as 129/SvJ (Fig 4B). A list of all of the SNPs

analyzed in the region and the subset that define the SLAM/CD2-family haplotype, along with the inbred laboratory strains analyzed, can be found in Table 5.

Although the *Sle1b* interval occurs as two stable haplotypes among the standard inbred strains, a detailed analysis of wild mice revealed extensive additional diversity and recombination throughout the entire region (Chapter 4). Fourteen fully inbred strains, derived from wild mouse stocks of different *Mus* sub-species, were also analyzed for the SLAM/CD2 family haplotype. Several of these strains carry recombinant versions of this region that share some alleles with B6, some with B6.*Sle1b*, and some unique alleles (Fig. 4B, Fig 5). Such recombinant strains may prove to be invaluable in further fine-mapping the gene(s) mediating autoimmunity in this region.

The prevalence of SLAM/CD2 haplotype 2 among non-autoimmune strains indicated that either this haplotype interacts with an additional gene(s) from the C57BL/6 genome to breach tolerance, or that an unidentified mutation unique to the SLAM/CD2 haplotype 2 in B6.*Sle1b* is responsible for the development of autoimmunity. To address this issue, we utilized marker-assisted selection to introgress a minimal congenic interval containing the SLAM/CD2 haplotype 2 from the non-autoimmune 129/SvJ strain onto the C57BL/6J background (253). As shown in Fig. 6A, although age-matched 129/SvJ mice are ANA negative, B6.*129c1* mice homozygous for the 129-derived SLAM/CD2 haplotype 2 on the B6 background have highly penetrant ANA production and are phenotypically indistinguishable from B6.*Sle1b*. Interestingly, Botto and co-workers recently reported a similar ANA phenotype in a B6.*129c1* congenic strain encompassing the *Sle1b* interval (7). These findings suggest that the SLAM/CD2 haplotype 2 of 129/SvJ and B6.*Sle1b* are equivalent in their capacity to mediate autoimmunity and that one or more additional allelic variations in the B6 genome interact with this haplotype to cause autoimmunity. This result illustrates the

importance of epistatic interactions with the B6 genome in the autoimmune phenotypes associated with *Sle1* (1,163). We also find that B6.*Castc1* congenic mice, which carry the “recombinant haplotype” CAST/Ei-derived *Sle1b* interval (Fig 4B and Fig5) introgressed onto the C57Bl/6 background (253), also develop highly penetrant ANA (Fig 6A). While the congenic interval in B6.*Castc1* is similar in size to that of B6.*Sle1* and consequently may contain other genes influencing autoimmunity (although CAST/Ei mice are not reported to be autoimmune-prone), a comparison of the structure of the *Sle1b* region in B6.*Castc1* with B6.*Sle1b* and B6.129c1 provides some useful insights. B6.*Castc1* carries alleles of *Nit1*, *Pxf*, *Nic*, and *Copa* that are similar or identical to B6 (Fig. 6B, Table 6), and different from B6.*Sle1b*, arguing against a role for these alleles in autoimmunity caused by *Sle1b*. B6.*Castc1* also excludes the amplification of *Cd244* as a candidate genetic polymorphism for *Sle1b*, in that B6.*Castc1* has a single *Cd244* gene closely related to that of B6. Two SLAM/CD2 family genes, *Cd229* and *Cs1*, are also unique alleles (in that they share some SNPs with B6 and others with B6.*Sle1b*), while the remaining SLAM/CD2 family alleles are shared by B6.*Castc1* and B6.*Sle1b*. Finally, the preferential expression of the *Ly108-1* splice isoform found in B6.*Sle1b*, has been found to be a property of haplotype 2-containing inbred strains, and has also been found in B6.*Castc1* (data from C. Nguyen, in 171). These results indicate that B6.*Castc1* carries a SLAM/CD2 family gene cluster that is most identical to B6.*Sle1b* in the telomeric portion of the haplotype.

Discussion

Genomic analysis of the critical interval for *Sle1b* has identified the SLAM/CD2 family gene cluster as the strongest candidate genes for the potent autoimmune phenotypes associated with *Sle1b*. The gene cluster is highly polymorphic, and autoimmunity is elicited in three independently-derived congenic strains carrying identical alleles for the telomeric portion of the SLAM/CD2 gene cluster. This suggests that the SLAM/CD2 haplotype 2-derived alleles of *Cd48*, *Cd150*, *Cd84*, and *Ly108* are the strongest susceptibility gene candidates. Although *Ly108* exhibits an intriguing preferential isoform expression, making it the strongest single gene candidate, it is equally feasible that more than one of these alleles participates in susceptibility to autoimmunity. In such a scenario, autoimmunity would be caused by the combined impact of two or more divergent alleles in the SLAM/CD2 family, possibly by influencing the functional properties of multiple immune cell lineages. The association of autoimmunity with a polymorphic haplotype, rather than a single allele, is reminiscent of the long established association of polymorphisms in the major histocompatibility complex with autoimmunity (258), as well as the recently reported association of Crohn's disease with polymorphisms in the human cytokine gene cluster (274).

SLAM/CD2 family molecules have been shown to transmit both stimulatory and inhibitory signals during cell-cell interactions between T cell, B cell, monocyte, and NK cell lineages (178,179,263). Each SLAM/CD2 family molecule is expressed in a specific set of immune cell lineages, and their expression is up-regulated by a variety of stimuli, including activation by antigen receptor systems, Toll receptors, and cytokines. Their co-stimulatory functions are activated via their adhesion during cognate antigen recognition between effector cells and APCs or targets. Phosphorylation of the ITSM motifs in their cytoplasmic domains activates their capacity to modulate a variety of immune functions, depending on the availability of downstream molecules in their signalling pathways (for reviews, see 177,178,262). Due to the complexities of these signalling processes, the functional

consequences of stimulation through these molecules are dependent upon a variety of factors, including their expression levels, functional avidity of the interactions involved, and the milieu of downstream signal transduction molecules expressed within the interacting cells. A variety of studies have demonstrated that their activation can modulate numerous immune functions, including T cell activation, cytokine secretion, and cytotoxicity (214,275).

Our analysis of *Sle1b* has revealed that the SLAM/CD2 gene cluster is extremely diversified in wild mice, and that two haplotypes are prevalent among standard laboratory mouse strains. SLAM/CD2 haplotypes 1 and 2 encode molecules that differ by multiple structural polymorphisms in regions critical to ligand binding, in expression levels on B and T lymphocytes, and in their preferential expression of specific isoforms. Such changes would be predicted to modulate their signalling properties during cellular interactions in the immune system and significantly impact immune activation. The preferential expression of a specific isoform of *Ly108* in SLAM/CD2 haplotype 2 is especially intriguing in this regard, since splice variants of *Cd244* have been shown to modulate between inhibitory and stimulatory functions for this molecule (276). Thus, the variation in *Ly108* splice variants that distinguish SLAM/CD2 haplotypes 1 and 2 may reflect a significant change in function for this molecule. Similar splice variations have been implicated in allelic variations associated with other autoimmune susceptibility genes (48,272,273).

The extensive diversity detected in immunoregulatory gene clusters such as the SLAM/CD2 gene cluster may be a consequence of pathogen-driven selection, which is anticipated to favour the maintenance of polymorphisms that functionally diversify immune responses against microbial pathogens (277). Several studies associate polymorphisms in the SLAM/CD2 family with resistance to viral diseases, including a prominent role in the regulation of EBV infections (reviewed in 263). This connection is intriguing with respect to the candidacy of SLAM/CD2 family polymorphisms as susceptibility alleles in human SLE. The human SLAM/CD2 family cluster is located in 1q23, a region in the human genome that has been associated with SLE susceptibility in multiple human linkage studies (16,17,19).

Interestingly, EBV infection has been implicated as an environmental trigger for SLE, raising the possibility that SLAM/CD2-cluster-mediated variations in the immune response to EBV infection may potentiate the development of autoimmunity (278-280). The link between autoimmunity and the SLAM/CD2 gene cluster is strengthened by evidence that mice deficient in the adaptor molecule SH2D1A or SLAM-associated protein (SAP), which directly binds to various members of this family of receptors, are protected from the experimental pristane-induced model of lupus (240). Given our association of variations in the SLAM/CD2 cluster with lupus susceptibility in mice, further work on the relationship of polymorphisms in the SLAM/CD2 cluster with susceptibility to SLE in humans is clearly warranted.

Our analyses demonstrate that SLAM/CD2 haplotype 2 alleles cause autoimmunity when they are expressed in the B6 strain, but not in several other laboratory strains, including 129/SvJ and NZW. These results suggest that it is the combination of the signalling properties of SLAM/CD2 haplotype 2 alleles *with* the downstream signal transduction pathways expressed in the B6 genome, which results in spontaneous autoimmunity. A variety of studies have demonstrated that the functional consequences of the signals transmitted by SLAM/CD2 molecules are dependent upon their interactions with several signal transduction pathways (reviewed in 177,177,178,262), and genetic variations effecting the functions of these pathways would be predicted to influence the consequences of SLAM/CD2 family signalling on the immune system. Thus, the signalling characteristics of SLAM/CD2 haplotype 2 is balanced by the downstream signal transduction properties expressed in the immune systems of inbred strains such as 129/SvJ, C3H, or BALB/c, and as a result, these mice are non-autoimmune. However, the combination of SLAM/CD2 haplotype 2 and the signal transduction milieu expressed in B6 mice results in a poorly regulated immune system that is prone to autoimmunity. The observed autoimmunity of B6.129c1 mice suggests caution in the interpretation of autoimmune phenotypes expressed in mice with gene ablations that have B6 X 129 hybrid genomes, as we and others have suggested previously (1, 7).

These results provide a clear example of the manner in which epistatic interactions between two polymorphic genetic systems can lead to autoimmune susceptibility. It is *in combination* with one or more polymorphic genes in the B6 genome that the SLAM/CD2 haplotype 2 alleles lead to an imbalanced immune system. The importance of contributions from the B6 genome to the autoimmune phenotypes of *Sle1* was previously revealed by our analysis of interactions between NZW and B6.*Sle1* in which we identified 4 loci in NZW that suppress autoimmunity elicited by B6.*Sle1*, which we designated *Sles1* through *Sles4* (for SLE suppressor, 163). It is tempting to speculate that some of these suppressive modifiers may impact the signal transduction pathways that interface with SLAM/CD2 family molecules.

Fig 1A. A complete BAC contig of the *Sle1b* congenic interval. Markers from the proximal to the distal end of the interval, used to order the BACs within the contig, are shown from left to right across the top of the figure. BAC clones are listed from top to bottom, with the markers that they were positive for highlighted. The smallest congenic interval that expressed the *Sle1b* component phenotype is carried by B6.*Sle1b* which has an NZM2410-derived genomic interval defined by an NZM2410 allele for *DIMit113* and B6 alleles for *DIMit148* on the proximal end and *DIMit149* on the distal end. The complete BAC contig of *Sle1b* consists of 100 BACs from the RPCI-23 and CalTech (indicated by the letter “C” before the BAC name) libraries, ensuring at least 6-fold coverage of the *Sle1b* region.

Fig 1B

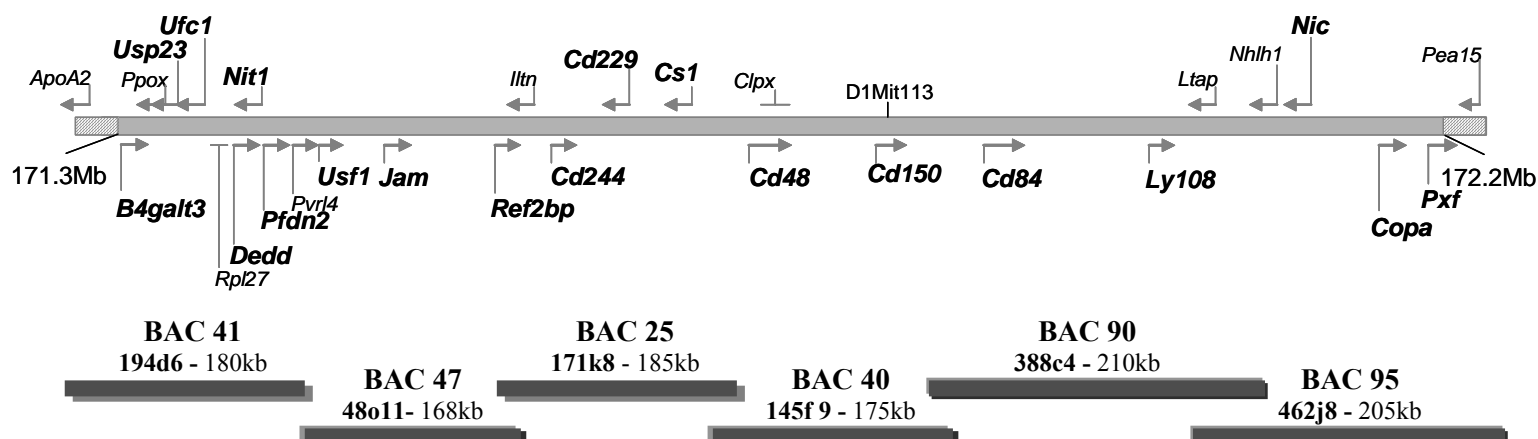


Fig 1B. A detailed molecular map of the *Sle1b* critical interval. A detailed transcriptional map was obtained by sequencing six overlapping B6-derived tiling path BACs. The peak linkage marker D1Mit113 resides within the CD150 gene. The gray bar denotes the area in the *Sle1b* region by congenic breakpoint mapping. Hatched bars denote the area outside the *Sle1b* interval. Arrows denote transcriptional direction of genes, and lines without arrows denote pseudogenes. Solid black bars denote the tiling path BACs used, with the BAC-numbers assigned to them in this study, and their respective RPCI-23 designations and sizes, indicated above each.

Table 3

	Non-synonymous SNPs	Synonymous SNPs
<i>B4galt3</i>	0	5
<i>Usp23</i>	1	2
<i>Ufc1</i>	0	0
<i>Dedd</i>	0	2
<i>Nit1</i>	1	1
<i>Pfdn2</i>	0	1
<i>Pvrl4</i>	0	5
<i>Usf1</i>	0	3
<i>Jam</i>	0	1
<i>Ref2bp</i>	1	1
<i>Cd244-1</i> ¹		(20) ²
<i>Cd244-2</i> ¹		(29) ²
<i>Cd244-3</i> ¹		(pseudogene)
<i>Cd244-4</i> ¹		(30) ²
<i>Cd229</i>	7	5
<i>Cs1</i>	2	0
<i>Cd48</i>	2	0
<i>Cd150</i>	0	2
<i>Cd84</i>	1	1
<i>Ly108</i>	0	3
<i>Nic</i>	3	5
<i>Copa</i>	3	7
<i>Pxf</i>	1	0

Table 3. Candidate gene analysis of the *Sle1b* congenic interval. All synonymous and non-synonymous coding-region SNPs between B6 and B6.*Sle1b* are shown. ¹The *Cd244* gene is expanded to four in B6.*Sle1b*, three of which are transcribed. ²The amino acid differences between B6 and the three transcribed B6.*Sle1b* *Cd244* genes were determined only for the extracellular IgV and IgC domains.

Table 4

Gene	Function	Genbank Accession Number	Position (amino acid)	Amino Acid Change ¹		Other Species ²	
				B6	NZW	Conserved	Not Conserved
<i>Usp23</i>	Intracellular protein breakdown and cell cycle regulation.	BAB27431	341	C	R	Human	Rat Drosophila Yeast
<i>Nit1</i>	Cleaves nitriles and organic amides.	NP_036179	22	T	I		Human
<i>Ref2bp</i>	RNA and export factor binding protein 2.	NP_062357	151	T	A	Human Rat Chicken Xenopus	Drosophila Arabidopsis
<i>Cd229</i>	Adhesion/costimulatory molecules that regulate activation threshold in many immune cell lineages.	NP_032560	58	I	T	Human	
			70	F	S		Human
			109	H	Y		Human
			118	I	T		Human
			345	K	N		Human
			356	E	K		Human
			571	G	E	Human	
<i>Cs1</i>	See <i>Cd229</i> .	AAH11154	248	M	T		Human
			253	G	R		Human
<i>Cd48</i>	See <i>Cd229</i> .	P18181	4	I	R	Human	Rat
			90	N	D	Rat	Human
<i>Cd84</i>	See <i>Cd229</i> .	NP_038517	27	V	M		Human
<i>Nic</i>	Integral membrane protein that interacts with presenilin-1 and -2.	AAH19998	21	S	F		Human
			678	T	I	Human	Drosophila C. elegans Arabidopsis
			680	V	I	Human Drosophila C. elegans	Arabidopsis
<i>Copa</i>	Housekeeping gene.	NP_034068	761	S	T	Human Drosophila Arabidopsis	C. elegans
			984	N	S	Human	Drosophila C. elegans Arabidopsis
			1110	N	S	Human Drosophila C. elegans	Arabidopsis
<i>Pxf</i>	Perioxysomal biogenesis.	NP_075528	55	P	S ³	Human Rat Hamster	Drosophila ³ C. elegans

Table 4. Candidate gene analysis of the *Sle1b* congenic interval. Amino acid changes between the B6 and NZW (B6.*Sle1b*) parental strains are evaluated for their possible significance, by examining whether they occur in evolutionarily conserved residues. ¹Amino acids listed in bold represent the conserved version. ²Sequence was not available for every species. ³S is conserved in Drosophila.

Fig 2A.

	A										
hCD2	KEIT	N	A	L	E	T	W	G	A	L	G
ratCd2	R	D	S	G	T	V	W	G	A	L	G
B6-Cd84	A	D	P	V	V	M	N	G	I	L	G
NZW-Cd84	A	D	P	M	V	M	N	G	I	L	G

Fig 2B.

	C												C'									
hCD2	D	I	D	D	I	K	W	E	-	K	T	S	D	K	K	K	I	A	Q	F	R	K
ratCd2	D	I	D	E	V	R	W	E	-	R	G	S	-	-	T	L	V	A	E	F	K	R
B6-Cd229	E	I	E	H	I	I	W	N	c	P	P	K	-	-	A	L	A	L	V	F	Y	K
NZW-Cd229	E	I	E	H	I	T	W	N	c	P	P	K	-	-	A	L	A	L	V	S	Y	K
		#	#			#								#	#	#					#	
		*	*			*		*						*	*	*		*			*	*

	F												G ➔			
hCD2	D	I	Y	K	V	S	I	Y	D	T	K	G	K	N	V	L
ratCd2	G	T	Y	N	V	T	V	Y	S	T	N	G	T	R	I	L
B6-Cd229	G	S	Y	H	A	Q	I	N	Q	K	N	V	I	L	T	T
NZW-Cd229	G	S	Y	Y	A	Q	I	N	Q	K	N	V	T	L	T	T
						#					#	#	#			
						*		*	*	*	*	*	*			

Fig 2. Candidate gene analysis of the *Sle1b* congenic interval. Sequence alignment of rat and human CD2 with B6 and NZW versions of **A.** Cd84 and **B.** Cd229 extracellular regions. β strand positions were determined from rat Cd2 structure and are marked by an overline. Boxed residues denote polymorphisms between the parental murine strains. #, Interface contact residues in the hCD2-hCD58 structure; *, residues in the interface.

Fig 3A

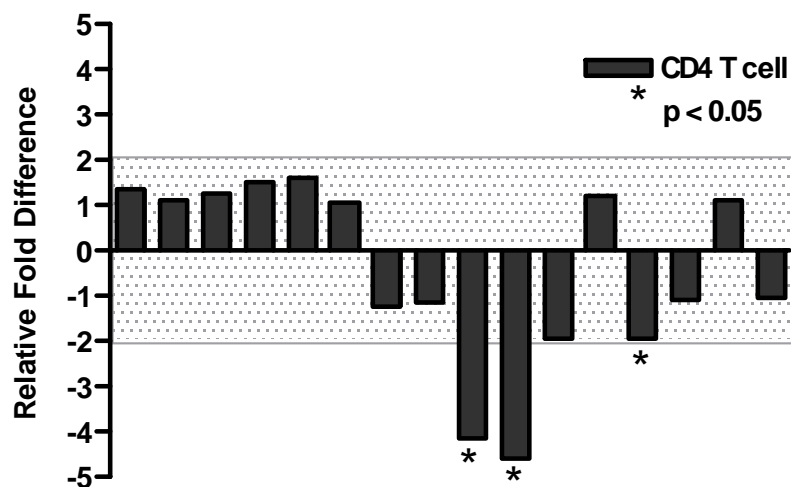


Fig 3B

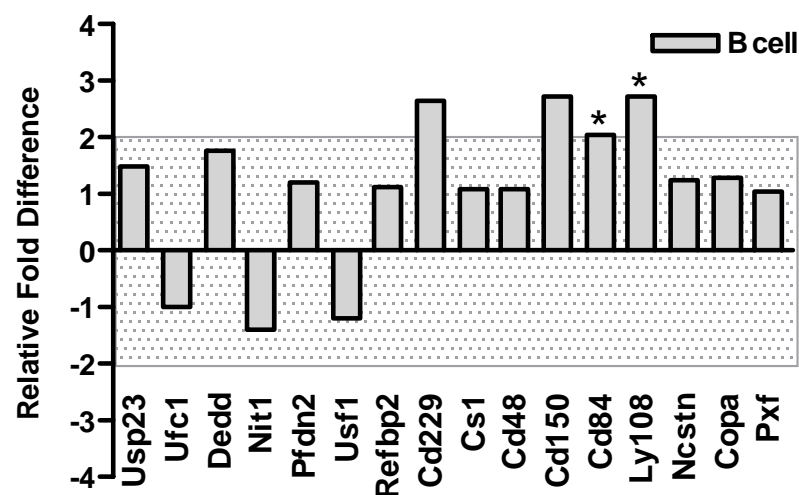


Fig 3. Candidate gene analysis of the *Sle1b* congenic interval, showing expression in splenic **A.** CD4⁺ T and **B.** B cells of candidate genes in 6-8 week old female B6 and B6.*Sle1b* mice (n=5 to 7) by real-time PCR. Data is expressed as relative fold difference compared to B6. The grey hatched box represents a 2-fold difference, used as the minimal cut-off for identifying genes that are differentially expressed.

Fig 4A.

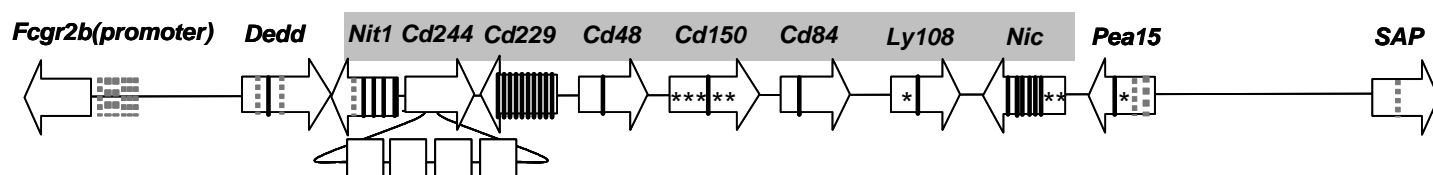


Fig 4B.

SLAM haplotype1 B6-Like	C57BL/6, C57BL6/By, C57BR/cdJ, C57L/J, RF/J, MOLF/EiJ, MOLE/EiJ
SLAM haplotype 2 Sle1b-Like	129/SvJ, A/J, AKR/J, BALB/cJ, C3H/HeJ, CBA/J, CE/J, DBA/2J, DDY/Jcl, LP/J, MRL/MpJ, NOD/Lt, NZB/B1WJ, NZW, P/J, PL/J, SB/Le, SEA/GnJ, SJL/J, SM/J, WB/Re, PERA/EiJ, PERA/RkJ, PERC/EiJ, SK/CamEiJ, SF/CamEiJ
Recombinants between haplotypes 1 and 2	CAST/EiJ, CASA/RkJ, CALB/RkJ, MOLC/EiJ, MOLD/EiJ, CZECHI/EiJ, SK/CamRkJ

Fig 4. Haplotype analysis of the *Sle1b* interval. **A.** The *Ig* domains of the *SLAM/CD2* genes, and a subset of SNPs from flanking genes, were sequenced in 34 inbred laboratory strains. Two stable, divergent haplotypes (Haplotypes1 and 2) were observed. SNPs that distinguish the two haplotypes are shown as solid black lines, and the genes falling into the haplotype-block are highlighted in grey. *Cd244* shows a gene expansion into a 4-gene locus, in Haplotype2. SNPs that lie outside the haplotype region and do not follow strain-specific patterns are shown as dotted grey lines. Asterisks represent additional SNPs found in a single strain. **B.** The mouse strains that share the B6-like version (*SLAM/CD2* haplotype1), and B6.*Sle1b*-like version (*SLAM/CD2* haplotype 2). Analysis of 14 wild-derived inbred strains identified additional strains carrying either haplotype, and some “recombinants” with part of haplotype 1 and part of haplotype 2.

Table 5

Gene Name	Genbank Accession	SNP Location	Nuc Postn (Genbank)	Nucleotide		Amino Acid		SNP distinguishes Haplotypes ¹
Fcgr2b	NM_010187	Promoter	362 285 261 174 83 30	C CAT GCTTGGAACCCTA C G G	T deleted deleted T A A	- - - - - -	- - - - - -	No No No No No No
Dedd	AJ011386	Exon	202 249 321	T T C	C C A	L R R	L R R	No Yes ² No
Nit1	NM_012049	3' UTR	1175	T	C	-	-	No
		Intron	638+45 638+10	T A	C G	- -	- -	Yes Yes
		Exon	567	A	G	P	P	Yes
		5' UTR	122	T	C	-	-	Yes ²
<i>Cd244</i> ³	<i>NM_018729</i>	<i>Gene</i>		<i>1 Gene Locus</i>	<i>Duplication to 4 loci</i>			<i>Yes</i> ⁴
Cd229	NM_008534	Exon	1187 1080 1049 879 367 339 338 320 223 187	C G G C T C C A T T	T A C A C T T G C C	N E K R I H Y K F I	N K N R T Y Y K S T	Yes ² Yes ² Yes ² Yes Yes Yes Yes Yes Yes Yes Yes
Cd48	X53526	Exon	318	A	G	N	D	Yes
Cd150	NM_013730	Exon	143 175 264 363 441 654	G C G A T C	C T A G G T	G L A S V H	G L A S V H	NZB only NZB only NZB only Yes NZB only NZB only

Table 5 (contd)

Gene Name	Genbank Accession	SNP Location	Nuc Postn (Genbank)	Nucleotide		Amino Acid		SNP distinguishes Haplotypes ¹
Cd84	AF043445	Exon	133	G	A	V	M	Yes
Ly108	AF248635	Exon	570 604	C C	T T	I L	T L	NZB only Yes ²
Nic	AF240469	3' UTR	2161	G	C	-	-	Yes
		Exon	2108	C	T	F	F	Yes
			2063	T	C	S	S	Yes
			2055	A	G	I	V	Yes
			2050	T	C	I	T	Yes
			1626	C	T	L	L	Yes
			1597	A	G	K	R	SWR only
			1547	C	T	I	I	PL/J only
Pea15	NM_008556	3' UTR	1362	T	C	-	-	Yes
			1350	T	C	-	-	PL/J only
			1226	G	A	-	-	No
		Exon	1106	deleted	GAA	none	E	No
SAP	MUSSAPRA	Intron	223+48	G	A	-	-	No

Table 5. Haplotype analysis of the *Sle1b* interval. This table shows the SNPs included in the haplotype analysis of extracellular *Ig* domains of the SLAM/CD2 gene cluster and flanking gene products, from the most proximal, to the distal.

¹Haplotype1 (B6-like) strains: C57Bl/6, C57Bl6/By, C57BR/cdJ, C57L/J, RF/J, and

Haplotype2 (B6.*Sle1b*-like) strains: 129/SvJ, A/J, Akrl/J, BALB/cJ, C3H/HeJ, CBA/J, CE/J, da/hsn, DBA/2J, ddy/j, fl/ire, FVB/NJ, htg/gosfsn, LP/J, MRL/MpJ, NOD/Lt, NZB/BINJ, NZW, NZW/LacJ, P/J, PL/J, r3/dmmob, SB/Le, SEA/GnJ, SJL/Bm, SJL/J, SM/J, SWR/J, WB/Re.

²There were two or less strain exceptions which “switched” haplotypes for these SNPs: Dedd¹: r3/dmmob; Nit1¹: AKR/J and r3/dmmob; CD229¹: SWR/J; Ly108¹: FVB/NJ and SWR/J

³More detailed information on the changes in Cd244 expanded locus extracellular domains can be found in Fig 2C.

⁴The 34 inbred lab strains were tested for the presence of B6-like Cd244 and the duplicated *Sle1b*-like Cd244 loci by PCR using allele-specific primers for each. AKR/J, DDY/JcL, FVB/NJ, and r3/dmmob were positive for 3 of the 4 duplicated *Sle1b*-like CD244 loci (types 2, 3 and 4, from Fig 2C). With these exceptions, the Cd244 duplication also fell into the two SLAM/CD2 haplotypes.

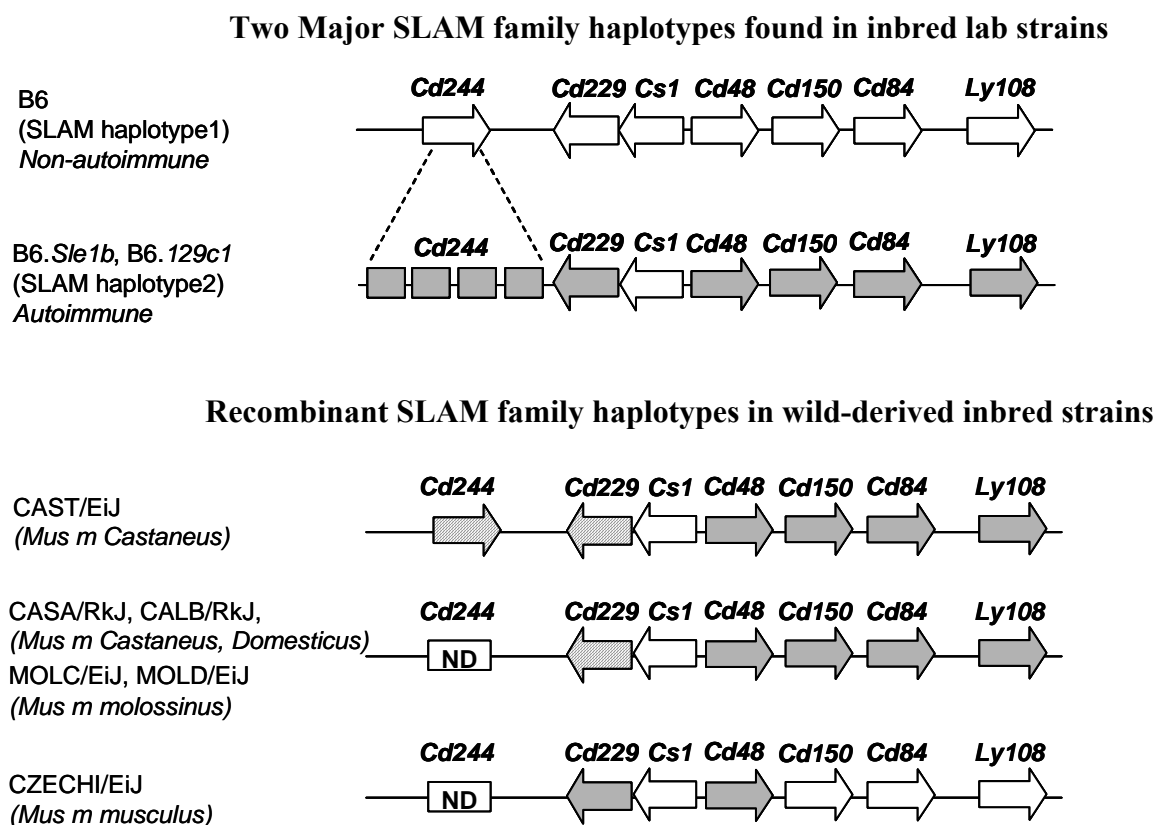
Fig 5

Fig 5. Haplotype analysis of the *Sle1b* interval. Recombinant SLAM/CD2 family haplotypes found in inbred strains derived from wild mouse stocks belonging to different *Mus* subspecies are shown. The extracellular *Ig* domains of the SLAM/CD2 family of genes were amplified by PCR and sequenced in 14 wild-derived inbred strain DNAs. Recombinant versions of the SLAM/CD2 haplotype, found in seven of these strains, are indicated. Arrows indicate transcriptional direction, and colors represent the different alleles: Clear for B6-like, grey for B6.*Sle1b*-like, and hatched for unique alleles. ND refers to strains in which the CD244 allele was not determined.

Fig 6A

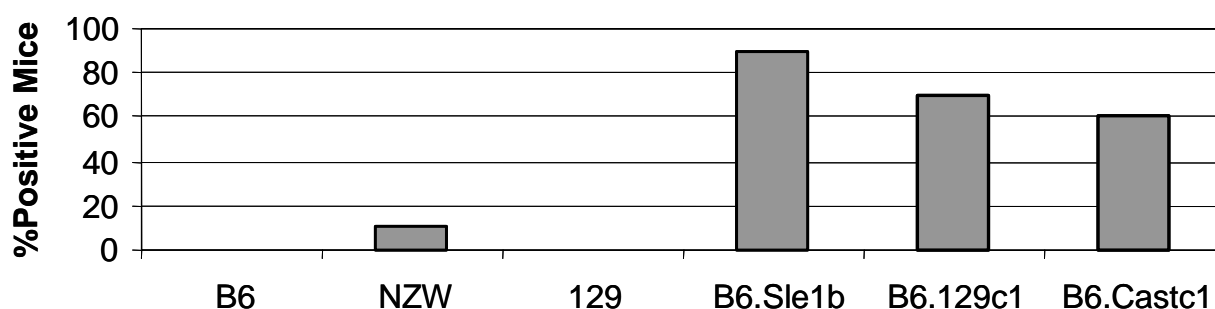


Fig 6B

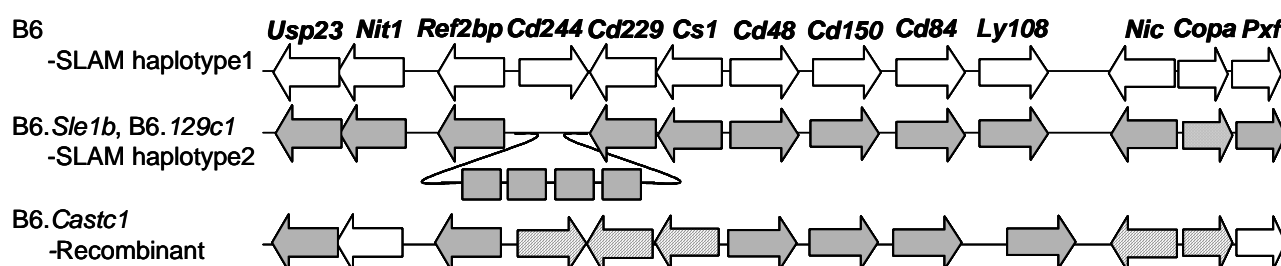


Fig 6. Analysis of mice congenic for the *Sle1b* locus, with intervals derived from NZM2410 (NZW), 129/SvJ, and CAST/Ei. **A.** Penetrance of ANA-production in *Sle1b*-region congenics. Sera from nine or more 9-month-old female mice were assayed for α -total histone/dsDNA IgG ANA by ELISA. Sera were assayed at a dilution of 1:800. For interplate comparisons, serial dilutions of a chromatin-specific hybridoma supernatant were included to construct a standard curve. Sera were considered positive if they scored higher than the mean value + 4 SD of eleven 12-month-old B6 females. **B.** Allelic comparisons between the autoimmune-prone B6.*Sle1b*, B6.*129c1*, and B6.*CASTc1* congenic mice and B6 were performed for all the productive polymorphisms previously found in the *Sle1b* candidate genes. B6 alleles are shown as white arrows. NZM2410 and 129/SvJ share the same alleles, shown as gray arrows. The exception is *Copa*, for which 129/SvJ differs from NZM2410 by a single productive SNP. CAST/Ei alleles not shared with B6 or B6.*Sle1b* are shown as hatched arrows.

Table 6

Gene	Function	Genbank Accession Number	Position (amino acid)	Amino Acid			
				B6	NZW	129	B6.CastC1
<i>Usp23</i>	Intracellular protein breakdown and cell cycle regulation.	BAB27431	341	C	R	R	R
<i>Nit1</i>	Cleaves nitriles and organic amides.	NP_036179	22	T	I	I	T
<i>Refbp2</i>	RNA and export factor binding protein 2.	NP_062357	151	T	A	A	A
<i>Cd229</i>	Adhesion/costimulatory molecules that regulate activation threshold in many immune cell lineages.	NP_032560	58	I	T	T	I
			70	F	S	S	S
			109	H	Y	Y	H
			118	I	T	T	T
			345	K	N	N	N
			356	E	K	K	K
<i>Cs1</i>	See <i>Cd229</i> .	AAH11154	248	M	T	T	T
			253	G	R	R	G
<i>Cd48</i>	See <i>Cd229</i> .	P18181	4	I	R	R	R
			90	N	D	D	D
<i>Cd84</i>	See <i>Cd229</i> .	NP_038517	27	V	M	M	M
<i>Ncstn</i>	Integral membrane protein that interacts with presenilin-1 and -2.	AAH19998	21	S	F	F	S
			678	T	I	I	I
			680	V	I	I	V
<i>Copa</i>	Housekeeping gene.	NP_034068	761	S	T	T	T
			984	N	S	S	N
			1110	N	S	N	N
<i>Pxf</i>	Perioxysomal biogenesis.	NP_075528	55	P	S	S	P

Table 6. Candidate gene analysis of the *Sle1b* interval. Non-synonymous SNPs previously found to distinguish between B6 and the NZW-derived B6.*Sle1b* congenic strain, were subsequently sequenced in 129 and B6.*CastC1*, to find the alleles common to all three autoimmune-prone congenic strains. This table shows the positions and identities of amino acid changes between B6 and NZW, along the residues found at these same positions in the 129 and B6.*CastC1* strains.

Chapter IV. Retention of Autoimmune Susceptibility Alleles in Natural Populations

Introduction

The genetic basis of complex autoimmune diseases like Systemic Lupus Erythematosus (SLE) and diabetes is well accepted; however, identification of their genetic underpinnings has proven to be quite elusive. Rare mutations that have strongly deleterious effects and act in a monogenic, Mendelian fashion can undoubtedly cause these diseases, as evidenced by the panoply of mouse models in which aberrant expression or function of genes due to their overexpression in transgenics or ablation in targeted mutants, causes autoimmunity (reviewed in 3, 42, 281). In humans as well, deficiencies in complement components *C1* and *C4* cause lupus with a high penetrance (reviewed in 1, 10). The highly deleterious nature of such aberrant alleles, however, makes them relatively rare in natural populations, and they account for a very small proportion of the observed autoimmunity in humans. Autoimmunity is more commonly mediated in a heterogeneous, polygenic manner, with multiple genes acting in concert to cause the overall phenotype. Numerous such susceptibility loci have been identified in human and mouse (1, 281); however, the identification of candidate genes within these loci remains a challenge.

Polymorphisms within a cluster of seven members of the SLAM/CD2 family of immunoregulatory receptors have recently been implicated in autoimmune susceptibility in a murine model of lupus (171, Chapter 3). *Cd244* (*2B4*), *Cd229* (*Ly9*), *Cs1*, *Cd48*, *Cd150* (*SLAM*), *Cd84*, and *Ly108* are located within the *Sle1b* susceptibility locus on telomeric mouse chromosome 1 and have been identified as the strongest candidates to mediate the loss in tolerance to chromatin that results in the production of anti-nuclear autoantibodies (ANAs) in B6.*Sle1b* congenic mice, which carry this NZW-derived locus on the C57BL/6 (B6)

genetic background (171). SLAM/CD2 family members are expressed on a variety of hematopoietic cells with dual activating and inhibitory co-receptor functions (for reviews, see 179, 177, 262). They belong to the immunoglobulin (Ig) receptor superfamily and are characterized extracellularly by an N-terminal IgV domain followed by a membrane-proximal, disulfide bonded IgC domain, encoded by exons 2 and 3 respectively. Sequence analysis of these exons (as well as exons 4 and 5 in *Cd229*, which has two IgV and two IgC domains) in a large panel of common inbred laboratory strains revealed that they form only two stable haplotypes across all of these strains. Haplotype 1 is found in B6, other C57-derived strains, and the RF/J strain. Haplotype 2 is far more common, being shared by numerous autoimmune-associated strains like NZW, NZB, NOD, and MRL, as well as non-autoimmune strains like 129, BALB/c, C3H, DBA/2 and many others. It can potentiate autoimmunity on the B6 genetic background in congenic strains that derive the region from different parental donors (NZW and 129; 7, 171). The two haplotypes are distinguished by numerous single nucleotide polymorphisms (SNPs) and an expansion of the *Cd244* gene into four loci in the autoimmune-linked Haplotype 2.

In order to assess whether both haplotypes are present even in wild outbred populations of mice, or whether the prevalence of Haplotype 2 reflects the artificial conditions of inbreeding in laboratory strains, the current study extends our analysis of the SLAM/CD2 family Ig regions to a panel of DNAs from 15 wild-derived inbred strains (listed in Table 7A) and 33 wild, natural (outbred) populations of mice (listed in Table 7B) that belong to five different species of *Mus* (*Musculus*, *Spretus*, *Macedonius*, *Spicilegus*, and *Pahari*). The polytypic *Mus musculus* species strains are further classified into the subspecies *Mus m musculus*, *Mus m domesticus*, *Mus m castaneus*, *Mus m molossinus*, and *Mus*

m Spp. A schematic representation of the estimated evolutionary distances and distributions of these strains is shown in Fig 7. The duplicated *Cd244* locus was omitted from this analysis.

We find that both haplotypes are present in the wild-derived inbred strains; however, there is a much greater degree of polymorphism, and no haplotypes discernable in the wild, outbred mice. Phylogenetic tree analyses reveal that each of these extracellular binding domains shows the presence of ancestral polymorphisms: multiple species and sub-species share branches or alleles, i.e., the alleles from one species are often closer to alleles from a widely divergent species, than other alleles from the same species. Such a pattern is indicative of the maintenance of these polymorphic alleles by balancing selection (282). As with the common laboratory strains, the autoimmune-linked Haplotype2 alleles are very prevalent amongst wild populations from different taxa. An analysis of the *CTLA4* gene demonstrates a similar phenomenon in the case of a silent SNP in exon 2, which has been associated with autoimmune susceptibility in the NOD mouse model of Type 1 diabetes (48). Codon-substitution analysis indicates that SLAM/CD2 members contain codons under selection in their ligand-binding domains, and this is most evident in the case of *Cd229*, *Cd48*, and *Cd84*. Finally, the positions of the specific codons under selection within these genes in their binding domains, indicate their functional relevance.

The maintenance of “disease” alleles in natural populations observed in this study supports the idea that the implicated polymorphisms are not deleterious *per se*, and may in fact even be advantageous in certain contexts of pathogen immunity and genetic background. Autoimmunity may simply be a by-product, occurring in the context of certain combinations of alleles. This is in keeping with previous studies which have shown that epistatic interactions between susceptibility loci and other polymorphic components of the genome can indeed profoundly affect disease outcome (163, 159, 259).

Results

SLAM/CD2 Haplotypes in common laboratory strains are present in multiple *Mus* sub-species.

Sequence analysis of the extracellular Ig domains of the SLAM/CD2 cluster in 15 wild-derived inbred strains of mice with well-defined taxonomic origins (Table 7A) revealed the presence of SLAM/CD2 Haplotypes 1 and 2 in multiple *Mus musculus* sub-species. As shown in Fig 8, two of the four *molossinus* strains share the B6-associated Haplotype 1, while five of the seven *musculus* strains contain the more common Haplotype 2 that potentiates autoimmunity on the B6 genetic background. The remaining wild-derived inbred strains (with the exception of *Mus Pahari*) share some SNPs with each, forming three additional recombinant versions of the cluster (Fig 8). The diversity among wild-derived inbred strains is only slightly greater than that found in the laboratory strains, with just five additional coding region SNPs found among the entire collection: three in *Cd229*, one in *Cd48*, and three in *Ly108*. The exception is the widely divergent *Mus Pahari*, a different *Mus* species.

An analysis of SLAM/CD2 in a more diverse wild, outbred collection revealed a much greater density of SNPs and extensive heterogeneity. Along with the wild-inbred strains, this collection represents five different species of *Mus*. It includes 40 *Mus Musculus* strains, further divided into the following sub-species: 15 *Mus m musculus* strains, 5 *Mus m molossinus*, 5 *Mus m castaneus*, 11 *Mus m domesticus*, and 4 *Mus m Spp*. 5 strains from the species *Mus Spretus*, and 1 each from *Mus Macedonius*, *Mus Spicilegus*, and *Mus Pahari* are also included. The various strains used and their species and sub-species, are listed in Tables 7A (wild-derived inbred) and 7B (wild outbred).

We sequenced the mitochondrial D-loop regulatory region, as a highly polymorphic genetic marker (283), in the wild and wild-derived inbred mice to give us an estimate of the evolutionary distances and patterns of clustering and overlap between the various DNAs used in our study. The mitochondrial sequences were used to generate a phylogenetic tree demonstrating the genetic relationships between the various strains. The analysis revealed that the DNAs do cluster, as expected, by sub-species and species (Fig 9), with some overlap between sub-species that are known to be sympatric and have been shown to interbreed in hybridization zones where their ranges overlap. Several of the *Mus m musculus* DNAs cluster together off a node, along with *Mus m Spp* strains (Bracket A). The *Mus m Spp* nomenclature is non-specific, simply denoting undesignated sub-species of *Mus musculus*, and the clustering of these DNAs with various sub-species is therefore to be expected. All of the *Mus m molossinus* strains are clustered together on one node, close to *Mus m musculus* (Bracket A), from which they are believed to have arisen through interbreeding with *Mus m castaneus* (284). The *castaneus* strains, with the exception of one wild-derived inbred (#34) cluster together (Bracket B). This one strain, somewhat unexpectedly, shares a node with several juxtaposed *Mus m musculus* and *Mus m domesticus* strains (Bracket C). It is known that there have been quite extensive genetic exchanges between these latter two sub-species over a large continuum of overlapping breeding ranges in Europe (285). All of the *musculus*, as well as many of *domesticus* DNAs on this node are indeed of European origin, with the remaining *domesticus* strains originating in the nearby North African/ Mediterranean region (see Table 7B for strain origins). Also within the area highlighted in Bracket C is the only occurrence in the Mitochondrial D-loop tree of strains from two different sub-species (#47, a *musculus* and #14, a *domesticus*) actually clustering together on a single branch. The entire polytypic *Mus musculus* complex of sub-species (*Mus m musculus*, *Mus m domesticus*, *Mus m castaneus*, *Mus m molossinus* and *Mus m Spp*), are more widely separated from each of the

other *Mus* species analyzed, than from each other. The longer evolutionary distances between species (estimated to be about 1.5 million years versus 0.75 million years between the *Mus musculus* sub-species; 285) is reflected in the fact that the *Mus Spretus*, *Mus Spicilegus*, and *Mus Macedonius* strains are separated by older nodes and show no overlap with the *Mus musculus* complex, or with each other. The furthest removed species is *Mus Pahari*. This distribution of species follows the accepted pattern of phylogenetic relationships between them, as obtained from hybridization studies on single copy nuclear DNA (reviewed in 285, shown in Fig 7). Data from sequences of a set of nuclear genes also yielded a very similar phylogenetic tree (286, 287), validating our use of mitochondrial DNA as a good measure of genetic variability and distribution of our DNAs.

Having established this baseline, we next moved on to analyze sequence data obtained from the SLAM/CD2 Ig regions. There are over 80 SNPs within the Ig regions of the six SLAM/CD2 genes in the wild outbred mice, almost a three-fold increase over the wild-derived inbred and laboratory strains, and tightly linked haplotypes are not evident in this sample of wild mice. To assess if there is any evidence of positive selection for polymorphisms in the SLAM/CD2 genes, we next completed phylogenetic analyses on the Ig-region sequences obtained from the wild-outbred and wild-derived inbred DNAs. In particular, the clustering of the autoimmune-associated Haplotype 2 with multiple sub-species would indicate that these alleles were present in ancestral *Mus* species and have been maintained in multiple sub-species subsequent to speciation.

The SLAM/CD2 family *Ig* regions show the presence of ancestral polymorphism

Phylogenetic trees generated from the Ig domain sequences of the SLAM/CD2 family, obtained from our panel of *Mus* taxa, show extensive clustering between different

sub-species and species. The trees generated from each of the members of the family are shown in Figs 10-15.

The most striking feature of the *Cd229* Ig domain tree (Fig 10) is the interspersed distribution of different *Mus* species, which is in contrast with their distribution in the mitochondrial D-loop tree or in phylogenetic analyses done with a variety of nuclear genes (286, 287). One *Mus Spretus* strain (#29), for instance, clusters closer with *Mus Macedonius* and *Mus Spicilegus*, and is separated from them by one node, away from the rest of the *Spretus* alleles (Bracket A). The *Spretus* cluster shares a node with a heterogeneous group of *Mus musculus* subspecies (Bracket B). The *Mus m castaneus* strains in particular show a very widespread distribution on this tree. The *castaneus* #6 is more divergent from the *Mus musculus* sub-species complex, than are any of the other species except *Mus Pahari* (Bracket C). More branches carry multiple sub-species on them than are observed in the mitochondrial tree, including *castaneus* with *domesticus*, and *musculus* with *domesticus*. Interestingly, the autoimmune Haplotype 2 allele is present in several *Mus m musculus* strains as well as *Mus m domesticus* (the outbred strains #7 and 33), while Haplotype 1 is found in *Mus m molossinus* (outbred # 22 and wild-inbred # 39 and 40). The occurrence of the autoimmune-associated allele in multiple sub-species suggests that it arose prior to the speciation event, and has persisted in these populations since.

Similar to *Cd229*, the *Cd48* tree (Fig 11) also fails to show the clear separation of the major *Mus* species from each other seen in the mitochondrial sequence tree. The two alleles from the heterozygous *Mus Spicilegus* strain (#32) are separated by three nodes, with 32B sharing a “younger” node with the *Mus musculus* sub-species, *Mus Macedonius*, and *Mus Spretus* (Bracket A). There are several instances where multiple *Mus musculus* sub-species

cluster together on one branch; this is a more pronounced feature of *Cd48* than of *Cd229*. The B6 Haplotype 1 allele is grouped on a single branch with *molossinus* (outbred #22 and wild-inbred #39 and 40), *musculus* (#19), and a *Mus m Spp* strain (#15). Significantly, the Haplotype 2 allele from B6.*Sle1b* is present in multiple strains from all of the *Mus musculus* sub-species (*musculus*: #45, 46, 47, 48; *domesticus*: #2, 7, 9, 13, 14, 35; *molossinus*: #37, 38; *castaneus*: #4, 5, 34, 36; *Spp*: 1, 15, 30). *Mus Pahari* remains a clear outlier in this distribution.

An impressive amount of ancestral polymorphism is also similarly observed in the trees generated from the other SLAM/CD2 family members analyzed (Figs 12-15). In the case of *Cd84* (Fig 12), *Ly108* (Fig 13), and *Cs1* (Fig 14), there is clustering, not only of different *Musculus* sub-species, but even multiple species on single branches. The level of ancestral polymorphism observed in these trees far exceeds that observed in the control Mitochondrial D-loop analysis, and cannot be completely accounted for by interbreeding between sympatric strains, indicating that it may be due to the persistence of polymorphisms that arose prior to speciation. This reflects balancing selection, possibly pathogen driven, acting on the ligand-binding domains of these genes (282). In addition, of particular interest is the fact that in every tree, multiple sub-species cluster on the same branch as the autoimmune-associated alleles of this cluster, showing that these potentially deleterious alleles have also persisted over evolutionary timespans.

Codon-substitution analyses on the SLAM/CD2 Ig show that *Cd229*, *Cd48* and *Cd84* are the best candidates for having codons under selection

The ratio of non-synonymous (change in amino acid) to synonymous (silent) substitutions ($\omega = d_N/d_S$) is a sensitive measure of the selective pressure acting on molecular

sequences. An equal number of nonsynonymous and synonymous substitutions ($\omega=d_N/d_S=1$) would be indicative of a neutral pattern of evolution, with no advantage being conferred by either preserving the original amino acid (purifying selection favoring synonymous substitutions; $\omega<1$), or by changing it (positive selection favoring non-synonymous substitutions; $\omega>1$). Since functional constraints limit nonsynonymous changes to discrete sites and times, codons are predominantly invariable, and averaging across all amino acid sites to obtain an overall ω value results in an underestimation of genes under selection. We therefore carried out a likelihood analysis of selection (Table 8) using Yang's codon-substitution models (257) as described in Chapter 2 (Methods). This allows for heterogeneous selection pressure at different amino acid sites, and is therefore more sensitive to selection operating on a subset of codons.

The difference in likelihood between the Neutral Model (M1) and the Discrete Model (M3, which allows for positive selection), shown as the Likelihood Ratio Test value, reaches significance only in the case of *Cd229* and *Cd48*, and *Cd84* (the latter only upon the inclusion of the widely divergent *Mus Pahari* line), suggesting that these genes have Ig-domains under selection (Table 8). As shown in the last column, ω_2 is greater than 1 in every case, showing that there is actually positive selection on this class or subset of codons in all of the SLAM/CD2 family genes. In most, however, the estimated number of codons that fall into this category is simply too small to make the overall result significant (Table 8). This is in keeping with a previous study which showed that SNPs associated with complex diseases tend to have much lower scores relative to the neutral model, than SNPs underlying Mendelian traits (288).

Protein-structure alignments of the Cd229 and Cd84 Ig-domains with those of human and rat CD2, for which the extracellular domain structure is known, are shown in Figs 16A and B respectively, with the specific residues that are under selection in each indicated. The locations of the selected codons point to their potential importance in the ligand-binding, and therefore, the function of the molecules. Singularly, in the case of both Cd229 and Cd84, these include all of the non-synonymous SNPs that distinguish the two major inbred-strain haplotypes. As shown in Fig 16A, Cd229 has eleven codons under selection, eight of which are within the IgV1 domain that aligns with the N-terminal IgV of rat-CD2. Of these, seven (including the four encoded by IgV1 region haplotype-SNPs) lie in β -strands known to be critical to ligand-binding by the CD2 molecule and/or actually correspond to residues that have specifically been shown to participate in its ligand-binding (264, 265). The C β -strand, which contains 2 such selected codons, has in fact also been shown to be important in homophilic ligand-binding of human Cd229 (234). The remaining three codons under selection (345 and 356, encoded by the remaining two haplotype-SNPs, and 359) lie within the IgC2 region, one of the two additional extracellular domains peculiar to Cd229.

Cd84 has eight IgV-region and four IgC-region codons under selection. Codons 27 (the one haplotype-SNP encoded residue) and 28 lie immediately proximal to the A β -sheet. Two other selected codons lie between β -strands, just proximal to C and C'', both important in CD2 ligand-binding, while codon 73 actually lies within the C'' β -strand. The remaining three codons lie within the D β -strand (Fig 16B). The IgC-region codons under selection include codons 193 in the F β -sheet, 203 and 204 in the G β -sheet, and 207 (data not shown). Across both analyses (of Cd229 and Cd84), only two of the codons under selection occur at positions that are conserved (identical) between human or rat CD2 and the gene in question. It has been shown that, while Mendelian trait-SNPs tend to occur at residues conserved between members of protein families, and may therefore be surmised to have strong effects

on function, complex trait-associated SNPs from affected individuals are not distributed significantly differently from those obtained from healthy ones (288). This supports the idea that they modulate, rather than interfere, with the basic ability of the protein to function.

Finally, the specific amino acid residues that are under selection in Cd48 include codon 36 in the IgV domain, and 171, 182, and 213 in the IgC region. The significance of these positions in ligand-binding is hard to assess, as they fall outside the region of alignment with human Cd58 (data not shown).

CTLA4 polymorphism linked to autoimmunity is common in multiple *Mus* species and sub-species

CTLA4 also has an autoimmune susceptibility allele that is shared by multiple strains from different *Mus* species and sub-species, indicating their maintenance in natural populations. A silent SNP at position 77 in exon 2 of this gene, which is located within the *Idd5.1* locus on chromosome 1, has been found to affect gene splicing, and is associated with disease susceptibility in the NOD murine model of Type 1 diabetes (48). The resistant strains B6 and B10 contain an “A” at this position, while the susceptible NOD carries the “G” allele.

We amplified and sequenced exon 2 of *CTLA4*, along with 5’ and 3’ flanking intron sequence in B6, NOD, and five other common laboratory strains, and our entire panel of wild and wild-derived inbred strains. As shown in Table 9, the autoimmune version is found in NZW, NZB, and BALB/cJ. No other SNPs were found in the exon 2 product amongst these strains. Amongst the wild-derived inbred strains, the B6 version was far more common, being present in all but 4 strains. The NOD allele was found in three strains, representing *Mus m molossinus* and *musculus*. Amongst the wild, outbred populations, however, the B6 allele was not present in any of the strains analyzed. Thirty-one of the 33 from this panel share the NOD version of the SNP, which is thus present in every *Mus* species and *Mus musculus* sub-

species analyzed, except the wild-inbred *Mus Pahari*. In contrast to the SLAM/CD2 Ig regions, d_N/d_S analysis shows that exon 2 of *CTLA4* does not have any codons in the p1 or p2 categories (Table 8), i.e., it has no non-synonymous mutations within exon 2. Thus, this region is perfectly conserved structurally across the entire panel used in this study, and it is the splice-SNP that shows evidence of being maintained in wild populations of mice.

Discussion

Polymorphisms within the extracellular ligand-binding domains of the SLAM/CD2 family of receptors can have important effects on their immuno-modulatory functions by changing their ability to bind ligands, or the affinity of their interactions. Numerous Ig-region SNPs distinguish 2 haplotypes of this gene cluster from each other in common inbred laboratory strains, one of which (Haplotype 2) is linked to autoimmunity, being able to potentiate the production of anti-nuclear antibodies (ANAs) in a highly penetrant manner. Somewhat surprisingly, this is nevertheless the haplotype shared by almost all of the commonly used laboratory strains.

One of the most striking findings of the current study is that, rather than being an artifact of the inbreeding that led to the derivation of the laboratory strains, the “pathogenic” SLAM/CD2 alleles are very common amongst natural, outbred populations of mice. This may not be as surprising as it seems at first glance, for a few reasons: *Sle1b* is a potent locus, mediating ANA-production and some degree of splenomegaly in a majority of B6.*Sle1b* mice (26, 171); however, by itself it is not associated with fatality. While the locus is important for disease initiation, it only has an effect on mortality, and possibly fitness, when it is combined with other susceptibility factors in the genome (259). Thus, it is only such deleterious *combinations* that are likely to be selected against (and therefore rarely found) in the wild, and it is not surprising that the individual alleles occur commonly, given their probable inability to affect reproductive fitness or life-span in isolation.

The presence of ancestral polymorphisms, as evidenced by phylogenetic tree analyses on the extracellular Ig regions, would indicate that some form of balancing selection, quite possibly pathogen-driven, may, in addition, be operating on these domains to actually

maintain the alleles (282). This is supported by our codon-substitution analyses, which show that at least a proportion of codons in each of the SLAM/CD2 family domains are indeed under positive selection, with non-synonymous, diversifying mutations being favored. The trend is most evident in *Cd229*, *Cd84*, and *Cd48*, where it reaches significance. Even in these genes, a comparison to the CD2 extracellular region shows that very few of the codons that are under selective pressure occur at conserved residues. This is in keeping with the idea that these SNPs, rather than having huge, deleterious effects on basic gene function by ablating critical residues, serve to modulate it in ways that may be differentially advantageous, with autoimmune susceptibility or resistance simply being by-products of the selected variations. In the case of the *CTLA4* gene, for example, it has been previously hypothesized that both the autoimmune-susceptible and non-autoimmune-associated variants may be common because they have been maintained for the advantages they each confer in fighting different kinds of pathogens (48). Our finding that the autoimmune allele is in fact very common amongst natural populations of mice does indeed support the idea that, rather than simply causing autoimmunity, it confers some advantage.

The nature of the selection operating on the SLAM/CD2 family is not known; however, it is tempting to speculate that it may be pathogen-driven. The SLAM/CD2 Ig domains are good candidates to be evolving under the influence of viral pathogens. Members of the morbillivirus family directly bind and use molecules belonging to this family as receptors. The measles virus, the canine distemper virus and rinderpest virus all bind *Cd150* (263). The importance of binding-domain structure in such interactions is illustrated by the fact that replacement of the human *Cd150* IgV domain with the mouse version abolishes the ability of the measles virus to enter cells (289). Thus, the extracellular domain polymorphisms included in this study, many of lie within regions important to ligand-binding

by analogy with CD2, could well have differential effects on their interaction with various such pathogens. In addition, they could modulate the ability and/or avidity of ligand-binding of family members to themselves or one another. Such variations in binding could in turn affect the strength and/or the nature of immune responses in a variety of contexts including pathogen-resistance, perhaps through differences in the degree or kind of downstream signaling molecules that are recruited upon receptor engagement (214, 262). SAP (SLAM-associated protein or SH2D1A), which acts directly downstream of this family, for instance, has been shown to play a role in Th2 regulation and cytokine production (250, 249). In addition, mutations in the adaptor molecule have been linked to a variety of diseases that result from dysregulations in viral immunity, including X-linked lymphoproliferative syndrome (XLP), which is caused by an inappropriate response to Epstein-Barr Virus (EBV) infection (263). EBV infection has also been implicated as an environmental trigger for SLE (279, 280), making an intriguing connection between these genes, viral immunity, and autoimmunity.

Table 7A

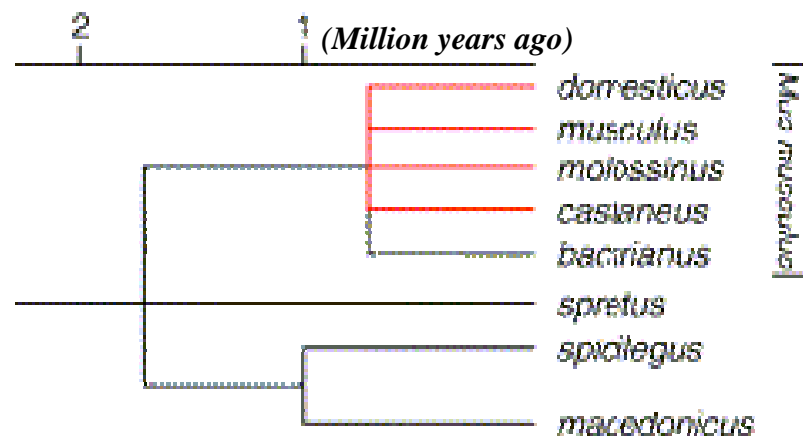
Strain Name	Assigned #	Species/Sub-species	Catalog #
PERA/Ei	42	<i>Mus m musculus</i>	000930
PERA/Rk	43	<i>Mus m musculus</i>	091057
PERC/Ei	44	<i>Mus m musculus</i>	001307
SF/CamEi	45	<i>Mus m musculus</i>	000280
SK/CamEi	46	<i>Mus m musculus</i>	090108
SK/CamRk	47	<i>Mus m musculus</i>	009328
CZECHi/Ei	48	<i>Mus m musculus</i>	002799
MOLC/Rk	37	<i>Mus m molossinus</i>	000731
MOLD/Rk	38	<i>Mus m molossinus</i>	000734
MOLE/Rk	39	<i>Mus m molossinus</i>	009163
MOLF/Ei	40	<i>Mus m molossinus</i>	000550
CASA/Rk	34	<i>Mus m castaneus</i>	000735
CAST/Ei	36	<i>Mus m castaneus</i>	000928
CALB/Rk	35	<i>Mus m domesticus</i>	001489
Mus Pahari	41	<i>Mus Pahari</i>	002655

Table 7A. Wild-derived inbred strains used in this study. Listed are the strains used, along with the numbers assigned to each and used throughout the study, sub-species information, and catalog numbers (Jackson Laboratories, Bar Harbor, ME).

Table 7B.

Strain	Assigned #	# Generations	Species/Sub-Species	Geographical Origin
MAM	17	8	<i>Mus m musculus</i>	Armenia: Megri
MGA	21	7	<i>Mus m musculus</i>	Georgia: Alazani
MBK	18	24	<i>Mus m musculus</i>	Bulgaria: Kranevo
MBS	19	25	<i>Mus m musculus</i>	Bulgaria: Sokolovo
MDH	20	10	<i>Mus m musculus</i>	Denmark: Hov
MPB	23	8	<i>Mus m musculus</i>	Poland: Bialowieza
MOL	22	21	<i>Mus m molossinus</i>	Japan: Mishima
CIM	4	8	<i>Mus m castaneus</i>	India: Masingudi
CTA	5	8	<i>Mus m castaneus</i>	Taiwan: He-mei
CTP	6	2	<i>Mus m castaneus</i>	Thailand: Pathumthani
BIK/g	2	31	<i>Mus m domesticus</i>	Israel: Haifa
BZO	3	27	<i>Mus m domesticus</i>	Algeria: Oran
DIK	11	1	<i>Mus m domesticus</i>	Israel: Keshet
DJO	12	19	<i>Mus m domesticus</i>	Italy: Orcetto
DMZ	13	11	<i>Mus m domesticus</i>	Morocco: Azzemour
DOT	14	25	<i>Mus m domesticus</i>	French Polynesia: Tahiti
22MO	33	26	<i>Mus m domesticus</i>	Tunisia: Monastir
DDO	7	18	<i>Mus m domesticus</i>	Denmark: Odis
DEB	8	2	<i>Mus m domesticus</i>	Spain: Barcelona
DGA	9	6	<i>Mus m domesticus</i>	Georgia: Adjarie
TEH	30	8	<i>Mus m Spp</i>	Iran: Tehran
BID	1	5	<i>Mus m Spp</i>	Iran: Birdjand
MAC	16	5	<i>Mus m Spp</i>	Iran: Machad
KAK	15	5	<i>Mus m Spp</i>	Iran: Khak
DHA	10	12	<i>Mus m Spp</i>	India: Delhi
MPR	24	9	<i>Mus m Spp</i>	Pakistan: Rawalpindi
SEG	26	36	<i>Mus spretus</i>	Spain: Grenada
SFM	27	26	<i>Mus spretus</i>	France: Montpellier
SMZ	28	11	<i>Mus spretus</i>	Morocco: Azzemour
STF	29	26	<i>Mus spretus</i>	Tunisia: Fondouk Djedid
SEB	25	2	<i>Mus spretus</i>	Spain: Barcelona
XBS	31	18	<i>Mus macedonius</i>	Bulgaria: Slantchev Briag
ZRU	32	15	<i>Mus spicilegus</i>	Ukraine

Table 7B. List of the wild, outbred-strain DNAs used in this study. These were obtained from Dr. Francois Bonhomme (Universite Montpellier II, Montpellier, France). Listed are the strains used, along with the numbers assigned to each and used throughout the study, the number of generations they have been maintained for at the facility, species and sub-species information, and areas of origin.

Fig 7

Mus Pahari: ~3-4 million years ago

Fig 7. Evolutionary distances and distribution of species within the Genus *Mus*. Adapted from a review by Guenet & Bonhomme (2003), these estimates are based on single-copy nuclear DNA hybridization studies, calibrated with respect to separation of *Mus* and *Rattus* (~10 million years ago). Studies on several nuclear genes by various other groups also yield similar phylogenies.

Fig 8

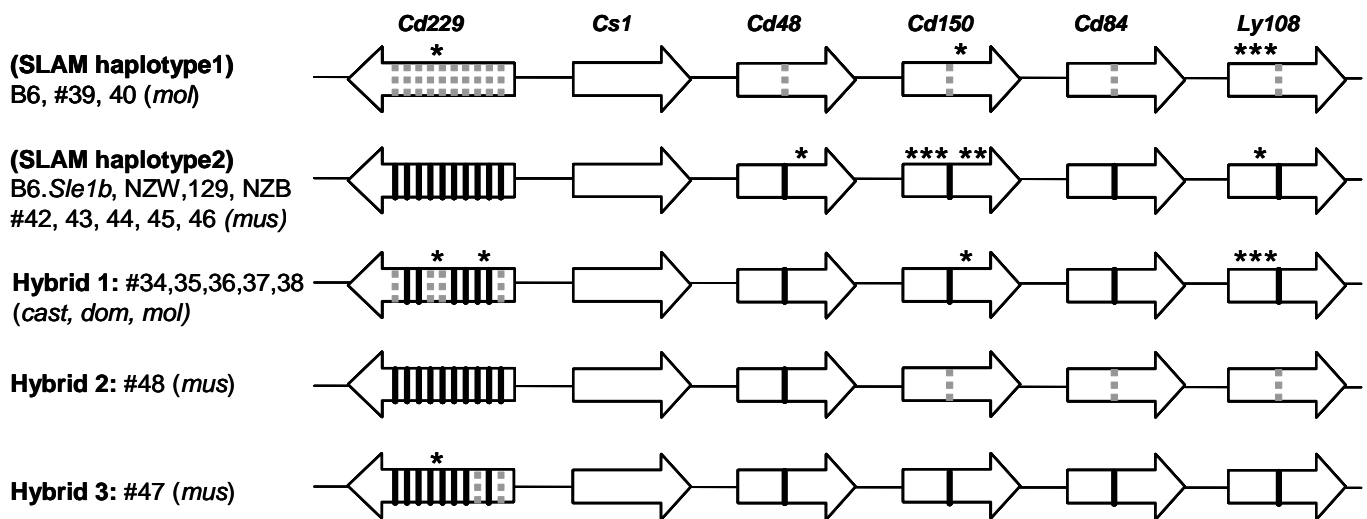


Fig 8. SLAM/CD2 haplotypes found in wild-derived inbred strains from distinct *Mus* taxa. The extracellular *Ig* domains of six members of the SLAM/CD2 family were sequenced in a panel of wild-derived inbred strains from five distinct *Mus musculus* sub-species. The two haplotypes originally found in common lab strains (Haplotype 1 and the autoimmune-associated Haplotype 2) are both present amongst the wild-inbred strains. Wild-derived inbred strains are designated by numbers (corresponding strain names with sub-species information can be found in Table 7A). The sub-species that share each haplotype are also indicated (*mol*: *Mus m molossinus*; *mus*: *Mus m musculus*; *cast*: *Mus m castaneus*; *dom*: *Mus m domesticus*). The arrows indicate the order and transcriptional direction of the genes, going from centromere to telomere on mouse chr 1. The SNPs that distinguish the two major haplotypes are indicated by dashed (Haplotype 1 alleles) or solid (Haplotype 2 alleles) lines. Asterisks indicate additional SNPs found in only a sub-set of the strains in each group.

Fig 9

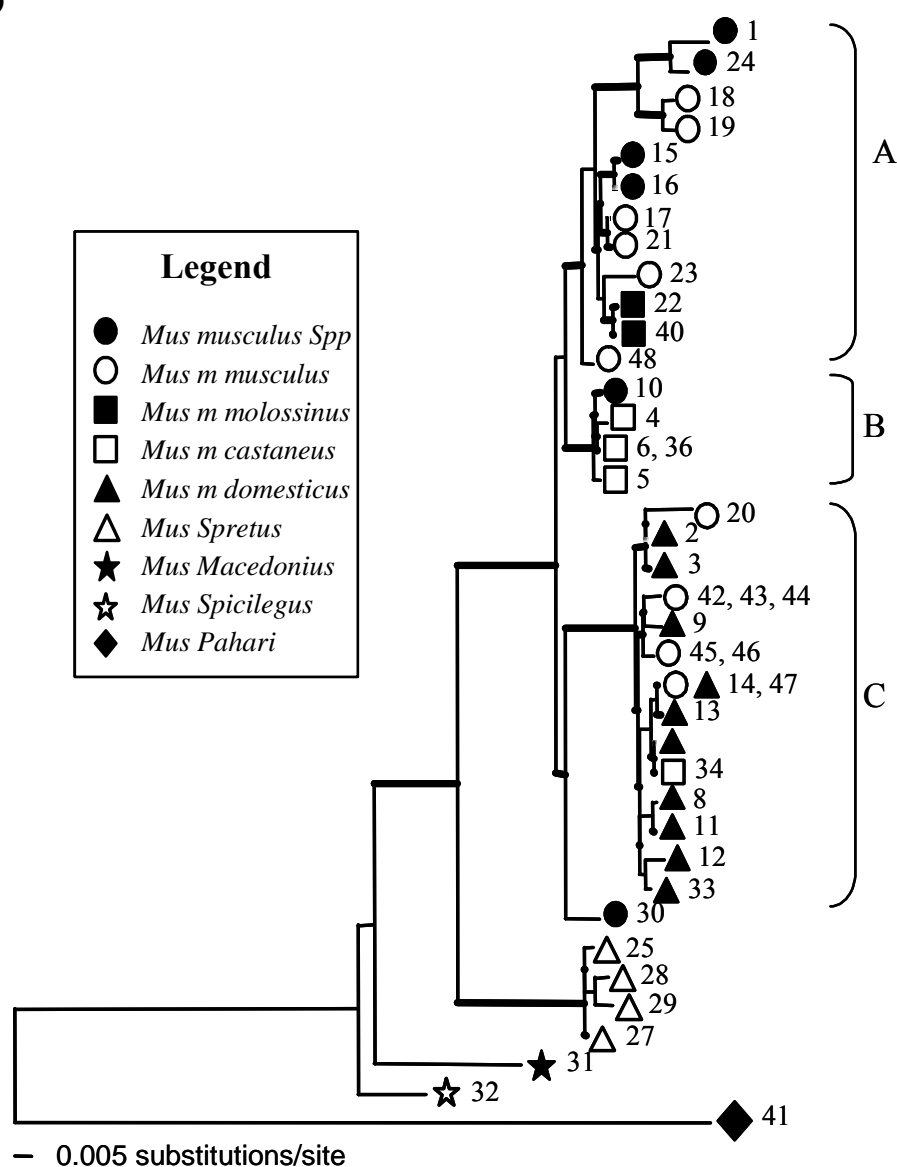


Fig 9. Phylogenetic analysis of Mitochondrial D-loop regulatory region sequences shows that mouse strains cluster by species. The tree generated by phylogenetic analysis of sequences generated from the non-coding D-loop region of mitochondria from 33 wild, outbred strains, and 15 wild-derived inbred strains from different *Mus* taxa is shown.

The legend lists the symbols used to denote the various *Mus* species.

Along with species, the individual strains on each branch are also indicated by their assigned numbers; corresponding strain names, along with sub-strain and geographic origin information can be found in Tables 7A and B.

Horizontal branch lengths correspond to the number of substitutions per amino acid site as indicated, showing the extent of diversification from the previous node.

The number of nodes separating one strain from another indicates how closely related their sequences are: strains on the same branch share the same allele, strains separated by a single node have more closely related alleles than those separated from them by three nodes, and so on.

Thicker lines indicate bootstrap values of >50% for the clustering of strains from the node that immediately follows. Brackets A, B and C are used to highlight regions that are described in the text.

Fig 10

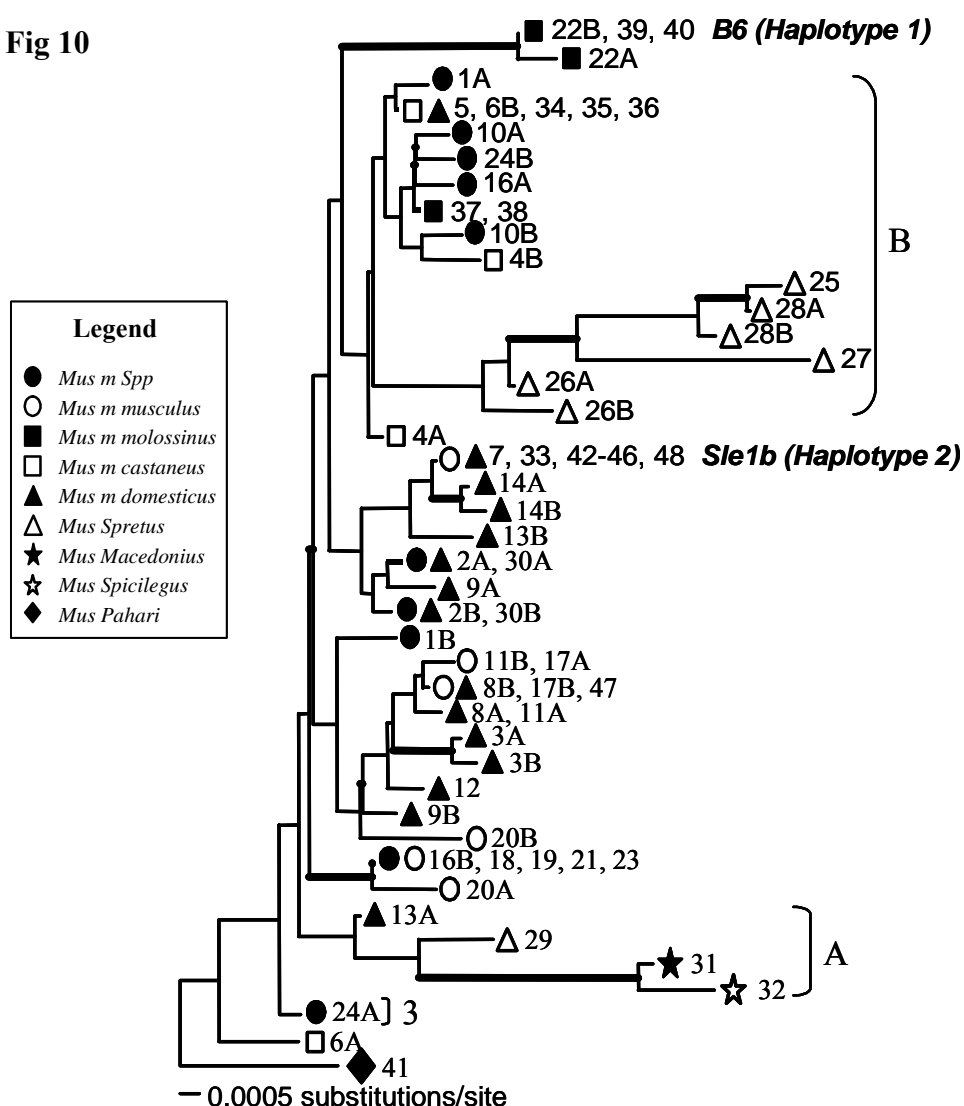


Fig 10. Phylogenetic analysis of the Cd229 Ig regions shows the presence of trans-species polymorphisms. The tree generated by phylogenetic analysis of sequences generated from the (IgV1+IgC1+IgV2+IgC2) domains from 33 wild, outbred strains, and 15 wild-derived inbred strains from different *Mus* taxa is shown.

Representative strains from Haplotype 1 (B6) and Haplotype 2 (B6.Sle1b, NZW, 129 and NZB) were also included.

The legend lists the symbols used to denote the various *Mus* species.

Along with species, the individual strains on each branch are also indicated by their assigned numbers. Heterozygous strain alleles are denoted by the strain names, followed by A or B (e.g. 22A and 22B). Corresponding strain names, along with sub-strain and geographic origin information can be found in Tables 7A and B.

Horizontal branch lengths correspond to the number of substitutions per amino acid site as indicated, showing the extent of diversification from the previous node.

The number of nodes separating one strain from another indicates how closely related their sequences are: strains on the same branch share the same allele, strains separated by a single node have more closely related alleles than those separated from them by three nodes, and so on.

Thicker lines indicate bootstrap values of >50% for the clustering of strains from the node that immediately follows. Brackets A and B are used to highlight regions that are described in the text.

Fig 11

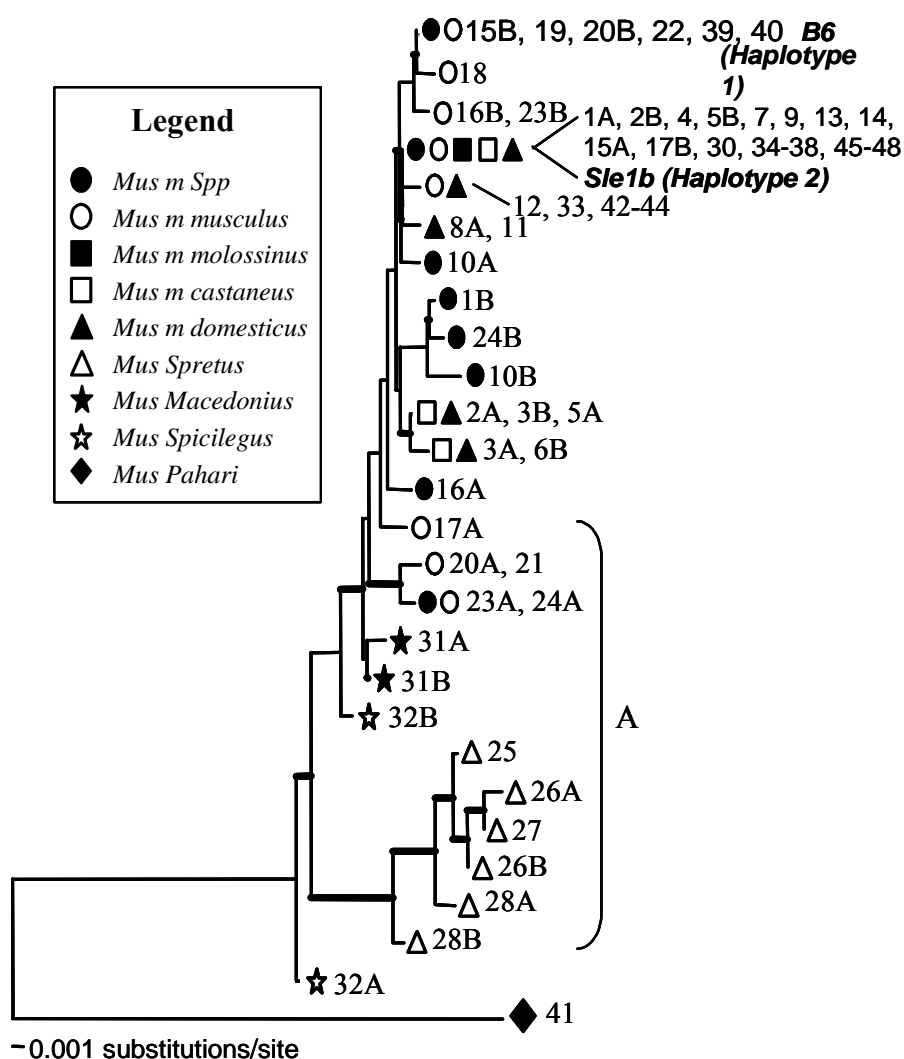


Fig 11. Phylogenetic analysis of the Cd48 Ig regions shows the presence of trans-species polymorphisms. The tree generated by phylogenetic analysis of sequences generated from the (IgV+IgC) domains from 33 wild, outbred strains, and 15 wild-derived inbred strains from different *Mus* taxa is shown.

Representative strains from Haplotype 1 (B6) and Haplotype 2 (B6.*Sle1b*, NZW, 129 and NZB) were also included.

The legend lists the symbols used to denote the various *Mus* species.

Along with species, the individual strains on each branch are also indicated by their assigned numbers.

Heterozygous strain alleles are denoted by the strain names, followed by A or B (e.g. 22A and 22B).

Corresponding strain names, along with sub-strain and geographic origin information can be found in Tables 7A and B.

Horizontal branch lengths correspond to the number of substitutions per amino acid site as indicated, showing the extent of diversification from the previous node.

The number of nodes separating one strain from another indicates how closely related their sequences are: strains on the same branch share the same allele, strains separated by a single node have more closely related alleles than those separated from them by three nodes, and so on.

Thicker lines indicate bootstrap values of >50% for the clustering of strains from the node that immediately follows. Bracket A is used to highlight regions that are described in the text.

Fig 12

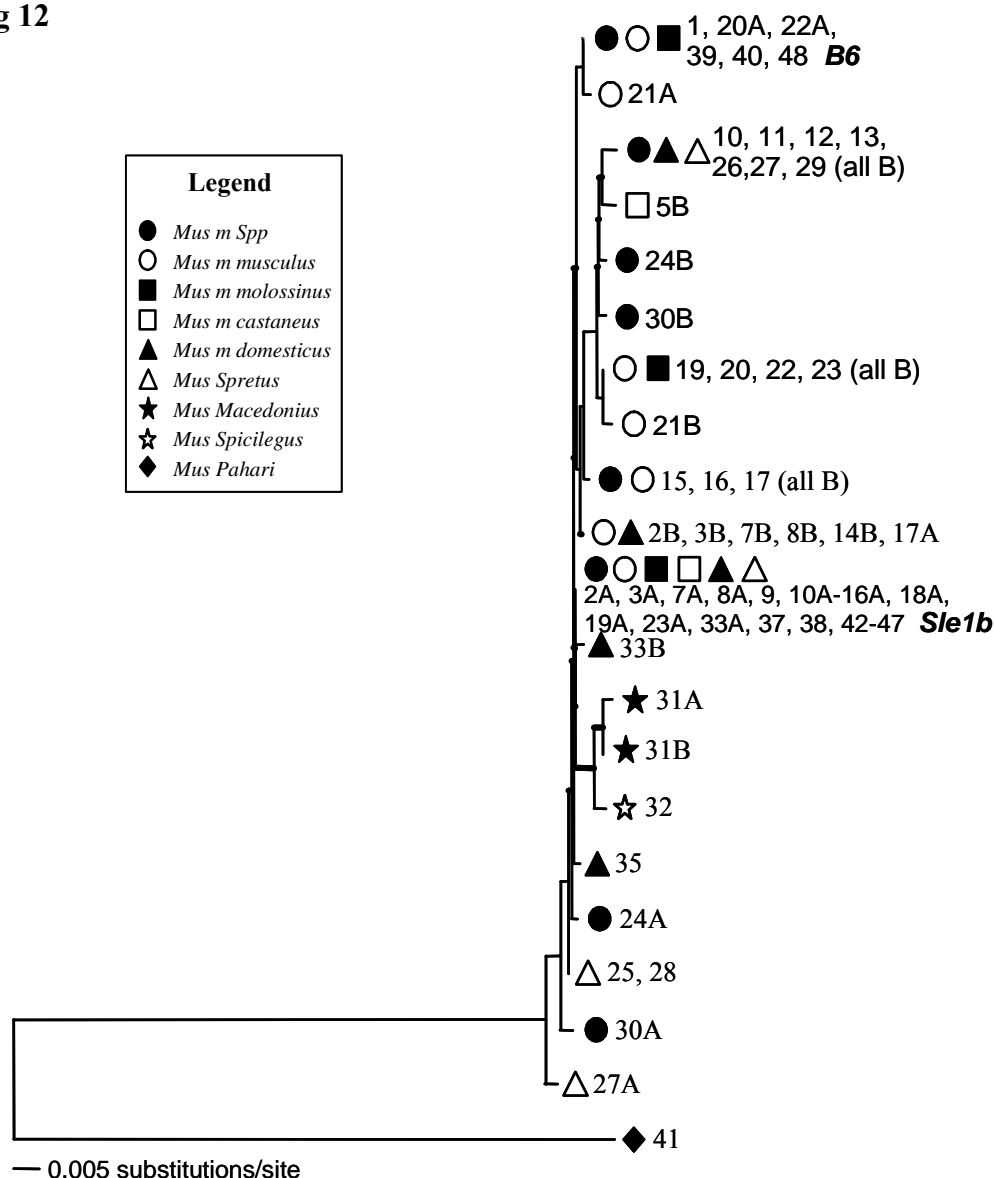


Fig 12. Phylogenetic analysis of the Cd84 Ig regions shows the presence of trans-species polymorphisms. The tree generated by phylogenetic analysis of sequences generated from the (IgV+IgC) domains from 33 wild, outbred strains, and 15 wild-derived inbred strains from different *Mus* taxa is shown.

Representative strains from Haplotype 1 (B6) and Haplotype 2 (B6.*Sle1b*, NZW, 129 and NZB) were also included.

The legend lists the symbols used to denote the various *Mus* species.

Along with species, the individual strains on each branch are also indicated by their assigned numbers.

Heterozygous strain alleles are denoted by the strain names, followed by A or B (e.g. 22A and 22B).

Corresponding strain names, along with sub-strain and geographic origin information can be found in Tables 7A and B.

Horizontal branch lengths correspond to the number of substitutions per amino acid site as indicated, showing the extent of diversification from the previous node.

The number of nodes separating one strain from another indicates how closely related their sequences are: strains on the same branch share the same allele, strains separated by a single node have more closely related alleles than those separated from them by three nodes, and so on.

Thicker lines indicate bootstrap values of >50% for the clustering of strains from the node that immediately follows.

Fig 13

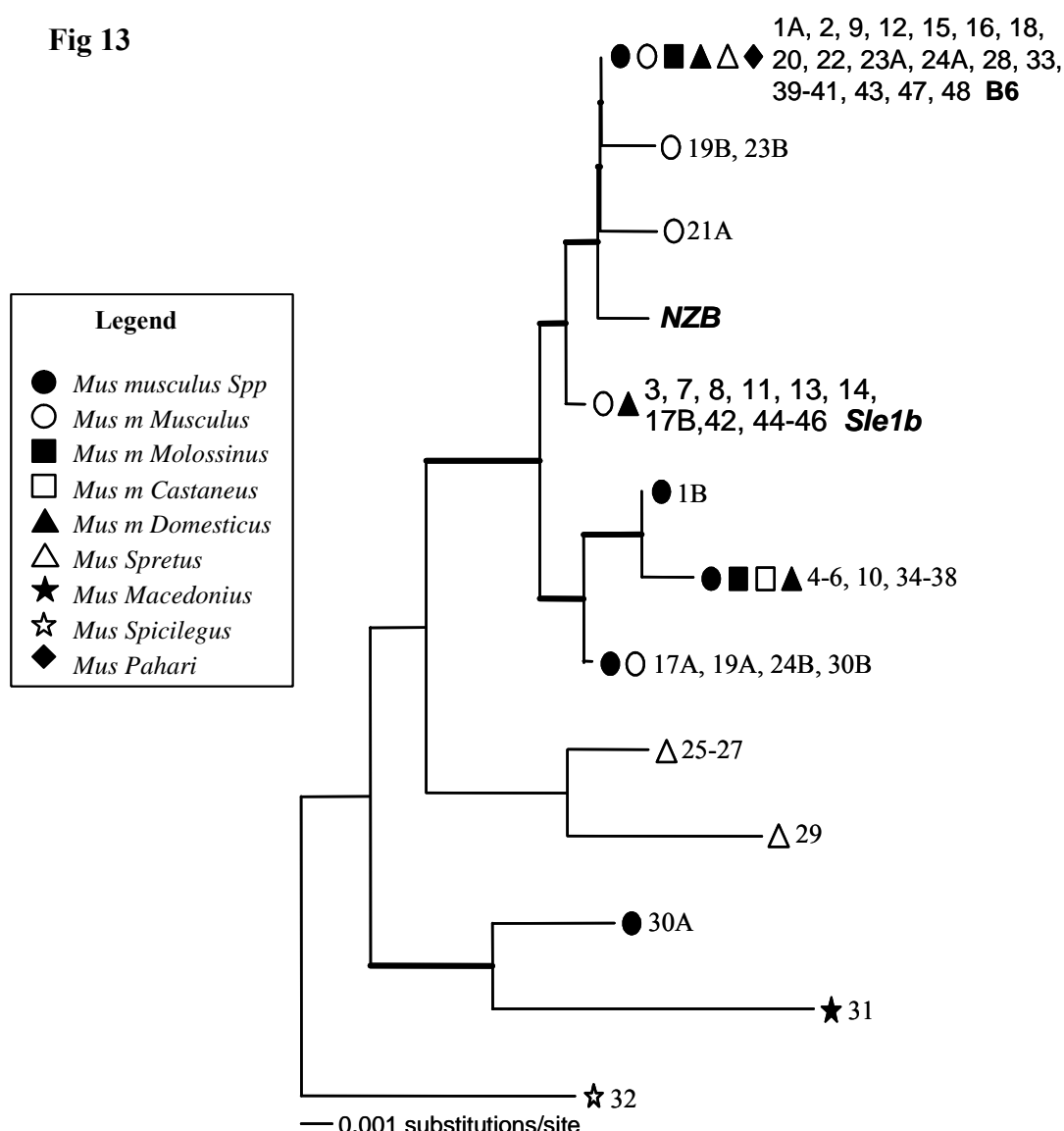


Fig 13. Phylogenetic analysis of the Ly108 Ig regions shows the presence of trans-species polymorphisms. The tree generated by phylogenetic analysis of sequences generated from the (IgV+IgC) domains from 33 wild, outbred strains, and 15 wild-derived inbred strains from different *Mus* taxa is shown.

Representative strains from Haplotype 1 (B6) and Haplotype 2 (B6.Sle1b, NZW, 129 and NZB) were also included.

The legend lists the symbols used to denote the various *Mus* species.

Along with species, the individual strains on each branch are also indicated by their assigned numbers.

Heterozygous strain alleles are denoted by the strain names, followed by A or B (e.g. 22A and 22B).

Corresponding strain names, along with sub-strain and geographic origin information can be found in Tables 7A and B.

Horizontal branch lengths correspond to the number of substitutions per amino acid site as indicated, showing the extent of diversification from the previous node.

The number of nodes separating one strain from another indicates how closely related their sequences are: strains on the same branch share the same allele, strains separated by a single node have more closely related alleles than those separated from them by three nodes, and so on.

Thicker lines indicate bootstrap values of >50% for the clustering of strains from the node that immediately follows.

Fig 14

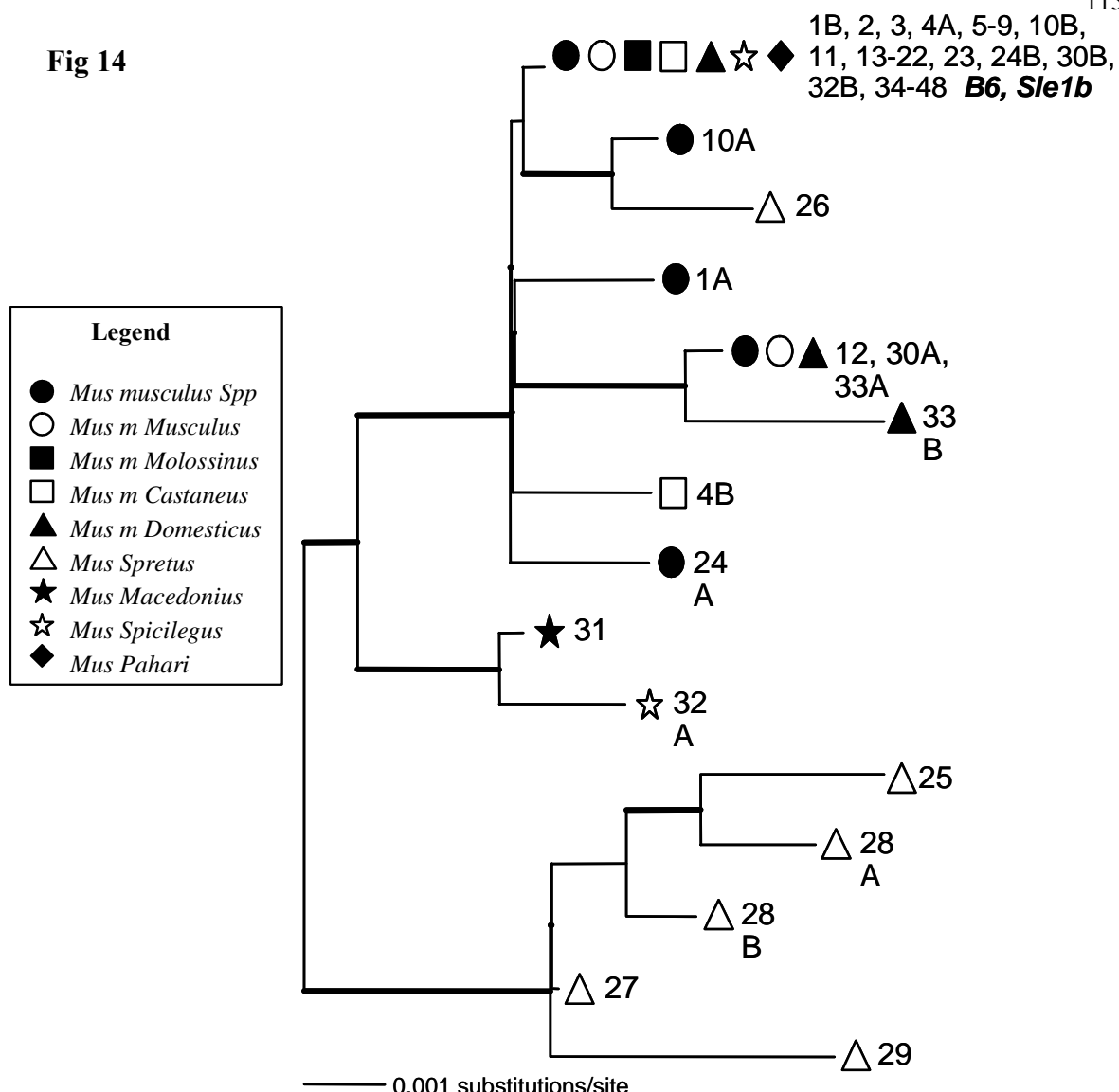


Fig 14. Phylogenetic analysis of the Cs1 Ig regions shows the presence of trans-species polymorphisms. The tree generated by phylogenetic analysis of sequences generated from the (IgV+IgC) domains from 33 wild, outbred strains, and 15 wild-derived inbred strains from different *Mus* taxa is shown.

Representative strains from Haplotype 1 (B6) and Haplotype 2 (B6.*Sle1b*, NZW, 129 and NZB) were also included.

The legend lists the symbols used to denote the various *Mus* species.

Along with species, the individual strains on each branch are also indicated by their assigned numbers.

Heterozygous strain alleles are denoted by the strain names, followed by A or B (e.g. 22A and 22B).

Corresponding strain names, along with sub-strain and geographic origin information can be found in Tables 7A and B.

Horizontal branch lengths correspond to the number of substitutions per amino acid site as indicated, showing the extent of diversification from the previous node.

The number of nodes separating one strain from another indicates how closely related their sequences are: strains on the same branch share the same allele, strains separated by a single node have more closely related alleles than those separated from them by three nodes, and so on.

Thicker lines indicate bootstrap values of >50% for the clustering of strains from the node that immediately follows.

Fig 15

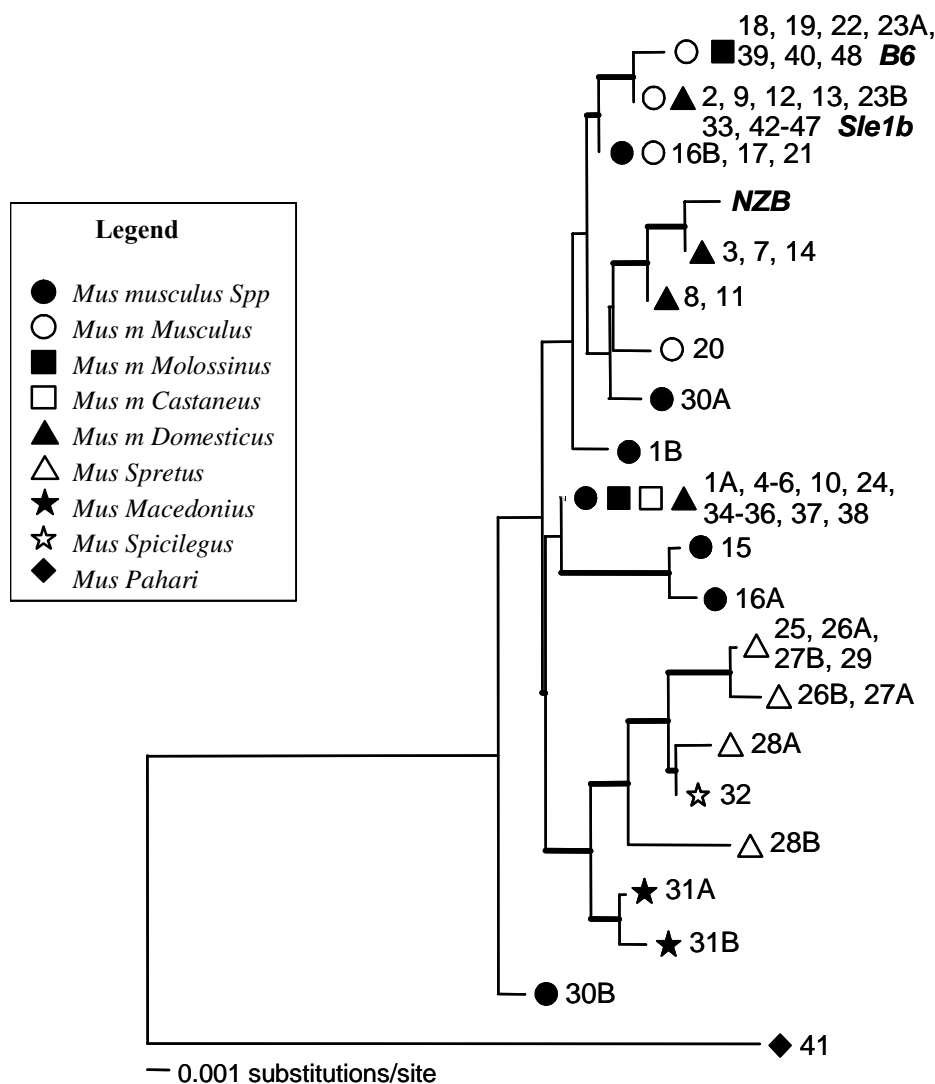


Fig 15. Phylogenetic analysis of the Cd150 Ig regions shows the presence of trans-species polymorphisms. The tree generated by phylogenetic analysis of sequences generated from the (IgV+IgC) domains from 33 wild, outbred strains, and 15 wild-derived inbred strains from different *Mus* taxa is shown.

Representative strains from Haplotype 1 (B6) and Haplotype 2 (B6.*Sle1b*, NZW, 129 and NZB) were also included.

The legend lists the symbols used to denote the various *Mus* species.

Along with species, the individual strains on each branch are also indicated by their assigned numbers.

Heterozygous strain alleles are denoted by the strain names, followed by A or B (e.g. 22A and 22B).

Corresponding strain names, along with sub-strain and geographic origin information can be found in Tables 7A and B.

Horizontal branch lengths correspond to the number of substitutions per amino acid site as indicated, showing the extent of diversification from the previous node.

The number of nodes separating one strain from another indicates how closely related their sequences are: strains on the same branch share the same allele, strains separated by a single node have more closely related alleles than those separated from them by three nodes, and so on.

Thicker lines indicate bootstrap values of >50% for the clustering of strains from the node that immediately follows.

Table 8

Locus	No. of Codons	Likelihood Ratio Test	Neutral Model (M1)		Discrete Model (M3)		
			$p0$ ($\omega0=0$)	$p1$ ($\omega1=1$)	$p0$ ($\omega0$)	$p1$ ($\omega1$)	$p2$ ($\omega2$)
Cd48	191	6.62207	0.69931	0.30069	0.82299 (0.00001)	0.11271 (2.78916)	0.06430 (6.75520)
Cd84	195	7.392841	0.42873	0.57127	0.61480 (0.00001)	0.38511 (3.94486)	0.00010 (3.94574)
Cd84 (<i>Mus Pahari</i> omitted)	195	3.086014	0.57502	0.42498	0.16982 (0.15467)	0.73934 (0.15473)	0.09084 (7.06495)
Cs1	191	-0.295038	0.22489	0.77511	0.54498 (0.75884)	0.44886 (0.75886)	0.00616 (36.35146)
Ly108	198	4.053447	0.27926	0.72074	0.00000 (0.00001)	0.99488 (0.71488)	0.00512 (77.69282)
Cd150	210	0.037811	0.87935	0.12065	0.09056 (0.00001)	0.79798 (0.0001)	0.11146 (1.14935)
Cd229	395	42.702684	0.79409	0.20591	0.20272 (0.16628)	0.76018 (0.16630)	0.03710 (20.38612)
CTLA4	116	2.312925	0.65334	0.34666	1 (0.23708)	0 (n/a)	0 (n/a)

Table 8. Codon substitution (d_N/d_S) analysis on the SLAM/Cd2 Ig domains and CTLA4 show that Cd229 and Cd48 are the most likely to be under positive selection. d_N/d_S analysis was carried out using Yang's codon substitution models as described in Methods. The number of codons included in the analysis from each gene is shown. Numbers under Likelihood Ratio Test show the difference between the log-likelihoods obtained for the Discrete Model (M3), and the Neutral Model (M1). Numbers in bold are those that reach significance, indicating there is positive selection. The Neutral Model columns indicate the proportion of conserved codons with $\omega0=d_N/d_S=0$ ($p0$), and the proportion under neutral selection ($p1$, with $\omega1=1$) under this model. The next three columns indicate the proportions of codons ($p0$, $p1$ and $p2$) from each gene, which are assigned to three classes in the Discrete Model, for which the d_N/d_S values are calculated. For each class, the d_N/d_S values ($\omega0$, $\omega1$ and $\omega2$ respectively) are also shown, in parenthesis. $\omega2>1$ indicates that the codons in this class are under positive selection. For CTLA4, $\omega1$ and $\omega2$ could not be estimated because all the exon 2 codons fall into one class, as indicated by $p0=1$.

Fig 16A

		A	B	C*	C*	C'*	D	
<i>M-Cd229</i>	36	GMLGGSVTFSL-NISKDAEIEHITWNCPPKALALVFYKKDITILDkgyNGRLK	VSE	D	G	y	S	94
<i>R-CD2</i>	8	GALGHGINLNIPNFQMTDDIDEVRWE-RGSTLVAAEFKRKMKEPFLK---	SGA	F	E	I	L	62
				58	61	65	70	87
		E	F*		G*		A	
<i>M-Cd229</i>	95	LYMSNLTKSDSGSYHAQINQKNVILTTNKEFTLHIYEKLOK	PQ	I	I	V	E	154
<i>R-CD2</i>	63	LKIKNLTRDDSGTYNVTVYSTNGTRILNKALDLRILEMVS	K	P	M	I	Y	114
			109	118		134		

Fig 16B

		A	B	C*	C*	C'*	D	
<i>M-Cd84</i>	31	GILGESVTF-LLNIQEPKKIDNIAWTSQSSVAFIKPGVNKA	EV	TL	TQ	G	T	89
<i>H-CD2</i>	11	GALGQDINLdIPSFQMSDDIDDIKWEKTS	DKK	K	I	A	Q	65
	27,28		45		70	73	79	83,84

Fig 16. Protein sequence alignment: **A.** Mouse Cd229 with Rat CD2 and **B.** Mouse Cd84 with Human CD2. β strand positions determined for CD2 are shown in shaded boxes with the strand name above. *: Strands known to form the CD2 binding interface. Codons under selection in Cd229/ Cd84 are boxed, with codon-numbers below. Selected codons encoded by SNPs distinguishing the two major laboratory strain haplotypes are boxed in bold. Codon numbers in bold represent selected codons corresponding to critical CD2 binding residues.

Table 9

	Diabetes Resistant: A at Position 77	Diabetes Susceptible: G at Position 77	
Inbred Lab Strains	MRL/MpJ, 129/SvJ, B6, B10	NZW, NOD NZB/BINJ,BALB/cJ	
Wild-derived Inbred	<i>Mus m musculus</i> (#42, 43, 45, 46, 47) <i>Mus m domesticus</i> (#35) <i>Mus m castaneus</i> (#34, 36) <i>Mus m molossinus</i> (#37, 38, 39)	<i>Mus m musculus</i> (#48) <i>Mus m molossinus</i> (#40)	
Wild, outbred	None	<i>Mus m musculus</i> <i>Mus m domesticus</i> <i>Mus m castaneus</i> <i>Mus m molossinus</i> <i>Mus m Spp</i>	<i>Mus Spicilegus</i> <i>Mus Macedonius</i> <i>Mus Spretus</i>

Table 9: The CTLA4 exon 2 SNP linked to Type 1 diabetes susceptibility is prevalent amongst populations from all *Mus* species analyzed. Sequence analysis of exon 2 of CTLA4 was carried out in the 33 wild-outbred, 15 wild-derived inbred, and 8 common lab strains. Wild outbred and wild-derived inbred strains are denoted by their assigned numbers. Mouse strains that share the B6 (diabetes resistant: A) version or the NOD version (diabetes susceptible: G) are listed along with species, or, in the case of *Mus Musculus* strains, their sub-species. The only exceptions are *Mus Pahari*, which has a T (synonymous) at this position, and the *Mus m Spp* strains 10 and 24, which are heterozygous (A/G) for the SNP.

**Chapter V. Identification of the *Sle1b* Gene by BAC-Transgenic Rescue:
SLAM/CD2 Members Remain the Strongest Candidates to Mediate Autoimmunity**

Introduction

The *Sle1b* locus, a ~900 kb interval on mouse chromosome 1, causes a break in tolerance to chromatin important in the initiation of pathogenesis in the NZM2410 spontaneous murine model of the complex autoimmune disease Systemic Lupus Erythematosus (SLE) (Chapter 3, 26, 171). B6.*Sle1b* congenic mice, which have this NZM2410-derived susceptibility interval alone introgressed onto the lupus-resistant C57BL/6 (B6) genetic background, are characterized by the production of serum anti-nuclear autoantibodies (ANAs), and elevated levels of activation markers on their splenic B and CD4⁺ T cells as they age (Chapter 3, 26, 171).

In an effort to identify the causative gene within the *Sle1b* region, we constructed a Bacterial Artificial Chromosome (BAC) contig of 100 BACs across the entire interval (Chapter 3). Each of these large, circular constructs carries a large segment of B6-derived genomic DNA, ranging from ~100-300 kb, and six of them together form a continuous, overlapping tiling path across the locus, as shown in Fig 1B of Chapter 3. By sequencing these six BACs, we were able to construct a transcriptional map of the region, which revealed the presence of 24 transcribed genes, 19 of which are spleen-expressed. Extensive candidate gene analysis, comparing the lupus-resistant B6 and lupus-susceptible B6.*Sle1b* strains for any functional polymorphisms in these genes, revealed that 14 have coding-region SNPs or transcriptional differences that distinguish the parental strain alleles, making them potential candidate genes. A polymorphic haplotype comprised of seven members of the SLAM/CD2 family of genes has been shown to be by far the strongest candidate to mediate the

phenotype, with a member of the family, Ly108, being the most attractive single candidate gene (Chapter 3, 171).

The *Sle1b*-associated autoimmune phenotype is strongly allele dose-dependent (26). Thus, while most (~90%) of aged B6.*Sle1b* females are ANA-positive, the presence of a B6 allele of *Sle1b* in (B6 X B6.*Sle1b*) F1 heterozygotes is able to reduce or “rescue” this phenotype to a large extent, and these mice show a large drop in the phenotype, to ~33%; B6 females are ANA-negative (Fig 17). We decided to harness this property of the *Sle1b* phenotype, and have employed a BAC-transgenic rescue strategy as a functional, *in vivo* method by which to localize and definitively identify the causative gene. A schematic outline of our strategy is shown in Fig 18: we reason that the expression of the B6 allele of the *Sle1b*-causative gene from a BAC-transgene may be able to reduce ANA production in B6.*Sle1b* mice, therefore allowing us to localize it to a single BAC. The use of other BACs from the region, harboring genes irrelevant to the phenotype, is not expected to have such an effect.

BACs have been successfully used in a similar capacity to localize and confirm the identity of genes mediating a wide variety of mutant phenotypes, by their ability to complement and rescue them (290, 291, 292, 293). Their main advantage over conventional transgenic constructs is that they mediate copy-number dependent expression of the genes they harbor, being less vulnerable to position effects (in which expression of a transgene is strongly influenced by its site of integration). These large genomic constructs are more than likely to carry 5' and 3' flanking, as well as intronic, regulatory elements required for optimal, endogenous-pattern gene expression (reviewed in 294, 295). In this particular instance, they also give us the ability to systematically interrogate the entire *Sle1b* locus for the presence of the causative gene in just six large, overlapping fragments contained in the tiling-path BACs, shown in Fig1B of Chapter 3, and in Table 10 of this Chapter.

The B6-BAC transgenics in this study were made on the B6 genetic background, due to ready availability of the large number of mice required for the process. Each transgene was then bred onto the B6.*Sle1b* background, and litters of “test-progeny” were generated, with the use of the breeding scheme illustrated in Fig 19. Once the transgenes were bred onto the B6.*Sle1b* background, we could assess copy number and test for the expression of the BAC-derived B6 alleles of candidate genes in each line. Since the B6 transgenes and B6.*Sle1b* endogenous alleles differ only by a series of single-nucleotide polymorphisms (SNPs), we use a sequencing-based SNP assay, described in detail in Chapter 2 (Methods), to characterize our transgenics. We were able to successfully generate and characterize germline-transmitting, candidate-gene expressing transgenic lines for five of the six BACs that we had hoped to; unfortunately, BAC 90, which carries our strongest candidate gene *Ly108*, was not one of these. BAC-heterozygous and homozygous females from each transgenic line and their BAC-negative littermates, all on the B6.*Sle1b* congenic background, were aged and phenotyped for rescue of the ANA-production phenotype at its peak, at nine months of age. FACs analysis on splenic lymphocytes was carried out and spleen weights were noted, to check for any gross abnormalities caused by the BAC-transgenes, or any reduction of the activation phenotypes associated with *Sle1b*.

We find that, while there are promising preliminary data from SLAM/CD2 family-containing transgenic lines, none of the BACs we have used thus far shows compelling, consistent evidence of rescue of the autoimmune phenotype. This study, however, remains preliminary, and will require the characterization of the *Ly108*-containing BAC 90 before any firm conclusions can be made. Nevertheless, none of the non-SLAM/CD2 BACs cause

any drop in ANA production despite the confirmed expression of their candidates genes, again supporting a role for the SLAM/CD2 family in mediating autoimmunity.

Results

Table 10 summarizes the B6-derived BAC-transgenic (BAC-Tg) lines that were successfully generated and characterized in this study in an effort to identify the gene mediating autoimmunity in B6.*Sle1b* mice. The efficiency of generation of BAC-Tg founders ranged from about 10% (of newborn pups being BAC Tg-positive) for BACs 41, 25, 40 and 90, to 21% for BAC 47, and 27% for BAC 95, in keeping with previous reports using BAC-transgenes (reviewed in 294). Of the 19 potential founders obtained in all, six failed to transmit their BAC-transgenes, and of the remaining, three were later found to fail to express the B6 (BAC-derived) alleles of their candidate genes on the B6.*Sle1b* genetic background. This left two lines per BAC (with the exception of BAC 90) that were useful (listed in Table 10), and these were further characterized. Copy numbers of the BAC-Tgs ranged from low (1-2 copies) in most lines, to medium (Med: 3-4) in the BAC 41 (1352) line, and very high (V. High: >10) in both BAC 40 lines and one BAC 25 (1118) line (Table 10). Again, this is in keeping with previous studies, which report a preponderance of low copy numbers with the use of BAC-transgenes (294). The one transmitting BAC 90-Tg line, carrying *Cd84* and *Ly108* (the latter the single most promising candidate gene in our region), unfortunately failed to express its BAC-derived genes, and was therefore eliminated from this study. Re-injection of this construct has yielded 17 potential founders that are being bred to B6.*Sle1b* mice, eight of which have successfully transmitted the transgene so far. Here we describe our initial characterization of the BAC-Tgs generated, in terms of their copy number, expression of candidate genes carried on each BAC, and their effect on ANA production and splenomegaly. Both copy number and relative expression of the B6-transgenes to the B6.*Sle1b*-endogenous alleles (termed simply the “*Sle1b*” alleles henceforth), were assessed using a sequencing based SNP assay on genomic or splenic cDNA, and details on the specific SNPs targeted in each of these assays can be found in Chapter 2 (Methods).

Characterization of BAC 41-Tg lines: B6-alleles of *Usp23* and *Nit1* on BAC 41 do not cause a drop in penetrance of ANA-production.

Ratios of peak heights from the B6 and *Sle1b* alleles of a SNP in the *Tnfrsf19* (*Dedd*) gene on BAC 41, obtained from genomic DNA of every BAC 41-Tg mouse set aside for aging, were used to categorize the mice from each of the two lines into heterozygous (Het) and homozygous (Hom) test progeny. B6 (transgene): *Sle1b* (endogenous) peak height ratios were in the range of 0.15 ± 0.004 (Hets) and 0.34 ± 0.019 (Homs) in BAC 41(1191) test progeny (Fig 20A). Thus, heterozygotes from this line have about half the B6: *Sle1b* SNP-allele ratio observed in (B6XB6.*Sle1b*) F1 mice (0.27 ± 0.11), which carry a 1:1 ratio of the two alleles. This would indicate that the number of B6-alleles carried in the BAC 41 (1191) line is about half the number of endogenous *Sle1b* alleles (2 copies in the B6.*Sle1b* genetic background), yielding a low copy number of 1 for this line. BAC 41(1191)-Homs, therefore, carry double this number, or 2 copies, of the B6-BAC. Similarly, the B6: *Sle1b* SNP-allele ratios were 0.73 ± 0.014 (Hets) and 0.92 ± 0.011 (Homs) in BAC 41(1352) test progeny, giving this line a copy number in the range of three to four (Fig 20A).

The candidate gene *Nit1* was found to be expressed in both lines, as shown in Fig 20B. Relative expression of the BAC-Tg derived B6 allele to the endogenous *Sle1b* allele was lower than might be expected, given the peak height ratios in cDNA from control (B6 X B6.*Sle1b*) F1 mice. This may indicate that some of the regulatory elements important to *Nit1* expression may be absent on the BAC construct, causing the gene to be more weakly expressed than expected in both lines. It should be noted that, while the overall ratios obtained from 41(1191)-Het cDNAs were low, the B6-peaks were very robust and unmistakably present in the assay (data not shown); the ratios reflect the greater heights of the *Sle1b*-peaks. *Nit1* expression seemed to correlate with copy number in general (albeit with the exception of the single BAC 41(1352)-Hom mouse tested), with mice carrying more

copies of the BAC-transgene expressing higher relative amounts of the B6 allele. B6 BAC-derived *Usp23* expression was absent in heterozygotes and homozygotes from the BAC 41(1191) line, indicating that there was incomplete integration of the BAC. In BAC 41(1352) mice, however, the B6-allele was expressed, at about double the relative amount as in (B6 X B6.*Sle1b*) F1's, in keeping with the estimated copy number (Fig 20C).

The expression of the genes on this BAC does not have an ameliorative effect on ANA-production (Fig 20D), and none of the groups of nine month old female test progeny shows a significant drop in penetrance relative to negative littermate controls. Only five 41(1191)-Hom mice have been obtained and aged to this point, making this group far too small to estimate penetrance with any reliability at all, and it is included here only for completeness. In addition, since a ratio of 1:2:1 of BAC-homozygous, BAC-heterozygous, and BAC-negative test progeny is expected (Fig 19), this number is actually about four-fold lower than it should be, given that at least 45 BAC 41(1191)-Hets have been obtained. This would indicate a deleterious effect of BAC-homozygosity in the line, probably attributable to disruption of a gene at the site of transgene-integration rather than over-expression of a gene on the BAC, since such an effect is not observed in the other, more highly expressing line. More mice continue to be aged to increase the numbers in the BAC 41(1352)-Het and 41(1352)-Hom groups, which are not yet ideally sized. Finally, the mild splenomegaly observed in B6.*Sle1b* mice (data not shown), does not seem to be affected by the presence of BAC 41, although the 41(1352)-Hom group may have slightly elevated spleen weights as compared to negative littermates; at present, they are not significantly different (Fig 20E).

Characterization of BAC 47- Tg lines: B6-*Ref2bp* does not cause a drop in ANA production.

The two BAC 47- Tg lines obtained and used in this study were both low in copy number. The ratios of B6:*Sle1b* alleles of a *Ref2bp* SNP, obtained from genomic DNA from these mice, were in the range of 1.6 ± 0.05 in BAC 47(1354), 2.18 ± 0.09 in 47(1429)-Hets, and 4.79 ± 0.38 in 47(1429)-Homs, as compared to 3.6 ± 0.05 in (B6 X B6.*Sle1b*) F1's (Fig 21A). None of the mice obtained from the 47(1354) line had a higher B6:*Sle1b* genomic allele ratio than that of the mice categorized as heterozygotes, indicating that the line is homozygous-lethal. This could be due to the site of integration, or, alternatively, due to over-expression of a gene on the BAC in homozygotes from this line, although the latter is less likely given the low copy number.

Relative expression of the B6 BAC-derived allele of *Ref2bp* reflects copy number in the two lines, and is about half that in (B6 X B6.*Sle1b*) F1's which carry equal amounts of both alleles (Fig 21B). While the transgene is expressed in the BAC 47(1354) mice, only the homozygotes from the 47(1429) line seem to express it: the heterozygotes have no detectable B6-peak.

The presence of this BAC does not cause any drop in penetrance of the ANA-production phenotype, adequate numbers of nine month old females having been assayed in each of the groups (Fig 21C), and nor does it affect spleen weight (Fig 21D).

Characterization of BAC 25-Tg lines: A modest but consistent drop in ANA penetrance caused by BAC 25, carrying the B6 alleles of SLAM/CD2 family members *Cd229* (*Ly9*), *Cs1*, and *Cd244* (2B4).

BAC 25 (1121) was found to be a low copy number line, with genomic B6:*Sle1b* *Cd229* SNP-allele ratios in the range of 0.16 ± 0.004 (Hets) and 0.29 ± 0.01 (Homs) as compared to 0.35 ± 0.00 in control (B6 X B6.*Sle1b*) F1's. The other line, 25 (1118), has a much higher copy number, with ratios of 2.8 ± 0.06 in heterozygotes, and 5.4 ± 0.16 in homozygotes, translating to a copy number of 16 (Fig 22A).

Expression of the B6 alleles of *Cd229* and *Cs1* were assessed using the SNP assay on splenic cDNA. Relative expression of transgenic B6 to endogenous *Sle1b* alleles of *Cd229* correlates well with copy number in the 25 (1121) line, and is comparable to relative levels of the two alleles in (B6 X B6.*Sle1b*) F1 splenic cDNA. Relative expression of the transgene is not as high as would be expected from copy number in the 25(1118) line, indicating that most of these copies are not intact. Relative allele expression is comparable to that of (B6 X B6.*Sle1b*) F1s in the 25 (1118)-Homs. Heterozygotes from this line, inexplicably, seem to express even more highly than the homs, and in fact have more than double the relative expression of B6: *Sle1b* as that in (B6 X B6.*Sle1b*) F1's (Fig 22B). This may indicate a shortcoming of the sequencing based SNP assay, which may be more suited to detection of transgene expression than quantification in the case of highly expressed transgenes, due to a ceiling effect. While relative allele expression of *Cs1* is comparable to (B6 X B6.*Sle1b*) F1's in the 25(1121)-Hets and about double in the 25(1121)-Homs, the high copy number 25(1118)-Hets expressed only about half, and homozygotes about the same ratios as the control mice (Fig 22C).

The availability of an antibody specific for the B6 allele of *Cd244* (B6-2B4; 296) allowed us to analyze B6 transgene expression by cell surface staining. CD244 is expressed

predominantly on NK cells and a proportion of CD8⁺ T cells (186, 187, 188). We therefore compared the expression of B6-2B4 in NK1.1⁺ (Fig 22D and E) and CD8⁺ (Fig 22F and G) splenocytes in B6 and B6.*Sle1b* control mice, and the two BAC 25-Tg lines. We also examined expression in B220⁺ cells (Fig 22H and I), the bulk of which are B cells, but which include subsets of NK and activated T cells, to examine how closely the pattern of expression of the BAC-transgene reflects endogenous patterns of CD244 expression. The percentage of cells expressing B6-2B4 (Figs 22D, F and H), as well as the intensity of staining within the B6-2B4⁺ populations (Figs 22E, G and I) were examined. In each case, inset panels show corresponding data from a small set of nine month old (B6 X B6.*Sle1b*) F1 females, along with age and sex-matched mice of the two parental strains, as a representation of the effect of carrying equivalent copies of the two alleles, on B6-2B4 cell surface expression.

As expected, a very large proportion of B6 NK cells express B6-2B4, as compared to B6.*Sle1b*, in which only about 25% of NK cells stain for the antibody (Fig 22D). 25(1121)-Hets and 25(1121)-Homs have percentages of B6-2B4⁺ NK cells comparable to those of B6 mice (Fig 22D), and the Median Fluorescence Intensity (MdFI) of these cells is also similar (Hets) or higher (Homs) as that of B6 NK cells. The small proportion of B6.*Sle1b* NK cells that do stain positive for the allele have a lower MdFI (Fig 22E). 25(1118)-Het and 25(1118)-Hom mice are intermediate between B6 and B6.*Sle1b* in terms of the percentage of B6-2B4⁺ NK cells, and similar to B6 for MdFI of the positive population (Figs 22D and E).

The data from CD8⁺ T cells is less clear, as the differences between the parental B6 and B6.*Sle1b* strains themselves are not significant. Unlike the NK cell population, B6.*Sle1b* mice have only very slightly lower percentages of CD8⁺ T cells positive for B6-2B4, and the positive populations actually have a slightly higher MdFI than those from B6 (Figs 22F and G). This is probably due to cross-reactivity of the antibody with one of the three expressed genes from the expanded *Cd244* (*2B4*) locus found in B6.*Sle1b*, as well as in most common

laboratory strains (Chapter 3). This cross-reactive B6.*Sle1b* allele seems to be expressed in only a small proportion of NK cells, but may be the predominantly expressed allele in the 2B4⁺ fraction of CD8⁺ cells. Both BAC Tg-lines express levels of B6-2B4 comparable to B6 or even higher, in terms of percentages of positive CD8⁺ cells (Fig 22F and G).

The pattern and level of expression of B6-2B4 in B220⁺ splenocytes from 25(1121) mice is similar to that of B6 mice, and higher than that of B6.*Sle1b* mice, although they fail to reach the level of significance of B6 (Figs 22H and I). 25(1118)-Hets have significantly higher percentages of B6-2B4⁺ B220 cells than B6.*Sle1b*, comparable to B6, and these percentages are even higher in 25(1118)-Homs (Fig 22H and I). The fact that this line actually has lower levels of B6-2B4⁺ NK and CD8⁺ T cells, but increased levels of B6-2B4⁺ B220⁺ cells, indicates that expression in this line may be less faithful to endogenous patterns of expression of the molecule.

The expression of the B6 alleles of the SLAM/CD2 members on BAC 25 causes a modest but consistent decrease in penetrance of ANA-production, from 87.5% in BAC Tg-negative littermates, to 62.5% in both the 25(1121)-Hets and Homs, 63.2% in the 25(1118)-Homs, and 68% in 25(1118)-Hets, with more than adequate numbers of mice having been assessed in all groups except 25(1121)-Het (Fig 22J). The presence of the BAC has no effect on spleen weight (Fig 22F).

Characterization of BAC 40-Tg lines: A significant, but inconsistent, drop in ANA production in the presence of the B6-BAC carrying SLAM/CD2 family members *Cd48* and *Cd150 (Slam)*.

Both BAC 40-Tg lines used in this study have very high copy numbers. The genomic B6: *Sle1b* *Cd48* SNP allele ratio was 14.18 ± 0.58 in heterozygotes and 26.07 ± 1.23 in

homozygotes from the BAC 40(1004) line, and 15.97 ± 0.44 in heterozygotes and 24.16 ± 0.93 in homozygotes from the 40(1006) line, compared to 1.65 ± 0.05 in (B6 X B6.*Sle1b*) F1 mice (Fig 23A).

The relative levels of expression of the transgenic (B6) to endogenous (*Sle1b*) alleles of *Cd48* were assessed using the SNP assay on splenic cDNAs, which showed somewhat erratic expression of the BAC-derived transgene at twelve months of age (Fig 23B). This could reflect the absence of some of the 5' elements important in faithful expression of the gene, which lies towards the proximal end of the BAC. The 40(1004)-Het group ranged from a relative level of expression 20-fold lower than that of control (B6 X B6.*Sle1b*) F1's in one mouse, to levels comparable to the controls in two others. 40(1004)-Homs had relative levels of expression ranging from that of the controls in one mouse, to about 15-fold higher in another. Relative B6: *Sle1b* expression of *Cd48* showed a similarly wide range in 40(1006)-Het mice, and was more consistent in the 40(1006)-Hom group, at about 10-fold that of control (B6 X B6.*Sle1b*) F1 mice (Fig 23B). Relative expression of B6:*Sle1b* alleles of *Cd150* was similarly erratic in 40(1004)-Hets and 40(1004)-Homs, which may reflect fragmented integration of the BAC in this line. The SNP allele ratios obtained from 40(1006)-Hets and 40(1006)-Homs were much more consistent, with both sets expressing relative levels about five to seven-fold higher than those in (B6 X B6.*Sle1b*) F1's (Fig 23C).

Total levels of CD48 cell surface expression were assessed with a staining antibody that recognizes both the B6 and *Sle1b* alleles, to look for any total upregulation of the molecule in splenocytes from the BAC-Tgs. CD48 is universally expressed on B, T and NK cells. We therefore examined the intensity of expression (MdFI) in CD4⁺ and CD8⁺ T cells, as well as B220⁺ B cells (Figs 23D, E and F). B6 mice show a small but significant, consistent increase in CD48 staining intensity as compared to B6.*Sle1b* mice (171, Figs 23D, E and F), which is most pronounced in the CD4⁺ population (Fig 23D), and is even more

clearly evident in the inset panels showing comparisons between B6, B6.*Sle1b*, and (B6 X B6.*Sle1b*) F1 mice. While the relative levels of B6: *Sle1b* *Cd48* alleles assessed using the SNP assay on splenic cDNA are erratic in both BAC Tg lines, the total levels of cell surface expression of CD48 are consistent within each group. BAC 40 (1004)-Hets and 40(1004)-Homs express the same amounts of surface CD48 as B6.*Sle1b* mice, despite their high copy number, so there is no obvious upregulation in total expression of this candidate gene in the line. BAC 40(1006)-Hets and 40(1006)-Homs express significantly higher levels than B6.*Sle1b* mice, and their level of expression also surpasses that of the B6 strain (Figs 23D, E and F). Both the heterozygotes and homozygotes express about the same amounts of the molecule, suggesting that total cell surface expression of CD48 may be under some form of regulation, and that doubling copy number in the 40(1006)-Homs does not increase expression any further.

Numerous differences between the two assays used to assess *Cd48* transgene expression could account for the differences in the data obtained: the SNP assays are carried out on bulk populations of all splenocytes, and assesses transcriptional levels of the two alleles relative to one another, while cell surface staining detects total cell surface protein expression in the three large cell subsets.

The only BAC-Tg group in this study to show a statistically significant drop in ANA production from 92% in littermate controls to 50% in 20 test progeny, was the BAC 40 (1004)-Het group (Fig 23G). This drop is not evident in the BAC 40(1004)-Hom test progeny, although the number of mice in this group (8) is smaller than desirable, and more mice are currently being aged to nine months to make a more conclusive assessment of ANA penetrance. There is no reduction in ANA production in the BAC 40 (1006)-Tg line, either amongst the Het or Hom groups, although this line expresses the B6-derived transgenes more

robustly than the “rescuing” line. This inconsistency would seem to suggest that the lowered penetrance in the BAC 40(1004)-Het group, while dramatic, may be the result of an extraneous, founder effect that will have to be more extensively investigated before it can be attributed to the presence of the B6 allele of the *Sle1b*-causative gene. Finally, the transgene has no effect on splenomegaly (Fig 23H).

Characterization of BAC 95-Tg lines: A mild and inconsistent drop in ANA-penetrance in BAC-Tgs with the B6 alleles of *Nicastrin*, *Copa*, and *Pxf*.

Two low copy number lines were obtained carrying BAC 95: BAC 95 (1254), with a genomic B6: *Sle1b Nic* SNP allele ratio of 1.68 ± 0.08 in heterozygotes and 3.9 ± 0.31 in homozygotes, yielding a copy number of one when normalized to the ratio of 3.8 ± 0.15 in (B6 X B6.*Sle1b*) F1's; and BAC 95 (1255), with ratios of 3.3 ± 0.08 in heterozygotes and 5.6 ± 0.28 in homozygotes, giving it a copy number of two (Fig 24A).

The relative expression levels of B6 to *Sle1b* alleles of *Nic* correlated quite well with copy number in these BAC- Tg lines (Fig 24B), with fairly low ratios in 95(1254)-Hets, approximately the same ratio as the control (B6 X B6.*Sle1b*) F1 mice in a 95(1254)-Hom and a 95(1255)-Het mouse, and about double the ratio in a 95(1255)-Hom mouse. *Copa* expression was about the same in both lines (Fig 24C), with heterozygotes expressing little more than half the relative ratio of (B6 X B6.*Sle1b*) F1 controls, and homozygotes expressing about double this ratio, despite the fact that 95(1255) has double the copy number of 95(1254). The *Pxf* gene lies only partially within the *Sle1b* interval. Thus, B6.*Sle1b* mice derive part of the gene from B6, and part of it from the NZW parent of NZM2410. A SNP between B6 and NZW in exon 6 of the gene was found to be identical in B6 and B6.*Sle1b* congenic mice (data not shown). We then harnessed an exon 2 SNP between B6 and NZW, with puzzling results. While B6 and B6.*Sle1b* clearly differ from each other, with the latter

sharing and expressing the NZW parental allele (data not shown), (B6 X B6.*Sle1b*) F1 mice seem to express the B6 allele exclusively, despite inheriting one copy of each. All of the BAC 95-Tg mice also follow this pattern of expression, showing only a single, B6 BAC Tg-derived peak in the SNP assay when it is carried out on splenic cDNA. The presence of two different peaks in B6 and B6.*Sle1b* splenic cDNA, and both peaks in genomic DNA from (B6 X B6.*Sle1b*) F1 mice, argues against this being an anomaly of the assay itself. Nevertheless, this does show that the B6-transgene seems to be expressed in both lines on the B6.*Sle1b* background (Fig 24D).

The expression of the B6 alleles of these genes caused a modest drop in ANA production, from 73% in BAC Tg-negative littermate controls, to about 65% in 95(1254)-Hets and 95(1255)-Hets. A similar reduction was not observed in homozygotes from either line, making it rather unconvincing (Fig 24E); more mice continue to be aged to obtain a sufficiently large 95(1254)-Hom group. Finally, there was no effect of the BAC-transgene on spleen weight (Fig 24F).

We went on to assess and compare titers of serum anti-total histone/ds DNA IgG in the subset of BAC-Tg lines which showed some drop in penetrance of the ANA phenotype, to see if these data could clarify which group, if any, showed a significant change from B6.*Sle1b* BAC Tg-negative littermate controls (Fig 25). As expected, a control group of B6 females had very low titers of ANAs, significantly lower than that of B6.*Sle1b* mice. None of the BAC-Tg lines, however, were significantly different from the background B6.*Sle1b* strain, when a non-parametric ANOVA was used to compare titers across the multiple groups. When each BAC-Tg line was individually compared to B6.*Sle1b* using Mann-Whitney tests, only the BAC 40(1004)-Het group reached significance ($p = 0.0334$). An

examination of the titers in the BAC 40 (1004)-Hom group shows that, while the overall penetrance in this group was not as low as that of the 40 (1004)-Hets, the titers in these mice are not as high, by and large, as those observed in the other groups, although they do not reach significance. The BAC 25 (1121)-Hom mice seem to show a bimodal distribution of serum ANA titers, with mice having either very high, or fairly low titers. Like the BAC 40(1004)-Hom mice, the few BAC 95 (1254)-Hom mice tested have titers that are not as high as some of the other lines, although these also fail to reach significance. As described in the following section, however, this latter observation probably reflects a drop in the overall percentage of CD19+ B cells observed in this line, rather than genuine “rescue” of autoimmunity by BAC 95.

Flow cytometric analysis of splenic cell populations in BAC-Tg lines: No obvious differences from the parental B6.*Sle1b* strain in any group except BAC 95(1254)-Hom.

Flow cytometric analysis was carried out on mice from the various BAC-Tg lines, as well as control B6 and B6.*Sle1b* mice, to assess for any gross abnormalities caused by over-expression of any of the genes present on the BAC-transgenes used (Table 11A), and to examine whether the known splenic lymphocyte differences between aged B6 and B6.*Sle1b* mice (26, Tables 11A, B and C, and unpublished data from S. Subramanian) are rescued by any of the BAC-transgenes. These FACs data were obtained over several separate experiments done on sets of six mice, each of which included at least one B6.*Sle1b* control, and several of which also included a B6 control.

In comparison to twelve-month old female B6's, B6.*Sle1b* mice have a significantly higher percentage of CD4+, and lower percentage of CD8+ T cells caused by a slight but consistent drop in the number of CD8+ T cells. They also have an increased percentage of CD11b+ cells (in bold in Table 11A, unpublished data from S. Subramanian). B6.*Sle1b* mice

show increased activation of their CD4⁺ T cells, with elevated expression of CD69 on their CD4⁺ T cells, and decreased percentages of Naïve (CD62L⁺CD44^{lo}) and increased percentages of Activated/memory (CD62L⁻CD44^{hi}) and Transitional phenotype (CD62L⁻CD44^{lo}) CD4⁺ T cells (in bold in Table 11B, unpublished data from S. Subramanian). Finally, lymphocyte activation is reflected in elevated CD69 expression on the B220⁺ (B cell) and CD3⁺ (T cell) populations in aged B6.*Sle1b* mice (in bold in Table 11C, unpublished data from S. Subramanian). While none of the BAC-Tg lines showed a significant difference from the parental B6.*Sle1b* strain, it should be noted that, as indicated in Tables 11A, B and C, most of the known, consistent differences between the B6 and B6.*Sle1b* groups did not reach significance when using non-parametric ANOVAs to compare across multiple groups, due to loss of statistical power. These differences become significant only when the two groups are compared just to each other, using parametric or non-parametric t-tests. Thus, to reliably detect any “rescue” of cellular phenotypes across multiple groups, much larger groups of mice would have to be analyzed. Alternatively, cohorts of mice from the various lines, along with age and sex-matched B6 and B6.*Sle1b* controls, would have to be run in discrete sets and compared, to avoid multiple-testing. Nevertheless, this analysis did show that, with the exception of BAC 95, none of the BAC-transgenes caused any gross changes in the cellular phenotypes examined. The two BAC 95 (1254)-Hom mice examined showed a large drop in the percentage of CD19⁺ B cells in their spleens, reflected in an increase in the percentages of CD4⁺ and CD8⁺ T cells, although the number of mice was too small to reach statistical significance (Table 11A). This reduction by about half of the B cell population could certainly have an extraneous effect on ANA production, and may account for the slightly lower titers in this group (Fig 25); no such drop was observed in the heterozygotes from this group.

Discussion

The use of BAC-transgenes in this study has not yet yielded strong, compelling evidence for any one BAC harboring the *Sle1b*-causative gene. One major shortcoming of our study as it stands, is the absence of a BAC carrying and expressing the B6 allele of our most promising candidate gene, *Ly108*, a member of the SLAM/CD2 cluster (Chapter 3, 171). Until test progeny from this BAC have also been generated, aged, and characterized, our results can only be considered preliminary, and efforts to do just this are underway. In addition, data gathered from growing numbers of mice from different groups have shown us that at least ten or more mice are needed within a group to give us an accurate, reliable measure of ANA-penetrance, which can fluctuate quite a lot with smaller numbers. Therefore, only the results from adequately sized groups should be considered, as additional mice continue to be aged and phenotyped where necessary.

There are nonetheless certain important conclusions we can draw at this point, primarily, that none of the non-SLAM/CD2 candidates, transgenes of all of which have been shown to be expressed in at least one line, succeed in rescuing the autoimmune phenotype. One BAC 40 line, carrying the SLAM/CD2 members *Cd48* and *Cd150* (*Slam*), and both BAC 25 lines, carrying the members *Cd229* (*Ly9*), *Cs1*, and *Cd244* (*2B4*), do show some evidence of being able to affect ANA production by B6.*Sle1b* mice. We consider the data from BAC 25 to be more convincing, given the consistency of the effect across both lines. The more dramatic BAC 40(1004)-Het effect, on the other hand, is not evident in the small BAC 40(1004)-Hom group, and nor is it observed in the BAC 40(1006) line, despite the fact that the latter is the more highly expressing of the two. It is not clear at this point, therefore, that it does not represent some extraneous founder effect, although there are no obvious disruptions

of the splenic lymphocyte populations examined, such as those observed in the case of the BAC 95 (1254)-Hom group.

It is very possible that ANA production in B6.*Sle1b* mice the effect of some *combination* of SLAM/CD2 family members, rather than any one gene. These molecules have overlapping functions resulting from homotypic and heterotypic interactions amongst themselves (177, 262, 178), and form two stable “haplotypes” of linked alleles across all inbred laboratory strains of mice studied, the more common of which is associated with autoimmunity (Chapter 3). If this is indeed the case, a more profound “rescue” effect would require the presence of the B6 alleles of multiple genes, for example, *Cd244* on BAC 25 and *Cd48* on BAC 40, which are known to interact with one another (183, 189, 195). These BACs-Tg lines can be bred to each other (or to other BAC-Tg lines) to test this hypothesis, in the event that an *Ly108*-containing BAC by itself fails to exhibit a convincing drop in penetrance.

As expected with the use of BAC-transgenes, many of our lines had low copy numbers, and correspondingly low expression of candidate genes. Given the strong effect of having equivalent copies of B6 and NZM-derived *Sle1b* alleles in (B6 X B6.*Sle1b*) F1 mice, which showed a ~60% drop in penetrance from B6.*Sle1b* mice, it seems likely that even slightly lower relative expression of the B6 allele of the causative gene, would nevertheless have some effect on ANA production. An issue that does need to be addressed, in the context of transgene expression in our study, is the fact that the relative expressions of the B6 BAC-derived alleles of several of our candidate genes do not reflect copy number. While copy-number dependent, position-effect independent expression is one of the main advantages of using BACs instead of conventional transgenic constructs, such expression requires that the

gene in question be optimally positioned towards the middle of the BAC, such that there is a good chance that 5' and 3' regulatory elements are also carried along with it (295). Genes that are less strategically positioned on a BAC may not have this advantage, and, lacking a strong engineered promoter to artificially drive expression (such as is often included in transgenic constructs), may in fact be even more vulnerable to the position-effects dictated by the site of integration. This would be especially true in cases where the transgenes are not integrated fully intact. Due to practical considerations, we did not have the luxury of positioning each of our 14 total candidate genes in the middle of a BAC, but instead chose to cover all of them as efficiently as possible. Multiple founder lines for each BAC were used, however, in order to control for just such variations in expression due to position and copy number effects, and to ensure reasonably adequate expression of the B6 allele of every candidate gene in at least one transgenic line.

This study represents the first such attempt to functionally identify the causative gene within a large locus linked to autoimmunity, by the ability of a polymorphic variant from a lupus-resistant strain, carried on a BAC-transgene, to correct the phenotype mediated by the lupus-susceptible endogenous version. Data obtained from these preliminary analyses will prove very useful in conjunction with similar studies testing the *Ly108*-containing BAC for its ability to rescue the B6.*Slc11b* strain. We are also in the process of generating a knock-out of the entire SLAM/CD2 family, and, by complementing it with each of our SLAM/CD2 BAC-transgenics, we hope to gain valuable insights about the functions mediated by the various members of the family.

Fig 17.

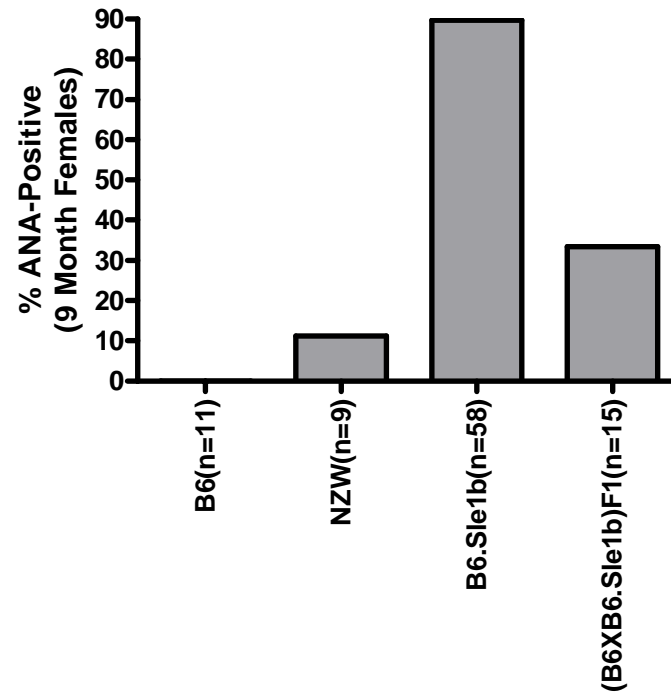


Fig 17. *Sle1b* has an allele-dose effect on ANA production on the B6 genetic

background. Nine month old female mice were assayed for the presence of serum anti-ds DNA/total histone IgG. Those with titers greater than the mean titer from a panel of eleven 12-month old B6 females + 4 SDs, were considered to be ANA-positive. The penetrance (percent of ANA-positive mice) of B6.*Sle1b* congenics is compared to that of (B6 X B6.*Sle1b*) F1 heterozygous mice, which carry one copy each of the B6 and *Sle1b* versions of the telomeric chromosome 1 interval, the parental B6 strain, and NZW, from which NZM2410 derives this interval.

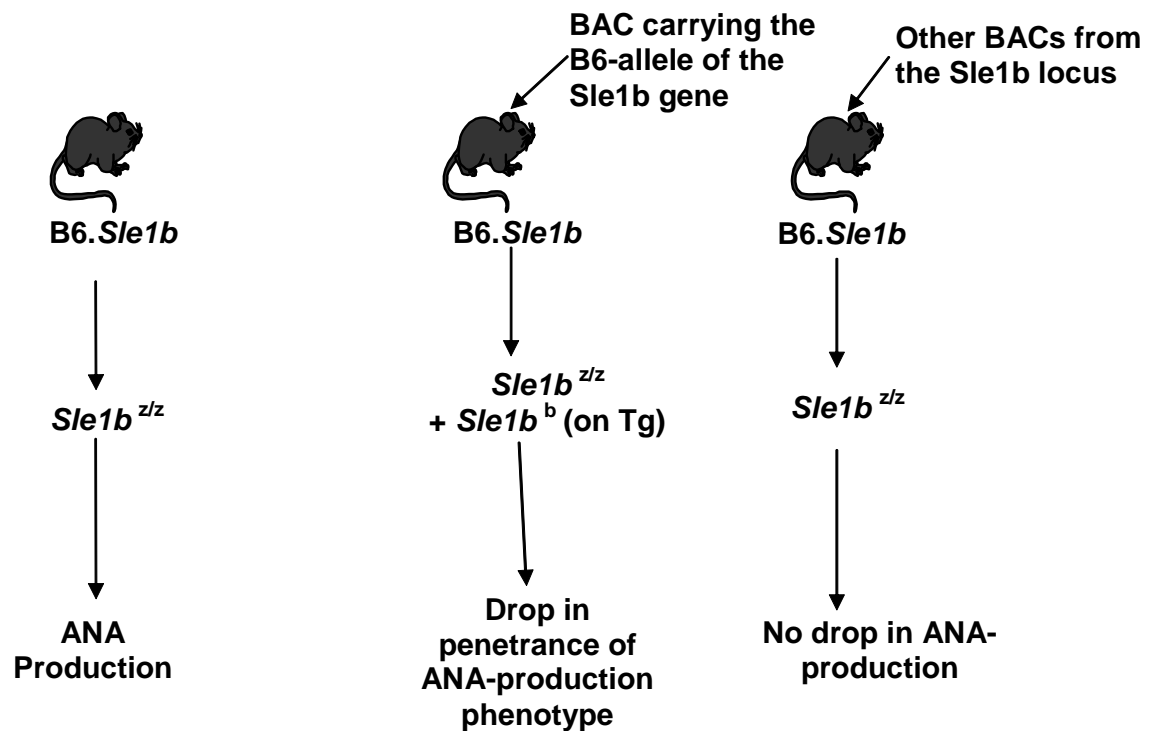
Fig 18

Fig 18. A schematic representation of the BAC-transgenic “rescue” strategy employed in this study. The presence of the B6 allele of the NZM-derived *Sle1b* gene (which mediates the autoimmune phenotype in *B6.Sle1b* congenic mice) on a BAC-transgene may “rescue” *B6.Sle1b* mice carrying that BAC from the ANA-production phenotype, resulting in a drop in penetrance. The presence of other BACs from the interval carrying B6 alleles of genes irrelevant to the phenotype, on the other hand, will fail to do so.

Table 10.

Assigned BAC Number	RPCI-23 Designation (Insert size)	Candidate Genes	BAC-Transgenic Lines
BAC41	194d6 (180 kb)	Usp23, Nit1	41(1191): Low Copy (1) 41(1352): Med Copy (3-4)
BAC47	48o11 (168 kb)	Ref2bp	47(1354): Low Copy (1) 47(1429): Low Copy (1)
BAC25	171k8 (185 kb)	Cd229(Ly9), Cs1, Cd244 (2B4)	25(1121): Low Copy (1) 25(1118): V. High Copy (16)
BAC40	145f9 (175 kb)	Cd48, Cd150 (Slam)	40(1004): V. High Copy (16) 40(1006): V. High Copy (18)
BAC90	388c4 (210 kb)	Ly108, Cd84	None
BAC95	462j8 (205 kb)	Nic, Copa, Pxf	95(1254): Low Copy (1) 95(1255): Low Copy (2)

Table 10. Six B6-derived BACs from the RPCI-23 library that form an overlapping tiling path were used to try to functionally identify the *Sle1b* gene by BAC-transgene mediated rescue of the ANA-production phenotype. Listed are the numbers assigned to each BAC used in this study (column 1), the corresponding RPCI designation and insert-size (column 2), and the candidate genes described in Chapter 1 that are included on each BAC (column 3). The successfully germline-transmitted, transgene-expressing lines that are characterized in this study are listed in column 4, with transgene-copy range (low/ medium/ high/ very high), and copy number indicated in brackets. BACs are listed in the order they occur, from the most centromeric to the most telomeric.

Fig 19

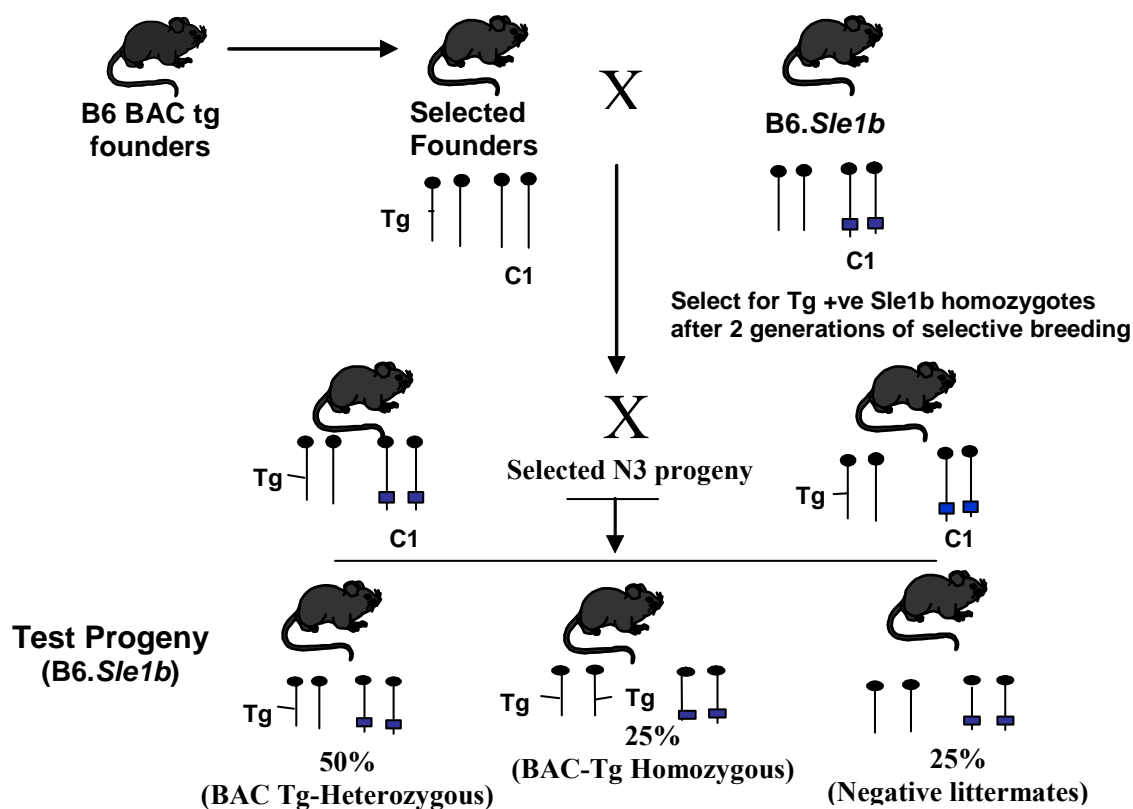


Fig 19. Breeding scheme employed to generate the BAC-transgenic “test progeny” that are assayed for transgene-mediated rescue. BAC-Tg founders generated on the B6 genetic background were bred onto the autoimmune B6.Sle1b background. BAC-Tg positive B6.Sle1b mice are intercrossed to yield BAC Tg- heterozygous and homozygous test progeny, as well as transgene-negative littermate controls, as shown.

Fig 20A. BAC41(*Usp23*, *Nit1*): *Tnfsf19*(*Dedd*)

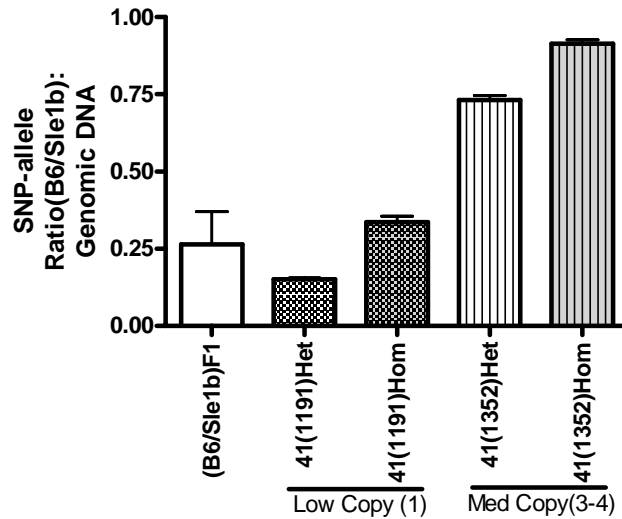


Fig 20B. BAC41-*Nit1* Expression

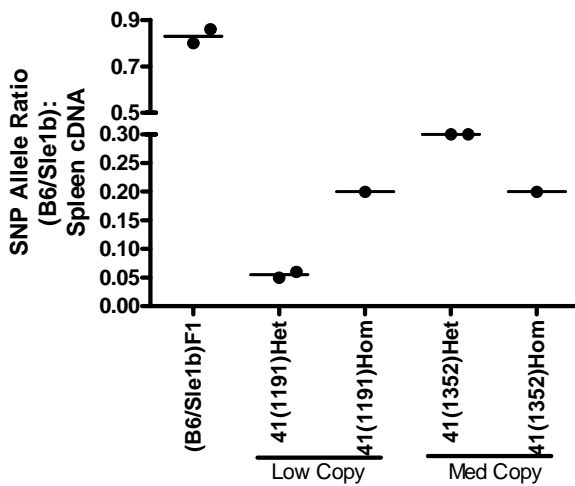


Fig 20C. BAC41-*Usp23* Expression

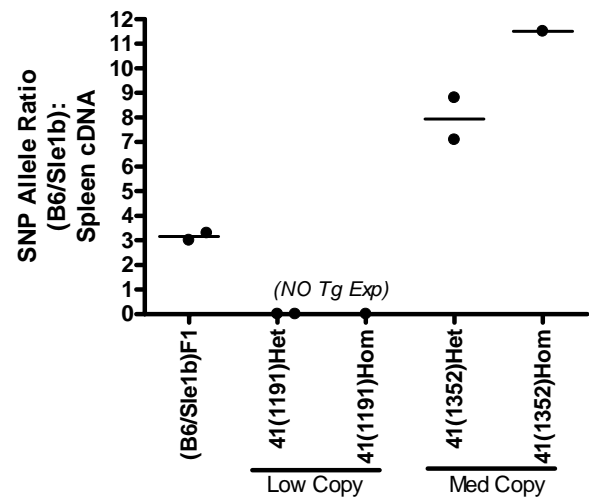


Fig 20. Initial characterization of BAC41-Tg (candidate genes: *Usp23*, *Nit1*) lines on the B6.*Sle1b* genetic background. A. Ratio of the peak heights of the B6: *Sle1b* SNP-alleles from the *Tnfsf19* (*Dedd*) gene present on the BAC, generated by a sequencing-based SNP assay performed on genomic tail DNA from **all** BAC 41-Tg test progeny generated so far from two separate lines. Ratios were used to distinguish between mice het vs hom for the BAC-Tg, and are shown as the Mean + SEM for each group. The ratio obtained from het mice in each line was normalized to that obtained from 4 (B6 X B6.*Sle1b*) F1 mice, which carry a 1:1 ratio of the B6 and *Sle1b* alleles, in order to calculate copy-number for each Tg-line, shown in brackets. **B. and C.** Ratio of the peak heights of B6: *Sle1b* SNP-alleles generated by the sequencing-based SNP assay performed on splenic cDNA from het and hom mice from each line, and control (B6 X B6.*Sle1b*) F1 mice, to assay for expression of the candidate genes on this BAC. Each spot represents the ratio obtained from one mouse at 12 months of age.

Fig 20D

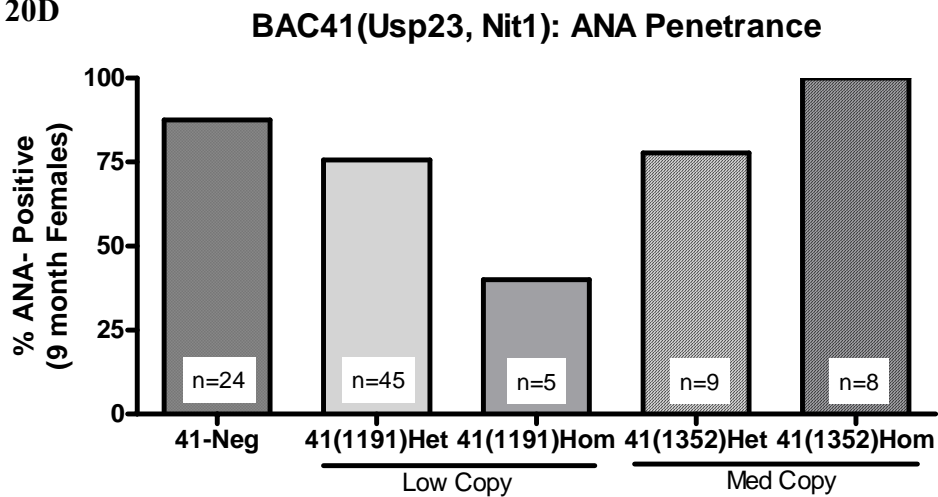


Fig 20E

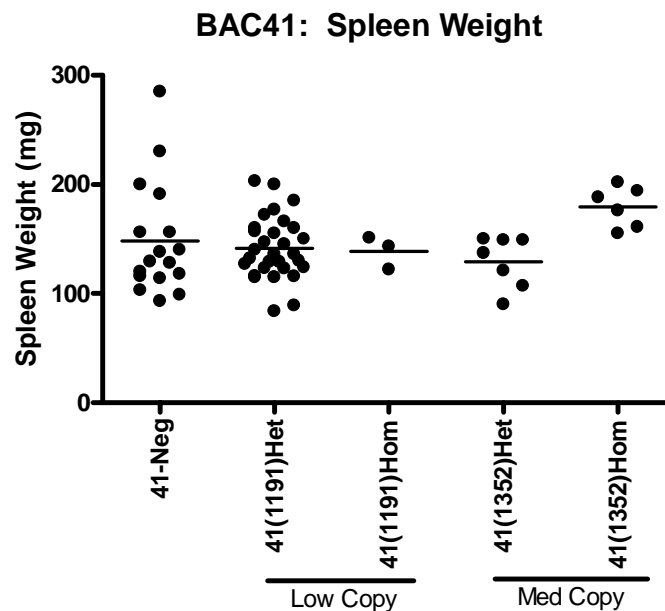


Fig 20. Initial characterization of BAC41-Tg (candidate genes: *Usp23*, *Nit1*) lines on the B6.*Slc1b* genetic background. D. Penetrance of ANA-production in BAC41-Tg mice. Percent of ANA-positive nine month old females ($> \text{B6 mean} + 4 \text{ SD}$) in het and hom groups from each BAC-Tg line, and BAC Tg-negative littermates from both lines, are shown. **E.** Spleen weights of BAC-Tg mice and negative littermates. Spleen weights were taken at the time of necropsy, at 12 months of age, from het and hom mice from each line, and BAC Tg-negative littermates from both lines. Each spot represents the spleen weight of one mouse.

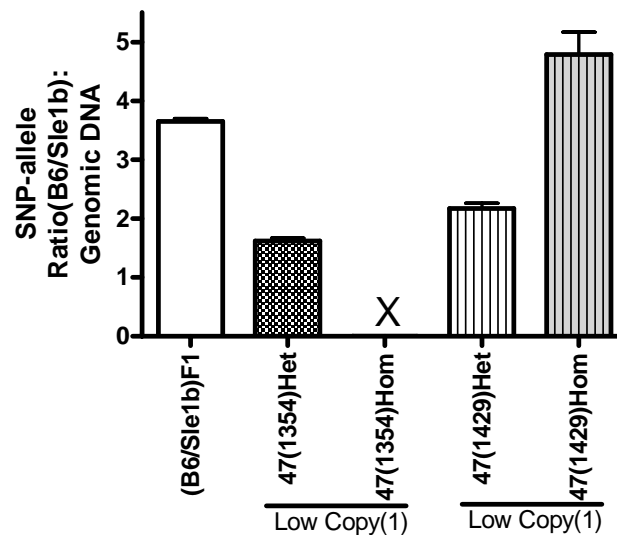


Fig 21B

BAC47-Ref2bp Expression

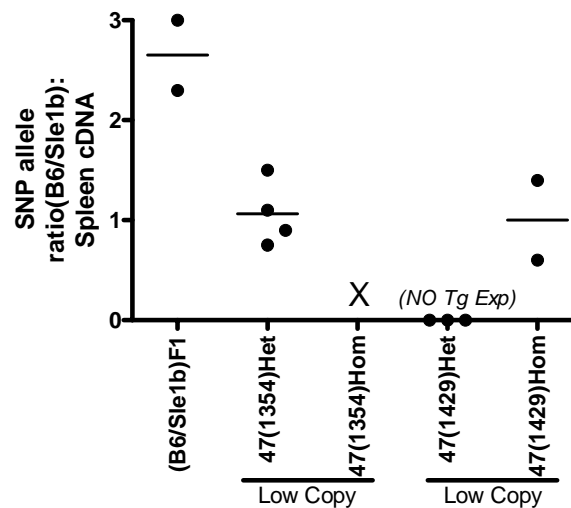


Fig 21. Initial characterization of BAC47-Tg (candidate gene: *Ref2bp*) lines on the B6.*Sle1b* genetic background. **A.** Ratio of the peak heights of the B6: *Sle1b* SNP-alleles from the *Ref2bp* gene present on the BAC, generated by a sequencing-based SNP assay performed on genomic tail DNA from **all** BAC47-Tg mice generated so far from two separate lines. Ratios were used to distinguish between mice het vs hom for the BAC-Tg, and are shown as the Mean + SEM for each group. The ratio obtained from the het mice in each line was normalized to that obtained from 4 (B6 X B6.*Sle1b*) F1 mice, which carry a 1:1 ratio of the B6 and *Sle1b* alleles, in order to calculate copy-number for each Tg-line, shown in brackets. **B.** Ratio of the peak heights of B6: *Sle1b* SNP-alleles generated by the sequencing-based SNP assay performed on splenic cDNA from het and hom mice from each Tg-line, and control (B6 X B6.*Sle1b*) F1 mice, to assay for expression of the candidate gene on this BAC. Each spot represents the ratio obtained from one mouse at 12 months of age. “X”: No mice obtained from this group.

Fig 21C

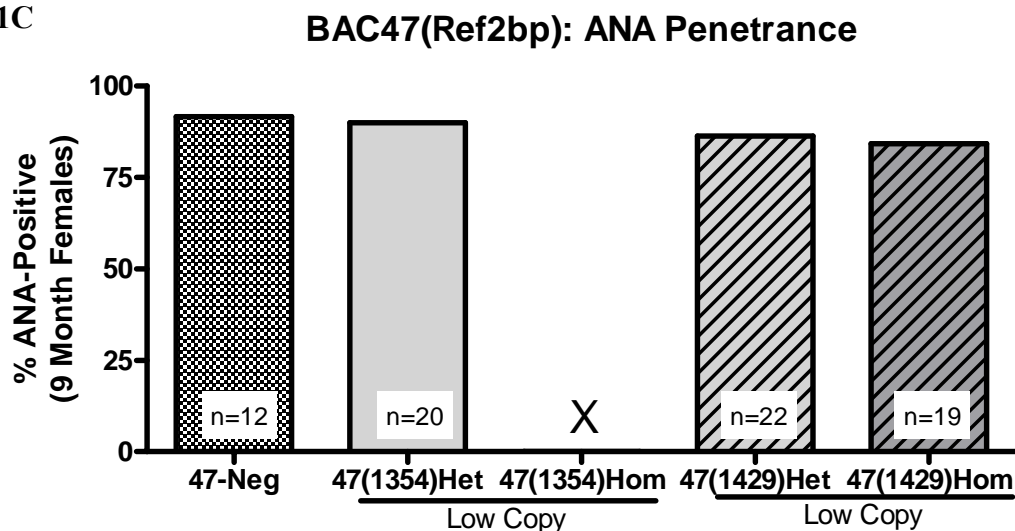


Fig 21D

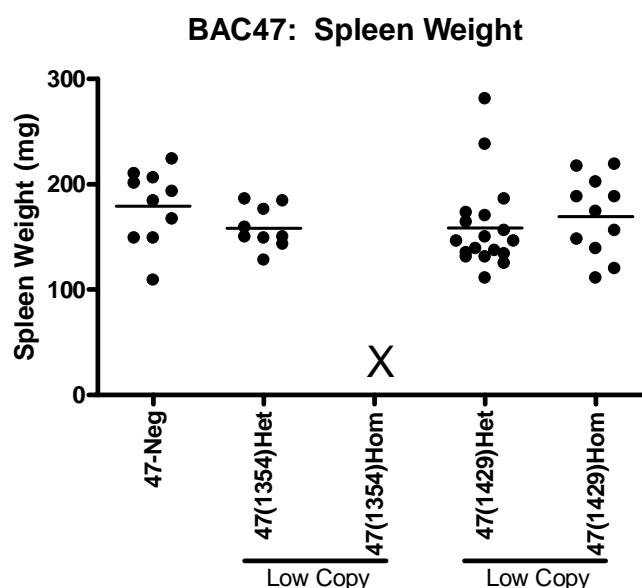


Fig 21. Initial characterization of BAC47-Tg (candidate gene: *Ref2bp*) lines on the B6.*Slc1b* genetic background. **C.** Penetrance of ANA-production in BAC47-Tg mice. Percent of ANA-positive nine month old females ($> \text{B6 mean} + 4 \text{ SD}$) in het and hom groups from each BAC-Tg line, and BAC Tg-negative littermates from both lines are shown. **D.** Spleen weights of BAC-Tg mice and their negative littermates. Spleen weights were taken at the time of necropsy, at 12 months of age, from het and hom mice from each line, and Tg-negative littermates from both lines. Each spot represents the spleen weight of one mouse. “X”: No mice obtained from this group.

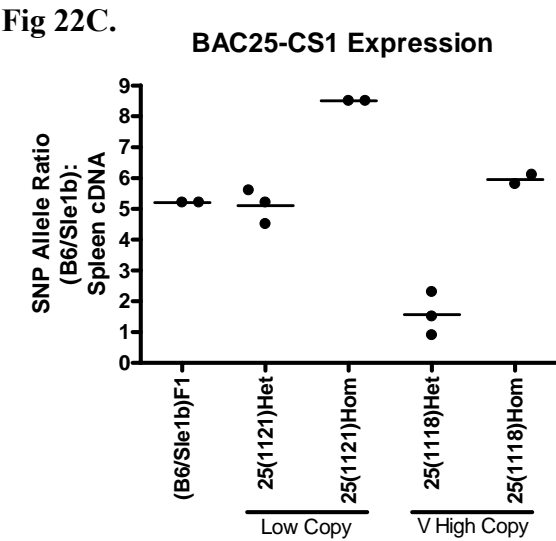
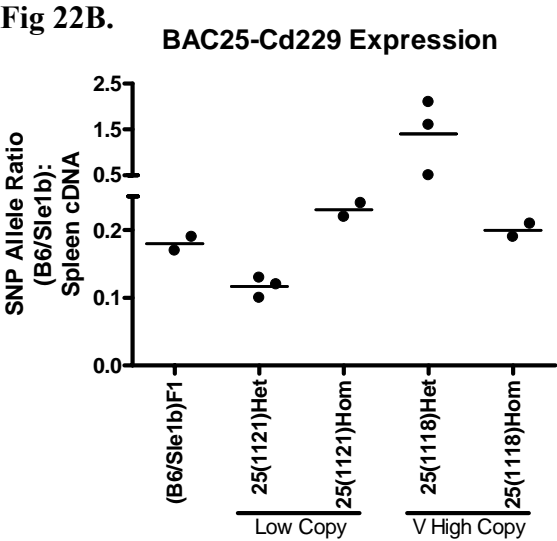
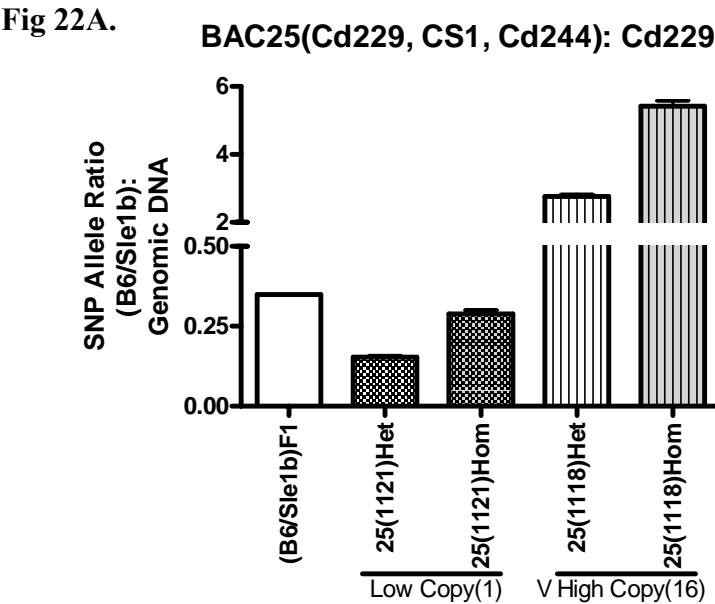


Fig 22. Initial characterization of BAC25-Tg (candidate genes: *Cd229*, *Cs1*, *Cd244*) lines on the *B6.Sle1b* genetic background. **A.** Ratio of the peak heights of the *B6: Sle1b* SNP-alleles from the *Cd229* (*Ly9*) gene present on the BAC, generated by a sequencing-based SNP assay performed on genomic tail DNA from **all** BAC25-Tg mice generated so far from two separate lines. Ratios were used to distinguish between mice het vs hom for the BAC-Tg, and are shown as the Mean + SEM for each group. The ratio obtained from the het mice in each line was normalized to that obtained from 4 (*B6* X *B6.Sle1b*) F1 mice, which carry a 1:1 ratio of the *B6* and *Sle1b* alleles, in order to calculate copy-number for each Tg-line, shown in brackets. **B. and C.** Ratio of the peak heights of *B6: Sle1b* SNP-alleles generated by the sequencing-based SNP assay performed on splenic cDNA from het and hom mice from each Tg line, and control (*B6* X *B6.Sle1b*) F1 mice, to assay for expression of the candidate genes on this BAC. Each spot represents the ratio obtained from one mouse at 12 months of age.

Fig 22D.

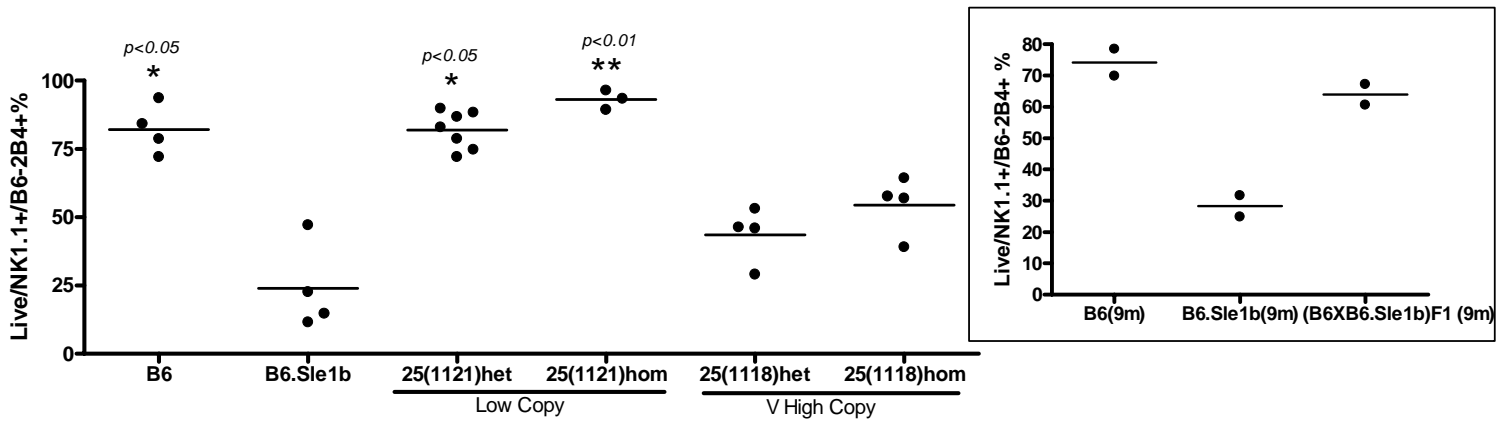


Fig 22E.

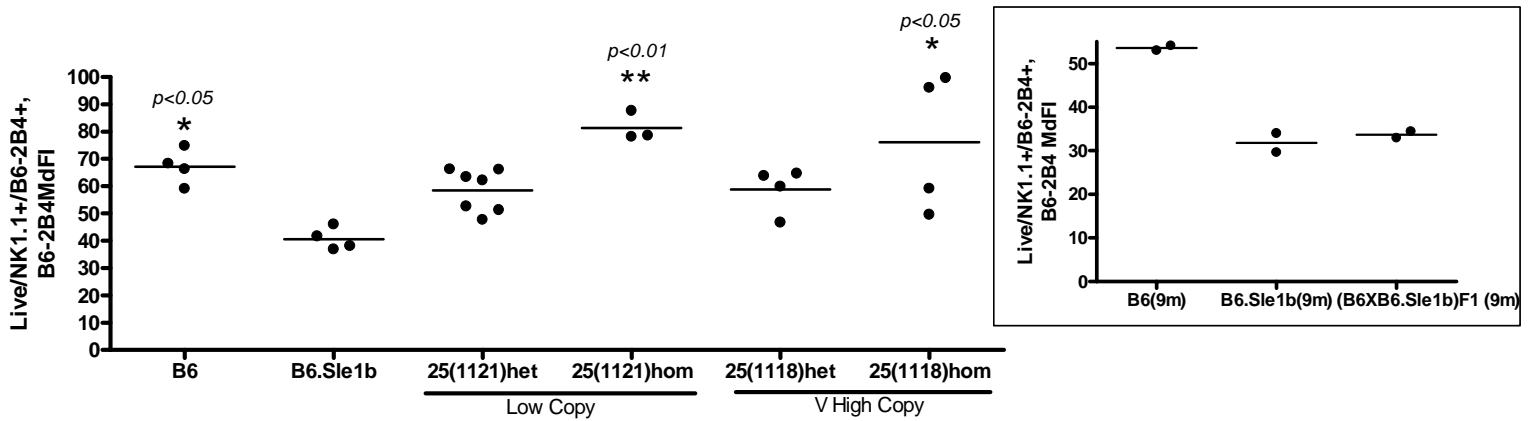


Fig 22. Initial characterization of BAC25-Tg (candidate genes: *Cd229*, *Cs1*, *Cd244*) lines on the *B6.Sle1b* genetic background. D-I. Flow cytometric analysis of cell-surface expression of the B6 allele of candidate gene *Cd244* (B6-2B4) on splenocytes from 12 month old female BAC25-Tg mice. **D.** The percentage of NK1.1+ cells that express B6-2B4 in age and sex-matched B6, *B6.Sle1b*, and BAC 25 Tg-*B6.Sle1b*. Each spot represents the percentage obtained from one mouse. **E.** Median fluorescence intensity (MdFI) of B6-2B4 in NK1.1+/B6-2B4+ cells. Each spot represents the MdFI from one mouse. For comparison, corresponding data obtained from two 9 month old B6, *B6.Sle1b*, and (*B6 X B6.Sle1b*)F1 heterozygous mice are shown in the inset panel beside each figure. *(*p* value): Groups significantly different from *B6.Sle1b*.

Fig 22F.

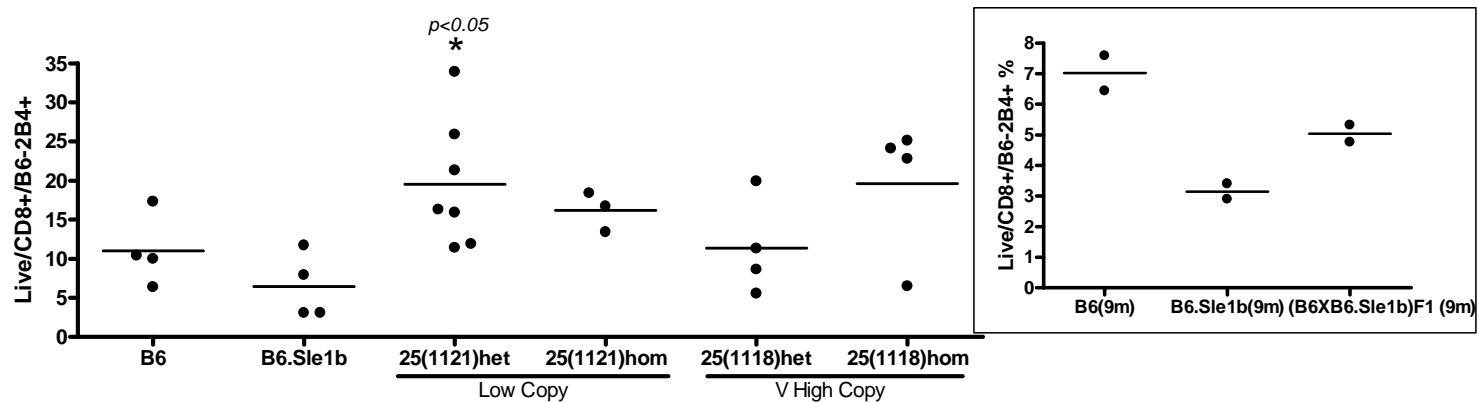


Fig 22G.

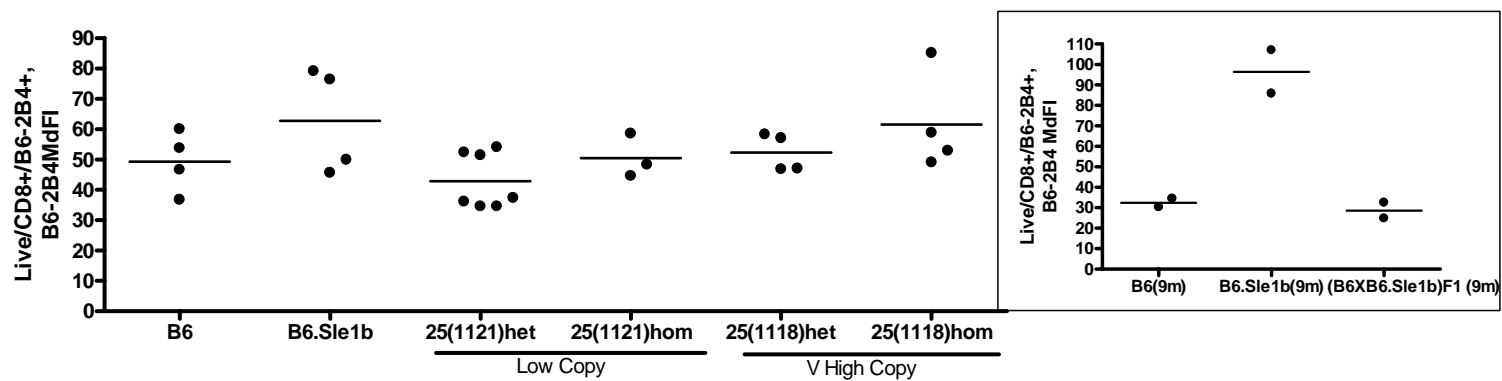


Fig 22. Initial characterization of BAC25-Tg (candidate genes: *Cd229*, *Cs1*, *Cd244*) lines on the B6.*Sle1b* genetic background. D-I. Flow cytometric analysis of cell-surface expression of the B6 allele of candidate gene *Cd244* (B6-2B4) on splenocytes from 12 month old female BAC25-Tg mice. **F.** The percentage of CD8+ T cells that express B6-2B4 in age and sex-matched B6, B6.*Sle1b*, and BAC 25 Tg-B6.*Sle1b*. Each spot represents the percentage obtained from one mouse. **G.** Median fluorescence intensity (MdFI) of B6-2B4 in CD8+/B6-2B4+ cells. Each spot represents the MdFI from one mouse. For comparison, corresponding data obtained from two 9 month old B6, B6.*Sle1b*, and (B6 X B6.*Sle1b*)F1 heterozygous mice are shown in the inset panel beside each figure. **(p value):* Groups that are significantly different from B6.*Sle1b*.

Fig 22H.

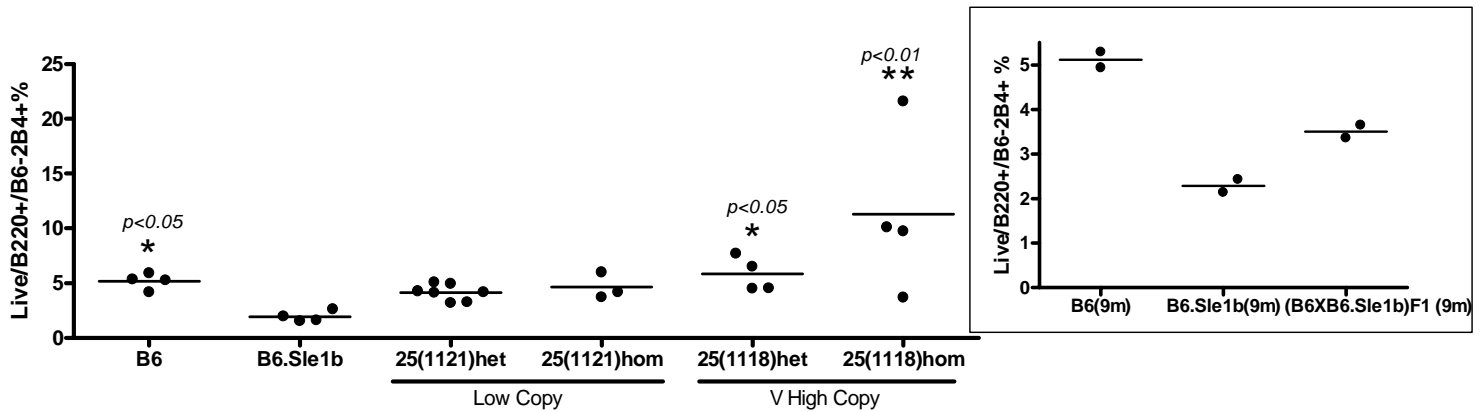


Fig 22I.

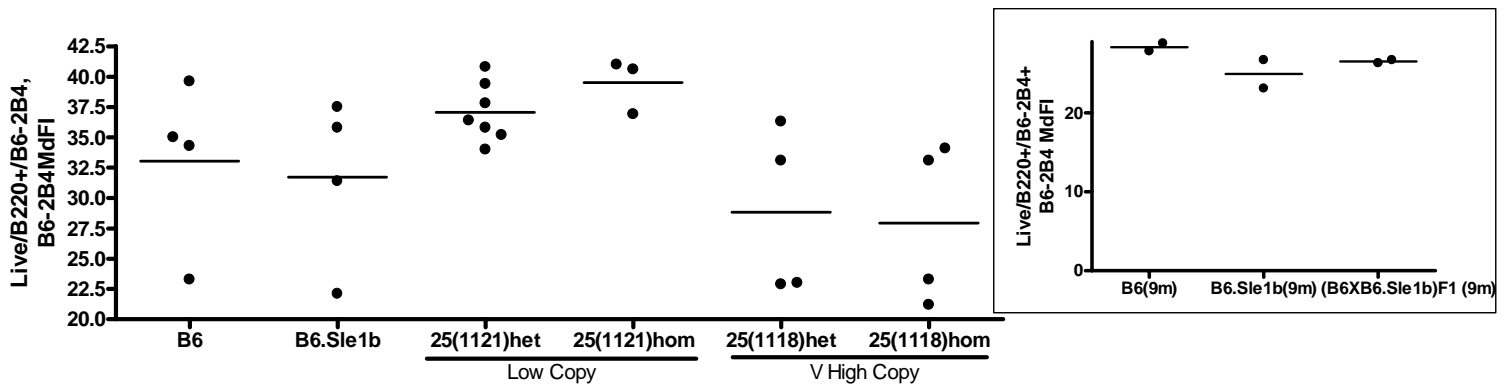


Fig 22. Initial characterization of BAC25-Tg (candidate genes: *Cd229*, *Cs1*, *Cd244*) lines on the B6.*Sle1b* genetic background. D-I. Flow cytometric analysis of cell-surface expression of the B6 allele of candidate gene *Cd244* (B6-2B4) on splenocytes from 12 month old female BAC25-Tg mice. **H.** The percentage of B220+ cells that express B6-2B4 in age and sex-matched B6, B6.*Sle1b*, and BAC 25 Tg-B6.*Sle1b*. Each spot represents the percentage obtained from one mouse. **I.** Median fluorescence intensity (MdFI) of B6-2B4 in B220+/B6-2B4+ cells. Each spot represents the MdFI from one mouse. For comparison, corresponding data obtained from two 9 month old B6, B6.*Sle1b*, and (B6 X B6.*Sle1b*)F1 heterozygous mice are shown in the inset panel beside each figure. *(*p* value): Groups that are significantly different from B6.*Sle1b*.

Fig 22J.

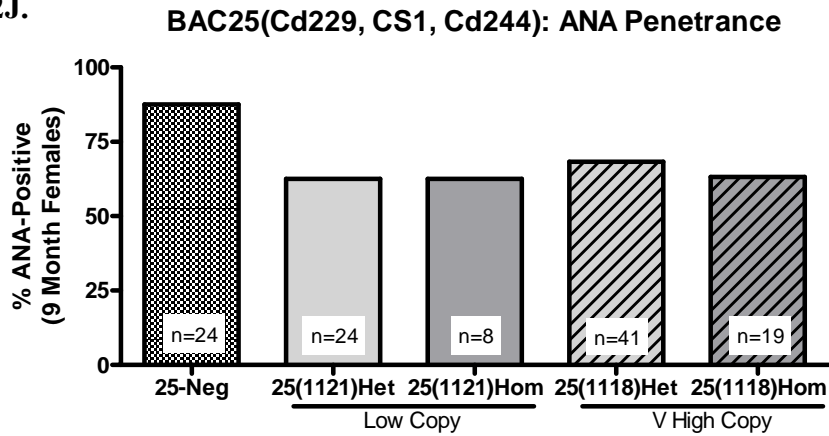


Fig 22K.

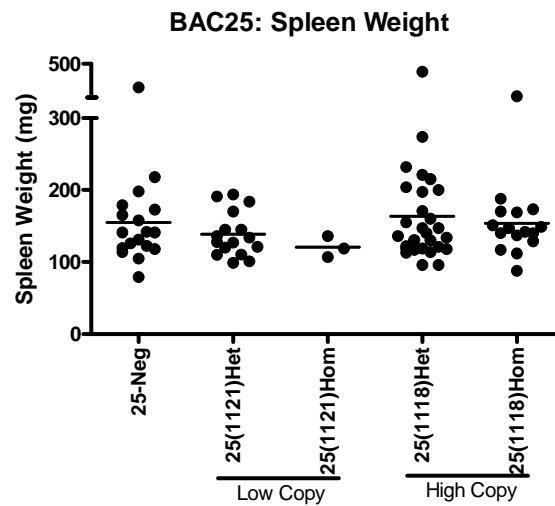


Fig 22. Initial characterization of BAC25-Tg (candidate genes: *Cd229*, *Cs1*, *Cd244*) lines on the B6.*Slc1b* genetic background. J. Penetrance of ANA-production in BAC25-Tg mice. Percent of ANA-positive nine month old females ($> \text{B6 mean} + 4 \text{ SD}$) in het and hom groups from each BAC-Tg line, and BAC Tg-negative littermates from both lines are shown. **K.** Spleen weights of BAC-Tg mice and their negative littermates. Spleen weights were taken at the time of necropsy, at 12 months of age, from het and hom mice from each line, and BAC Tg-negative littermates from both lines. Each spot represents the spleen weight of one mouse.

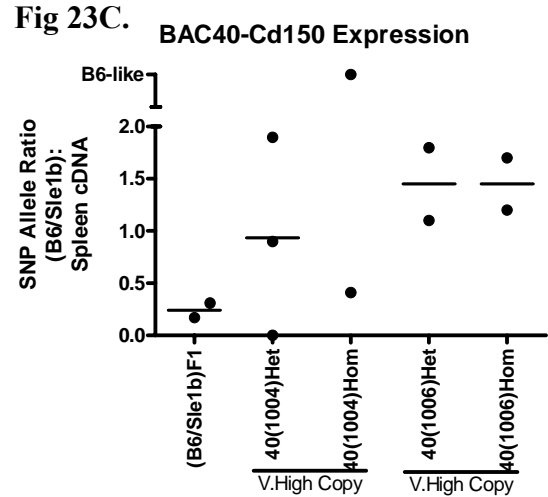
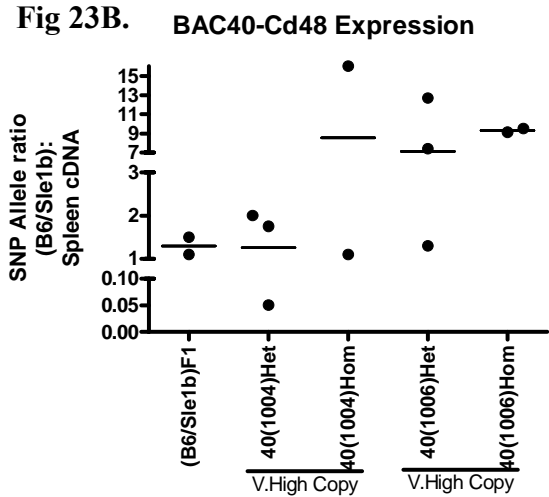
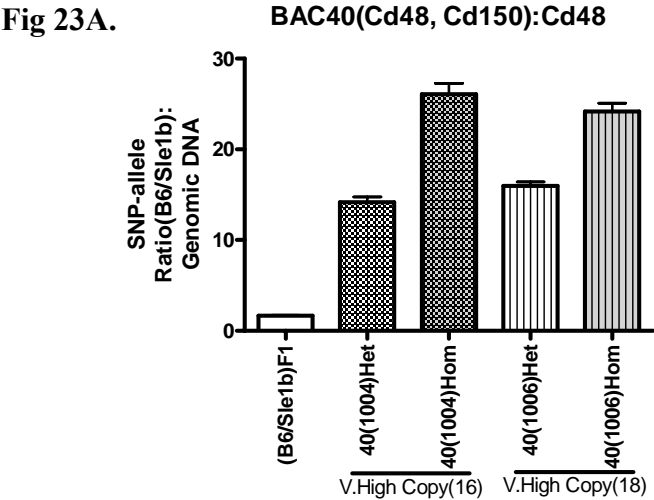


Fig 23. Initial characterization of BAC40-Tg (candidate genes: *Cd48*, *Cd150*) lines on the B6.*Sle1b* genetic background. **A.** Ratio of the peak heights of the B6: *Sle1b* SNP-alleles from the *Cd48* gene present on the BAC, generated by a sequencing-based SNP assay performed on genomic tail DNA from **all** BAC40-Tg mice generated so far from two separate lines. Ratios were used to distinguish between mice het vs hom for the BAC-Tg, and are shown as the Mean + SEM for each group. The ratio obtained from the het mice in each line was normalized to that obtained from 4 (B6 X B6.*Sle1b*) F1 mice, which carry a 1:1 ratio of the B6 and *Sle1b* alleles, in order to calculate copy-number for each Tg-line, shown in brackets. **B. and C.** Ratio of the peak heights of B6: *Sle1b* SNP-alleles generated by the sequencing-based SNP assay performed on splenic cDNA from het and hom mice from each Tg-line, and control (B6 X B6.*Sle1b*) F1 mice, to assay for expression of the candidate genes on this BAC. Each spot represents the ratio obtained from one mouse at 12 months of age.

Fig 23D.

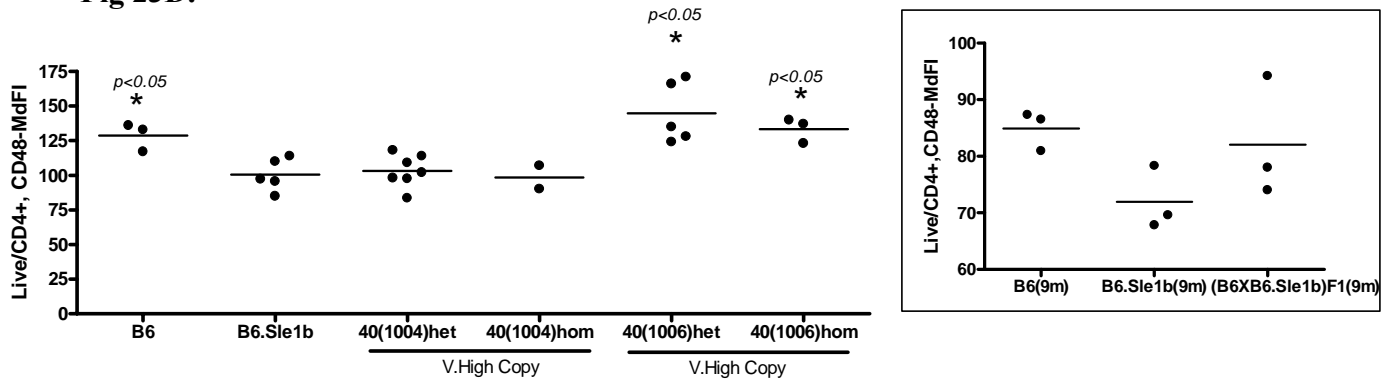


Fig 23E.

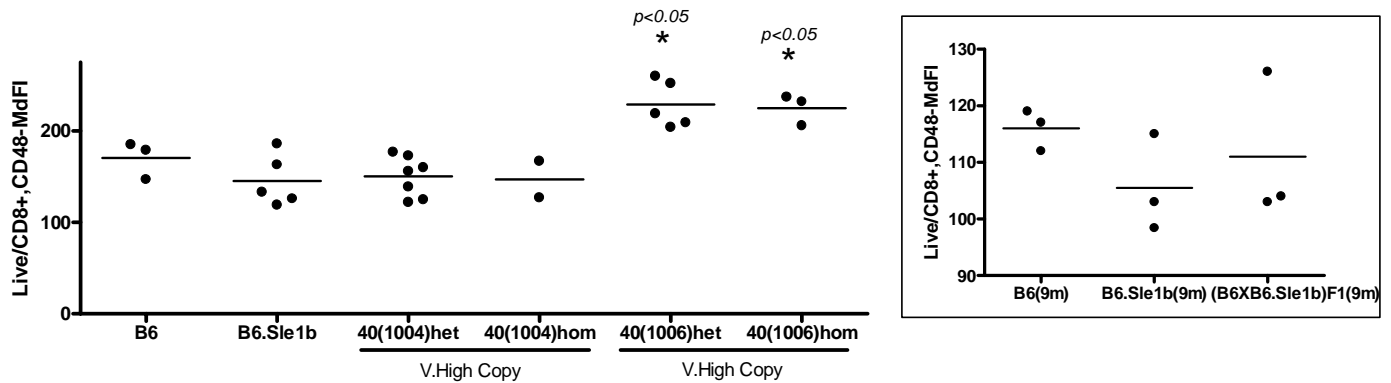


Fig 23F.

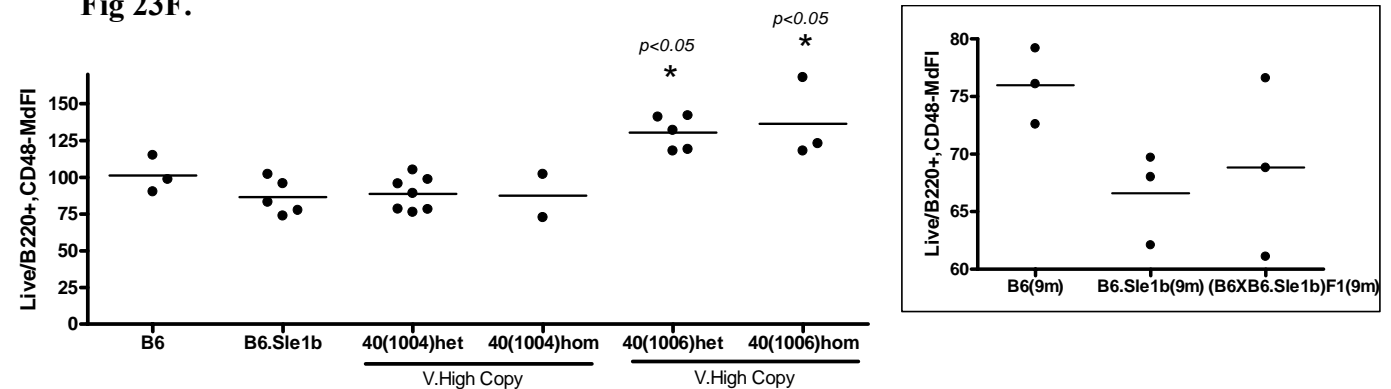


Fig 23. Initial characterization of BAC40-Tg (candidate genes: *Cd48*, *Cd150*) lines on the B6.*Sle1b* genetic background. D-F. Flow cytometric analysis of overall total cell-surface expression of CD48 (B6 and *Sle1b* alleles) on splenocytes from 12 month old female BAC40-Tg mice. All splenocytes express CD48 on their cell surface; the Median fluorescence intensities (MdFI) of CD48 on: **D.** CD4⁺; **E.** CD8⁺; and **F.** B220⁺ cells are shown. Each spot represents the MdFI from one mouse. For comparison, corresponding data obtained from three 9 month old B6, B6.*Sle1b*, and (B6 X B6.*Sle1b*)F1 heterozygous mice are shown in the inset panel beside each figure.

Fig 23G.

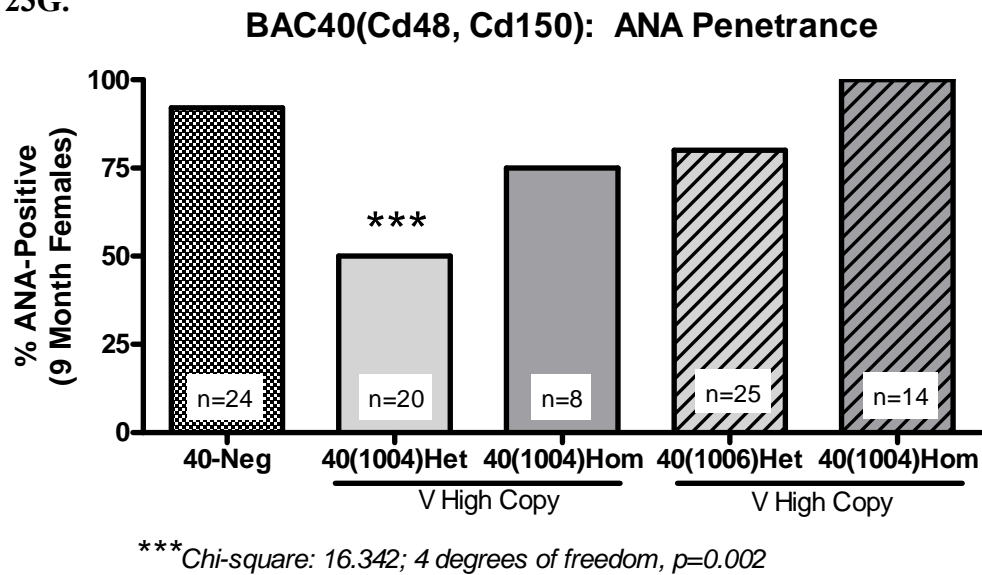


Fig 23H.

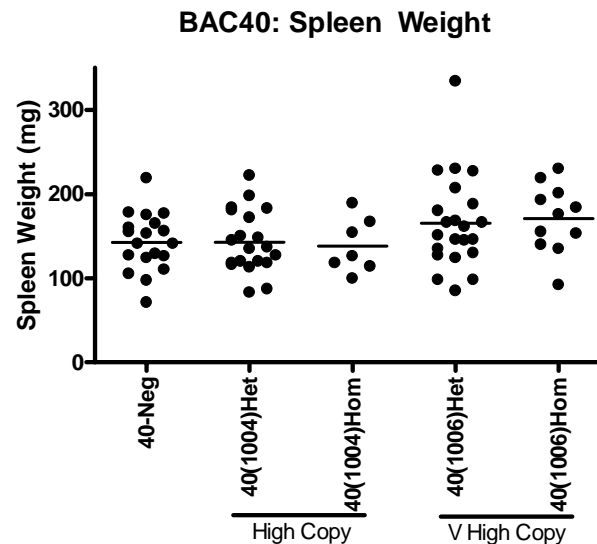


Fig 23. Initial characterization of BAC40-Tg (candidate genes: *Cd48*, *Cd150*) lines on the B6.*Slc1b* genetic background. G. Penetrance of ANA-production in BAC40-Tg mice. Percent of ANA-positive nine month old females ($> \text{B6 mean} + 4 \text{ SD}$) in het and hom groups from each BAC-Tg line, and BAC Tg-negative littermates from both lines are shown. **H.** Spleen weights of BAC-Tg mice and their negative littermates. Spleen weights were taken at the time of necropsy, at 12 months of age, from het and hom mice from each line, and BAC Tg-negative littermates from both lines. Each spot represents the spleen weight of one mouse. ***: Significantly different distribution from negative littermates.

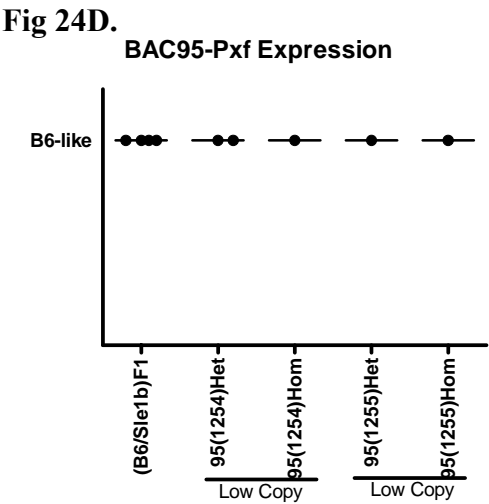
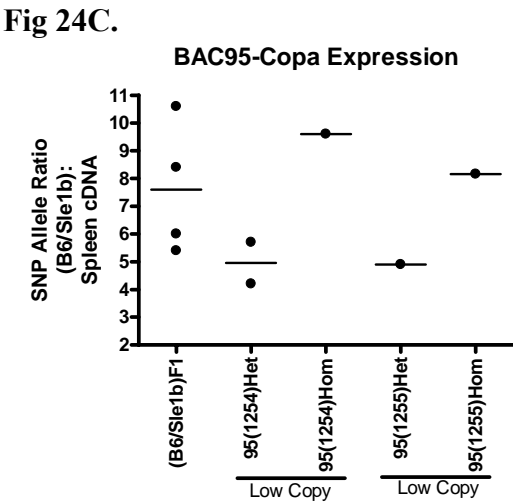
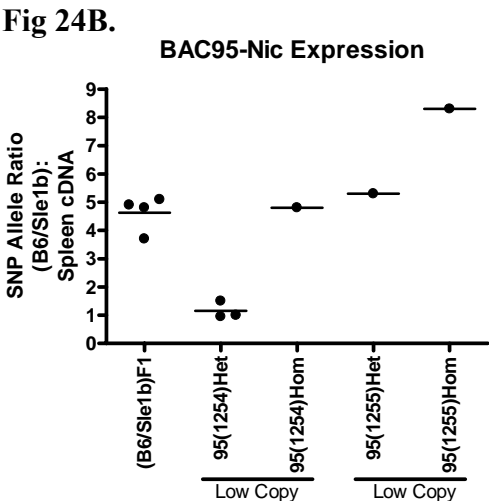
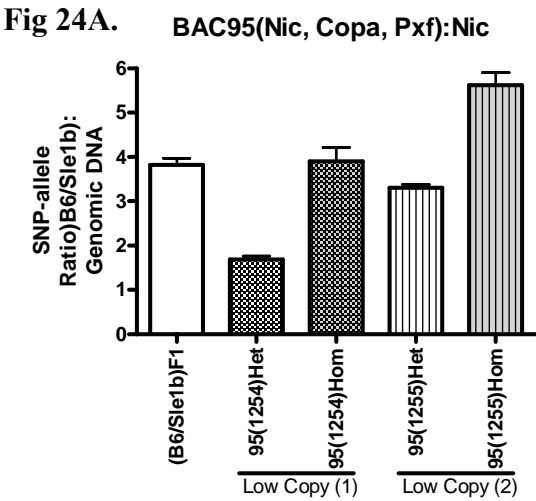


Fig 24. Initial characterization of BAC95-Tg (candidate genes: *Nic*, *Copa*, *Pxf*) lines on the B6.*Sle1b* genetic background. **A.** Ratio of the peak heights of the B6: *Sle1b* SNP-alleles from the *Nicastrin* gene present on the BAC, generated by a sequencing-based SNP assay performed on genomic tail DNA from **all** BAC95-Tg mice generated so far from two separate lines. Ratios were used to distinguish between mice het vs hom for the BAC-Tg, and are shown as the Mean + SEM for each group. The ratio obtained from het mice in each line was normalized to that obtained from 4 (B6 X B6.*Sle1b*) F1 mice, which carry a 1:1 ratio of the B6 and *Sle1b* alleles, in order to calculate copy-number for each Tg-line, shown in brackets. **B., C and D.** Ratio of the peak heights of B6: *Sle1b* SNP-alleles generated by the sequencing-based SNP assay performed on splenic cDNA from het and hom mice from each Tg-line, and control (B6 X B6.*Sle1b*) F1 mice, to assay for expression of the candidate genes on this BAC. Each spot represents the ratio obtained from one mouse at 12 months of age.

Fig 24E.

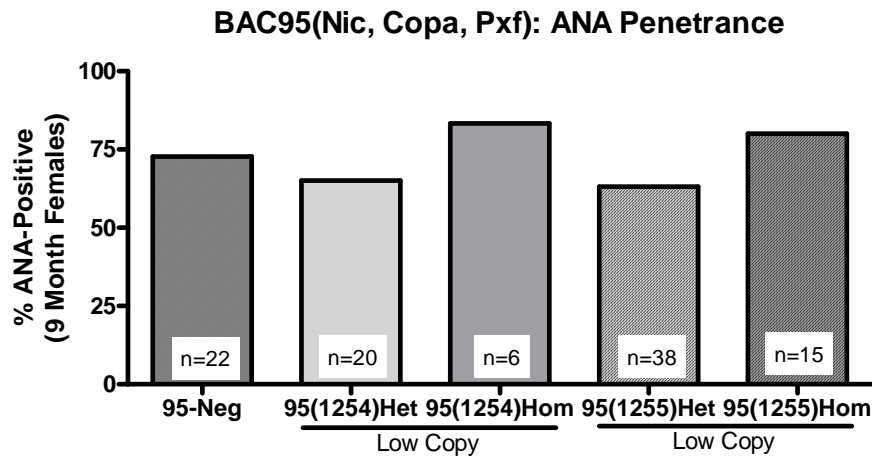


Fig 24F.

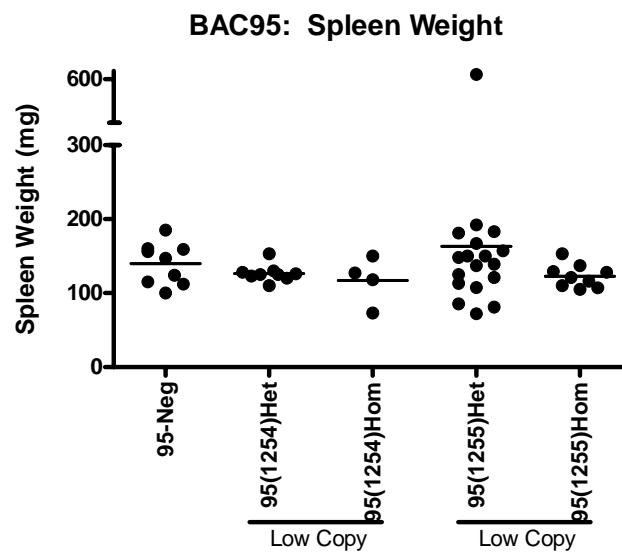


Fig 24. Initial characterization of BAC95-Tg (candidate genes: *Nic*, *Copa*, *Pxf*) lines on the B6.*Sle1b* genetic background. E. Penetrance of ANA-production in BAC95-Tg mice. Percent of ANA-positive nine month old females ($> \text{B6 mean} + 4 \text{ SD}$) in het and hom groups from each BAC-Tg line, and BAC Tg-negative littermates from both lines are shown. **F.** Spleen weights of BAC-Tg mice and their negative littermates. Spleen weights were taken at the time of necropsy, at 12 months of age, from het and hom mice from each line, and Tg-negative littermates from both lines. Each spot represents the spleen weight of one mouse.

Fig 25.

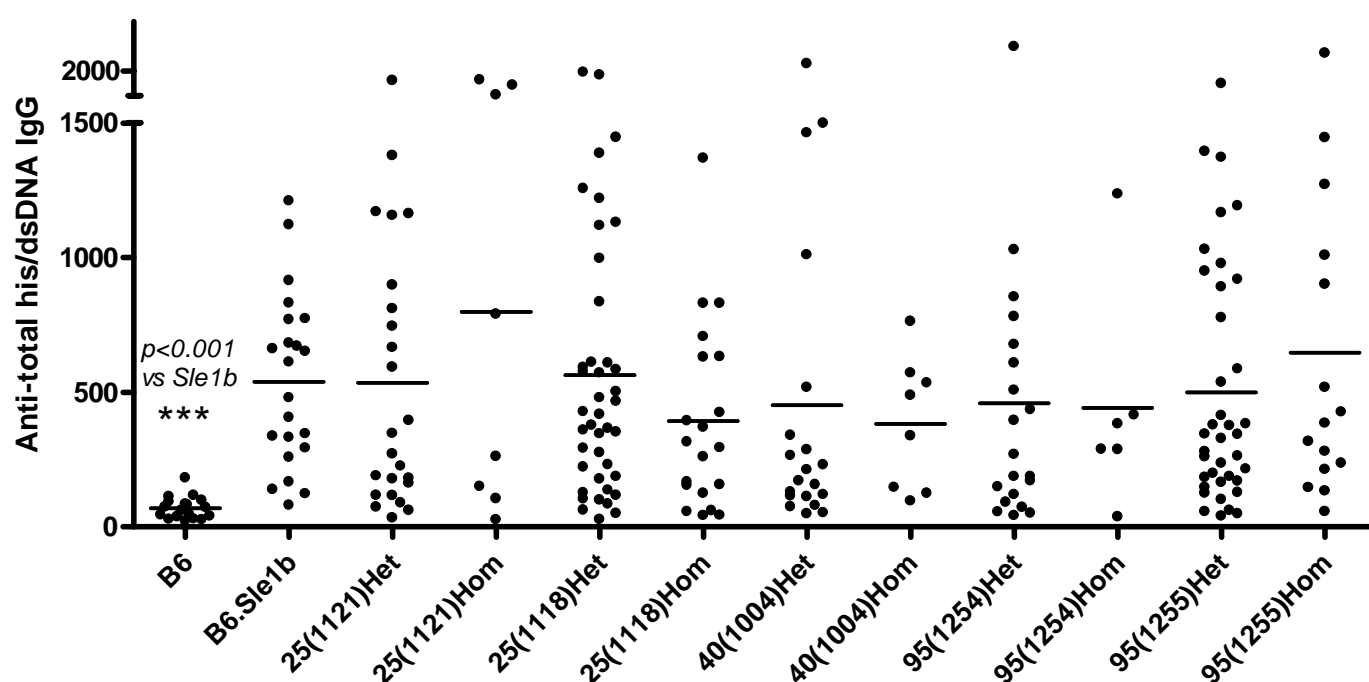


Fig 25. Anti-ds DNA/total histone IgG titers in a subset of BAC-Tg lines, which showed some drop in penetrance of ANA-production. Sera from the 9 month old female mice from BAC-Tg lines that showed some indication of a drop in penetrance (BAC25(1121) and (1118), 40(1004), and 95(1954) and (1955)), were assayed for their ANA-titers by ELISA in a single batch, and compared to a group of age-matched B6.*Sle1b* Tg-negative female littermates, and 12 month old B6 females. Titers are represented as arbitrary concentrations based on a standard curve of serial dilutions of a dsDNA/total histone-specific hybridoma supernatant, included on every plate. *(*p value*): Groups significantly different from B6.*Sle1b*.

Table 11A

Strain	CD4+%	CD8+%	CD19+%	CD11b+, CD19- %	NK1.1+, CD3- %	NK1.1+, CD3+ %
B6 (n=8)	13.13 ± 0.46	9.50 ± 0.92	52.09 ± 3.06	4.79 ± 0.31	3.65 ± 0.27	2.52 ± 0.31
Sle1b (n=18)	15.29 ± 0.42	7.47 ± 0.47	48.53 ± 3.36	6.25 ± 0.55	3.84 ± 0.25	2.76 ± 0.17
BAC41 (Usp23, Nit1):						
1191(Low) Het (n=4)	14.98 ± 0.89	6.92 ± 0.59	54.5 ± 2.82	6.85 ± 0.86	3.29 ± 0.53	1.85 ± 0.19
1191(Low) Hom (n=2)	15.90 ± 0.10	7.85 ± 0.35	46.85 ± 2.25	8.07 ± 0.81	4.59 ± 1.18	3.31 ± 0.13
1352 (Med) Hom (n=3) (Het ND)	18.80 ± 1.11	6.38 ± 0.91	49.23 ± 0.73	8.32 ± 0.58	3.22 ± 0.52	2.59 ± 0.19
BAC47 (Ref 2bp):						
1354(Low) Het (n=4) (hom lethal?)	16.54 ± 0.73	9.90 ± 0.73	49.36 ± 1.77	9.29 ± 1.45	3.99 ± 0.20	2.46 ± 0.12
1429(Low)-Het (n=3)	13.83 ± 1.14	6.61 ± 0.64	59.57 ± 1.54	6.59 ± 0.29	5.40 ± 0.48	3.34 ± 0.19
1429(Low)-Hom (n=5)	15.80 ± 0.73	6.57 ± 0.96	48.80 ± 1.74	9.43 ± 1.14	4.28 ± 0.60	2.85 ± 0.22
BAC25 (Cd229, Cs1, Cd244):						
1121(Low)-Het (n=7)	14.41 ± 1.18	7.86 ± 1.10	53.01 ± 2.52	6.68 ± 0.88	3.51 ± 0.28	2.81 ± 0.23
1121(Low)-Hom (n=3)	13.77 ± 0.99	9.75 ± 0.82	58.73 ± 1.34	4.70 ± 1.25	3.96 ± 0.49	2.37 ± 0.11
1118(V High)-Het (n=4)	12.78 ± 0.63	9.71 ± 1.82	53.95 ± 2.78	6.75 ± 1.40	3.92 ± 0.37	3.56 ± 0.32
1118(V High)-Hom (n=4)	12.60 ± 0.91	8.29 ± 1.30	52.15 ± 3.91	6.06 ± 0.75	4.39 ± 0.86	3.76 ± 0.74
BAC40 (Cd48, Cd150):						
1004(V High)-Het (n=7)	14.44 ± 1.02	9.66 ± 1.20	54.81 ± 1.73	5.88 ± 0.35	4.54 ± 0.50	2.94 ± 0.28
1004(V High)- Hom (n=2)	13.90 ± 1.30	9.43 ± 1.98	54.65 ± 4.75	5.56 ± 0.97	5.17 ± 1.55	2.91 ± 0.75
1006(V High)- Het (n=5)	16.02 ± 1.11	5.58 ± 0.69	54.70 ± 1.85	5.52 ± 0.68	3.57 ± 0.09	2.91 ± 0.15
1006(V High)-Hom (n=3)	16.37 ± 1.15	5.12 ± 0.22	47.40 ± 2.64	9.27 ± 2.28	3.69 ± 1.02	3.25 ± 0.43
BAC95 (Nic, Copa, Pxf):						
1254(Low)-Het (n=4)	14.65 ± 0.37	5.97 ± 0.84	53.80 ± 2.53	6.07 ± 0.76	3.35 ± 0.29	2.49 ± 0.21
1254(Low)-Hom (n=2)	17.90 ± 1.00	14.15 ± 1.25	23.05 ± 2.65	8.18 ± 1.36	4.92 ± 1.99	3.03 ± 0.01
1255(Low)-Het (n=4)	16.25 ± 0.85	7.00 ± 0.77	53.70 ± 2.53	6.11 ± 0.42	4.14 ± 0.29	2.67 ± 0.32
1255(Low)-Hom (n=2)	15.55 ± 2.15	7.63 ± 1.93	55.90 ± 6.41	6.10 ± 0.93	3.52 ± 0.76	2.00 ± 0.31

Table 11. Flow cytometric analysis of splenic lymphocyte populations in BAC-Tg mice. Cell populations are shown as mean percentages of total live lymphocytes ± SEM, from the indicated number of 12 month old BAC-Tg, B6, and B6.*Sle1b* mice. **Bold*****: groups significantly different from B6.*Sle1b* (non-parametric ANOVA: *p<0.05, **p<0.01, ***p<0.001). **Bold**: Indicative of perturbation in a cell compartment, but does not reach significance; OR B6 vs B6.*Sle1b* significant when compared only to each other (t-test or Mann-Whitney). **Bold(ital)**: B6 vs B6.*Sle1b* significant only when using paired t-test on the 8 paired samples done in the same set of experiments. **A.** Basic characterization of splenic cell lineages showing percentages of CD4+ and CD8+ (T cells), CD19+ (B cells), CD11b+ (macrophages), NK1.1+ (NK cells), and NK1.1+CD3+ (NKT cells).

Table 11B.

Strain	CD4/CD69%	CD4/CD69+, MdFI	CD4/ Naïve% (CD62L+CD44lo)	CD4/Act-Mem% (CD62L-CD44hi)	CD4/Transit% (CD62L-CD44lo)
B6 (n=8)	27.04 ± 1.07	78.29 ± 6.38	26.79 ± 3.49	25.90 ± 1.10	44.41 ± 2.81
Sle1b (n=18)	37.30 ± 1.64	85.17 ± 5.96	13.84 ± 1.52	33.09 ± 1.36	49.92 ± 1.71
BAC41 (Usp23, Nit1): 1191(Low) Het (n=4)	37.60 ± 4.14	64.83 ± 2.83	11.00 ± 1.97	41.40 ± 2.35	44.53 1.70
1191(Low) Hom (n=2)	35.50 ± 1.70	89.65 ± 0.95	2.36 ± 0.48	30.55 ± 2.15	66.15 1.65
1352 (Med) Hom (n=3) (Het ND)	44.93 ± 1.26	78.70 ± 0.99	8.90 ± 1.61	33.33 ± 1.42	55.20 1.23
BAC47 (Ref 2bp): 1354(Low) Het (n=4) (hom lethal?)	30.08 ± 1.56	80.38 ± 12.95	18.88 ± 2.71	30.70 ± 3.25	47.36 2.04
1429(Low)-Het (n=3)	36.37 ± 2.05	80.20 ± 0.78	11.30 ± 0.90	33.37 ± 3.42	52.73 2.67
1429(Low)-Hom (n=5)	38.18 ± 3.48	120.1 ± 14.65	7.34 ± 1.39	35.46 ± 1.62	55.26 3.20
BAC25 (Cd229, Cs1, Cd244): 1121(Low)-Het (n=7)	42.21 ± 1.58	110.1 ± 4.87	10.83 ± 3.12	34.04 ± 2.58	52.69 3.49
1121(Low)-Hom (n=3)	30.70 ± 4.14	98.53 ± 9.74	21.83 ± 0.52	27.10 ± 3.91	47.63 4.30
1118(V High)-Het (n=4)	33.93 ± 4.86	96.05 ± 10.95	20.73 ± 6.09	28.40 ± 2.54	47.95 3.74
1118(V High)-Hom (n=4)	39.13 ± 7.62	95.60 ± 9.99	15.04 ± 7.47	30.45 ± 3.38	51.98 4.37
BAC40 (Cd48, Cd150): 1004(V High)-Het (n=7)	30.74 ± 3.30	73.53 ± 7.41	25.55 ± 5.14	28.87 ± 1.67	42.34 3.84
1004(V High)- Hom (n=2)	31.20 ± 4.00	92.95 ± 21.05	24.65 ± 6.95	28.10 ± 3.30	44.15 4.55
1006(V High)- Het (n=5)	45.82 ± 1.83	79.56 ± 9.42	10.34 ± 0.77	36.52 ± 2.65	50.14 2.72
1006(V High)-Hom (n=3)	51.20 ± 1.10	96.50 ± 5.20	7.52 ± 1.33	36.93 ± 1.27	53.10 1.95
BAC95 (Nic, Copa, Pxf): 1254(Low)-Het (n=4)	44.05 ± 2.08	68.05 ± 8.37	9.92 ± 2.63	33.95 ± 4.00	52.53 1.72
1254(Low)-Hom (n=2)	35.25 ± 7.35	73.65 ± 27.35	11.59 ± 3.71	27.50 ± 0.90	57.90 3.80
1255(Low)-Het (n=4)	41.13 ± 2.99	78.48 ± 6.69	11.84 ± 4.02	30.55 ± 1.65	55.10 3.78
1255(Low)-Hom (n=2)	43.70 ± 6.80	89.80 ± 17.20	13.70 ± 0.60	31.80 ± 1.00	51.85 0.35

Table 11. Flow cytometric analysis of splenic lymphocyte populations in BAC-Tg mice. Cell populations are shown as mean percentages of total live lymphocytes ± SEM, from the indicated number of 12 month old BAC-Tg, B6, and B6.*Sle1b* mice. **Bold*****: groups significantly different from B6.*Sle1b* (non-parametric ANOVA: *p<0.05, **p<0.01, ***p<0.001). **Bold**: Indicative of perturbation in a cell compartment, but does not reach significance; OR B6 vs B6.*Sle1b* significant when compared only to each other (t-test or Mann-Whitney). **Bold(ital)**: B6 vs B6.*Sle1b* significant only when using paired t-test on the 8 paired samples done in the same set of experiments. **B**. Activation/memory and naïve populations of CD4+ T cells in BAC-transgenic mice showing the percentage of CD4+ T cells expressing the activation marker CD69, the MdFI of CD69+ CD4 T cells, and the percentage of naïve, activated/memory, and transitional CD4+ T cells.

Table 11C.

Strain	CD3/CD69%	CD3/CD69+, MdFI	B220/CD69+%	B220/CD69+, MdFI
B6 (n=8)	26.63 ± 2.15	68.03 ± 2.89	3.43 ± 0.21***	37.19 ± 2.59
Sle1b (n=18)	36.19 ± 1.74	76.33 ± 2.16	6.32 ± 0.41	37.31 ± 1.91
BAC41 (Usp23, Nit1): 1191(Low) Het (n=4)	31.48 ± 3.20	67.80 ± 3.44	5.20 ± 0.69	25.20 ± 0.61
1191(Low) Hom (n=2)	37.15 ± 0.35	81.75 ± 1.85	6.87 ± 0.09	33.85 ± 0.75
1352 (Med) Hom (n=3) (Het ND)	44.43 ± 2.53	92.77 ± 1.32	5.17 ± 0.47	33.67 ± 0.32
BAC47 (Ref 2bp): 1354(Low) Het (n=4) (hom lethal?)	32.16 ± 1.61	70.04 ± 6.41	5.75 ± 0.80	37.00 ± 3.89
1429(Low)-Het (n=3)	38.33 ± 1.39	82.87 ± 2.45	6.44 ± 0.62	29.87 ± 0.35
1429(Low)-Hom (n=5)	38.34 ± 2.56	91.98 ± 6.46	7.40 ± 0.94	46.22 ± 5.34
BAC25 (Cd229, Cs1, Cd244): 1121(Low)-Het (n=7)	41.04 ± 2.23	82.07 ± 3.28	6.80 ± 0.59	39.40 ± 2.98
1121(Low)-Hom (n=3)	31.60 ± 1.80	65.43 ± 6.22	4.81 ± 0.60	46.80 ± 6.07
1118(V High)-Het (n=4)	32.50 ± 5.15	75.23 ± 2.42	4.99 ± 0.67	40.10 ± 1.15
1118(V High)-Hom (n=4)	40.08 ± 7.31	75.23 ± 7.98	6.67 ± 1.76	39.40 ± 2.15
BAC40 (Cd48, Cd150): 1004(V High)-Het (n=7)	28.39 ± 4.62	70.96 ± 5.10	4.37 ± 0.63	37.30 ± 2.53
1004(V High)- Hom (n=2)	29.60 ± 5.00	87.85 ± 2.85	4.93 ± 1.01	32.60 ± 4.10
1006(V High)- Het (n=5)	42.64 ± 3.06	75.42 ± 6.93	6.35 ± 0.57	42.70 ± 2.83
1006(V High)-Hom (n=3)	44.13 ± 4.09	83.80 ± 2.30	7.75 ± 0.64	40.30 ± 1.31
BAC95 (Nic, Copa, Pxf): 1254(Low)-Het (n=4)	40.73 ± 2.57	64.55 ± 1.54	6.60 ± 1.07	34.23 ± 1.22
1254(Low)-Hom (n=2)	34.65 ± 12.65	64.10 ± 10.50	8.44 ± 1.45	33.45 ± 4.45
1255(Low)-Het (n=4)	39.10 ± 3.23	76.73 ± 3.11	6.64 ± 0.46	32.45 ± 2.26
1255(Low)-Hom (n=2)	43.45 ± 10.25	78.20 ± 1.80	6.69 ± 2.18	36.50 ± 3.90

Table 11. Flow cytometric analysis of splenic lymphocyte populations in BAC-Tg mice. Cell populations are shown as mean percentages of total live lymphocytes ± SEM, from the indicated number of 12 month old BAC-Tg, B6, and B6.*Sle1b* mice. **Bold*****: groups significantly different from B6.*Sle1b* (non-parametric ANOVA: *p<0.05, **p<0.01, ***p<0.001). **Bold**: Indicative of perturbation in a cell compartment, but does not reach significance; OR B6 vs B6.*Sle1b* significant when compared only to each other (t-test or Mann-Whitney). **Bold(ital)**: B6 vs B6.*Sle1b* significant only when using paired t-test on the 8 paired samples done in the same set of experiments. **C**. Expression of activation markers on CD3+ and B220+ cell populations, showing the percentages of these cells expressing CD69, and the MdFI of CD69+ fractions of each.

Chapter VI. Discussion

Our identification of the SLAM/CD2 family as mediators of a break in tolerance to chromatin that initiates pathogenesis in the NZM2410 model of lupus, gives us a very promising set of candidate genes to examine for associations with autoimmunity in human populations. The region has been linked to lupus-like phenotypes in multiple autoimmune-prone mouse strains (165, 167, 168,169), which, as we have gone on to find, actually share the same alleles of these genes, making it possible that they play a fundamental role in pathogenesis of the disease. In addition, the regulatory differences in expression of this family that we observe early on between B6 and B6.*Sle1b* mice are also observed in other autoimmune strains. MRL/+, BXSB, and pristane-treated 129 mice, which develop an experimentally-induced lupus-like disease, have elevated levels of Ly108 and Cd150 (Slam) in their peripheral blood leukocytes, as compared to BALB/c, B6 or saline-treated control 129 mice (240). Significantly, the SLAM/CD2 region is also syntenic to a locus consistently linked to SLE susceptibility in humans (16, 17, 18). It is possible that, as with several other candidate gene regions, associations will be detected with a haplotype of SNPs spanning more than one of these family members, rather than with any one SNP or allele. These associations are also likely to occur only in certain populations, given the complexity and heterogeneity typical of the genetics underlying lupus.

We ourselves have not yet been able to definitively identify which gene, or combination of genes within the SLAM/CD2 haplotype, is actually mediating the phenotype. The small size of the *Sle1b* congenic region, and the presence of this tightly linked set of alleles within it, makes further recombinational analysis a less attractive tool by which to tackle this question. Instead, we have chosen to use a BAC-transgenic rescue approach,

which allows us to break the region down into six separate parts, each of which can be assessed for its ability to rescue the autoimmune phenotype. We are certainly hopeful that the completion of this study, with the generation of an Ly108-containing BAC, will yield a definitive answer as to the identity of the *Sle1b* gene(s). Even in the absence of this last piece of the puzzle, however, we have succeeded in eliminating any of the other non-SLAM/CD2 candidate genes as causative of the ANA-production in B6.*Sle1b* mice.

An alternative approach is to harness the wild-derived inbred strains that we have found carry “recombinant” haplotypes of B6 and B6.*Sle1b*-like alleles of the SLAM/CD2 genes. The use of the B6.*Castc1* congenic strain, which shares the telomeric part of the SLAM/CD2 haplotype with 129 and NZW and produces ANAs, implicates the region containing Cd48, Cd150, Cd84, and Ly108. We have begun using a similar strategy with the CZECHI/Ei strain, in which the recombinant haplotype consists of B6-like alleles of Cd150, Cd84, and Ly108, and B6.*Sle1b*-like alleles of Cd244 (PCR with Cd244 allele-specific primers, in unpublished data from A.Chan in the lab), Cd229, Cs1, and Cd48. Whether or not a congenic strain carrying the CZECHI-SLAM/CD2 region on the B6 genetic background makes ANAs, will tell us which half of the haplotype is linked to autoimmunity, and, in combination with our data from B6.*Castc1* mice and the BAC-transgenics, should allow us to identify the elusive *Sle1b* gene.

Another exciting avenue of further research on this gene family in humans is microarray analysis on sorted B and CD4⁺ T cell populations in PBMCs from patients, which would tell us if the dysregulations in the SLAM/CD2 family members observed in these cell types in our and other autoimmune-prone mice (171, 240), are also observed in humans. These differences in expression are a feature of the autoimmune-associated genomic

haplotype of the SLAM/CD2 family, and occur very early on before any detectable disease-related changes like ANA-production or lymphocyte activation. This supports the idea that any similar changes detected in human patients as compared to controls, may reflect early events that play a role in disease initiation, rather than the consequences of chronic autoimmune activation.

The discovery that it is the common alleles of the SLAM/CD2 family, rather than some rare mutations, that are associated with autoimmune susceptibility, has many important implications. It highlights the importance of epistasis in complex diseases like lupus. The same genes that are seemingly innocuous in 129 or NZW mice, cause a highly penetrant ANA-production phenotype in combination with the downstream signaling components on the B6 genetic background (Fig 26), and, when put together with other susceptibility loci, actually result in fatal GN (159,159,164). The presence of epistatic loci like *Sles1*(163) that hold the effects of these genes in check, provides at least part of the explanation for why these alleles are so prevalent, even in natural outbred populations of mice.

The presence of the autoimmune-associated alleles of SLAM/CD2 in 129 mice provides us with a likely explanation for why targeted deletions of genes in this region, such as *FcgRIIb* and Serum Amyloid Factor P (SAP), generated in 129 and bred onto B6 and other strains, sometimes show such strongly background-dependent autoimmune effects (118, 126). When these targeted deletions are bred onto B6, they carry with them a congenic interval that includes the B6.*Sle1b*-like, 129-derived SLAM/CD2 region. This region from 129, even in the absence of any targeted deficiencies or other perturbations, has been shown to be able to mediate autoimmunity on the B6 genetic background (171, 7). Thus, the gene deficiencies may not actually cause the lupus-like phenotypes, but may instead serve to exacerbate

autoimmunity once it is initiated by the SLAM/CD2 family on the B6 (171, 7), but not other genetic backgrounds like BALB/c or 129 (118,127). Supporting this hypothesis is the fact that the expression of a human SAP transgene fails to rescue autoimmunity on the SAP-deficient B6 background (127). In addition, an examination of genetic modifiers of the FcγRIIb-deficient phenotype has identified a chromosome 17 locus that coincides with the *Sles1* locus previously shown to modify *Sle1*-mediated autoimmunity (163, 297). Just as B6.129c1 mice show an autoimmune phenotype similar to B6.*Sle1* and B6.*Sle1b* mice, preliminary data from S. Subramanian and K. Belobrajdic in the lab show that the homozygous chromosome 17 *Sles1* region from 129 also has a suppressive effect similar to that observed in the presence of the corresponding NZW-derived locus. This gives us several advantages in trying to localize and functionally analyze and identify the *Sles1* gene. One is the existence of is a BAC library for 129, not available for NZW, which will allow us to employ a 129-BAC mediated gene identification strategy. The fact that B6 and 129 share the same H2^b MHC haplotype (298), would seem to position *Sles1* outside this cluster, although it is possible that polymorphisms within the highly related MHC-regions between the two strains account for their differential ability to suppress autoimmunity. The common MHC between the two strains will nevertheless allow us to carry out mixed bone marrow chimera experiments to try and identify which cell compartment the *Sles1* gene is critical in. This is not possible with the NZW-derived *Sles1* congenics, in which the MHC mismatch would cause graft rejection.

Examination of the SLAM/CD2 alleles in multiple *Mus* species and *Mus musculus* sub-species shows that they have actually been retained over evolutionary time-spans. Such a sharing of alleles between long-diverged species is indicative of balancing selection (282). The association of autoimmunity with a haplotype rather than a single gene, the highly

polymorphic nature of this family, and the long coalescence times observed for these alleles, are all reminiscent of the major histocompatibility complex (299, 49,300). It is tempting to speculate that the selection operating on members of the SLAM/CD2 family is, similarly, pathogen driven. Given the strong link between Cd150 and SAP and viral immunity (reviewed in 263, 178, 243), it is likely that selection, in this case, is driven by viral pathogens. Furthermore, these forces may be operating, not just at the level of direct binding of pathogens to receptors, as in the case of Cd150 and the morbilivirus family (263), but also at the level of selecting for the nature or type of immune response to various infections. Many of the SLAM/CD2 family members play a role in modulating Th1/Th2 responses (237, 228, 220), and SAP-deficient mice, which fail to produce Th2-cytokines and are defective in T-dependent humoral autoimmunity, fail to mount an appropriate long-term anti-viral response to LCMV (252). Th1 versus Th2 responses are demonstrably more or less appropriate and effective, depending on the particular pathogenic context; for instance, in mice, the Th1 responses of B6 mice can more effectively control the intracellular parasite *Leishmania* than the Th2 responses of BALB/c (221). Conversely, as observed in the case of the SAP-deficient strains, a Th2 response is necessary for the appropriate control of certain viral pathogens like LCMV (252).

It is very interesting that the SLAM/CD2 family, linked here to lupus susceptibility in mice, has a signaling partner directly downstream which is critical to EBV-directed responses in humans (178), as studies have shown defective control of EBV in SLE patients (279, 280). It is possible that the polymorphisms in this family that potentiate lupus-susceptibility also have a deleterious effect on immunity to EBV, which would mean, in addition, that the same, or intersecting, pathways are involved. The identification of specific infectious models that are demonstrably affected in their infectivity or pathogenicity by the SLAM/CD2 haplotype,

using B6 and B6.*Sle1b* mice, which differ only in this regard, would be of great use. Many such pathogens are well-characterized with regard to disease mechanisms and pathways, and this information could potentially give us insights about the complex processes involved in the initiation of autoimmunity.

Fig 26

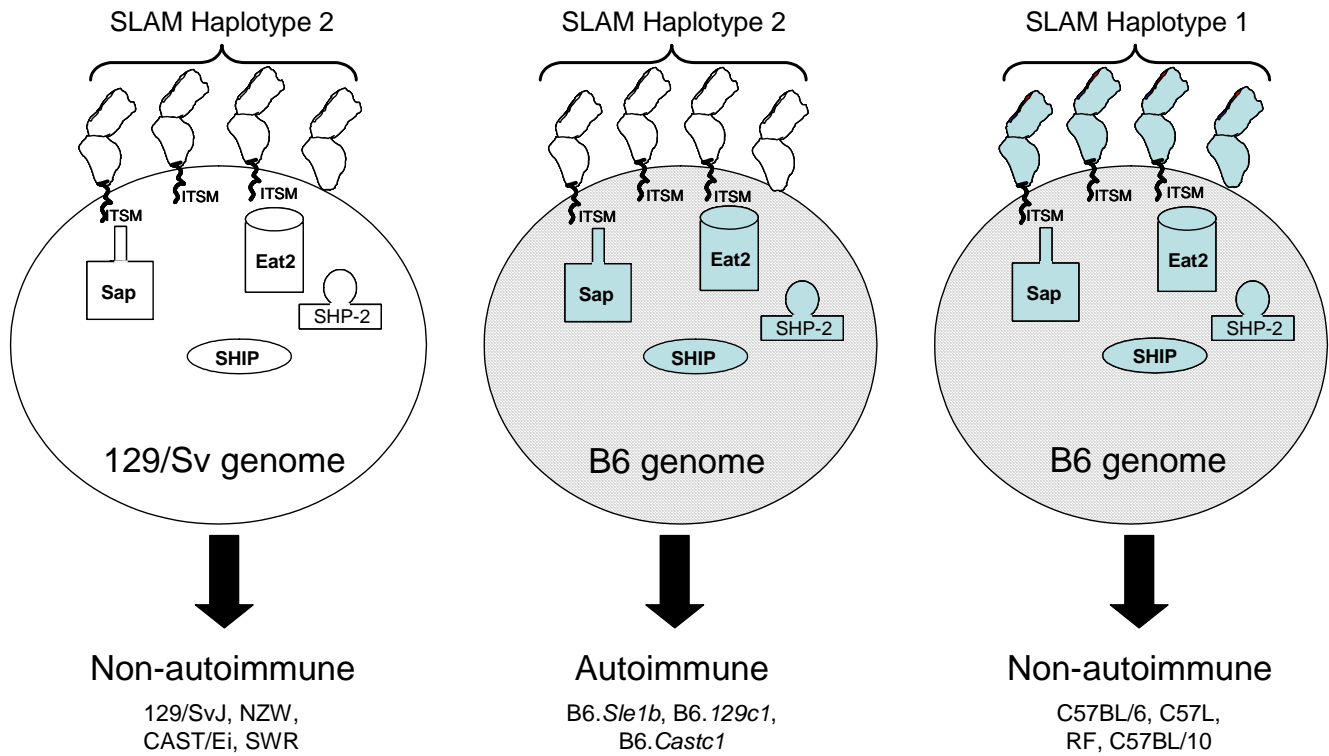


Fig 26. A model depicting how SLAM/CD2 Haplotype 2 mediates autoimmunity in the context of the B6 genome. We propose that the autoimmunity mediated by *Sle1b* is a consequence of the SLAM/CD2 family alleles, in combination with genetic variations in downstream signaling molecules. In the context of the 129/SvJ or BALB/c genomes, SLAM/CD2 haplotype 2 does not cause ANAs. On the other hand, the imbalance between the SLAM/CD2 haplotype 2 alleles and signaling molecules found in the B6 genome (shown in the center panel) results in spontaneous autoimmunity, as seen in the B6.*Sle1b*, B6.*129c1* and B6.*Castc1* congenic lines.

References

1. Wakeland, E. K., K. Liu, R. R. Graham, and T. W. Behrens. 2001. Delineating the genetic basis of systemic lupus erythematosus. *Immun* 15:397.
2. Vyse, T. J., and B. L. Kotzin. 1998. Genetic susceptibility to systemic lupus erythematosus. *Annu Rev Immunol* 16:261.
3. Wandstrat, A. E., and E. K. Wakeland. 2001. The Genetics of Complex Autoimmune Diseases: non-MHC Susceptibility Genes. *Nature Immunology* 2:802.
4. Pickering, M. C., M. Botto, P. R. Taylor, P. J. Lachmann, and M. J. Walport. 2000. Systemic lupus erythematosus, complement deficiency, and apoptosis. *Adv. Immunol.* 76:227.
5. Mitchell, D. A., M. C. Pickering, J. Warren, L. Fossati-Jimack, J. Cortes-Hernandez, H. T. Cook, M. Botto, and M. J. Walport. 2002. C1q deficiency and autoimmunity: the effects of genetic background on disease expression. *J. Immunol.* 168:2538.
6. Trendelenburg, M., A. P. Manderson, L. Fossati-Jimack, M. J. Walport, and M. Botto. 2004. Monocytosis and accelerated activation of lymphocytes in C1q-deficient autoimmune-prone mice. *Immunology* 113:80.
7. Bygrave, A. E., K. L. Rose, J. Cortes-Hernandez, J. Warren, R. J. Rigby, H. T. Cook, M. J. Walport, T. J. Vyse, and M. Botto. 2004. Spontaneous autoimmunity in 129 and C57BL/6 mice-implications for autoimmunity described in gene-targeted mice. *PLoS. Biol.* 2:E243.

8. Botto, M., C. Dell'Agnola, A. E. Bygrave, E. M. Thompson, H. T. Cook, F. Petry, M. Loos, P. P. Pandolfi, and M. J. Walport. 1998. Homozygous C1q deficiency causes glomerulonephritis associated with multiple apoptotic bodies. *Nature Gen.* 19:56.
9. Yang, Y., K. Lhotta, E. K. Chung, P. Eder, F. Neumair, and C. Y. Yu. 2004. Complete complement components C4A and C4B deficiencies in human kidney diseases and systemic lupus erythematosus. *J. Immunol.* 173:2803.
10. Walport, M. J. 2002. Complement and systemic lupus erythematosus. *Arthritis Res.* 4 Suppl 3:S279-S293.
11. Yang, Y., E. K. Chung, B. Zhou, K. Lhotta, L. A. Hebert, D. J. Birmingham, B. H. Rovin, and C. Y. Yu. 2004. The intricate role of complement component C4 in human systemic lupus erythematosus. *Curr. Dir. Autoimmun.* 7:98.
12. Chen, Z., S. B. Koralov, and G. Kelsoe. 2000. Complement C4 inhibits systemic autoimmunity through a mechanism independent of complement receptors CR1 and CR2. *J. Exp. Med.* 192:1339.
13. Paul, E., O. O. Pozdnyakova, E. Mitchell, and M. C. Carroll. 2002. Anti-DNA autoreactivity in C4-deficient mice. *Eur. J. Immunol.* 32:2672.
14. Sullivan, K. E., M. A. Petri, B. J. Schmeckpeper, R. H. McLean, and J. A. Winkelstein. 1994. Prevalence of a mutation causing C2 deficiency in systemic lupus erythematosus. *J. Rheumatol.* 21:1128.
15. Carroll, M. C. 2004. The complement system in B cell regulation. *Mol. Immunol.* 41:141.

16. Moser, K. L., B. R. Neas, J. E. Salmon, H. Yu, C. Gray-McGuire, N. Asundi, G. R. Bruner, J. Fox, J. Kelly, S. Henshall, D. Bacino, M. Dietz, R. Hogue, G. Koelsch, L. Nightingale, T. Shaver, N. I. Abdou, D. A. Albert, C. Carson, M. Petri, E. L. Treadwell, J. A. James, and J. B. Harley. 1998. Genome scan of human systemic lupus erythematosus: Evidence for linkage on chromosome 1q in african-american pedigrees. *Proc Natl Acad Sci USA* 95:14869.
17. Shai, R., F. Quismorio Jr., L. Li, O.-J. Kwon, J. Morrison, D. Wallace, C. Neuwelt, C. Brautbar, W. Gauderman, and C. O. Jacob. 1999. Genome-wide screen for systemic lupus erythematosus susceptibility genes in multiplex families. *Human Molecular Genetics* 8:639.
18. Cantor, R. M., J. Yuan, S. Napier, N. Kono, J. M. Grossman, B. H. Hahn, and B. P. Tsao. 2004. Systemic lupus erythematosus genome scan: support for linkage at 1q23, 2q33, 16q12-13, and 17q21-23 and novel evidence at 3p24, 10q23-24, 13q32, and 18q22-23. *Arthritis Rheum.* 50:3203.
19. Tsao, B. P., R. M. Cantor, C. Kalunian, C.-J. Chen, H. Badsha, R. Singh, D. J. Wallace, R. C. Kitridou, S. Chen, N. Shen, Y. W. Song, D. A. Isenberg, C.-L. Yu, B. H. Hahn, and J. I. Rotter. 1997. Evidence for linkage of a candidate chromosome 1 region to human systemic lupus erythematosus. *J. Clin. Invest.* 99:725.
20. Gaffney, P. M., G. M. Kearns, K. B. Shark, W. A. Ortmann, S. A. Selby, M. L. Malmgren, K. E. Rohlf, T. C. Ockenden, R. P. Messner, S. Rich, and T. W. Behrens. 1998. A genome-wide search for susceptibility genes in human systemic lupus erythematosus sib-pair families. *Proc Natl Acad Sci USA* 95:14875.

21. Gaffney, P. M., W. A. Ortmann, S. A. Selby, K. B. Shark, T. C. Ockenden, K. E. Rohlf, N. L. Walgrave, W. P. Boyum, M. L. Malmgren, M. E. Miller, G. M. Kearns, R. P. Messner, R. A. King, S. S. Rich, and T. W. Behrens. 2000. Genome screening in human systemic lupus erythematosus: results from a second Minnesota cohort and combined analyses of 187 sib-pair families. *Am J Hum Genet* 66:547.
22. Moser, K. L., C. Gray-McGuire, J. Kelly, N. Asundi, H. Yu, G. R. Bruner, M. Mange, R. Hogue, B. R. Neas, and J. B. Harley. 1999. Confirmation of genetic linkage between human systemic lupus erythematosus and chromosome 1q41. *Arthritis Rheum* 42:1902.
23. Graham, R. R., C. D. Langefeld, P. M. Gaffney, W. A. Ortmann, S. A. Selby, E. C. Baechler, K. B. Shark, T. C. Ockenden, K. E. Rohlf, K. L. Moser, W. M. Brown, S. E. Gabriel, R. P. Messner, R. A. King, P. Horak, J. T. Elder, P. E. Stuart, S. S. Rich, and T. W. Behrens. 2001. Genetic linkage and transmission disequilibrium of marker haplotypes at chromosome 1q41 in human systemic lupus erythematosus.
24. Tsao, B. P., R. M. Cantor, J. Grossman, N. Shen, N. Teophilov, D. C. Wallace, F. C. Arnett, K. Hartung, R. Goldstein, K. Kalunian, B. Hahn, and J. Rotter. 1999. PARP alleles within the linked chromosomal region are associated with systemic lupus erythematosus. *J Clin Invest* 103:1135.
25. Criswell, L. A., K. L. Moser, P. M. Gaffney, S. Inda, W. A. Ortmann, D. Lin, J. J. Chen, H. Li, M. Gray, B. R. Neas, S. S. Rich, J. B. Harley, T. W. Behrens, and M. F. Seldin. 2000. PARP alleles and SLE: failure to confirm association with disease susceptibility. *J Clin Invest* 105:1501.

26. Morel, L., K. R. Blenman, B. P. Croker, and E. K. Wakeland. 2001. The major murine systemic lupus erythematosus susceptibility locus, Sle1, is a cluster of functionally related genes. *Proc Natl Acad Sci U S A* 98:1787.
27. Lindqvist, A. K., K. Steinsson, B. Johanneson, H. Kristjansdottir, A. Arnasson, G. Grondal, I. Jonasson, V. Magnusson, G. Sturfelt, L. Truedsson, E. Svenungsson, I. Lundberg, J. D. Terwilliger, U. B. Gyllensten, and M. E. Alarcon-Riquelme. 2000. A susceptibility locus for human systemic lupus erythematosus (hSLE1) on chromosome 2q. *J Autoimmun* 14:169.
28. Gray-McGuire, C., K. L. Moser, P. M. Gaffney, J. Kelly, H. Yu, J. M. Olson, C. M. Jedrey, K. B. Jacobs, R. P. Kimberly, B. R. Neas, S. S. Rich, T. W. Behrens, and J. B. Harley. 2000. Genome scan of human systemic lupus erythematosus by regression modeling: evidence of linkage and epistasis at 4p16-15.2. *Am J Hum Genet* 67:1460.
29. Ogura, Y., D. K. Bonen, N. Inohara, D. L. Nicolae, F. F. Chen, R. Ramos, H. Britton, T. Moran, R. Karaliuskas, R. H. Duerr, J. P. Achkar, S. R. Brant, T. M. Bayless, B. S. Kirschner, S. B. Hanauer, G. Nunez, and J. H. Cho. 2001. A frameshift mutation in NOD2 associated with susceptibility to Crohn's disease. *Nature* 411:603.
30. Johansson, C. M., R. Zunec, M. A. Garcia, H. R. Scherbarth, G. A. Tate, S. Paira, S. M. Navarro, C. E. Perandones, S. Gamron, A. Alvarellos, C. E. Graf, J. Manni, G. A. Berbotto, S. A. Palatnik, L. J. Catoggio, C. G. Battagliotti, G. D. Sebastiani, S. Migliaresi, M. Galeazzi, B. A. Pons-Estel, and M. E. arcon-Riquelme. 2004. Chromosome 17p12-q11 harbors susceptibility loci for systemic lupus erythematosus. *Hum. Genet.* 115:230.

31. Nath, S. K., A. I. Quintero-Del-Rio, J. Kilpatrick, L. Feo, M. Ballesteros, and J. B. Harley. 2004. Linkage at 12q24 with systemic lupus erythematosus (SLE) is established and confirmed in Hispanic and European American families. *Am. J. Hum. Genet.* 74:73.
32. Quintero-Del-Rio, A. I., J. A. Kelly, J. Kilpatrick, J. A. James, and J. B. Harley. 2002. The genetics of systemic lupus erythematosus stratified by renal disease: linkage at 10q22.3 (SLEN1), 2q34-35 (SLEN2), and 11p15.6 (SLEN3). *Genes Immun.* 3 Suppl 1:S57-S62.
33. Scofield, R. H., G. R. Bruner, J. A. Kelly, J. Kilpatrick, D. Bacino, S. K. Nath, and J. B. Harley. 2003. Thrombocytopenia identifies a severe familial phenotype of systemic lupus erythematosus and reveals genetic linkages at 1q22 and 11p13. *Blood* 101:992.
34. Nath, S. K., B. Namjou, J. Kilpatrick, C. P. Garriott, G. R. Bruner, R. H. Scofield, and J. B. Harley. 2004. A candidate region on 11p13 for systemic lupus erythematosus: a linkage identified in African-American families. *J. Investig. Dermatol. Symp. Proc.* 9:64.
35. Kelly, J. A., K. Thompson, J. Kilpatrick, T. Lam, S. K. Nath, C. Gray-McGuire, J. Reid, B. Namjou, C. E. Aston, G. R. Bruner, R. H. Scofield, and J. B. Harley. 2002. Evidence for a susceptibility gene (SLEH1) on chromosome 11q14 for systemic lupus erythematosus (SLE) families with hemolytic anemia. *Proc. Natl. Acad. Sci. U. S. A* 99:11766.
36. Nath, S. K., J. A. Kelly, B. Namjou, T. Lam, G. R. Bruner, R. H. Scofield, C. E. Aston, and J. B. Harley. 2001. Evidence for a susceptibility gene, SLEV1, on

chromosome 17p13 in families with vitiligo-related systemic lupus erythematosus.

Am. J. Hum. Genet. 69:1401.

37. Namjou, B., S. K. Nath, J. Kilpatrick, J. A. Kelly, J. Reid, J. A. James, and J. B. Harley. 2002. Stratification of pedigrees multiplex for systemic lupus erythematosus and for self-reported rheumatoid arthritis detects a systemic lupus erythematosus susceptibility gene (SLER1) at 5p15.3. *Arthritis Rheum.* 46:2937.
38. Nath, S. K., B. Namjou, C. P. Garriott, S. Frank, P. A. Joslin, J. Kilpatrick, J. A. Kelly, and J. B. Harley. 2004. Linkage analysis of SLE susceptibility: confirmation of SLER1 at 5p15.3. *Genes Immun.* 5:209.
39. Namjou, B., S. K. Nath, J. Kilpatrick, J. A. Kelly, J. Reid, M. Reichlin, J. A. James, and J. B. Harley. 2002. Genome scan stratified by the presence of anti-double-stranded DNA (dsDNA) autoantibody in pedigrees multiplex for systemic lupus erythematosus (SLE) establishes linkages at 19p13.2 (SLED1) and 18q21.1 (SLED2). *Genes Immun.* 3 Suppl 1:S35-S41.
40. Sawalha, A. H., B. Namjou, S. K. Nath, J. Kilpatrick, A. Germundson, J. A. Kelly, D. Hutchings, J. James, and J. Harley. 2002. Genetic linkage of systemic lupus erythematosus with chromosome 11q14 (SLEH1) in African-American families stratified by a nucleolar antinuclear antibody pattern. *Genes Immun.* 3 Suppl 1:S31-S34.
41. Nath, S. K., J. A. Kelly, J. Reid, T. Lam, C. Gray-McGuire, B. Namjou, C. E. Aston, and J. B. Harley. 2002. SLEB3 in systemic lupus erythematosus (SLE) is strongly related to SLE families ascertained through neuropsychiatric manifestations. *Hum. Genet.* 111:54.

42. Raman, K., and C. Mohan. 2003. Genetic underpinnings of autoimmunity--lessons from studies in arthritis, diabetes, lupus and multiple sclerosis. *Curr. Opin. Immunol.* 15:651.
43. Bottini, N., L. Musumeci, A. Alonso, S. Rahmouni, K. Nika, M. Rostamkhani, J. MacMurray, G. F. Meloni, P. Lucarelli, M. Pellecchia, G. S. Eisenbarth, D. Comings, and T. Mustelin. 2004. A functional variant of lymphoid tyrosine phosphatase is associated with type I diabetes. *Nat. Genet.* 36:337.
44. Begovich, A. B., V. E. Carlton, L. A. Honigberg, S. J. Schrodi, A. P. Chokkalingam, H. C. Alexander, K. G. Ardlie, Q. Huang, A. M. Smith, J. M. Spoerke, M. T. Conn, M. Chang, S. Y. Chang, R. K. Saiki, J. J. Catanese, D. U. Leong, V. E. Garcia, L. B. McAllister, D. A. Jeffery, A. T. Lee, F. Batliwalla, E. Remmers, L. A. Criswell, M. F. Seldin, D. L. Kastner, C. I. Amos, J. J. Sninsky, and P. K. Gregersen. 2004. A missense single-nucleotide polymorphism in a gene encoding a protein tyrosine phosphatase (PTPN22) is associated with rheumatoid arthritis. *Am. J. Hum. Genet.* 75:330.
45. Kyogoku, C., C. D. Langefeld, W. A. Ortmann, A. Lee, S. Selby, V. E. Carlton, M. Chang, P. Ramos, E. C. Baechler, F. M. Batliwalla, J. Novitzke, A. H. Williams, C. Gillett, P. Rodine, R. R. Graham, K. G. Ardlie, P. M. Gaffney, K. L. Moser, M. Petri, A. B. Begovich, P. K. Gregersen, and T. W. Behrens. 2004. Genetic Association of the R620W Polymorphism of Protein Tyrosine Phosphatase PTPN22 with Human SLE. *Am. J. Hum. Genet.* 75:504.
46. Orozco, G., E. Sanchez, M. A. Gonzalez-Gay, M. A. Lopez-Nevot, B. Torres, R. Caliz, N. Ortego-Centeno, J. Jimenez-Alonso, D. Pascual-Salcedo, A. Balsa, P. R. de, A. Nunez-Roldan, M. F. Gonzalez-Escribano, and J. Martin. 2005. Association of a

- functional single-nucleotide polymorphism of PTPN22, encoding lymphoid protein phosphatase, with rheumatoid arthritis and systemic lupus erythematosus. *Arthritis Rheum.* 52:219.
47. Kristiansen, O. P., Z. M. Larsen, and F. Pociot. 2000. CTLA-4 in autoimmune diseases--a general susceptibility gene to autoimmunity? *Genes Immun.* 1:170.
 48. Ueda, H., J. M. Howson, L. Esposito, J. Heward, H. Snook, G. Chamberlain, D. B. Rainbow, K. M. Hunter, A. N. Smith, G. G. Di, M. H. Herr, I. Dahlman, F. Payne, D. Smyth, C. Lowe, R. C. Twells, S. Howlett, B. Healy, S. Nutland, H. E. Rance, V. Everett, L. J. Smink, A. C. Lam, H. J. Cordell, N. M. Walker, C. Bordin, J. Hulme, C. Motzo, F. Cucca, J. F. Hess, M. L. Metzker, J. Rogers, S. Gregory, A. Allahabadia, R. Nithiyananthan, E. Tuomilehto-Wolf, J. Tuomilehto, P. Bingley, K. M. Gillespie, D. E. Undlien, K. S. Ronningen, C. Guja, C. Ionescu-Tirgoviste, D. A. Savage, A. P. Maxwell, D. J. Carson, C. C. Patterson, J. A. Franklyn, D. G. Clayton, L. B. Peterson, L. S. Wicker, J. A. Todd, and S. C. Gough. 2003. Association of the T-cell regulatory gene CTLA4 with susceptibility to autoimmune disease. *Nature* 423:506.
 49. Vyse, T. J., and J. A. Todd. 1996. Genetic analysis of autoimmune disease. *Cell* 85:311.
 50. Dawkins, R. L., C. Leelayuwat, S. Gaudieri, G. Tay, J. Hui, S. Cattley, P. Martinez, and J. Kulski. 1999. Genomics of the major histocompatibility complex: haplotypes, duplication, retroviruses and disease. *Immunol. Rev.* 167:275.
 51. Graham, R. R., W. A. Ortmann, C. D. Langefeld, D. Jawaheer, S. A. Selby, P. R. Rodine, E. C. Baechler, K. E. Rohlf, K. B. Shark, K. J. Espe, L. E. Green, R. P. Nair, P. E. Stuart, J. T. Elder, R. A. King, K. L. Moser, P. M. Gaffney, T. L. Bugawan, H.

- A. Erlich, S. S. Rich, P. K. Gregersen, and T. W. Behrens. 2002. Visualizing human leukocyte antigen class II risk haplotypes in human systemic lupus erythematosus. *Am. J. Hum. Genet.* 71:543.
52. Tan, F. K., and F. C. Arnett. 1998. The genetics of lupus. *Curr. Opin. Rheumatol.* 10:399.
 53. Truedsson, L., G. Sturfelt, P. Johansen, O. Nived, and B. Thuresson. 1995. Sharing of MHC haplotypes among patients with systemic lupus erythematosus from unrelated Caucasian multicase families: disease association with the extended haplotype [HLA-B8, SC01, DR17]. *J. Rheumatol.* 22:1852.
 54. Jonsen, A., A. A. Bengtsson, G. Sturfelt, and L. Truedsson. 2004. Analysis of HLA DR, HLA DQ, C4A, FcgammaRIIa, FcgammaRIIIa, MBL, and IL-1Ra allelic variants in Caucasian systemic lupus erythematosus patients suggests an effect of the combined FcgammaRIIa R/R and IL-1Ra 2/2 genotypes on disease susceptibility. *Arthritis Res. Ther.* 6:R557-R562.
 55. Wilson, A. G., F. S. di Giovine, and G. W. Duff. 1995. Genetics of tumour necrosis factor-alpha in autoimmune, infectious, and neoplastic diseases. *J. Inflamm.* 45:1.
 56. Studnicka-Benke, A., G. Steiner, P. Petera, and J. S. Smolen. 1996. Tumour necrosis factor alpha and its soluble receptors parallel clinical disease and autoimmune activity in systemic lupus erythematosus. *Br. J. Rheumatol.* 35:1067.
 57. Aringer, M., E. Feierl, G. Steiner, G. H. Stummvoll, E. Hofler, C. W. Steiner, I. Radda, J. S. Smole, and W. B. Graninger. 2002. Increased bioactive TNF in human systemic lupus erythematosus: associations with cell death. *Lupus* 11:102.

58. Wilson, A. G., C. Gordon, F. S. di Giovine, V. N. de, L. B. van de Putte, P. Emery, and G. W. Duff. 1994. A genetic association between systemic lupus erythematosus and tumor necrosis factor alpha. *Eur. J. Immunol.* 24:191.
59. Rood, M. J., M. V. van Krugten, E. Zanelli, M. W. van der Linden, V. Keijsers, G. M. Schreuder, W. Verduyn, R. G. Westendorp, R. R. de Vries, F. C. Breedveld, C. L. Verweij, and T. W. Huizinga. 2000. TNF-308A and HLA-DR3 alleles contribute independently to susceptibility to systemic lupus erythematosus. *Arthritis Rheum* 43:129.
60. van der Linden, M. W., A. R. van der Slik, E. Zanelli, M. J. Giphart, E. Pieterman, G. M. Schreuder, R. G. Westendorp, and T. W. Huizinga. 2001. Six microsatellite markers on the short arm of chromosome 6 in relation to HLA-DR3 and TNF-308A in systemic lupus erythematosus. *Genes Immun.* 2:373.
61. Sullivan, K. E., C. Wooten, B. J. Schmeckpeper, D. Goldman, and M. A. Petri. 1997. A promoter polymorphism of tumor necrosis factor alpha associated with systemic lupus erythematosus in African-Americans. *Arthritis Rheum.* 40:2207.
62. Rudwaleit, M., M. Tikly, M. Khamashta, K. Gibson, J. Klinke, G. Hughes, and P. Wordsworth. 1996. Interethnic differences in the association of tumor necrosis factor promoter polymorphisms with systemic lupus erythematosus. *J. Rheumatol.* 23:1725.
63. Tsuchiya, N., A. Kawasaki, B. P. Tsao, T. Komata, J. M. Grossman, and K. Tokunaga. 2001. Analysis of the association of HLA-DRB1, TNFalpha promoter and TNFR2 (TNFRSF1B) polymorphisms with SLE using transmission disequilibrium test. *Genes Immun.* 2:317.

64. Parks, C. G., J. P. Pandey, M. A. Dooley, E. L. Treadwell, C. E. St, G. S. Gilkeson, C. L. Feghali-Botswick, and G. S. Cooper. 2004. Genetic polymorphisms in tumor necrosis factor (TNF)-alpha and TNF-beta in a population-based study of systemic lupus erythematosus: associations and interaction with the interleukin-1alpha-889 C/T polymorphism. *Hum. Immunol.* 65:622.
65. Chen, C. J., J. H. Yen, W. C. Tsai, C. S. Wu, W. Chiang, J. J. Tsai, and H. W. Liu. 1997. The TNF2 allele does not contribute towards susceptibility to systemic lupus erythematosus. *Immunol. Lett.* 55:1.
66. Abraham, L. J., and K. M. Kroeger. 1999. Impact of the -308 TNF promoter polymorphism on the transcriptional regulation of the TNF gene: relevance to disease. *J. Leukoc. Biol.* 66:562.
67. Bayley, J. P., R. H. de, P. J. van den Elsen, T. W. Huizinga, and C. L. Verweij. 2001. Functional analysis of linker-scan mutants spanning the -376, -308, -244, and -238 polymorphic sites of the TNF-alpha promoter. *Cytokine* 14:316.
68. Komata, T., N. Tsuchiya, M. Matsushita, K. Hagiwara, and K. Tokunaga. 1999. Association of tumor necrosis factor receptor 2 (TNFR2) polymorphism with susceptibility to systemic lupus erythematosus. *Tissue Anti.* 53:527.
69. Morita, C., T. Horiuchi, H. Tsukamoto, N. Hatta, Y. Kikuchi, Y. Arinobu, T. Otsuka, T. Sawabe, S. Harashima, K. Nagasawa, and Y. Niho. 2001. Association of tumor necrosis factor receptor type II polymorphism 196R with Systemic lupus erythematosus in the Japanese: molecular and functional analysis. *Arthritis Rheum.* 44:2819.

70. Takahashi, M., H. Hashimoto, M. Akizuki, T. Sasazuki, N. Nishikimi, H. Ouchi, Y. Kobayashi, F. Numano, and A. Kimura. 2001. Lack of association between the Met196Arg polymorphism in the TNFR2 gene and autoimmune diseases accompanied by vasculitis including SLE in Japanese. *Tissue Anti.* 57:66.
71. Al-Ansari, A. S., W. E. Ollier, J. Villarreal, J. Ordi, L. S. Teh, and A. H. Hajeer. 2000. Tumor necrosis factor receptor II (TNFRII) exon 6 polymorphism in systemic lupus erythematosus. *Tissue Anti.* 55:97.
72. Khoa, P. D., T. Sugiyama, and T. Yokochi. 2004. Polymorphism of interleukin-10 promoter and tumor necrosis factor receptor II in Vietnamese patients with systemic lupus erythematosus. *Clin. Rheumatol.*
73. Hasegawa, K., F. Martin, G. Huang, D. Tumas, L. Diehl, and A. C. Chan. 2004. PEST domain-enriched tyrosine phosphatase (PEP) regulation of effector/memory T cells. *Science* 303:685.
74. Cloutier, J. F., and A. Veillette. 1999. Cooperative inhibition of T-cell antigen receptor signaling by a complex between a kinase and a phosphatase. *J. Exp. Med.* 189:111.
75. Magnusson, V., A. K. Lindqvist, C. Castillejo-Lopez, H. Kristjansdottir, K. Steinsson, G. Grondal, G. Sturfelt, L. Truedsson, E. Svenungsson, I. Lundberg, I. Gunnarsson, A. I. Bolstad, H. J. Haga, R. Jonsson, L. Klareskog, J. cocer-Varela, D. arcon-Segovia, J. D. Terwilliger, U. B. Gyllensten, and M. E. arcon-Riquelme. 2000. Fine mapping of the SLEB2 locus involved in susceptibility to systemic lupus erythematosus. *Genomics* 70:307.

76. Okazaki, T., Y. Iwai, and T. Honjo. 2002. New regulatory co-receptors: inducible co-stimulator and PD-1. *Curr. Opin. Immunol.* 14:779.
77. Prokunina, L., C. Castillejo-Lopez, F. Oberg, I. Gunnarsson, L. Berg, V. Magnusson, A. J. Brookes, D. Tentler, H. Kristjansdottir, G. Grondal, A. I. Bolstad, E. Svenungsson, I. Lundberg, G. Sturfelt, A. Jonssen, L. Truedsson, G. Lima, J. cocer-Varela, R. Jonsson, U. B. Gyllensten, J. B. Harley, D. arcon-Segovia, K. Steinsson, and M. E. arcon-Riquelme. 2002. A regulatory polymorphism in PDCD1 is associated with susceptibility to systemic lupus erythematosus in humans. *Nat. Genet.* 32:666.
78. Tokuhiro, S., R. Yamada, X. Chang, A. Suzuki, Y. Kochi, T. Sawada, M. Suzuki, M. Nagasaki, M. Ohtsuki, M. Ono, H. Furukawa, M. Nagashima, S. Yoshino, A. Mabuchi, A. Sekine, S. Saito, A. Takahashi, T. Tsunoda, Y. Nakamura, and K. Yamamoto. 2003. An intronic SNP in a RUNX1 binding site of SLC22A4, encoding an organic cation transporter, is associated with rheumatoid arthritis. *Nat. Genet.* 35:341.
79. Helms, C., L. Cao, J. G. Krueger, E. M. Wijsman, F. Chamian, D. Gordon, M. Heffernan, J. A. Daw, J. Robarge, J. Ott, P. Y. Kwok, A. Menter, and A. M. Bowcock. 2003. A putative RUNX1 binding site variant between SLC9A3R1 and NAT9 is associated with susceptibility to psoriasis. *Nat. Genet.* 35:349.
80. Nielsen, C., H. Laustrop, A. Voss, P. Junker, S. Husby, and S. T. Lillevang. 2004. A putative regulatory polymorphism in PD-1 is associated with nephropathy in a population-based cohort of systemic lupus erythematosus patients. *Lupus* 13:510.
81. Ferreira-Vidal, I., J. J. Gomez-Reino, F. Barros, A. Carracedo, P. Carreira, F. Gonzalez-Escribano, M. Liz, J. Martin, J. Ordi, J. L. Vicario, and A. Gonzalez. 2004.

Association of PDCD1 with susceptibility to systemic lupus erythematosus: evidence of population-specific effects. *Arthritis Rheum.* 50:2590.

82. Nishimura, H., M. Nose, H. Hiai, N. Minato, and T. Honjo. 1999. Development of lupus-like autoimmune diseases by disruption of the PD-1 gene encoding an ITIM motif-carrying immunoreceptor. *Immun* 11:141.
83. Nishimura, H., N. Minato, T. Nakano, and T. Honjo. 1998. Immunological studies on PD-1 deficient mice: implication of PD-1 as a negative regulator for B cell responses. *Int. Immunol.* 10:1563.
84. Nishimura, H., T. Okazaki, Y. Tanaka, K. Nakatani, M. Hara, A. Matsumori, S. Sasayama, A. Mizoguchi, H. Hiai, N. Minato, and T. Honjo. 2001. Autoimmune dilated cardiomyopathy in PD-1 receptor-deficient mice. *Science* 291:319.
85. Parks, C. G., L. L. Hudson, G. S. Cooper, M. A. Dooley, E. L. Treadwell, E. W. St Clair, G. S. Gilkeson, and J. P. Pandey. 2004. CTLA-4 gene polymorphisms and systemic lupus erythematosus in a population-based study of whites and African-Americans in the southeastern United States. *Lupus* 13:784.
86. Ahmed, S., K. Ihara, S. Kanemitsu, H. Nakashima, T. Otsuka, K. Tsuzaka, T. Takeuchi, and T. Hara. 2001. Association of CTLA-4 but not CD28 gene polymorphisms with systemic lupus erythematosus in the Japanese population. *Rheumatology. (Oxford)* 40:662.
87. Barreto, M., E. Santos, R. Ferreira, C. Fesel, M. F. Fontes, C. Pereira, B. Martins, R. Andreia, J. F. Viana, F. Crespo, C. Vasconcelos, C. Ferreira, and A. M. Vicente. 2004. Evidence for CTLA4 as a susceptibility gene for systemic lupus erythematosus. *Eur. J. Hum. Genet.* 12:620.

88. Torres, B., F. Aguilar, E. Franco, E. Sanchez, J. Sanchez-Roman, J. J. Alonso, A. Nunez-Roldan, J. Martin, and M. F. Gonzalez-Escribano. 2004. Association of the CT60 marker of the CTLA4 gene with systemic lupus erythematosus. *Arthritis Rheum.* 50:2211.
89. Gibson, A. W., J. C. Edberg, J. Wu, R. G. Westendorp, T. W. Huizinga, and R. P. Kimberly. 2001. Novel single nucleotide polymorphisms in the distal IL-10 promoter affect IL-10 production and enhance the risk of systemic lupus erythematosus. *J. Immunol.* 166:3915.
90. Chong, W. P., W. K. Ip, W. H. Wong, C. S. Lau, T. M. Chan, and Y. L. Lau. 2004. Association of interleukin-10 promoter polymorphisms with systemic lupus erythematosus. *Genes Immun.* 5:484.
91. Houssiau, F. A., C. Lefebvre, B. M. Vanden, M. Lambert, J. P. Devogelaer, and J. C. Renaud. 1995. Serum interleukin 10 titers in systemic lupus erythematosus reflect disease activity. *Lupus* 4:393.
92. Capper, E. R., J. K. Maskill, C. Gordon, and A. I. Blakemore. 2004. Interleukin (IL)-10, IL-1ra and IL-12 profiles in active and quiescent systemic lupus erythematosus: could longitudinal studies reveal patient subgroups of differing pathology? *Clin. Exp. Immunol.* 138:348.
93. Llorente, L., Y. Richaud-Patin, J. Couderc, D. arcon-Segovia, R. Ruiz-Soto, N. cocer-Castillejos, J. cocer-Varela, J. Granados, S. Bahena, P. Galanaud, and D. Emilie. 1997. Dysregulation of interleukin-10 production in relatives of patients with systemic lupus erythematosus. *Arthritis Rheum.* 40:1429.

94. Llorente, L., W. Zou, Y. Levy, Y. Richaud-Patin, J. Wijdenes, J. cocer-Varela, B. Morel-Fourrier, J. C. Brouet, D. arcon-Segovia, P. Galanaud, and . 1995. Role of interleukin 10 in the B lymphocyte hyperactivity and autoantibody production of human systemic lupus erythematosus. *J. Exp. Med.* 181:839.
95. Lauwerys, B. R., N. Garot, J. C. Renauld, and F. A. Houssiau. 2000. Interleukin-10 blockade corrects impaired in vitro cellular immune responses of systemic lupus erythematosus patients. *Arthritis Rheum.* 43:1976.
96. Llorente, L., Y. Richaud-Patin, C. Garcia-Padilla, E. Claret, J. Jakez-Ocampo, M. H. Cardiel, J. cocer-Varela, L. Grangeot-Keros, D. arcon-Segovia, J. Wijdenes, P. Galanaud, and D. Emilie. 2000. Clinical and biologic effects of anti-interleukin-10 monoclonal antibody administration in systemic lupus erythematosus. *Arthritis Rheum.* 43:1790.
97. Salmon, J. E., and L. Pricop. 2001. Human receptors for immunoglobulin G: key elements in the pathogenesis of rheumatic disease. *Arthritis Rheum.* 44:739.
98. Warmerdam, P. A., J. G. van de Winkel, A. Vlug, N. A. Westerdaal, and P. J. Capel. 1991. A single amino acid in the second Ig-like domain of the human Fc gamma receptor II is critical for human IgG2 binding. *J. Immunol.* 147:1338.
99. Koene, H. R., M. Kleijer, J. Algra, D. Roos, A. E. von dem Borne, and H. M. de. 1997. Fc gammaRIIIa-158V/F polymorphism influences the binding of IgG by natural killer cell Fc gammaRIIIa, independently of the Fc gammaRIIIa-48L/R/H phenotype. *Blood* 90:1109.

100. Davies, K. A., A. M. Peters, H. L. Beynon, and M. J. Walport. 1992. Immune complex processing in patients with systemic lupus erythematosus. In vivo imaging and clearance studies. *J. Clin. Invest* 90:2075.
101. Salmon, J. E., J. C. Edberg, and R. P. Kimberly. 1990. Fc gamma receptor III on human neutrophils. Allelic variants have functionally distinct capacities. *J. Clin. Invest* 85:1287.
102. Salmon, J. E., S. S. Millard, N. L. Brogle, and R. P. Kimberly. 1995. Fc gamma receptor IIIb enhances Fc gamma receptor IIa function in an oxidant-dependent and allele-sensitive manner. *J. Clin. Invest* 95:2877.
103. Manger, K., R. Repp, B. M. Spriewald, A. Rascu, A. Geiger, R. Wassmuth, N. A. Westerdal, B. Wentz, B. Manger, J. R. Kalden, and J. G. van de Winkel. 1998. Fc gamma receptor IIa polymorphism in Caucasian patients with systemic lupus erythematosus: association with clinical symptoms. *Arthritis Rheum.* 41:1181.
104. Norsworthy, P., E. Theodoridis, M. Botto, P. Athanassiou, H. Beynon, C. Gordon, D. Isenberg, M. J. Walport, and K. A. Davies. 1999. Overrepresentation of the Fc gamma receptor type IIA R131/R131 genotype in caucasoid systemic lupus erythematosus patients with autoantibodies to C1q and glomerulonephritis. *Arthritis Rheum.* 42:1828.
105. Manger, K., R. Repp, M. Jansen, M. Geisselbrecht, R. Wassmuth, N. A. Westerdal, A. Pfahlberg, B. Manger, J. R. Kalden, and J. G. van de Winkel. 2002. Fc gamma receptor IIa, IIIa, and IIIb polymorphisms in German patients with systemic lupus erythematosus: association with clinical symptoms. *Ann. Rheum. Dis.* 61:786.

106. Chen, J. Y., C. M. Wang, K. C. Tsao, Y. H. Chow, J. M. Wu, C. L. Li, H. H. Ho, Y. J. Wu, and S. F. Luo. 2004. Fcgamma receptor IIa, IIIa, and IIIb polymorphisms of systemic lupus erythematosus in Taiwan. *Ann. Rheum. Dis.* 63:877.
107. Zuniga, R., S. Ng, M. G. Peterson, J. D. Reveille, B. A. Baethge, G. S. Alarcon, and J. E. Salmon. 2001. Low-binding alleles of Fcgamma receptor types IIA and IIIA are inherited independently and are associated with systemic lupus erythematosus in Hispanic patients. *Arthritis Rheum.* 44:361.
108. Magnusson, V., B. Johanneson, G. Lima, J. Odeberg, D. arcon-Segovia, and M. E. arcon-Riquelme. 2004. Both risk alleles for FcgammaRIIA and FcgammaRIIIA are susceptibility factors for SLE: a unifying hypothesis. *Genes Immun.* 5:130.
109. Kyogoku, C., H. M. Dijstelbloem, N. Tsuchiya, Y. Hatta, H. Kato, A. Yamaguchi, T. Fukazawa, M. D. Jansen, H. Hashimoto, J. G. van de Winkel, C. G. Kallenberg, and K. Tokunaga. 2002. Fcgamma receptor gene polymorphisms in Japanese patients with systemic lupus erythematosus: contribution of FCGR2B to genetic susceptibility. *Arthritis Rheum.* 46:1242.
110. Siriboonrit, U., N. Tsuchiya, M. Sirikong, C. Kyogoku, S. Bejrachandra, P. Suthipinittharm, K. Luangtrakool, D. Srinak, R. Thongpradit, K. Fujiwara, D. Chandanayingyong, and K. Tokunaga. 2003. Association of Fcgamma receptor IIb and IIIb polymorphisms with susceptibility to systemic lupus erythematosus in Thais. *Tissue Anti.* 61:374.
111. Chu, Z. T., N. Tsuchiya, C. Kyogoku, J. Ohashi, Y. P. Qian, S. B. Xu, C. Z. Mao, J. Y. Chu, and K. Tokunaga. 2004. Association of Fcgamma receptor IIb polymorphism

- with susceptibility to systemic lupus erythematosus in Chinese: a common susceptibility gene in the Asian populations. *Tissue Anti.* 63:21.
112. Clynes, R., and J. V. Ravetch. 1995. Cytotoxic antibodies trigger inflammation through Fc receptors. *Immun* 3:21.
 113. Clynes, R., C. Dumitru, and J. V. Ravetch. 1998. Uncoupling of immune complex formation and kidney damage in autoimmune glomerulonephritis. *Science* 279:1052.
 114. Suzuki, Y., I. Shirato, K. Okumura, J. V. Ravetch, T. Takai, Y. Tomino, and C. Ra. 1998. Distinct contribution of Fc receptors and angiotensin II-dependent pathways in anti-GBM glomerulonephritis. *Kidney Int* 54:1166.
 115. van Lent, P. L., A. J. van Vuuren, A. B. Blom, A. E. Holthuysen, L. B. van de Putte, J. G. van de Winkel, and W. B. van den Berg. 2000. Role of Fc receptor gamma chain in inflammation and cartilage damage during experimental antigen-induced arthritis. *Arthritis Rheum.* 43:740.
 116. Jiang, Y., S. Hirose, M. Abe, R. Sanokawa-Akakura, M. Ohtsuji, X. Mi, N. Li, Y. Xiu, D. Zhang, J. Shirai, Y. Hamano, H. Fujii, and T. Shirai. 2000. Polymorphisms in IgG Fc receptor IIB regulatory regions associated with autoimmune susceptibility. *Immunogenetics* 51:429.
 117. Xiu, Y., K. Nakamura, M. Abe, N. Li, X. S. Wen, Y. Jiang, D. Zhang, H. Tsurui, S. Matsuoka, Y. Hamano, H. Fujii, M. Ono, T. Takai, T. Shimokawa, C. Ra, T. Shirai, and S. Hirose. 2002. Transcriptional regulation of Fcgr2b gene by polymorphic promoter region and its contribution to humoral immune responses. *J. Immunol.* 169:4340.

118. Bolland, S., and J. V. Ravetch. 2000. Spontaneous autoimmune disease in Fc(gamma)RIIB-deficient mice results from strain-specific epistasis. *Immun* 13:277.
119. McGaha, T. L., B. Sorrentino, and J. V. Ravetch. 2005. Restoration of tolerance in lupus by targeted inhibitory receptor expression. *Science* 307:590.
120. Fukuyama, H., F. Nimmerjahn, and J. V. Ravetch. 2005. The inhibitory Fcgamma receptor modulates autoimmunity by limiting the accumulation of immunoglobulin G⁺ anti-DNA plasma cells. *Nat. Immunol.* 6:99.
121. Russell, A. I., D. S. Cunninghame Graham, C. Shepherd, C. A. Robertson, J. Whittaker, J. Meeks, R. J. Powell, D. A. Isenberg, M. J. Walport, and T. J. Vyse. 2004. Polymorphism at the C-reactive protein locus influences gene expression and predisposes to systemic lupus erythematosus. *Hum. Mol. Genet.* 13:137.
122. Du Clos, T. W. 2003. C-reactive protein as a regulator of autoimmunity and inflammation. *Arthritis Rheum.* 48:1475.
123. Carroll, M. 2001. Innate immunity in the etiopathology of autoimmunity. *Nat. Immunol.* 2:1089.
124. Szalai, A. J., C. T. Weaver, M. A. McCrory, F. W. van Ginkel, R. M. Reiman, J. F. Kearney, T. N. Marion, and J. E. Volanakis. 2003. Delayed lupus onset in (NZB x NZW)F1 mice expressing a human C-reactive protein transgene. *Arthritis Rheum.* 48:1602.
125. Gaip, U. S., J. Brunner, T. D. Beyer, R. E. Voll, J. R. Kalden, and M. Herrmann. 2003. Disposal of dying cells: a balancing act between infection and autoimmunity. *Arthritis Rheum.* 48:6.

126. Bickerstaff, M. C., M. Botto, W. L. Hutchinson, J. Herbert, G. A. Tennent, A. Bybee, D. A. Mitchell, H. T. Cook, P. J. Butler, M. J. Walport, and M. B. Pepys. 1999. Serum amyloid P component controls chromatin degradation and prevents antinuclear autoimmunity. *Nat Med* 5:694.
127. Gillmore, J. D., W. L. Hutchinson, J. Herbert, A. Bybee, D. A. Mitchell, R. P. Hasserjian, K. Yamamura, M. Suzuki, C. A. Sabin, and M. B. Pepys. 2004. Autoimmunity and glomerulonephritis in mice with targeted deletion of the serum amyloid P component gene: SAP deficiency or strain combination? *Immunology* 112:255.
128. Napirei, M., H. Karsunky, B. Zevnik, H. Stephan, H. G. Mannherz, and T. Moroy. 2000. Features of systemic lupus erythematosus in Dnase1-deficient mice. *Nat Genet* 25:177.
129. Cohen, P. L., R. Caricchio, V. Abraham, T. D. Camenisch, J. C. Jennette, R. A. Roubey, H. S. Earp, G. Matsushima, and E. A. Reap. 2002. Delayed apoptotic cell clearance and lupus-like autoimmunity in mice lacking the c-mer membrane tyrosine kinase. *J. Exp. Med.* 196:135.
130. Xue, D., H. Shi, J. D. Smith, X. Chen, D. A. Noe, T. Cedervall, D. D. Yang, E. Eynon, D. E. Brash, M. Kashgarian, R. A. Flavell, and S. L. Wolin. 2003. A lupus-like syndrome develops in mice lacking the Ro 60-kDa protein, a major lupus autoantigen. *Proc. Natl. Acad. Sci. U. S. A* 100:7503.
131. Watanabe-Fukunaga, R., C. I. Brannan, N. G. Copeland, N. A. Jenkins, and S. Nagata. 1992. Lymphoproliferation disorder in mice explained by defects in Fas antigen that mediates apoptosis. *Nature* 356:314.

132. Takahashi, T., M. Tanaka, C. I. Brannan, N. A. Jenkins, N. G. Copeland, T. Suda, and S. Nagata. 1994. Generalized lymphoproliferative disease in mice, caused by a point mutation in the Fas ligand. *Cell* 76:969.
133. Adachi, M., S. Suematsu, T. Suda, D. Watanabe, H. Fukuyama, J. Ogasawara, T. Tanaka, N. Yoshida, and S. Nagata. 1996. Enhanced and accelerated lymphoproliferation in Fas-null mice. *Proc. Natl. Acad. Sci. U. S. A* 93:2131.
134. Weintraub, J. P., V. Godfrey, P. A. Wolthusen, R. L. Cheek, R. A. Eisenberg, and P. L. Cohen. 1998. Immunological and pathological consequences of mutations in both Fas and Fas ligand. *Cell Immunol.* 186:8.
135. Strasser, A., S. Whittingham, D. L. Vaux, M. L. Bath, J. M. Adams, S. Cory, and A. W. Harris. 1991. Enforced BCL2 expression in B-lymphoid cells prolongs antibody responses and elicits autoimmune disease. *P. N. A. S.* 88:8661.
136. Bouillet, P., D. Metcalf, D. C. Huang, D. M. Tarlinton, T. W. Kay, F. Kontgen, J. M. Adams, and A. Strasser. 1999. Proapoptotic Bcl-2 relative Bim required for certain apoptotic responses, leukocyte homeostasis, and to preclude autoimmunity. *Science* 286:1735.
137. Zhang, Y., S. F. Schlossman, R. A. Edwards, C. N. Ou, J. Gu, and M. X. Wu. 2002. Impaired apoptosis, extended duration of immune responses, and a lupus-like autoimmune disease in IEX-1-transgenic mice. *Proc. Natl. Acad. Sci. U. S. A* 99:878.
138. Drappa, J., L. A. Kamen, E. Chan, M. Georgiev, D. Ashany, F. Marti, and P. D. King. 2003. Impaired T cell death and lupus-like autoimmunity in T cell-specific adapter protein-deficient mice. *J. Exp. Med.* 198:809.

139. Di, C. A., P. Kotsi, Y. F. Peng, C. Cordon-Cardo, K. B. Elkon, and P. P. Pandolfi. 1999. Impaired Fas response and autoimmunity in Pten^{+/-} mice. *Science* 285:2122.
140. Borlado, L. R., C. Redondo, B. Alvarez, C. Jimenez, L. M. Criado, J. Flores, M. A. Marcos, A. Martinez, D. Balomenos, and A. C. Carrera. 2000. Increased phosphoinositide 3-kinase activity induces a lymphoproliferative disorder and contributes to tumor generation in vivo. *FASEB J.* 14:895.
141. Khare, S. D., I. Sarosi, X. Z. Xia, S. McCabe, K. Miner, I. Solovyev, N. Hawkins, M. Kelley, D. Chang, G. Van, L. Ross, J. Delaney, L. Wang, D. Lacey, W. J. Boyle, and H. Hsu. 2000. Severe B cell hyperplasia and autoimmune disease in TALL-1 transgenic mice. *Proc Natl Acad Sci U S A* 97:3370.
142. Seshasayee, D., P. Valdez, M. Yan, V. M. Dixit, D. Tumas, and I. S. Grewal. 2003. Loss of TACI causes fatal lymphoproliferation and autoimmunity, establishing TACI as an inhibitory BLYS receptor. *Immunity*. 18:279.
143. Miwa, T., M. A. Maldonado, L. Zhou, X. Sun, H. Y. Luo, D. Cai, V. P. Werth, M. P. Madaio, R. A. Eisenberg, and W. C. Song. 2002. Deletion of decay-accelerating factor (CD55) exacerbates autoimmune disease development in MRL/lpr mice. *Am. J. Pathol.* 161:1077.
144. Higuchi, T., Y. Aiba, T. Nomura, J. Matsuda, K. Mochida, M. Suzuki, H. Kikutani, T. Honjo, K. Nishioka, and T. Tsubata. 2002. Cutting Edge: Ectopic expression of CD40 ligand on B cells induces lupus-like autoimmune disease. *J. Immunol.* 168:9.
145. Yu, C. C., T. S. Yen, C. A. Lowell, and A. L. DeFranco. 2001. Lupus-like kidney disease in mice deficient in the Src family tyrosine kinases Lyn and Fyn. *Curr. Biol.* 11:34.

146. Miyamoto, A., K. Nakayama, H. Imaki, S. Hirose, Y. Jiang, M. Abe, T. Tsukiyama, H. Nagahama, S. Ohno, S. Hatakeyama, and K. I. Nakayama. 2002. Increased proliferation of B cells and auto-immunity in mice lacking protein kinase Cdelta. *Nature* 416:865.
147. Salvador, J. M., M. C. Hollander, A. T. Nguyen, J. B. Kopp, L. Barisoni, J. K. Moore, J. D. Ashwell, and A. J. Fornace, Jr. 2002. Mice lacking the p53-effector gene Gadd45a develop a lupus-like syndrome. *Immunity*. 16:499.
148. Nguyen, C., N. Limaye, and E. K. Wakeland. 2002. Susceptibility genes in the pathogenesis of murine lupus. *Arthritis Res.* 4 Suppl 3:S255-S263.
149. Rudofsky, U. H., B. D. Evans, S. L. Balaban, V. D. Mottironi, and A. E. Gabrielsen. 1993. Differences in expression of lupus nephritis in New Zealand mixed H-2z homozygous inbred strains of mice derived from New Zealand black and New Zealand white mice. Origins and initial characterization. *Laboratory Investigations* 68:419.
150. Morel, L., and E. K. Wakeland. 1998. Susceptibility to lupus nephritis in the NZB/W model system. *Curr Opin Immunol* 10:718.
151. Morel, L., U. H. Rudofsky, J. A. Longmate, J. Schiffenbauer, and E. K. Wakeland. 1994. Polygenic control of susceptibility to murine systemic lupus erythematosus. *Immun* 1(3):219.
152. Morel, L., Y. Yu, K. R. Blenman, R. A. Caldwell, and E. K. Wakeland. 1996. Production of congenic mouse strains carrying SLE-susceptibility genes derived from the SLE-prone NZM/Aeg2410 strain. *Mamm. Genome* 7:335.

153. Morel, L., C. Mohan, J. Schiffenbauer, U. H. Rudofsky, J. Tian, J. Longmate, and E. K. Wakeland. 1999. Multiplex inheritance of component phenotypes in a murine model of lupus. *Mamm. Genome* 10:176.
154. Morel, L., C. Mohan, B. P. Croker, X.-H. Tian, and E. K. Wakeland. 1997. Functional dissection of systemic lupus erythematosus using congenic mouse strains. *J. Immunol.* 158:6019.
155. Mohan, C., L. Morel, P. Yang, H. Watanabe, B. P. Croker, G. S. Gilkeson, and E. K. Wakeland. 1999. Genetic dissection of lupus pathogenesis: A recipe for nephrophilic autoantibodies. *J. Clin. Invest.* 103:1685.
156. Mohan, C., E. Alas, L. Morel, P. Yang, and E. K. Wakeland. 1998. Genetic dissection of SLE pathogenesis: *Sle1* on murine chromosome 1 leads to a selective loss of tolerance to H2A/H2B/DNA subnucleosomes. *J. Clin. Invest.* 101:1362.
157. Sobel, E. S., C. Mohan, L. Morel, J. Schiffenbauer, and E. K. Wakeland. 1999. Genetic dissection of SLE pathogenesis: Adoptive transfer of *Sle1* mediates the loss of tolerance by bone marrow-derived B cells. *Journal of Immunology* 162:2415.
158. Sobel, E. S., M. Satoh, Y. Chen, E. K. Wakeland, and L. Morel. 2002. The major murine systemic lupus erythematosus susceptibility locus *Sle1* results in abnormal functions of both B and T cells. *J. Immunol.* 169:2694.
159. Morel, L., B. P. Croker, K. R. Blenman, C. Mohan, G. Huang, G. Gilkeson, and E. K. Wakeland. 2000. Genetic reconstitution of systemic lupus erythematosus immunopathology with polycongenic murine strains. *Proc Natl Acad Sci U S A* 97:6670.

160. Mohan, C., L. Morel, P. Yang, and E. K. Wakeland. 1997. Genetic dissection of SLE pathogenesis: *Sle2* on murine chromosome 4 leads to B-cell hyperactivity. *Journal of Immunology* 159:454.
161. Mohan, C., Y. Yu, L. Morel, P. Yang, and E. K. Wakeland. 1999. Genetic dissection of SLE pathogenicity: *Sle3* on murine chromosome 7 impacts T cell activation, differentiation, and cell death. *Journal of Immunology* 162:6492.
162. Vyse, T. J., L. Morel, F. J. Tanner, E. K. Wakeland, and B. L. Kotzin. 1996. Backcross analysis of genes linked to autoantibody production in New Zealand white mice. *J. Immunol.* 157:2719.
163. Morel, L., X.-H. Tian, B. P. Croker, and E. K. Wakeland. 1999. Epistatic modifiers of autoimmunity in a murine model of lupus nephritis. *Immun* 11:131.
164. Shi, X., C. Xie, D. Kreska, J. A. Richardson, and C. Mohan. 2002. Genetic dissection of SLE: SLE1 and FAS impact alternate pathways leading to lymphoproliferative autoimmunity. *J. Exp. Med.* 196:281.
165. Hogarth, M. B., J. H. Slingsby, P. J. Allen, E. M. Thompson, P. Chandler, K. A. Davies, E. Simpson, B. J. Morley, and M. J. Walport. 1998. Multiple lupus susceptibility loci map to chromosome 1 in BXSB mice. *J Immunol* 161:2753.
166. Haywood, M. E., N. J. Rogers, S. J. Rose, J. Boyle, A. McDermott, J. M. Rankin, V. Thiruudaian, M. R. Lewis, L. Fossati-Jimack, S. Izui, M. J. Walport, and B. J. Morley. 2004. Dissection of BXSB lupus phenotype using mice congenic for chromosome 1 demonstrates that separate intervals direct different aspects of disease. *J. Immunol.* 173:4277.

167. Xie, S., S. Chang, P. Yang, C. Jacob, A. Kaliyaperumal, S. K. Datta, and C. Mohan. 2001. Genetic contributions of nonautoimmune SWR mice toward lupus nephritis. *J. Immunol.* 167:7141.
168. Vyse, T. J., S. J. Rozzo, C. G. Drake, S. Izui, and B. L. Kotzin. 1997. Control of multiple autoantibodies linked with a lupus nephritis susceptibility locus in New Zealand black mice. *J Immunol* 158:5566.
169. Kono, D. H., R. W. Burlingame, D. G. Owens, A. Kuramochi, R. S. Balderas, D. Balomenos, and A. N. Theofilopoulos. 1994. Lupus susceptibility loci in New Zealand mice. *Proceedings of the National Academy of Sciences USA* 91:10168.
170. Rozzo, S. J., J. D. Allard, D. Choubey, T. J. Vyse, S. Izui, G. Peltz, and B. L. Kotzin. 2001. Evidence for an interferon-inducible gene, Ifi202, in the susceptibility to systemic lupus. *Immunity.* 15:435.
171. Wandstrat, A. E., C. Nguyen, N. Limaye, A. Y. Chan, S. Subramanian, X. H. Tian, Y. S. Yim, A. Pertsemlidis, H. R. Garner, Jr., L. Morel, and E. K. Wakeland. 2004. Association of extensive polymorphisms in the SLAM/CD2 gene cluster with murine lupus. *Immunity.* 21:769.
172. Boackle, S. A., V. M. Holers, X. Chen, G. Szakonyi, D. R. Karp, E. K. Wakeland, and L. Morel. 2001. Cr2, a candidate gene in the murine Sle1c lupus susceptibility locus, encodes a dysfunctional protein. *Immunity.* 15:775.
173. Wilson, J. G., W. D. Ratnoff, P. H. Schur, and D. T. Fearon. 1986. Decreased expression of the C3b/C4b receptor (CR1) and the C3d receptor (CR2) on B lymphocytes and of CR1 on neutrophils of patients with systemic lupus erythematosus. *Arthritis Rheum.* 29:739.

174. Marquart, H. V., A. Svendsen, J. M. Rasmussen, C. H. Nielsen, P. Junker, S. E. Svehag, and R. G. Leslie. 1995. Complement receptor expression and activation of the complement cascade on B lymphocytes from patients with systemic lupus erythematosus (SLE). *Clin. Exp. Immunol.* 101:60.
175. Takahashi, K., Y. Kozono, T. J. Waldschmidt, D. Berthiaume, R. J. Quigg, A. Baron, and V. M. Holers. 1997. Mouse complement receptors type 1 (CR1;CD35) and type 2 (CR2;CD21): expression on normal B cell subpopulations and decreased levels during the development of autoimmunity in MRL/lpr mice. *J. Immunol.* 159:1557.
176. Prodeus, A. P., S. Goerg, L. M. Shen, O. O. Pozdnyakova, L. Chu, E. M. Alicot, C. C. Goodnow, and M. C. Carroll. 1998. A critical role for complement in maintenance of self-tolerance. *Immun* 9:721.
177. Veillette, A., and S. Latour. 2003. The SLAM family of immune-cell receptors. *Curr. Opin. Immunol.* 15:277.
178. Engel, P., M. J. Eck, and C. Terhorst. 2003. The SAP and SLAM families in immune responses and X-linked lymphoproliferative disease. *Nat. Rev. Immunol.* 3:813.
179. Tangye, S. G., J. H. Phillips, and L. L. Lanier. 2000. The CD2-subset of the Ig superfamily of cell surface molecules: receptor-ligand pairs expressed by NK cells and other immune cells. *Semin Immunol* 12:149.
180. Kingsmore, S. F., C. A. Souryal, M. L. Watson, D. D. Patel, and M. F. Seldin. 1995. Physical and genetic linkage of the genes encoding Ly-9 and CD48 on mouse and human chromosomes 1. *Immunogenetics* 42:59.

181. Reiser, H. 1990. sgp-60, a signal-transducing glycoprotein concerned with T cell activation through the T cell receptor/CD3 complex. *J. Immunol.* 145:2077.
182. Kato, K., M. Koyanagi, H. Okada, T. Takanashi, Y. W. Wong, A. F. Williams, K. Okumura, and H. Yagita. 1992. CD48 is a counter-receptor for mouse CD2 and is involved in T cell activation. *J Exp Med* 176:1241.
183. Brown, M. H., K. Boles, P. Anton van der Merwe, V. Kumar, P. A. Mathew, and A. N. Barclay. 1998. 2B4, the natural killer and T cell immunoglobulin superfamily surface protein, is a ligand for CD48. *J Exp Med* 188:2083.
184. Davis, S. J., and d. van. 1996. The structure and ligand interactions of CD2: implications for T-cell function. *Immunol Today* 17:177.
185. Gonzalez-Cabrero, J., C. J. Wise, Y. Latchman, G. J. Freeman, A. H. Sharpe, and H. Reiser. 1999. CD48-deficient mice have a pronounced defect in CD4(+) T cell activation. *Proc Natl Acad Sci U S A* 96:1019.
186. Garni-Wagner, B. A., A. Purohit, P. A. Mathew, M. Bennett, and V. Kumar. 1993. A novel function-associated molecule related to non-MHC-restricted cytotoxicity mediated by activated natural killer cells and T cells. *J Immunol* 151:60.
187. Nakajima, H., M. Cella, H. Langen, A. Friedlein, and M. Colonna. 1999. Activating interactions in human NK cell recognition: the role of 2B4-CD48. *Eur. J. Immunol.* 29:1676.
188. Romero, X., D. Benitez, S. March, R. Vilella, M. Miralpeix, and P. Engel. 2004. Differential expression of SAP and EAT-2-binding leukocyte cell-surface molecules CD84, CD150 (SLAM), CD229 (Ly9) and CD244 (2B4). *Tissue Anti.* 64:132.

189. Kambayashi, T., E. Assarsson, B. J. Chambers, and H. G. Ljunggren. 2001. Cutting edge: Regulation of CD8(+) T cell proliferation by 2B4/CD48 interactions. *J Immunol* 167:6706.
190. Stepp, S. E., J. D. Schatzle, M. Bennett, V. Kumar, and P. A. Mathew. 1999. Gene structure of the murine NK cell receptor 2B4: presence of two alternatively spliced isoforms with distinct cytoplasmic domains. *Eur. J. Immunol.* 29:2392.
191. Schatzle, J. D., S. Sheu, S. E. Stepp, P. A. Mathew, M. Bennett, and V. Kumar. 1999. Characterization of inhibitory and stimulatory forms of the murine natural killer cell receptor 2B4. *Proc. Natl. Acad. Sci. U. S. A* 96:3870.
192. Mooney, J. M., J. Klem, C. Wulfig, L. A. Mijares, P. L. Schwartzberg, M. Bennett, and J. D. Schatzle. 2004. The murine NK receptor 2B4 (CD244) exhibits inhibitory function independent of signaling lymphocytic activation molecule-associated protein expression. *J. Immunol.* 173:3953.
193. Lee, K. M., M. E. McNerney, S. E. Stepp, P. A. Mathew, J. D. Schatzle, M. Bennett, and V. Kumar. 2004. 2B4 acts as a non-major histocompatibility complex binding inhibitory receptor on mouse natural killer cells. *J. Exp. Med.* 199:1245.
194. Lee, K. M., S. Bhawan, T. Majima, H. Wei, M. I. Nishimura, H. Yagita, and V. Kumar. 2003. Cutting edge: the NK cell receptor 2B4 augments antigen-specific T cell cytotoxicity through CD48 ligation on neighboring T cells. *J. Immunol.* 170:4881.
195. Assarsson, E., T. Kambayashi, J. D. Schatzle, S. O. Cramer, B. A. von, P. E. Jensen, H. G. Ljunggren, and B. J. Chambers. 2004. NK cells stimulate proliferation of T and NK cells through 2B4/CD48 interactions. *J. Immunol.* 173:174.

196. Vaidya, S. V., S. E. Stepp, M. E. McNerney, J. K. Lee, M. Bennett, K. M. Lee, C. L. Stewart, V. Kumar, and P. A. Mathew. 2005. Targeted disruption of the 2B4 gene in mice reveals an in vivo role of 2B4 (CD244) in the rejection of B16 melanoma cells. *J. Immunol.* 174:800.
197. Boles, K. S., H. Nakajima, M. Colonna, S. S. Chuang, S. E. Stepp, M. Bennett, V. Kumar, and P. A. Mathew. 1999. Molecular characterization of a novel human natural killer cell receptor homologous to mouse 2B4. *Tissue Anti.* 54:27.
198. Tangye, S. G., H. Cherwinski, L. L. Lanier, and J. H. Phillips. 2000. 2B4-mediated activation of human natural killer cells. *Mol. Immunol.* 37:493.
199. Sivori, S., S. Parolini, M. Falco, E. Marcenaro, R. Biassoni, C. Bottino, L. Moretta, and A. Moretta. 2000. 2B4 functions as a co-receptor in human NK cell activation. *Eur J Immunol* 30:787.
200. Tangye, S. G., J. H. Phillips, L. L. Lanier, and K. E. Nichols. 2000. Functional requirement for SAP in 2B4-mediated activation of human natural killer cells as revealed by the X-linked lymphoproliferative syndrome. *J Immunol* 165:2932.
201. Parolini, S., C. Bottino, M. Falco, R. Augugliaro, S. Giliani, R. Franceschini, H. D. Ochs, H. Wolf, J. Y. Bonnefoy, R. Biassoni, L. Moretta, L. D. Notarangelo, and A. Moretta. 2000. X-linked lymphoproliferative disease. 2B4 molecules displaying inhibitory rather than activating function are responsible for the inability of natural killer cells to kill Epstein-Barr virus-infected cells. *J Exp Med* 192:337.
202. Chen, R., F. Relouzat, R. Roncagalli, A. Aoukaty, R. Tan, S. Latour, and A. Veillette. 2004. Molecular dissection of 2B4 signaling: implications for signal transduction by SLAM-related receptors. *Mol. Cell Biol.* 24:5144.

203. Sayos, J., K. B. Nguyen, C. Wu, S. E. Stepp, D. Howie, J. D. Schatzle, V. Kumar, C. A. Biron, and C. Terhorst. 2000. Potential pathways for regulation of NK and T cell responses: differential X-linked lymphoproliferative syndrome gene product SAP interactions with SLAM and 2B4. *Int. Immunol.* 12:1749.
204. Sidorenko, S. P., and E. A. Clark. 1993. Characterization of a cell surface glycoprotein IPO-3, expressed on activated human B and T lymphocytes. *J. Immunol.* 151:4614.
205. Tatsuo, H., N. Ono, K. Tanaka, and Y. Yanagi. 2000. SLAM (CDw150) is a cellular receptor for measles virus. *Nature* 406:893.
206. Cocks, B. G., C. C. Chang, J. M. Carballido, H. Yssel, V. de, and G. Aversa. 1995. A novel receptor involved in T-cell activation. *Nature* 376:260.
207. Castro, A. G., T. M. Hauser, B. G. Cocks, J. Abrams, S. Zurawski, T. Churakova, F. Zonin, D. Robinson, S. G. Tangye, G. Aversa, K. E. Nichols, J. E. De Vries, L. L. Lanier, and A. O'Garra. 1999. Molecular and functional characterization of mouse signaling lymphocytic activation molecule (SLAM): differential expression and responsiveness in Th1 and Th2 cells. *J Immunol* 163:5860.
208. Aversa, G., C. C. Chang, J. M. Carballido, B. G. Cocks, and J. E. De Vries. 1997. Engagement of the signaling lymphocytic activation molecule (SLAM) on activated T cells results in IL-2-independent, cyclosporin A-sensitive T cell proliferation and IFN-gamma production. *J. Immunol.* 158:4036.
209. Mavaddat, N., D. W. Mason, P. D. Atkinson, E. J. Evans, R. J. Gilbert, D. I. Stuart, J. A. Fennelly, A. N. Barclay, S. J. Davis, and M. H. Brown. 2000. Signaling

- lymphocytic activation molecule (CDw150) is homophilic but self-associates with very low affinity. *J Biol Chem* 275:28100.
210. Punnonen, J., B. G. Cocks, J. M. Carballido, B. Bennett, D. Peterson, G. Aversa, and V. de. 1997. Soluble and membrane-bound forms of signaling lymphocytic activation molecule (SLAM) induce proliferation and Ig synthesis by activated human B lymphocytes. *J Exp Med* 185:993.
 211. Sayos, J., C. Wu, M. Morra, N. Wang, X. Zhang, D. Allen, S. van Schaik, L. Notarangelo, R. Geha, M. G. Roncarolo, H. Oettgen, J. E. De Vries, G. Aversa, and C. Terhorst. 1998. The X-linked lymphoproliferative-disease gene product SAP regulates signals induced through the co-receptor SLAM [see comments]. *Nature* 395:462.
 212. Lewis, J., L. J. Eiben, D. L. Nelson, J. I. Cohen, K. E. Nichols, H. D. Ochs, L. D. Notarangelo, and C. S. Duckett. 2001. Distinct interactions of the X-linked lymphoproliferative syndrome gene product SAP with cytoplasmic domains of members of the CD2 receptor family. *Clin. Immunol.* 100:15.
 213. Howie, D., S. Okamoto, S. Rietdijk, K. Clarke, N. Wang, C. Gullo, J. P. Bruggeman, S. Manning, A. J. Coyle, E. Greenfield, V. Kuchroo, and C. Terhorst. 2002. The role of SAP in murine CD150 (SLAM)-mediated T-cell proliferation and interferon gamma production. *Blood* 100:2899.
 214. Shlapatska, L. M., S. V. Mikhalap, A. G. Berdova, O. M. Zelensky, T. J. Yun, K. E. Nichols, E. A. Clark, and S. P. Sidorenko. 2001. CD150 association with either the SH2-containing inositol phosphatase or the SH2-containing protein tyrosine phosphatase is regulated by the adaptor protein SH2D1A. *Jour. Imm.* 166:5480.

215. Latour, S., G. Gish, C. D. Helgason, R. K. Humphries, T. Pawson, and A. Veillette. 2001. Regulation of SLAM-mediated signal transduction by SAP, the X-linked lymphoproliferative gene product. *Nat. Immunol.* 2:681.
216. Chan, B., A. Lanyi, H. K. Song, J. Griesbach, M. Simarro-Grande, F. Poy, D. Howie, J. Sumegi, C. Terhorst, and M. J. Eck. 2003. SAP couples Fyn to SLAM immune receptors. *Nat. Cell Biol.* 5:155.
217. Simarro, M., A. Lanyi, D. Howie, F. Poy, J. Bruggeman, M. Choi, J. Sumegi, M. J. Eck, and C. Terhorst. 2004. SAP increases FynT kinase activity and is required for phosphorylation of SLAM and Ly9. *Int. Immunol.* 16:727.
218. Carballido, J. M., G. Aversa, K. Kaltoft, B. G. Cocks, J. Punnonen, H. Yssel, K. Thestrup-Pedersen, and J. E. De Vries. 1997. Reversal of human allergic T helper 2 responses by engagement of signaling lymphocytic activation molecule. *J. Immunol.* 159:4316.
219. Quiroga, M. F., G. J. Martinez, V. Pasquinelli, M. A. Costas, M. M. Bracco, A. Malbran, L. M. Olivares, P. A. Sieling, and V. E. Garcia. 2004. Activation of signaling lymphocytic activation molecule triggers a signaling cascade that enhances Th1 responses in human intracellular infection. *J. Immunol.* 173:4120.
220. Wang, N., A. Satoskar, W. Faubion, D. Howie, S. Okamoto, S. Feske, C. Gullo, K. Clarke, M. R. Sosa, A. H. Sharpe, and C. Terhorst. 2004. The cell surface receptor SLAM controls T cell and macrophage functions. *J. Exp. Med.* 199:1255.
221. Sacks, D., and N. Noben-Trauth. 2002. The immunology of susceptibility and resistance to *Leishmania major* in mice. *Nat. Rev. Immunol.* 2:845.

222. Tovar, V., V. J. del, N. Zapater, M. Martin, X. Romero, P. Pizcueta, J. Bosch, C. Terhorst, and P. Engel. 2002. Mouse novel Ly9: a new member of the expanding CD150 (SLAM) family of leukocyte cell-surface receptors. *Immunogenetics* 54:394.
223. Boles, K. S., and P. A. Mathew. 2001. Molecular cloning of CS1, a novel human natural killer cell receptor belonging to the CD2 subset of the immunoglobulin superfamily. *Immunogenetics* 52:302.
224. Bouchon, A., M. Cella, H. L. Grierson, J. I. Cohen, and M. Colonna. 2001. Activation of NK cell-mediated cytotoxicity by a SAP-independent receptor of the CD2 family. *J. Immunol.* 167:5517.
225. Kumaresan, P. R., W. C. Lai, S. S. Chuang, M. Bennett, and P. A. Mathew. 2002. CS1, a novel member of the CD2 family, is homophilic and regulates NK cell function. *Mol. Immunol.* 39:1.
226. Lee, J. K., K. S. Boles, and P. A. Mathew. 2004. Molecular and functional characterization of a CS1 (CRACC) splice variant expressed in human NK cells that does not contain immunoreceptor tyrosine-based switch motifs. *Eur. J. Immunol.* 34:2791.
227. Palou, E., F. Pirotto, J. Sole, J. H. Freed, B. Peral, C. Vilardell, R. Vilella, J. Vives, and A. Gaya. 2000. Genomic characterization of CD84 reveals the existence of five isoforms differing in their cytoplasmic domains. *Tissue Anti.* 55:118.
228. Martin, M., X. Romero, I. de, V. Tovar, N. Zapater, E. Esplugues, P. Pizcueta, J. Bosch, and P. Engel. 2001. CD84 functions as a homophilic adhesion molecule and enhances IFN-gamma secretion: adhesion is mediated by Ig-like domain 1. *J Immunol* 167:3668.

229. de la Fuente, M. A., V. Tovar, P. Pizcueta, M. Nadal, J. Bosch, and P. Engel. 1999. Molecular cloning, characterization, and chromosomal localization of the mouse homologue of CD84, a member of the CD2 family of cell surface molecules. *Immunogenetics* 49:249.
230. Sayos, J., M. Martin, A. Chen, M. Simarro, D. Howie, M. Morra, P. Engel, and C. Terhorst. 2001. Cell surface receptors Ly-9 and CD84 recruit the X-linked lymphoproliferative disease gene product SAP. *Blood* 97:3867.
231. Tangye, S. G., K. E. Nichols, N. J. Hare, and B. C. van de Weerd. 2003. Functional requirements for interactions between CD84 and Src homology 2 domain-containing proteins and their contribution to human T cell activation. *J. Immunol.* 171:2485.
232. de la Fuente, M. A., V. Tovar, N. Villamor, N. Zapater, P. Pizcueta, E. Campo, J. Bosch, and P. Engel. 2001. Molecular characterization and expression of a novel human leukocyte cell-surface marker homologous to mouse Ly-9. *Blood* 97:3513.
233. Sandrin, M. S., T. P. Gumley, M. M. Henning, H. A. Vaughan, L. J. Gonez, J. A. Trapani, and I. F. McKenzie. 1992. Isolation and characterization of cDNA clones for mouse Ly-9. *J Immunol* 149:1636.
234. Romero, X., N. Zapater, V. Tovar, C. Ockeloen, and P. Engel. 2004. Cd229 (Ly9) cell-surface molecule functions as a homophilic receptor and relocalizes to the immune synapse.
235. Peck, S. R., and H. E. Ruley. 2000. Ly108: a new member of the mouse CD2 family of cell surface proteins. *Immunogenetics* 52:63.

236. Bottino, C., M. Falco, S. Parolini, E. Marcenaro, R. Augugliaro, S. Sivori, E. Landi, R. Biassoni, L. D. Notarangelo, L. Moretta, and A. Moretta. 2001. NTB-A [correction of GNTB-A], a novel SH2D1A-associated surface molecule contributing to the inability of natural killer cells to kill Epstein-Barr virus-infected B cells in X-linked lymphoproliferative disease. *J Exp Med* 194:235.
237. Valdez, P. A., H. Wang, D. Seshasayee, C. M. van Lookeren, A. Gurney, W. P. Lee, and I. S. Grewal. 2004. NTB-A, a new activating receptor in T cells that regulates autoimmune disease. *J. Biol. Chem.* 279:18662.
238. Flaig, R. M., S. Stark, and C. Watzl. 2004. Cutting edge: NTB-A activates NK cells via homophilic interaction. *J. Immunol.* 172:6524.
239. Falco, M., E. Marcenaro, E. Romeo, F. Bellora, D. Marras, F. Vely, G. Ferracci, L. Moretta, A. Moretta, and C. Bottino. 2004. Homophilic interaction of NTBA, a member of the CD2 molecular family: induction of cytotoxicity and cytokine release in human NK cells. *Eur. J. Immunol.* 34:1663.
240. Hron, J. D., L. Caplan, A. J. Gerth, P. L. Schwartzberg, and S. L. Peng. 2004. SH2D1A regulates T-dependent humoral autoimmunity. *J. Exp. Med.* 200:261.
241. Coffey, A. J., R. A. Brooksbank, O. Brandau, T. Ohashi, G. R. Howell, J. M. Bye, A. P. Cahn, J. Durham, P. Heath, P. Wray, R. Pavitt, J. Wilkinson, M. Leversha, E. Huckle, S. Shaw, A. Dunham, S. Rhodes, V. Schuster, G. Porta, L. Yin, P. Serafini, B. Sylla, M. Zollo, B. Franco, and D. R. Bentley. 1998. Host response to EBV infection in X-linked lymphoproliferative disease results from mutations in an SH2-domain encoding gene. *Nat Genet* 20:129.

242. Nichols, K. E., D. P. Harkin, S. Levitz, M. Krainer, K. A. Kolquist, C. Genovese, A. Bernard, M. Ferguson, L. Zuo, E. Snyder, A. J. Buckler, C. Wise, J. Ashley, M. Lovett, M. B. Valentine, A. T. Look, W. Gerald, D. E. Housman, and D. A. Haber. 1998. Inactivating mutations in an SH2 domain-encoding gene in X-linked lymphoproliferative syndrome. *Proc. Natl. Acad. Sci. U. S. A* 95:13765.
243. Latour, S., and A. Veillette. 2003. Molecular and immunological basis of X-linked lymphoproliferative disease. *Immunol. Rev.* 192:212.
244. Nagy, N., C. Cerboni, K. Mattsson, A. Maeda, P. Gogolak, J. Sumegi, A. Lanyi, L. Szekely, E. Carbone, G. Klein, and E. Klein. 2000. SH2D1A and SLAM protein expression in human lymphocytes and derived cell lines. *Int. J. Cancer* 88:439.
245. Morra, M., J. Lu, F. Poy, M. Martin, J. Sayos, S. Calpe, C. Gullo, D. Howie, S. Rietdijk, A. Thompson, A. J. Coyle, C. Denny, M. B. Yaffe, P. Engel, M. J. Eck, and C. Terhorst. 2001. Structural basis for the interaction of the free SH2 domain EAT-2 with SLAM receptors in hematopoietic cells. *EMBO J* 20:5840.
246. Hwang, P. M., C. Li, M. Morra, J. Lillywhite, D. R. Muhandiram, F. Gertler, C. Terhorst, L. E. Kay, T. Pawson, J. D. Forman-Kay, and S. C. Li. 2002. A "three-pronged" binding mechanism for the SAP/SH2D1A SH2 domain: structural basis and relevance to the XLP syndrome. *EMBO J.* 21:314.
247. Czar, M. J., E. N. Kersh, L. A. Mijares, G. Lanier, J. Lewis, G. Yap, A. Chen, A. Sher, C. S. Duckett, R. Ahmed, and P. L. Schwartzberg. 2001. Altered lymphocyte responses and cytokine production in mice deficient in the X-linked lymphoproliferative disease gene SH2D1A/DSHP/SAP. *Proc Natl Acad Sci U S A* 98:7449.

248. Wu, C., K. B. Nguyen, G. C. Pien, N. Wang, C. Gullo, D. Howie, M. R. Sosa, M. J. Edwards, P. Borrow, A. R. Satoskar, A. H. Sharpe, C. A. Biron, and C. Terhorst. 2001. SAP controls T cell responses to virus and terminal differentiation of TH2 cells. *Nat Immunol* 2:410.
249. Cannons, J. L., L. J. Yu, B. Hill, L. A. Mijares, D. Dombroski, K. E. Nichols, A. Antonellis, G. A. Koretzky, K. Gardner, and P. L. Schwartzberg. 2004. SAP regulates T(H)2 differentiation and PKC-theta-mediated activation of NF-kappaB1. *Immunity*. 21:693.
250. Davidson, D., X. Shi, S. Zhang, H. Wang, M. Nemer, N. Ono, S. Ohno, Y. Yanagi, and A. Veillette. 2004. Genetic evidence linking SAP, the X-linked lymphoproliferative gene product, to Src-related kinase FynT in T(H)2 cytokine regulation. *Immunity*. 21:707.
251. Murphy, K. M., and S. L. Reiner. 2002. The lineage decisions of helper T cells. *Nat. Rev. Immunol.* 2:933.
252. Crotty, S., E. N. Kersh, J. Cannons, P. L. Schwartzberg, and R. Ahmed. 2003. SAP is required for generating long-term humoral immunity. *Nature* 421:282.
253. Wakeland, E. K., L. Morel, K. Achey, M. Yui, and J. Longmate. 1997. Speed congenics: A classic technique moves into the fast lane (relatively speaking). *Immunol. Today*. 18:473.
254. Stanier, P., H. Abu, J. N. Murdoch, J. Eddleston, and A. J. Copp. 1998. Paralogous sm22alpha (Tagln) genes map to mouse chromosomes 1 and 9: further evidence for a paralogous relationship. *Genomics* 51:144.

255. Bergstrom, D. E., L. H. Gagnon, and E. M. Eicher. 1999. Genetic and physical mapping of the dreher locus on mouse chromosome 1. *Genomics* 59:291.
256. Underhill, D. A., K. J. Vogan, Z. Kibar, J. Morrison, J. Rommens, and P. Gros. 2000. Transcription mapping and expression analysis of candidate genes in the vicinity of the mouse Loop-tail mutation. *Mamm Genome* 11:633.
257. Yang, Z., R. Nielsen, N. Goldman, and A. M. Pedersen. 2000. Codon-substitution models for heterogeneous selection pressure at amino acid sites. *Genetics* 155:431.
258. Vyse, T. J., and J. A. Todd. 1996. Genetic analysis of autoimmune disease. . *Cell* 85:311.
259. Croker, B. P., G. Gilkeson, and L. Morel. 2003. Genetic interactions between susceptibility loci reveal epistatic pathogenic networks in murine lupus. *Genes Immun.* 4:575.
260. Osoegawa, K., M. Tateno, P. Y. Woon, E. Frengen, A. G. Mammoser, J. J. Catanese, Y. Hayashizaki, and J. de. 2000. Bacterial artificial chromosome libraries for mouse sequencing and functional analysis. *Genome Res* 10:116.
261. Shizuya, H., B. Birren, U. J. Kim, V. Mancino, T. Slepak, Y. Tachiiri, and M. Simon. 1992. Cloning and stable maintenance of 300-kilobase-pair fragments of human DNA in Escherichia coli using an F-factor-based vector. *Proc. Natl. Acad. Sci. U. S. A* 89:8794.
262. Veillette, A. 2004. SLAM Family Receptors Regulate Immunity with and without SAP-related Adaptors. *J. Exp. Med.* 199:1175.

263. Sidorenko, S. P., and E. A. Clark. 2003. The dual-function CD150 receptor subfamily: the viral attraction. *Nat. Immunol.* 4:19.
264. Somoza, C., P. C. Driscoll, J. G. Cyster, and A. F. Williams. 1993. Mutational analysis of the CD2/CD58 interaction: the binding site for CD58 lies on one face of the first domain of human CD2. *J. Exp. Med.* 178:549.
265. Jining, L., I. Makagiansar, H. Yusuf-Makagiansar, V. T. Chow, T. J. Siahaan, and S. D. Jois. 2004. Design, structure and biological activity of beta-turn peptides of CD2 protein for inhibition of T-cell adhesion. *Eur. J. Biochem.* 271:2873.
266. Sacksteder, K. A., J. M. Jones, S. T. South, X. Li, Y. Liu, and S. J. Gould. 2000. PEX19 binds multiple peroxisomal membrane proteins, is predominantly cytoplasmic, and is required for peroxisome membrane synthesis. *J Cell Biol* 148:931.
267. Smith, T. S., and C. Southan. 2000. Sequencing, tissue distribution and chromosomal assignment of a novel ubiquitin-specific protease USP23. *Biochim Biophys Acta* 1490:184.
268. Pekarsky, Y., M. Campiglio, Z. Siprashvili, T. Druck, Y. Sedkov, S. Tillib, A. raganescu, P. ermuth, J. H. othman, K. uebner, A. M. uchberg, A. azo, C. renner, and C. M. roce. 1998. Nitrilase and Fhit homologs are encoded as fusion proteins in *Drosophila melanogaster* and *Caenorhabditis elegans*. *Proc Natl Acad Sci U S A* 95:8744.
269. Yu, G., M. Nishimura, S. Arawaka, D. Levitan, L. Zhang, A. Tandon, Y. Q. Song, E. Rogaeva, F. Chen, T. Kawarai, A. Supala, L. Levesque, H. Yu, D. S. Yang, E. Holmes, P. Milman, Y. Liang, D. M. Zhang, D. H. Xu, C. Sato, E. Rogaev, M. Smith, C. Janus, Y. Zhang, R. Aebersold, L. S. Farrer, S. Sorbi, A. Bruni, P. Fraser, and P. St

- George-Hyslop. 2000. Nicastrin modulates presenilin-mediated notch/glp-1 signal transduction and betaATP processing. *Nature* 407:48.
270. Quek, H. H., and V. T. Chow. 1997. Molecular and cellular studies of the human homolog of the 160-kD alpha-subunit of the coatmer protein complex. *DNA Cell Biol* 16:275.
271. Kimberly, W. T., and M. S. Wolfe. 2003. Identity and function of gamma-secretase. *J. Neurosci. Res.* 74:353.
272. Blomhoff, A., B. A. Lie, A. G. Myhre, E. H. Kemp, A. P. Weetman, H. E. Akselsen, E. S. Huseby, and D. E. Undlien. 2004. Polymorphisms in the Cytotoxic T Lymphocyte Antigen-4 Gene Region Confer Susceptibility to Addison's Disease. *J. Clin. Endocrinol. Metab* 89:3474.
273. Muschen, M., U. Warskulat, A. Perniok, J. Even, C. Moers, B. Kismet, N. Temizkan, D. Simon, M. Schneider, and D. Haussinger. 1999. Involvement of soluble CD95 in Churg-Strauss syndrome. *Am. J. Pathol.* 155:915.
274. Rioux, J. D., M. J. Daly, M. S. Silverberg, K. Lindblad, H. Steinhart, Z. Cohen, T. Delmonte, K. Kocher, K. Miller, S. Guschwan, E. J. Kulbokas, S. O'Leary, E. Winchester, K. Dewar, T. Green, V. Stone, C. Chow, A. Cohen, D. Langelier, G. Lapointe, D. Gaudet, J. Faith, N. Branco, S. B. Bull, R. S. McLeod, A. M. Griffiths, A. Bitton, G. R. Greenberg, E. S. Lander, K. A. Siminovitch, and T. J. Hudson. 2001. Genetic variation in the 5q31 cytokine gene cluster confers susceptibility to Crohn disease. *Nat. Genet.* 29:223.

275. Howie, D., M. Simarro, J. Sayos, M. Guirado, J. Sancho, and C. Terhorst. 2002. Molecular dissection of the signaling and costimulatory functions of CD150 (SLAM): CD150/SAP binding and CD150-mediated costimulation. *Blood* 99:957.
276. Schatzle, J. D., S. Sheu, S. E. Stepp, P. A. Mathew, M. Bennett, and V. Kumar. 1999. Characterization of inhibitory and stimulatory forms of the murine natural killer cell receptor 2B4. *Proc Natl Acad Sci U S A* 96:3870.
277. Slev, P. R., and W. K. Potts. 2002. Disease consequences of pathogen adaptation. *Curr. Opin. Immunol.* 14:609.
278. James, J. A., B. R. Neas, K. L. Moser, T. Hall, G. R. Bruner, A. L. Sestak, and J. B. Harley. 2001. Systemic lupus erythematosus in adults is associated with previous Epstein-Barr virus exposure. *Arthritis Rheum* 44:1122.
279. Moon, U. Y., S. J. Park, S. T. Oh, W. U. Kim, S. H. Park, S. H. Lee, C. S. Cho, H. Y. Kim, W. K. Lee, and S. K. Lee. 2004. Patients with systemic lupus erythematosus have abnormally elevated Epstein-Barr virus load in blood. *Arthritis Res. Ther.* 6:R295-R302.
280. Kang, I., T. Quan, H. Nolasco, S. H. Park, M. S. Hong, J. Crouch, E. G. Pamer, J. G. Howe, and J. Craft. 2004. Defective control of latent Epstein-Barr virus infection in systemic lupus erythematosus. *J. Immunol.* 172:1287.
281. Wakeland, E. K., A. E. Wandstrat, K. Liu, and L. Morel. 1999. Genetic dissection of systemic lupus erythematosus. *Curr Opin Immunol* 11:701.
282. Klein, J. 1987. Origin of major histocompatibility complex polymorphism: The trans-species hypothesis. *Hum. Immunol.* 19:155.

283. Nachman, M. W., S. N. Boyer, J. B. Searle, and C. F. Aquadro. 1994. Mitochondrial DNA variation and the evolution of Robertsonian chromosomal races of house mice, *Mus domesticus*. *Genetics* 136:1105.
284. Yonekawa, H., K. Moriwaki, O. Gotoh, N. Hiyashita, Y. Matsushima, L. Shi, W. S. Cho, X. L. Zhen, and Y. Tagashira. 1988. Hybrid origin of japanese mice *Mus musculus molossinus*: evidence from restriction analysis of mitochondrial DNA. *Mol. Biol. Ev.* 5:63.
285. Guenet, J. L., and F. Bonhomme. 2003. Wild mice: an ever-increasing contribution to a popular mammalian model. *Trends Genet.* 19:24.
286. Jansa, S. A., B. L. Lundrigan, and P. K. Tucker. 2003. Tests for positive selection on immune and reproductive genes in closely related species of the murine genus *mus*. *J. Mol. Evol.* 56:294.
287. Lundrigan, B. L., S. A. Jansa, and P. K. Tucker. 2002. Phylogenetic relationships in the genus *mus*, based on paternally, maternally, and biparentally inherited characters. *Syst. Biol.* 51:410.
288. Thomas, P. D., and A. Kejariwal. 2004. Coding single-nucleotide polymorphisms associated with complex vs. Mendelian disease: evolutionary evidence for differences in molecular effects. *Proc. Natl. Acad. Sci. U. S. A* 101:15398.
289. Ono, N., H. Tatsuo, K. Tanaka, H. Minagawa, and Y. Yanagi. 2001. V domain of human SLAM (CDw150) is essential for its function as a measles virus receptor. *J. Virol.* 75:1594.

290. Antoch, M. P., E.-J. Song, A.-M. Chang, M. H. Vitaterna, Y. Zhao, L. D. Wilsbacher, A. M. Sangoram, D. P. King, L. H. Pinto, and J. S. Takahashi. 1997. Functional identification of the mouse circadian *clock* gene by transgenic BAC rescue. *Cell* 89:655.
291. Probst, F. J., R. A. Fridell, Y. Raphael, T. L. Saunders, A. Wang, Y. Liang, R. J. Morell, J. W. Touchman, R. H. Lyons, K. Hoben-Trauth, T. B. Friedman, and S. A. Camper. 1998. Correction of deafness in shaker-2 mice by an unconventional myosin in a BAC transgene. *Science* 280:1447.
292. Kibar, Z., S. Gauthier, S. H. Lee, S. Vidal, and P. Gros. 2003. Rescue of the neural tube defect of loop-tail mice by a BAC clone containing the *Ltap* gene. *Genomics* 82:397.
293. De, G. R., V. L. Friedrich, G. M. Perez, E. Senturk, P. H. Wen, K. Kelley, G. A. Elder, and M. A. Gama Sosa. 2004. Transgenic rescue of Krabbe disease in the twitcher mouse. *Gene Ther.* 11:1188.
294. Giraldo, P., and L. Montoliu. 2001. Size matters: use of YACs, BACs and PACs in transgenic animals. *Transgenic Res.* 10:83.
295. Heintz, N. 2000. Analysis of mammalian central nervous system gene expression and function using bacterial artificial chromosome-mediated transgenesis. *Hum Mol Genet* 9:937.
296. Kumaresan, P. R., V. T. Huynh, and P. A. Mathew. 2000. Polymorphism in the 2B4 gene of inbred mouse strains. *Immunogenetics* 51:758.

297. Bolland, S., Y. S. Yim, A. Tutter, E. K. Wakeland, and J. V. Ravetch. 2002. Genetic modifiers of systemic lupus erythematosus in FcgammaRIIB^{-/-} Mice. *J. Exp. Med.* 195:1167.
298. Klein, J., F. Figueroa, and C. S. David. 1983. H-2 haplotypes, genes and antigens: second listing. II. The H-2 complex. *Immunogenetics* 17:553.
299. Edwards, S. V., K. Chesnut, Y. Satta, and E. K. Wakeland. 1997. Ancestral polymorphism of Mhc class II genes in mice: implications for balancing selection and the mammalian molecular clock. *Genetics* 146:655.
300. McConnell, T. J., W. S. Talbot, R. A. McIndoe, and E. K. Wakeland. 1988. The origin of MHC class II gene polymorphism within the genus *Mus*. *Nature* 332:651.

VITAE

Nisha Limaye was born in New Delhi, India on July 9, 1974, the daughter of Malathi Limaye and Udaya Kumar Limaye. After graduating from the Frank Anthony Public School in Bangalore, India, she entered Mount Carmel College, Bangalore University, and received a Bachelor of Arts degree in Psychology, English Literature and Journalism in 1995. She moved to Dallas in 1995 and completed a Bachelor of Science degree with a major in Psychology at the University of Texas at Arlington in 1998. She entered the Graduate School of Biomedical Sciences at the University of Texas Southwestern Medical Center in August, 1998. She completed her studies in April, 2005, and was awarded the degree of Doctor of Philosophy, with an emphasis on immunology, in June, 2005.

Permanent Address: 11609 Larch Valley Drive

Austin, Texas 78754